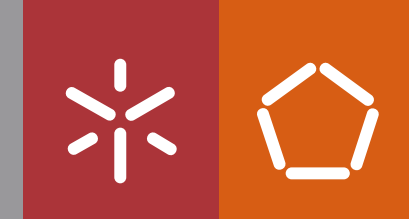




Daniela Sofia Rodrigues Martins

**Bacterial Cellulose: One Material,
Multiple Products**

Universidade do Minho
Escola de Engenharia





Universidade do Minho
Escola de Engenharia

Daniela Sofia Rodrigues Martins

**Bacterial Cellulose:
One Material, Multiple Products**

Doctoral Thesis
Doctorate in Chemical and Biological Engineering

Work developed under the supervision of:
Professor Doctor Francisco Miguel Portela da Gama
and
Professor Doctor Elvira Maria Correia Fortunato

July 2021

DIREITOS DE AUTOR E CONDIÇÕES DE UTILIZAÇÃO DO TRABALHO POR TERCEIROS

Este é um trabalho académico que pode ser utilizado por terceiros desde que respeitadas as regras e boas práticas internacionalmente aceites, no que concerne aos direitos de autor e direitos conexos.

Assim, o presente trabalho pode ser utilizado nos termos previstos na licença abaixo indicada.

Caso o utilizador necessite de permissão para poder fazer um uso do trabalho em condições não previstas no licenciamento indicado, deverá contactar o autor, através do RepositóriUM da Universidade do Minho.

Licença concedida aos utilizadores deste trabalho



Atribuição-NãoComercial-SemDerivações
CC BY-NC-ND

<https://creativecommons.org/licenses/by-nc-nd/4.0/>

ACKNOWLEDGEMENTS

A doctoral degree is given as an individual title but, in truth, many people were involved and contributed in some extent to the work hereby presented. To them, and many others which I may have forgotten during this “long” journey, I thank here with sincere appreciation.

To my supervisor, Professor Miguel Gama, for recognizing my value and giving me the opportunity to start a research career. I thank him for pushing me out of my comfort zone and encouraging me to start this doctoral degree (even when I didn’t believe I was able to accomplish it), for having confidence in my work.

To Professor Elvira Fortunato, for accepting to co-supervise in a field that was still unknown to me.

To the University of Minho; to the Centre of Biological Engineering (CEB) and all its technical staff, for always ensuring the necessary means to all researchers; a special thank you to Paula Pereira and Maura Guimarães, always around and willing to help when I needed.

To all the people from LTEB lab at CEB, for their companionship, for the productive discussions about science and for all the good times at the lab. I want to thank particularly to Fernando Dourado, Ricardo Carvalho and Ana Cristina Rodrigues for their help and direct contributions to this work during the years.

To all people from CEB that helped me at some point with experimental work or their knowledge: Doctor Eduardo Gudiña, Doctor Cristina Rocha, Doctor Rui Rodrigues, Cátia Braga, Pedro Silva, among others.

To Marta Leal, Ana Fontão, Helena Fertuzinhos and Daniela Faria from Satisfibre.

To my friends, the old ones who stayed and the new ones who came, for all the support. Even more important, thank you all for taking my mind out of work and worries, keeping me sane and happy.

To my parents. Although they will never read or understand any of this, it was their education that made who I am, and their work, effort and investment that carried me to where I am.

To my boyfriend and my brother, for their unconditional support, encouragement, and love. They call me back to reason when I’ve lost it and they correct me when I’m wrong. Every day I grow because of them.

Lastly, I gratefully acknowledge Fundação Portuguesa para Ciência e Tecnologia (FCT) for the PhD scholarship ref. SFRH/BD/115917/2016, and all the entities supporting this work: FCT under the scope of the strategic funding of UIDB/04469/2020 unit and COMPETE 2020 (POCI-01-0145-FEDER-006684) and BioTecNorte operation (NORTE-01-0145-FEDER-000004) funded by the European Regional Development Fund (ERDF) under the scope of Norte2020 - Programa Operacional Regional do Norte.

STATEMENT OF INTEGRITY

I hereby declare having conducted this academic work with integrity. I confirm that I have not used plagiarism or any form of undue use of information or falsification of results along the process leading to its elaboration.

I further declare that I have fully acknowledged the Code of Ethical Conduct of the University of Minho.

Bacterial cellulose: one material, multiple products

ABSTRACT

In the scope of this doctoral thesis, bacterial cellulose (BC) dry formulations were produced, using carboxymethyl cellulose (CMC) as a co-drying agent to prevent hornification and improve colloidal stability. Dry BC:CMC in a mass ratio of 1:1 is able to redisperse in aqueous media in few minutes, under low-energy mixing, preserving the properties of the never-dried mixture: high viscosity, reduction of the oil/water interfacial tension and the ability to stabilize heterogeneous systems.

To study the effect of processing parameters in the formulation's properties, different wet-grinding, drying and comminution methods were employed. The size of wet BC fibre bundles was found to be the most relevant parameter, as a reduction in the $Dv(50)$ from 1228 to 55 μm resulted in a decrease in viscosity, interfacial activity and suspending ability of the respective BC:CMC (1:1) formulations. At a concentration of 0.15 %, BC:CMC showed better particle suspending ability than several commercial cellulose products. A spray-dried BC:CMC (1:1) formulation, with a Zeta Potential of (-67.0 ± 3.9) mV and a $Dv(50)$ of (601 ± 19.7) μm , was employed as stabilizer of oil-in-water emulsions. It was able to impart a high viscosity, decrease the oil/water interfacial tension and to form a three-dimensional network structuring the continuous phase, key characteristics for providing emulsion stability. Indeed, at a concentration of 0.50 %, the dry BC:CMC formulation was able to stabilize emulsions against coalescence or creaming for up to 90 days, confirming the potential of BC as a Pickering stabilizer.

Cosmetic cream analogues were prepared by partially or completely replacing the surfactants of a traditional cosmetic emulsion with only 0.75% freeze-dried BC:CMC (1:1). BC-stabilized creams consistently showed similar results to the surfactant-stabilized control cream, and allowed to mimic relevant properties such as storage stability, rheologic behaviour and texture. BC:CMC was also able to stabilize cosmetic emulsions at lower concentration when compared with two commercial cosmetic grade microcrystalline celluloses.

Finally, the BC:CMC ratio was increased to 1:0.5, leading to improved rheological properties. In a benchmark with commercial xanthan gum, BC:CMC 1:0.5 showed higher values of zero-shear viscosity, presented a measurable yield stress of (1.54 ± 0.17) Pa (for a 0.5 % aqueous dispersion) and the highest storage modulus, indicating a stronger solid-like character and better stabilizing properties. Contrarily to xanthan gum, the viscosity of all BC:CMC dispersions was independent from the pH and ionic strength.

Keywords - Bacterial cellulose; dry additive; food and cosmetics; heterogeneous systems; stabilizer and thickener.

Celulose bacteriana: um material, múltiplos produtos

RESUMO

No âmbito desta tese de doutoramento foram produzidas formulações secas de celulose bacteriana (BC), usando carboximetil celulose (CMC) como coadjuvante de secagem para prevenir a agregação irreversível das fibras e melhorar a estabilidade coloidal. A BC:CMC seca, com rácio de 1:1, redispersa em água em poucos minutos e com baixa energia de agitação, preservando as propriedades da mistura não seca: alta viscosidade, redução da tensão interfacial óleo/água e capacidade de estabilizar sistemas heterogéneos. Para estudar o efeito dos parâmetros de processamento nas propriedades da formulação, foram usados diferentes métodos de trituração em húmido, secagem e cominuição. Constatou-se que o tamanho dos agregados de fibras húmidas de BC é o parâmetro mais relevante, já que uma redução do Dv(50) de 1228 para 55 μm causou uma diminuição da viscosidade, da atividade interfacial e da capacidade de suspensão das respetivas formulações BC:CMC (1:1). A uma concentração de 0.15 %, a BC:CMC demonstrou melhor capacidade de suspensão de partículas do que várias celulosas comerciais.

Uma formulação de BC:CMC (1:1) seca por *spray-drying*, com um potencial Zeta de (-67.0 ± 3.9) mV e um Dv(50) de (601 ± 19.7) μm , foi usada como estabilizante de emulsões óleo-em-água. Esta foi capaz de promover alta viscosidade, diminuir a tensão interfacial e formar uma rede tridimensional a estruturar a fase contínua, características chave para estabilizar emulsões. De facto, a uma concentração de 0.5 % a formulação de BC:CMC foi capaz de estabilizar emulsões contra coalescência e *creaming* até 90 dias. Foram preparados análogos de cremes cosméticos substituindo completa ou parcialmente os surfactantes de uma emulsão cosmética por apenas 0.75 % de BC:CMC 1:1 liofilizada. Os cremes estabilizados com BC mostraram consistentemente resultados similares aos do controlo estabilizado com surfactantes, permitindo reproduzir propriedades relevantes como a estabilidade de armazenamento, o comportamento reológico e a textura. A BC:CMC foi capaz de estabilizar emulsões cosméticas com menor concentração do que duas celulosas microcristalinas comerciais usadas na cosmética.

Por fim, o rácio de BC:CMC foi aumentado para 1:0.5, levando à melhoria das propriedades reológicas. Num estudo comparativo com xantano, a BC:CMC 1:0.5 apresentou maior viscosidade em repouso, uma tensão de cedência de (1.54 ± 0.17) Pa (para uma concentração de 0.5 %) e módulo elástico superior, indicativo de um carácter sólido pronunciado e melhores propriedades estabilizantes. Contrariamente ao xantano, a viscosidade das dispersões de BC:CMC mostrou-se independente do pH e da força iónica.

Palavras chave - Celulose bacteriana; aditivo seco; alimentar e cosmética; sistemas heterogéneos; estabilizante e espessante.

LIST OF CONTENTS

Chapter 1 - Introduction	18
1.1 - Context and Motivation	19
1.2 - Objectives.....	20
1.3 - Thesis Outline.....	21
1.4 - Dissemination and Communications	22
1.5 - Bibliographic references.....	24
Chapter 2 - Literature Review	26
2.1 - Introduction to cellulose materials.....	27
2.2 - BC biosynthesis and production	30
2.3 - BC's properties and characterization.....	34
2.4 - Stabilization of heterogeneous systems	37
2.4.1 - Particle-stabilized systems: Pickering emulsions and foams	39
2.4.2 - Cellulose particles as Pickering stabilizers	42
2.5 - Applications of BC in Food and Cosmetics.....	48
2.5.1 - Food Applications	49
2.5.2 - Cosmetic applications	51
2.6 - Bibliographic references.....	52
Chapter 3 - Dry BC:CMC formulations with interfacial-active performance: processing conditions and redispersion	64
3.1 - Introduction	65
3.2 - Materials and Methods.....	67
3.2.1 - Preparation of the BC:CMC powders	67
3.2.2 - Evaluation of the dispersibility	69
3.2.3 - Microscopic observations	69
3.2.4 - Size measurements	69
3.2.5 - Viscosity measurements.....	70
3.2.6 - Interfacial tension	70
3.2.7 - Effect of BC:CMC formulations on the suspension stability of cocoa beverage	71
3.3 - Results	72
3.3.1 - Effect of wet-grinding method on BC bundle size.....	72

3.3.2 - Properties of the never-dried BC formulations after CMC addition.....	73
3.3.3 - Effect of drying and redispersion methods	76
3.3.4 - Effect of dry comminution	79
3.3.5 - Functionality assessment: Suspension Stability of a Cocoa Beverage.....	82
3.4 - Conclusions.....	84
3.5 - Bibliographic references.....	84
Chapter 4 - A Dry and Fully Dispersible BC Formulation as a Stabilizer for Oil-in-Water Emulsions	87
4.1 - Introduction	88
4.2 - Materials and Methods.....	89
4.2.1 - Materials and Reagents.....	89
4.2.2 - BC:CMC preparation.....	89
4.2.3 - Contact angles of BC and BC:CMC.....	90
4.2.4 - Particles Zeta Potential and size measurements	90
4.2.5 - Interfacial tension measurements.....	91
4.2.6 - Emulsions' preparation	91
4.2.7 - Microscopy	92
4.2.8 - Rheological analysis of the emulsions.....	92
4.3 - Results and Discussion	93
4.3.1 - Assessment of the surface hydrophilicity by contact angles measurement	95
4.3.2 - Surface charge assessment through Zeta Potential measurements	96
4.3.3 - Interfacial tension	97
4.3.4 - Emulsion stability over time.....	99
4.3.5 - Rheological analysis.....	102
4.4 - Conclusions.....	104
4.5 - Bibliographic references.....	105
Chapter 5 - BC:CMC dry formulation as stabilizer and texturizing agent for surfactant-free cosmetic formulations	108
5.1 - Introduction	109
5.2 - Materials and Methods.....	111
5.2.1 - Materials and Reagents.....	111
5.2.2 - BC:CMC preparation.....	111

5.2.3 - Emulsions preparation	111
5.2.4 - Evaluation of stability	113
5.2.5 - Rheological analysis of the emulsions.....	113
5.2.6 - Textural analysis	114
5.2.7 - Confocal Laser Scanning Microscopy (CLSM)	115
5.3 - Results and Discussion	115
5.3.1 - Evaluation of stability over time	115
5.3.2 - Rheological assessment.....	119
5.3.3 - Texture assessment.....	130
5.4 - Conclusions.....	132
5.5 - Bibliographic references.....	133
Chapter 6 - Effect of ionic strength and pH in the behaviour of re-dispersed BC:CMC - a comparative study with Xanthan Gum.....	136
6.1 - Introduction	137
6.2 - Materials and Methods.....	138
6.2.1 - Materials and reagents.....	138
6.2.2 - Preparation of BC:CMC dry formulations	138
6.2.3 - Physicochemical characterization of the polysaccharides	139
6.2.4 - Preparation of aqueous dispersions.....	139
6.2.5 - Rheological analysis.....	140
6.3 - Results and Discussion	141
6.3.1 - Characterization of the polysaccharides and BC:CMC formulations	141
6.3.2 - Rheological characterization of the aqueous dispersions	142
6.3.3 - Effect of concentration	144
6.3.4 - Effect of salinity and pH	146
6.4 - Conclusions.....	149
6.5 - Bibliographic References.....	150
Chapter 7 - Conclusions and Future Work.....	153
Conclusions.....	154
Future work	155

LIST OF FIGURES

Figure 2.1 – Structure of a single cellulose chain, showing cellobiose as the repeating unit and the number of glucose residues as the degree of polymerization.....	27
Figure 2.2 – (A) Schematic example of the organization of cellulose molecules into elementary fibrils, microfibrils and fibres (adapted from [8]); (B) representation of crystalline and amorphous regions in cellulose fibrils and result after hydrolysis.....	28
Figure 2.3 – Examples of different cellulose particles. Scanning electron microscope images of (A) wood pulp fibres (retrieved from [11]), (B) hydrocolloidal microcrystalline cellulose Avicel CM2159, (C) bacterial cellulose from <i>K. xylinus</i> , and (D) transmission electron micrograph of ramie cellulose nanocrystals (retrieved from [12]).	29
Figure 2.4 - (A) Schematic illustration of the metabolic pathways of cellulose production in bacteria (adapted from [13]); bacterial cellulose membranes in (B) wet and (C) dry state, and respective scanning electron micrographs (D and E).	31
Figure 2.5 – Amphiphilic character of cellulose: (A) side and front view of a cellulose chain, with dashed lines marking the hydrophobic and hydrophilic parts of the molecule (adapted from [58]); (B) schematic representation of the transverse section of a cellulose nanocrystal (I β allomorph) at the oil/water interface, exposing the hydrophobic edge plane (200) to the oil phase (retrieved from [59]).	36
Figure 2.6 – Representation of the destabilization mechanisms of emulsion systems (adapted from [109]).	39
Figure 2.7 – Wettability of a solid surface, as measured by contact angle with a water drop (top); position of a spherical solid particle at a planar oil/water (or air/water) interface, according to its contact angle, and corresponding position at a curved interface resulting in oil-in-water or water-in-oil emulsions (bottom).	41
Figure 2.8 – Scanning electron microscope images of polymerised styrene-in-water emulsions stabilised by CNCs of different aspect ratios: (a) cotton nanocrystals with aspect ratio of 13; (b) bacterial cellulose nanocrystals with aspect ratio of 47; (c) <i>Cladophora</i> nanocrystals with aspect ratio of 160 (retrieved from [127]).	44
Figure 2.9 - Confocal laser scanning micrographs of a pickering emulsion stabilized with cotton CNCs containing 10 % of internal phase, and the resulting HIPE with 85.6% of internal phase (retrieved from [130]).	45

Figure 3.1 - Scheme of the several steps and processing conditions used in this work to obtain the different dry BC:CMC powders.	67
Figure 3.2 - Viscosity profiles of 0.5% (m/v) of CMC and never-dried BC:CMC mixtures with BC from the different grinding methods, diluted and dispersed using Ultra-turrax.....	74
Figure 3.3 - Effect of wet grinding of BC on the Interfacial Tension of Isohexadecane/Water containing 0.5 % (m/v) never-dried BC:CMC. Results are expressed as average of triplicate measurements and bars are representative of the Standard Deviation. All datasets were compared with each other using one-way ANOVA followed by Tukey's Multiple Comparison Test (significant at *p <0.05, ***p < 0.001, when compared with the H ₂ O control; ns – not significant comparing HB with HPH-1).	75
Figure 3.4 - Classification of the dispersibility of dry BC:CMC formulations in water, at 0.5 % (m/v): 1 - sample is homogeneous and no visible particles or aggregates are observable; 2 - sample contains some very small particles or aggregates; 3 – the sample contains some larger particles or aggregates; 4 – non-dispersible, the water remains transparent and the well separated particles or aggregates are observed.	77
Figure 3.5 - Dynamic viscosity profiles of 0.5 % (m/v) BC:CMC powders redispersed in water, following different drying (hot plate or oven) and comminution (to sizes <300 µm or <100 µm), and redispersed using UT homogenizer or Magnetic stirring.	78
Figure 3.6 - SEM images of BC:CMC powders obtained from HB processed BC, (A) dried in a Hot plate, ground and sieved to <300 µm; (B) dried in an Oven, ground and sieved to <300 µm; (C) dried in a Hot plate, ground and sieved to <100 µm; (D) dried in an Oven, ground and sieved to <100 µm. All white scale bars correspond to 300 µm.	80
Figure 4.1 - Cryo-SEM images (2000X magnification) of (A) 0.50 % non-dried BC:CMC; (B) 0.50 % dried and redispersed BC:CMC; (C) SEM image (890X magnification) of spray-dried BC:CMC. All black scale bars correspond to 20 µm.	94
Figure 4.2 - Optical micrographs (10X magnification) of ground BC (left) and redispersed BC:CMC formulation after spray-drying (right), stained with Calcofluor White. Scale bars correspond to 100 µm.	94
Figure 4.3 - Optical micrographs (20X magnification) of Avicel LM310, Avicel RT1133 and Novagel RCN15, dispersed in water and stained with Calcofluor White, before and after activation. Scale bars correspond to 50 µm.	95

Figure 4.4 - (A) Micrographs of the evolution of a 2 μ L water drop on top of BC and BC:CMC dry films over time (glass was used as a control); (B) Contact angles of water with BC and BC:CMC films over time, as determined by the sessile drop method..... 95

Figure 4.5 - Isohexadecane/water interfacial tension measurements performed by (A) Du Noüy Ring method and (B) Pendant Drop method, in the presence of (1) different concentrations of the BC:CMC dry formulation (0.10 %, 0.25 % and 0.50 %) and 0.50 % CMC, and (2) 0.50 % of plant celluloses (Avicel RT1133, Avicel LM310, Novagel RCN15, Celluforce NCC) and Xanthan gum. Results are the average of triplicate measurements and bars represent standard deviation. All the results were compared with the control (H_2O) using one-way ANOVA and Tukey's Multiple Comparison Test (ns – not significant, * $p < 0.05$, ** $p < 0.01$, *** $p < 0.001$). 98

Figure 4.6 - Photographs and optical micrographs (10X magnification) of 10 % isohexadecane-in-water emulsions prepared with different concentrations of BC:CMC dry formulation (0.10 %, 0.25 % and 0.50 %) and with 0.50 % CMC, taken 1 day after preparation and after a storage time of 30 and 90 days, at room temperature. Black scale bars correspond to 100 μ m..... 100

Figure 4.7 - Photographs and optical micrographs (10X magnification) of 10 % isohexadecane-in-water emulsions prepared with 0.50 % of different materials (Avicel RT1133, Avicel LM310, Novagel RCN15, Celluforce NCC and Xanthan gum), taken 1 day after preparation and after a storage time of 30 days at room temperature. Black scale bars correspond to 100 μ m. 100

Figure 4.8 - Cryo-SEM images (different magnifications) of 10 % isohexadecane-in-water emulsions prepared with (A) 0.10 %, (B) 0.25 % and (C) 0.50 % of the BC:CMC dry formulation in the day after preparation. All black scale bars correspond to 20 μ m. 101

Figure 4.9 - Flow sweep curves of 10 % isohexadecane-in-water emulsions prepared with (A) different concentrations of the BC:CMC dry formulation (0.10 %, 0.25 % and 0.50 %); (B) 0.50 % of different materials (Avicel RT1133, Avicel LM310, Novagel RCN15, Celluforce NCC, Xanthan gum and CMC), obtained from the average of triplicate samples. 103

Figure 4.10 - Oscillatory frequency sweep curves of 10 % isohexadecane-in-water emulsions prepared with 0.50 % BC:CMC and Xanthan gum, obtained from the average of triplicate samples. Bars represent standard deviation..... 103

Figure 5.1 - Photographs of the cosmetic emulsions stabilized with different concentrations of BC:CMC, Avicel PC-591 and Avicel PC-611, taken 1 day after preparation and after 30 days of storage, at room temperature. Red arrows indicate visible lines of phase separation, creaming effect or sedimentation..... 116

Figure 5.2 - Optical micrographs (10X magnification) of the cosmetic emulsions stabilized with different concentrations of BC:CMC, Avicel PC-591 and Avicel PC-611, taken after a storage time of 1 day and 30 days, at room temperature. Scale bars correspond to 100 μm	117
Figure 5.3 - CLSM micrographs (10x magnification) of NS 0.5 BC:CMC. Oil phase is stained in red by Nile Red dye, and BC fibers are stained blue by Calcofluor White stain. Scale bars correspond to 100 μm	119
Figure 5.4 - Flow curves of aqueous dispersions of the polymers used in this study, at different concentrations. Results are the average of triplicate samples, obtained from the third consecutive flow sweep (FS3). Bars represent standard deviation.	120
Figure 5.5 - Rheological evaluation of the FF and LSF after 1 day of storage at room temperature: flow curves taken from (a) the first flow sweep, FS1, and (b) the third consecutive flow sweep, FS3; (c) storage modulus, G' , and (d) loss modulus, G'' , taken from oscillatory frequency sweep tests. Results are the average of triplicate samples. Bars represent standard deviation.....	121
Figure 5.6 - Rheological evaluation of the FF and LSF after 30 days of storage at room temperature: flow curves taken from (a) the first flow sweep, FS1, and (b) the third consecutive flow sweep, FS3; (c) storage modulus, G' , and (d) loss modulus, G'' , taken from oscillatory frequency sweep tests. Results are the average of triplicate samples. Bars represent standard deviation.....	123
Figure 5.7 - Oscillatory strain sweeps of the FF and LSF after 1 day of storage at room temperature.	124
Figure 5.8 - Rheological evaluation of NSF after 1 day of storage at room temperature: flow curves taken from (a) the first flow sweep, FS1, and (b) the third consecutive flow sweep, FS3; (c) storage modulus, G' , and loss modulus, G'' , taken from oscillatory frequency sweep tests. Results are the average of triplicate samples. Bars represent standard deviation.	126
Figure 5.9 - Rheological evaluation of NSF after 30 days of storage at room temperature: flow curves taken from (a) the first flow sweep, FS1, and (b) the third consecutive flow sweep, FS3; (c) storage modulus, G' , and loss modulus, G'' , taken from oscillatory frequency sweep tests. Results are the average of triplicate samples. Bars represent standard deviation.	127
Figure 5.10 – Three interval thixotropy flow curves of the cosmetic cream analogues after 1 day of storage, at room temperature.....	128
Figure 5.11 - Temperature dependence of G' in oscillatory temperature cycles, between 10 $^{\circ}\text{C}$ and 50 $^{\circ}\text{C}$, of the cosmetic cream analogues after 1 day of storage at room temperature.....	129

Figure 5.12 - Textural parameters of the cosmetic emulsions after 1 day of storage at room temperature: Firmness (a) and Consistency (b) were taken from a puncture test; Firmness and Cohesiveness (c), Consistency and Index of Viscosity (d) were taken from a back-extrusion test. Results are the average of triplicate samples and bars represent standard deviation. All the results were compared with the FF cream using one-way ANOVA and Tukey's Multiple Comparison Test (* $p < 0.05$, ** $p < 0.01$, *** $p < 0.001$)..... 131

Figure 6.1 - Characterization of BC:CMC formulations, CMC and XG in dry state by: (A) Differential scanning calorimetry, between 20 °C and 400 °C, at a heat rate of 10 °C/min under N₂ atmosphere; (B) Attenuated total reflection-Fourier transform infrared spectroscopy, in absorbance mode in the range of 400 cm⁻¹ to 4000 cm⁻¹..... 141

Figure 6.2 - Rheological characterization of BC:CMC and XG dispersions at a concentration of 0.5 % (w/w) in distilled water, plus XG in 150 mM NaCl: (A) viscosity and (B) shear stress, as function of shear rate taken from flow sweep tests in the range of 0.01 to 300 s⁻¹; (C) storage modulus, G' and (D) loss modulus, G'', taken from oscillatory frequency sweep tests in the range of 0.01 to 40 Hz. Samples were analysed at 25 °C. Results are the average of triplicate samples and bars represent standard deviations..... 143

Figure 6.3 - Mass percentage concentration dependence of the (A) zero-shear viscosity, η_0 , and (B) yield stress, σ_0 , for BC:CMC and XG dispersions in distilled water, plus XG in 150 mM NaCl, at 25 °C. Results are the average of triplicate samples and bars represent standard deviations. 145

Figure 6.4 - Effect of NaCl concentration in the flow curves (viscosity vs shear rate) of 0.5 % (w/w) dispersions of (A) XG, (B) BC:CMC 1:1, (C) BC:CMC 1:0.75, and (D) BC:CMC 1:0.5. Samples were analysed at 25 °C. Results are the average of triplicate samples and bars represent standard deviations. 147

Figure 6.5 - Effect of pH in the flow curves (viscosity vs shear rate) of 0.5 % (w/w) dispersions of (A) XG, (B) BC:CMC 1:1, (C) BC:CMC 1:0.75, and (D) BC:CMC 1:0.5. Samples were analysed at 25 °C. Results are the average of triplicate samples and bars represent standard deviations..... 149

LIST OF TABLES

Table 3.1 - Percentiles and Mean Diameters of the particle size distribution (by volume) of BC samples wet-ground by different methods, and respective micrographs (scale bars correspond to 100 μm). All measurements satisfy the quality criteria since the Residuals (%) and Weighted Residuals (%) are $\leq 1\%$	73
Table 3.2 - Dispersibility of BC:CMC mixtures after drying, grinding and sieving to a particle size of $<300\ \mu\text{m}$	77
Table 3.3 - Dispersibility of BC:CMC mixtures after drying, grinding and sieving to a particle size $<100\ \mu\text{m}$	81
Table 3.4 - Stabilization of cocoa particles in chocolate milk, with BC:CMC, added at 0.15% (m/v), at room temperature (c.s. – complete sedimentation).....	83
Table 4.1 - Zeta Potential (Z) and particle size of different cellulose aqueous suspensions, represented as the average and standard deviation (a- Before activation; b- After activation; c – Information provided by the supplier).....	96
Table 5.1 - Composition, in mass fraction (% w/w), of the generic cosmetic cream emulsions (* - Full formulation of the generic cream, prepared according to Gilbert et al. [29–31]).....	112
Table 6.1 - Salinity (dimensionless) and conductivity (mS/cm) of the NaCl solutions in distilled water prepared at concentrations ranging from 0 to 350 mM, at room temperature	146
Table 6.2 - Salinity (dimensionless) and conductivity (mS/cm) of the buffer solutions in distilled water prepared at a concentration of 50 mM, with pH values ranging from 2.8 to 10.4, at 25 °C	148

LIST OF ABBREVIATIONS

BC	– Bacterial Cellulose
BC:CMC	– Bacterial Cellulose and Carboxymethyl Cellulose mixture
BCNC	– Bacterial Cellulose Nanocrystals
BCNF	– Bacterial Cellulose Nanofibrils
CLSM	– Confocal Laser Scanning Microscope
CMC	– Carboxymethyl Cellulose
CNC	– Cellulose Nanocrystals
CNF	– Cellulose Nanofibrils
CTE	– Coefficient of Thermal Expansion
DP	– Degree of Polymerization
FF	– Full Formulation
GRAS	– Generally Recognized as Safe
HB	– Hand Blender
HIPE	– High Internal Phase Emulsion
HEC	– Hydroxyethyl Cellulose
HP	– Hot Plate
HPH	– High-Pressure Homogenization
HPMC	– Hydroxypropyl Methyl Cellulose
HS	– Hestrin and Schramm medium
IFT	– Interfacial Tension
LBG	– Locust Bean Gum
LSF	– Low Surfactants Formulations
MC	– Methyl Cellulose
MCC	– Microcrystalline Cellulose
MFC	– Microfibrillated Cellulose
MHI	– Microcut Head Impeller
MS	– Magnetic Stirring
NFC	– Nanofibrillated Cellulose
NSF	– No Surfactants Formulations
OV	– Oven

SEM – Scanning Electron Microscope

TC – Terminal Complex

TEMPO – 2,2,6,6-tetramethylpiperidine-1-oxyl

TGA – Thermogravimetric Analysis

TS – Total Solids

UT – Ultra-Turrax homogenizer

XG – Xanthan Gum

Chapter 1

Introduction

In this first chapter, the context and motivation that supported this thesis are explained; the objectives of the work are delineated, and the content of this manuscript is outlined for the reader. Finally, the scientific dissemination outcomes of the performed work (research papers and communications in science meetings) are reported.

1.1 - CONTEXT AND MOTIVATION

Cellulose is now – and has been throughout the years - one of the most used bulk commodities, owing to its outstanding properties. Paper and textiles, buildings and furniture are examples of traditional uses of cellulose, either purified or combined with lignin and other polysaccharides, as is produced in the plant kingdom. Microcrystalline cellulose from plant sources is used as an additive in food and cosmetics, as a stabilizing and thickening agent [1,2]. Many cellulose derivatives, as carboxymethyl cellulose, cellulose acetate, hydroxyethyl cellulose and others, are found in food, pharmaceutical, medical and chemical industries [3–5]. Cellulose is used as reinforcement for construction materials and auto parts, and regenerated cellulose is now used in more eco-friendly textiles [6–9]. The development of low-cost, paper-based biodegradable electronics and sensors is an emerging area holding great potential [10,11]. New cellulose-based high-value products are still being researched and developed with success. Through improved processing, using mechanical or enzymatic treatments, cellulose can be made available from biomass in different morphologies, such as micro and nano crystals, fibres and rods [12–15].

However, inevitably, the widespread and intensive use of cellulose started to raise environmental concerns related to the sustainability of the forest exploitation, as well as to the massive use of water and pesticides required to, e.g., grow cotton [16–18]. In response, a new research trend emerged for alternative materials, new ways to process and add value to the biomass residues, and for the search for more sustainable sources of cellulose. One of these alternative sources resides in the biotechnological production of cellulose by fermentation. Although known for many years, this process is not yet exploited industrially to large extent, although it could provide a more sustainable route and yield a product with unique and highly performant properties [19].

Bacterial Cellulose (BC) is produced in the pure state during fermentation by different microorganisms, most efficiently by acetic acid bacteria of the genus *Komagataeibacter*. It is chemically identical to cellulose produced by plants, but radically different in its macromolecular assembly and overall morphology. As a raw material, BC can be obtained by sustainable and economical processes, from low-cost fermentation substrates and in a short time [20–22]. When produced in static culture, BC membranes are made of entangled networks of long and pure cellulose nanofibrils, holding a high-water content. In wet or dry state, BC membranes are now being used for different advanced applications requiring low cost yet highly performant materials. Many uses have already been studied and developed for cellulose membranes, for example in the field of biomedicine as wound dressings and dura matter substitutes [23–25]. However, BC's full potential is yet to be unveiled: there are still applications and

markets to be explored, and there is still a need to validate the possibility of replacing plant-based cellulose in some of its uses. Also, it remains to be ascertained whether the increased cost of BC, as compared to wood derived cellulose, is balanced by the superior performance in some applications.

The use of BC in the food industry mainly concerns nata de coco, a dessert produced in Asian countries. Although cellulose-based additives are used in the food industry, and although several studies support BC as a very efficient stabilizer for heterogeneous systems (as are many foods and beverages), this application is not used industrially, perhaps due to the legal issues regarding the introduction of novel food ingredients [26,27]. Given its distinct characteristics from commonly used stabilizers and the advantages inherent to nano-sized materials, BC might in fact show a great potential in this area. These features are also appealing for other areas: the technological potential of BC for the development of cosmetic applications, for instance, is well stated in patents by multinational companies; yet, surprisingly, no publications systematically addressing this topic can be found in other scientific literature.

1.2 - OBJECTIVES

The work presented in this thesis aims to contribute to the knowledge and development of new and value-added applications for BC and its composites. With that in vision, this project was conducted in two specific domains: food technology and cosmetic formulations. The use of BC in food and cosmetics stems from its properties as thickener and as a stabilizer of different heterogeneous systems.

The main objectives of this work are the following:

- Development of BC powder formulations, a step towards attracting the attention of the industry to this new hydrocolloid and facilitating its future commercialization. This will be accomplished by mixing wet-ground BC with edible polysaccharides in different ratios, as co-drying agents, and finding a suitable drying method. A formulation with good redispersing ability and colloidal stability over a wide range of temperatures, salt concentrations and pH conditions is envisioned.
- Characterization of the developed dry formulations and understanding of the mechanisms behind the stabilizing effect of BC fibres, highlighting its potential as a novel hydrocolloid.
- Application of a dry BC formulation in the food technology field, as a novel functional ingredient and stabilizer of different food matrices: oil-in-water emulsions, resembling spoonable or pourable dressings; suspensions of solid particles in liquids, such as chocolate milk beverages; edible aqueous foams, such as smoothies or whipped cream.
- Application of a dry BC formulation as stabilizer and texturing agent in the cosmetic field: given

the surfactant-like activity of BC, the development of low-surfactant or surfactant-free cosmetic emulsions, with the same rheological and organoleptic properties of traditional creams, is envisioned.

- In parallel with the previous objectives, conducting benchmarking studies with hydrocolloidal polysaccharides already marketed for food and cosmetic applications, such as microcrystalline cellulose and xanthan gum. The goal is to highlight the superior performance of BC formulations and prove its potential as a multifaceted additive.

In this perspective, this project aims at presenting the ground basis for the development of innovative bacterial cellulose products with excellent technological properties that meet emerging needs.

1.3 - THESIS OUTLINE

This thesis is divided into 7 main chapters, some of which were published as research papers in scientific journals.

Chapter 2 - Literature Review, is a scientific state-of-the-art review on the subject of the present thesis. The features of BC that make it a unique and outstanding material are discussed, highlighting how it differs from other celluloses.

Chapter 3 - Dry BC:CMC formulations with interfacial-active performance: processing conditions and redispersion, reports the results from laboratorial production of BC powder formulations with carboxymethyl cellulose (CMC). For this work, different processing parameters were employed in the production of dry BC:CMC powders: the extent of grinding of the BC membranes and final fibre bundle size, drying method and final dry particle size. The properties of the prepared powders, their dispersibility and their ability to stabilize a heterogeneous solid-in-liquid system, composed of milk and cocoa powder (as in a chocolate milk beverage), were assessed. A benchmarking test was made using several plant-derived commercial celluloses. This was the first systematic study envisioning the understanding of the relevant processing conditions for the development of dry BC:CMC formulations.

In *Chapter 4 - A dry and fully dispersible BC formulation as a stabilizer for oil-in-water emulsions*, a more in-depth study is made on the emulsion stabilizing properties of dry BC:CMC formulations. A spray-dried BC:CMC formulation was characterized and employed as a stabilizer in 10 % isohexadecane emulsions, in parallel with commercial plant celluloses and xanthan gum. A low concentration of the dry BC:CMC was shown to prevent emulsion creaming and phase separation for a 90-day time period. Reduction of the interfacial tension, Pickering effect and continuous phase structuring were investigated as the

mechanisms responsible for the observed stabilizing properties.

In another work, the same dry formulation was applied in a different type of emulsion, as reported in *Chapter 5 – BC:CMC dry formulation as stabilizer and texturizing agent for surfactant-free cosmetic formulations*. Generic cosmetic oil-in-water emulsions were prepared using dry BC:CMC as a more natural stabilizer, to partially or completely replace surfactants, diminishing the associated skin irritation issues. A simple protocol was employed, with short time mixing, and two commercial hydrocolloidal microcrystalline celluloses (commonly used as thickeners and stabilizing aids in cosmetics) were tested alongside as a benchmarking study. In this first report of a dry BC:CMC additive for replacement of surfactants in cosmetic emulsions, cream analogues were effectively stabilized while delivering similar rheological and textural characteristics of a traditional surfactant-stabilized cream.

In *Chapter 6 – Effect of ionic strength and pH in the behaviour of re-dispersed BC:CMC - a comparative study with Xanthan Gum*, BC:CMC dry formulations were prepared in different mass ratios, 1:1, 1:0.75 and 1:0.5. Several rheological parameters were studied, namely dynamic viscosity and shear stress, zero-shear viscosity, yield stress and dynamic moduli, and compared with a commercial xanthan gum. The effect of the ionic strength and pH of the aqueous media in the viscosity of the dispersions was assessed. The increase in the BC:CMC ratio showed to improve the rheological properties of the dispersions, while their behaviour remained constant despite the environmental conditions, in contrast with xanthan gum. Finally, in *Chapter 7 – Conclusions and future work*, a final overview of the thesis is made, highlighting the main findings and conclusions, and adding some suggestions for the continuation of the work with dry BC formulations.

1.4 - DISSEMINATION AND COMMUNICATIONS

The experimental and research work presented in this thesis was disseminated through several publications in international journals, as well as communications in national and international science meetings. The scientific output originated from this work is listed below.

Publications in peer-reviewed journals

- Martins, D., Estevinho, B., Rocha, F., Dourado, F. & Gama, M. (2020). *A Dry and Fully Dispersible Bacterial Cellulose Formulation as a Stabilizer for Oil-in-Water Emulsions*. Carbohydrate Polymers, 230, 115657.

<https://doi.org/10.1016/j.carbpol.2019.115657>

- Martins, D., de Carvalho Ferreira, D., Gama, M. & Dourado, F. (2020). *Dry Bacterial Cellulose and Carboxymethyl Cellulose formulations with interfacial-active performance: processing conditions and redispersion*. Cellulose, 27, 6505–6520.
<https://doi.org/10.1007/s10570-020-03211-9>
- Martins, D., Rocha, C., Dourado, F. & Gama, M. (2021). *Bacterial Cellulose-Carboxymethyl Cellulose (BC:CMC) dry formulation as stabilizer and texturizing agent for surfactant-free cosmetic formulations*. Colloids and Surfaces A: Physicochemical and Engineering Aspects, 617, 126380.
<https://doi.org/10.1016/j.colsurfa.2021.126380>.

Manuscripts in preparation

- Martins, D., Dourado, F., Coimbra, M. A. & Gama, M. (2021). *Effect of ionic strength and pH in the behaviour of re-dispersed BC:CMC - a comparative study with Xanthan Gum*.

Oral Communications

- Martins, D., Dourado, F. & Gama, M., *A Dry Bacterial Cellulose-Carboxymethyl Cellulose Formulation as Stabilizer for Oil-in-Water Emulsions*. Glupor 13 - 13^o Reunião do Grupo de Glúcidos, Porto (Portugal), 3 – 6 September 2019.
- Martins, D., Dourado, F. & Gama, M., *A Dry Bacterial Cellulose-Carboxymethyl Cellulose Formulation as Stabilizer for Pickering Oil-in-Water Emulsions*. 4th International Symposium on Bacterial NanoCellulose, Porto (Portugal), 2 – 4 October 2019.

Poster Presentations

- Martins, D., Almeida Garrett, F., Fontão, A., Leal, M., Dourado, F. & Gama, F.M., *Bacterial cellulose as a novel stabilizer and texturizer for cosmetic and food applications*. Glupor 12 - 12^o Reunião do Grupo de Glúcidos, Aveiro (Portugal), 11 -13 September 2017.
- Martins, D., Fontão, A., Dourado, F. & Gama, M. *Bacterial Cellulose as a stabilizer for oil-in-water emulsions*. ChemPor 2018 - 13th International Chemical and Biological Engineering Conference, Aveiro (Portugal), 2 – 4 October 2018.
- Martins, D., Dourado, F. & Gama, F. M. *A Dry Bacterial Cellulose-Carboxymethyl Cellulose*

Formulation as Stabilizer for Pickering Oil-in-Water Emulsions. Materials Research Society Fall Meeting and Exhibit, Boston, Massachusetts (United States of America), 1 – 6 December 2019.

1.5 - BIBLIOGRAPHIC REFERENCES

- [1] J. Nsor-Atindana, M. Chen, H.D. Goff, F. Zhong, H.R. Sharif, Y. Li, Functionality and nutritional aspects of microcrystalline cellulose in food, *Carbohydr. Polym.* 172 (2017) 159–174. <https://doi.org/10.1016/j.carbpol.2017.04.021>.
- [2] D. Trache, M.H. Hussin, C.T. Hui Chuin, S. Sabar, M.R.N. Fazita, O.F.A. Taiwo, T.M. Hassan, M.K.M. Haafiz, Microcrystalline cellulose: Isolation, characterization and bio-composites application—A review, *Int. J. Biol. Macromol.* 93 (2016) 789–804. <https://doi.org/10.1016/j.ijbiomac.2016.09.056>.
- [3] D. Saha, S. Bhattacharya, Hydrocolloids as thickening and gelling agents in food: A critical review, *J. Food Sci. Technol.* 47 (2010) 587–597. <https://doi.org/10.1007/s13197-010-0162-6>.
- [4] M. Oprea, S.I. Voicu, Recent advances in composites based on cellulose derivatives for biomedical applications, *Carbohydr. Polym.* 247 (2020) 116683. <https://doi.org/10.1016/j.carbpol.2020.116683>.
- [5] X. He, W. Lu, C. Sun, H. Khalesi, A. Mata, R. Andaleeb, Y. Fang, Cellulose and cellulose derivatives: Different colloidal states and food-related applications, *Carbohydr. Polym.* 255 (2021) 117334. <https://doi.org/10.1016/j.carbpol.2020.117334>.
- [6] C. Felgueiras, N.G. Azoia, C. Gonçalves, M. Gama, F. Dourado, Trends on the Cellulose-Based Textiles: Raw Materials and Technologies, *Front. Bioeng. Biotechnol.* 9 (2021) 1–20. <https://doi.org/10.3389/fbioe.2021.608826>.
- [7] M. Ardanuy, J. Claramunt, R.D. Toledo Filho, Cellulosic fiber reinforced cement-based composites: A review of recent research, *Constr. Build. Mater.* 79 (2015) 115–128. <https://doi.org/10.1016/j.conbuildmat.2015.01.035>.
- [8] L. Jiao, M. Su, L. Chen, Y. Wang, H. Zhu, H. Dai, Natural cellulose nanofibers as sustainable enhancers in construction cement, *PLoS One*. 11 (2016) 1–13. <https://doi.org/10.1371/journal.pone.0168422>.
- [9] S.J. Eichhorn, A. Dufresne, M. Aranguren, N.E. Marcovich, J.R. Capadona, S.J. Rowan, C. Weder, W. Thielemans, M. Roman, S. Renneckar, W. Gindl, S. Veigel, J. Keckes, H. Yano, K. Abe, M. Nogi, A.N. Nakagaito, A. Mangalam, J. Simonsen, A.S. Benight, A. Bismarck, L.A. Berglund, T. Peijs, Review: Current international research into cellulose nanofibres and nanocomposites, 2010. <https://doi.org/10.1007/s10853-009-3874-0>.
- [10] D. Tobjörk, R. Österbacka, Paper electronics, *Adv. Mater.* 23 (2011) 1935–1961. <https://doi.org/10.1002/adma.201004692>.
- [11] Y. Lin, D. Gritsenko, Q. Liu, X. Lu, J. Xu, Recent Advancements in Functionalized Paper-Based Electronics, *ACS Appl. Mater. Interfaces*. 8 (2016) 20501–20515. <https://doi.org/10.1021/acsami.6b04854>.
- [12] K. Dhali, M. Ghasemlou, F. Daver, P. Cass, B. Adhikari, A review of nanocellulose as a new material towards environmental sustainability, *Sci. Total Environ.* 775 (2021) 145871. <https://doi.org/10.1016/j.scitotenv.2021.145871>.
- [13] R.J. Moon, A. Martini, J. Nairn, J. Simonsen, J. Youngblood, Cellulose nanomaterials review: Structure, properties and nanocomposites, 2011. <https://doi.org/10.1039/c0cs00108b>.
- [14] Y. Habibi, L.A. Lucia, O.J. Rojas, Cellulose nanocrystals: Chemistry, self-assembly, and applications, *Chem. Rev.* 110 (2010) 3479–3500. <https://doi.org/10.1021/cr900339w>.
- [15] D. Klemm, E.D. Cranston, D. Fischer, M. Gama, S.A. Kedzior, D. Kralisch, F. Kramer, T. Kondo, T. Lindström, S. Nietzsche, K. Petzold-Welcke, F. Rauchfuß, Nanocellulose as a natural source for groundbreaking

- applications in materials science: Today's state, *Mater. Today*. 21 (2018) 720–748. <https://doi.org/10.1016/j.mattod.2018.02.001>.
- [16] D.C. Zemp, C.F. Schleussner, H.M.J. Barbosa, A. Rammig, Deforestation effects on Amazon forest resilience, *Geophys. Res. Lett.* 44 (2017) 6182–6190. <https://doi.org/10.1002/2017GL072955>.
- [17] L.Y. Khor, T. Feike, Economic sustainability of irrigation practices in arid cotton production, *Water Resour. Econ.* 20 (2017) 40–52. <https://doi.org/10.1016/j.wre.2017.10.004>.
- [18] O. Damette, P. Delacote, Unsustainable timber harvesting, deforestation and the role of certification, *Ecol. Econ.* 70 (2011) 1211–1219. <https://doi.org/10.1016/j.ecolecon.2011.01.025>.
- [19] F. Dourado, A.I. Fontão, M. Leal, A.C. Rodrigues, M. Gama, Process Modeling and Techno-Economic Evaluation of an Industrial Bacterial NanoCellulose Fermentation Process, in: M. Gama, F. Dourado, S. Bielecki (Eds.), *Bact. Nanocellulose - From Biotechnol. to Bio- Econ.* ., Elsevier B.V., 2016. <https://doi.org/https://doi.org/10.1016/B978-0-444-63458-0.00012-3>.
- [20] L. Stasiak, S. Błaejak, Acetic acid bacteria-perspectives of application in biotechnology-a review, *Polish J. Food Nutr. Sci.* 59 (2009) 17–23.
- [21] A.F. Jozala, R.A.N. Pértile, C.A. dos Santos, V. de Carvalho Santos-Ebinuma, M.M. Seckler, F.M. Gama, A. Pessoa, Bacterial cellulose production by *Gluconacetobacter xylinus* by employing alternative culture media, *Appl. Microbiol. Biotechnol.* 99 (2015) 1181–1190. <https://doi.org/10.1007/s00253-014-6232-3>.
- [22] M.U. Islam, M.W. Ullah, S. Khan, N. Shah, J.K. Park, Strategies for cost-effective and enhanced production of bacterial cellulose, *Int. J. Biol. Macromol.* 102 (2017) 1166–1173. <https://doi.org/10.1016/j.ijbiomac.2017.04.110>.
- [23] K. Ludwicka, M. Jedrzejczak-Krzepkowska, K. Kubiak, M. Kolodziejczyk, T. Pankiewicz, S. Bielecki, Medical and Cosmetic Applications of Bacterial NanoCellulose, in: M. Gama, F. Dourado, S. Bielecki (Eds.), *Bact. Nanocellulose - From Biotechnol. to Bio-Economy*, Elsevier B.V., 2016: pp. 145–165.
- [24] H.G. de Oliveira Barud, R.R. da Silva, H. da Silva Barud, A. Tercjak, J. Gutierrez, W.R. Lustri, O.B. de Oliveira, S.J.L. Ribeiro, A multipurpose natural and renewable polymer in medical applications: Bacterial cellulose, *Carbohydr. Polym.* 153 (2016) 406–420. <https://doi.org/10.1016/j.carbpol.2016.07.059>.
- [25] H. Ullah, H.A. Santos, T. Khan, Applications of bacterial cellulose in food, cosmetics and drug delivery, *Cellulose*. 23 (2016) 2291–2314. <https://doi.org/10.1007/s10570-016-0986-y>.
- [26] F. Dourado, M. Leal, D. Martins, A. Fontão, A. Cristina Rodrigues, M. Gama, Celluloses as Food Ingredients/Additives: Is There a Room for BNC?, in: M. Gama, F. Dourado, S. Bielecki (Eds.), *Bact. Nanocellulose From Biotechnol. to Bio-Economy*, Elsevier B.V., 2016: pp. 123–133. <https://doi.org/10.1016/B978-0-444-63458-0.00007-X>.
- [27] Z. Shi, Y. Zhang, G.O. Phillips, G. Yang, Utilization of bacterial cellulose in food, *Food Hydrocoll.* 35 (2014) 539–545. <https://doi.org/10.1016/j.foodhyd.2013.07.012>.

Chapter 2

Literature Review

This chapter provides a state-of-the-art review on the subject of the present thesis. Initially is presented a brief introduction to cellulosic materials and their general features. Emphasis is then given to bacterial cellulose by referring some relevant aspects of its biosynthesis and pointing out its distinctive characteristics in relation to other cellulose particles. Next are described the mechanisms of stabilization of heterogeneous systems by solid particles (Pickering stabilization); the particular features that make BC suitable for Pickering stabilization are discussed in more detail. Finally are presented some examples of the already studied applications of BC fibres, specifically within the food and cosmetic areas.

2.1 - INTRODUCTION TO CELLULOSE MATERIALS

Cellulose is the most abundant biopolymer on earth, produced by plants, algae, some bacterial species and even an animal species, tunicates. In plants and algae, it is present within the cell wall, where it plays an important structural role; in tunicates and bacteria it acts as an external protective coat. The actual most significant and abundant sources of cellulose are wood and plants such as cotton, flax, ramie, wheat, and others [1–3].

Cellulose is a high molecular weight linear homopolymer of glucose ($C_6H_{12}O_6$). The polymeric chemical structure can be written as $(C_6H_{10}O_5)_n$, since cellulose is composed of anhydro-D-glucose (more specifically anhydro-D-glucopyranose) units linked together through β -1,4 glycosidic bonds. This means that one oxygen atom is both covalently bonded to the C1 of one glucose residue and to the C4 of the following one, being each single glucopyranose unit rotated 180° relative to the adjacent units. Thus cellobiose, a glucose dimer, is the repeating chemical unit in the structure. The degree of polymerization (DP), i.e., the number of glucose units, is used to characterize the size of the cellulose chains. Besides the covalent bonds, there are intra-chain hydrogen bonding interactions between adjacent molecules that stabilize the linear configuration, and inter-chain hydrogen bonds that result in organized chain assemblies [1,4–6]. The structure of a single cellulose chain is represented in Figure 2.1.

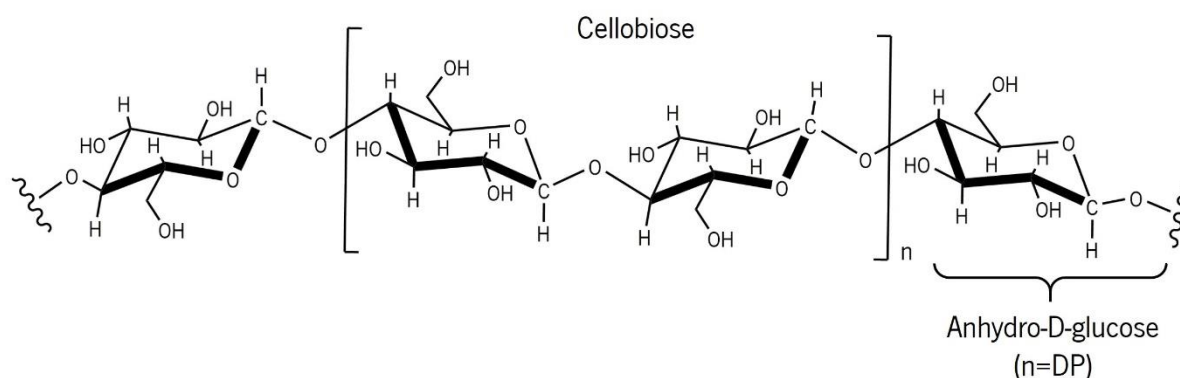


Figure 2.1 – Structure of a single cellulose chain, showing cellobiose as the repeating unit and the number of glucose residues as the degree of polymerization.

Cellulose biosynthesis occurs in enzymatic complexes located on the cell membrane, called terminal complexes (TC). Each TC has several subunits with multiple catalytic sites where single cellulose chains are polymerized, and further aggregate and crystallize. Different cellulose-synthesizing organisms or species have different TC configurations, which results in varied fibril architectures (despite the chains chemical similarity) and ultimately impacts the material's morphology. In a general way, each TC subunit

secretes multiple chains bonded together in ordered sheets by van der Waals forces; these sheets assemble in elementary fibrils within the TC by inter-chain hydrogen bonds; several elementary fibrils aggregate in microfibrils, and these can further organize in more complex fibre structures [1,4,7]. Figure 2.2-A shows an example of the organization of cellulose molecules in elementary fibrils, microfibrils and fibres.

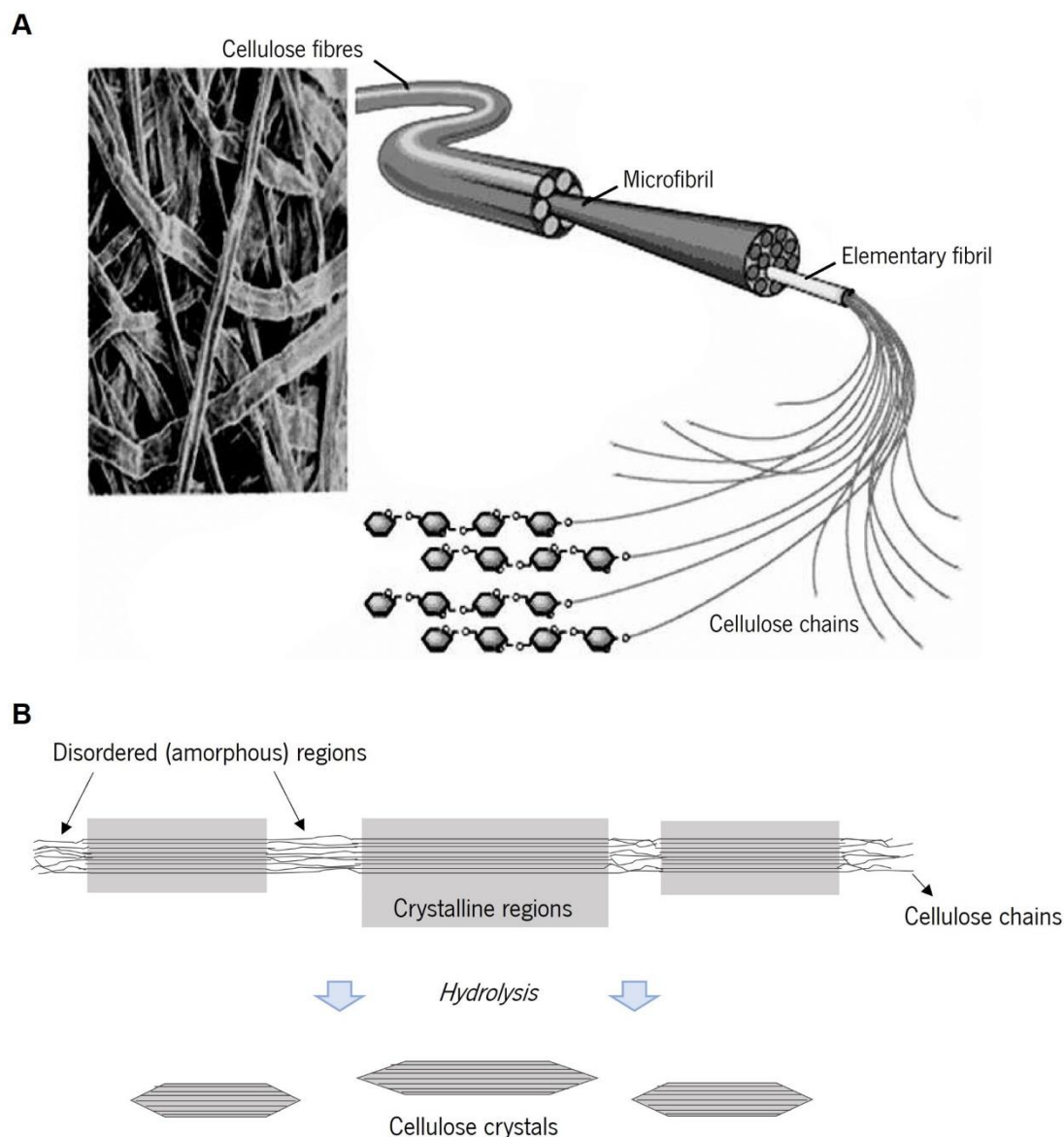


Figure 2.2 – (A) Schematic example of the organization of cellulose molecules into elementary fibrils, microfibrils and fibres (adapted from [8]); (B) representation of crystalline and amorphous regions in cellulose fibrils and result after hydrolysis.

Although this molecular organization results in an overall crystalline structure, in some regions the fibrils are disordered – amorphous regions. Crystalline and amorphous regions appear alternated along the fibril length, as depicted in Figure 2.2-B. The crystallinity of cellulose, like the DP, is highly dependent on

the source.

Cellulose particles with different sizes, morphology, and crystallinity can be obtained, depending on the way the raw material is processed. In the case of wood or plant biomass, an initial pre-treatment is needed to remove hemicellulose and lignin. Cellulose fibres purified from wood and plant have the largest particles, with low crystallinity, but can be processed into several different types of smaller particles. Examples of different cellulose particles are shown in Figure 2.3.

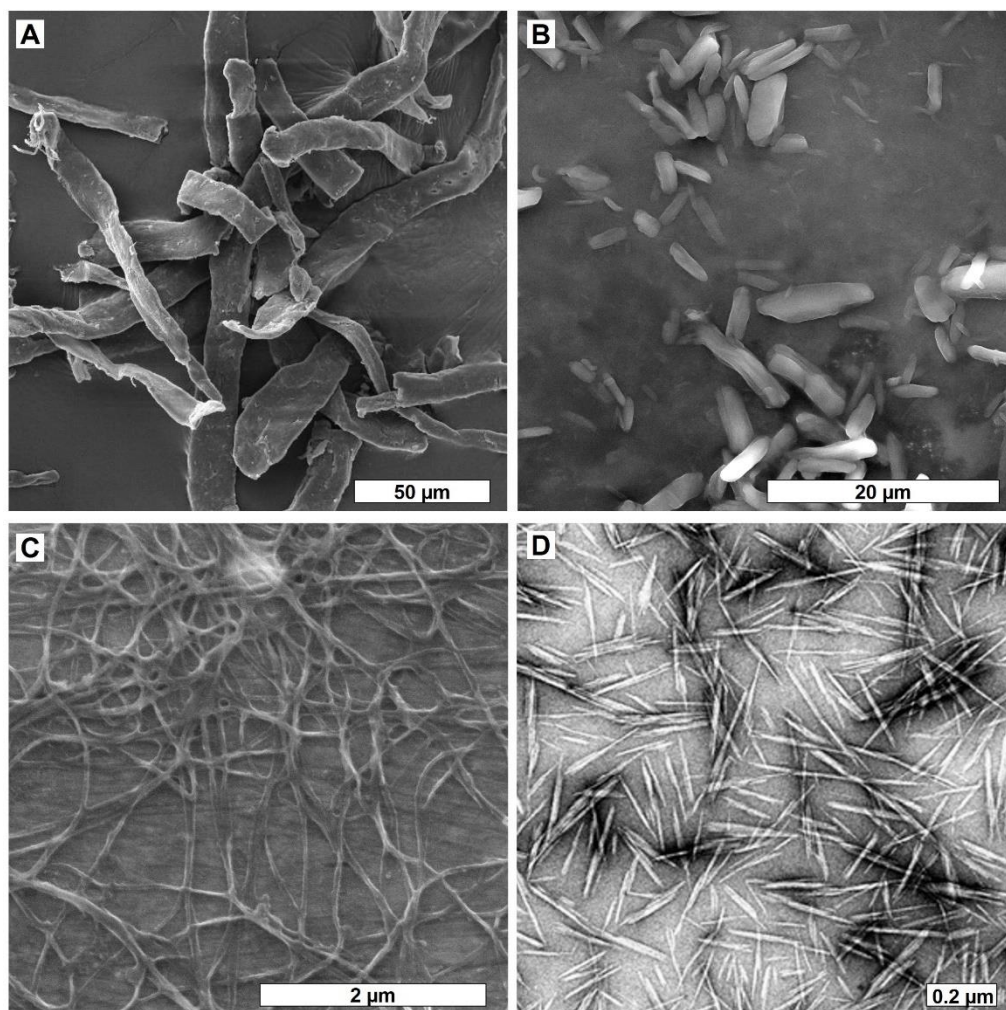


Figure 2.3 – Examples of different cellulose particles. Scanning electron microscope images of (A) wood pulp fibres (retrieved from [11]), (B) hydrocolloidal microcrystalline cellulose Avicel CM2159, (C) bacterial cellulose from *K. xylinus*, and (D) transmission electron micrograph of ramie cellulose nanocrystals (retrieved from [12]).

When wood pulp is refined through mechanical processes, such as high-pressure homogenization (HPH), fibre cleavage happens along the longitudinal axis and it is possible to separate the microfibrils, yielding micro-fibrillated cellulose (MFC, 10 – 100 nm wide, 0.5 – 10's µm length); alternatively, by removing the amorphous segments via acid hydrolysis, microcrystalline cellulose (MCC, 10–50 µm wide, 10 – 50 µm

in length) is obtained, containing mainly crystalline regions. Despite the denomination, MFC is in fact considered a nanocellulose since it has nanoscale width, and it is also extracted from algae and produced by bacteria. A more intensive disintegration of pulps or MFC into the elementary fibrils produces nanofibrillated cellulose (NFC, 4 - 20 nm wide, 500 - 2000 nm in length); and finally, cellulose nanocrystals (CNC, 3 - 50 nm wide, 50 - 4000 nm in length) can be isolated from all the above-mentioned materials by acid hydrolysis. CNCs can also be produced from algae, tunicate and bacterial cellulose [1,2,4].

It must be noticed that the terminology for cellulose particles is not normalized the same way in all reports. For example, the term cellulose nanofibrils (CNF) is often employed instead of NFC; the terms NFC and MFC are used interchangeably since both share nanoscale width; and “cellulose nanowhiskers” is used as synonym of CNCs. Also, the sizes presented are merely indicative since they are highly dependent on the source and the applied treatments.

Among the above referred cellulose materials, nanocelluloses – micro or nanofibrils obtained by mechanical processes, nanocrystals extracted by hydrolysis, and bacterial cellulose produced by fermentation – have attracted particular interest. Having at least one dimension in the nanoscale, these materials exhibit specific properties such as high aspect ratio (ratio between length and width) and high surface area for interaction (with water, chemical compounds, particles or cells). BC is a particularly interesting source of nanocellulose because it consists of pure microfibrils with high crystallinity and aspect ratio, not requiring much refinement or treatment to be fully functional in diverse applications [2,6,9,10].

2.2 - BC BIOSYNTHESIS AND PRODUCTION

Bacterial cellulose - also referred to as bacterial nanocellulose, microbial cellulose or biocellulose - is a sophisticated material produced biotechnologically in the pure state by different microorganisms, but most efficiently by acetic acid bacteria of the genus *Komagataeibacter* (formerly designated *Gluconacetobacter*). Acetic acid bacteria are strict anaerobes, capable of growing in acidic and alcoholic media. They can metabolize and use carbon sources such as ethanol, sugars (mainly glucose, but also arabinose, fructose, galactose, mannose, ribose and xylose) and organic acids (such as acetic acid). *K. xylinus* in particular is very well known for its high cellulose productivity, *K. hansenii* being also frequently used [6,13–15].

During the fermentation process, bacterial cells secrete cellulose elementary fibrils from synthetic sites

along their longitudinal axis (2 - 6 nm in width), which assemble in microfibrils outside the cell (40 - 80 nm in width). Due to the bacteria movement during growth in the culture medium, the cellulose microfibrils twist and entangle, forming a polymer network that entraps water and supports bacterial growth. In the macroscopic scale, a gel-like membrane is visible in the air – liquid interface [13,14,16].

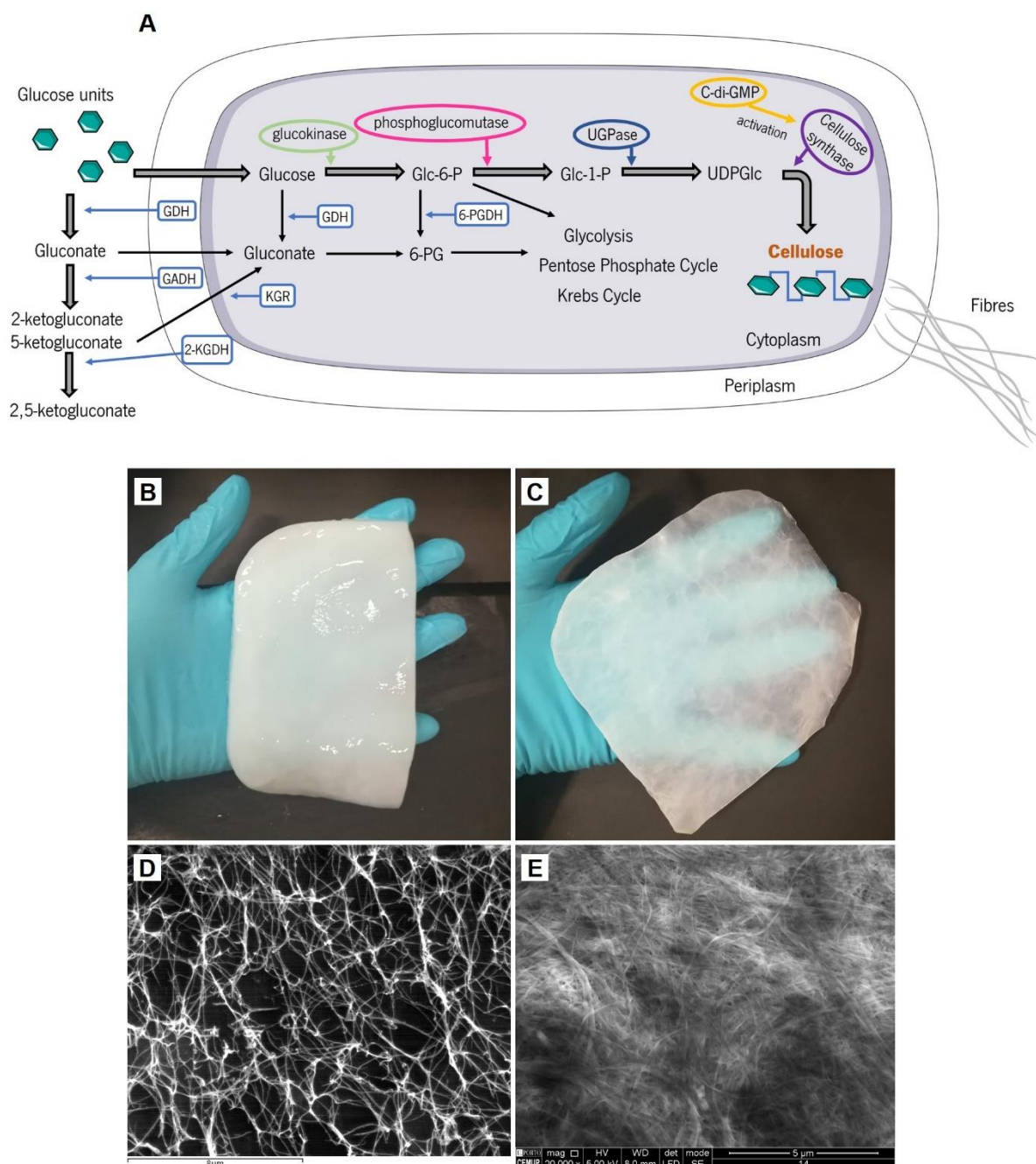


Figure 2.4 - (A) Schematic illustration of the metabolic pathways of cellulose production in bacteria (adapted from [13]); bacterial cellulose membranes in (B) wet and (C) dry state, and respective scanning electron micrographs (D and E).

After being washed and purified, this pellicle or membrane is composed of pure cellulose and up to 99 % water [6,17,18]. Figure 2.4 presents a schematic of cellulose biosynthesis in bacteria, with the major metabolic pathways, and sample photographs of wet and dry membranes.

It has been suggested that bacteria produce this cellulose pellicle as a protective coat, against UV light and as a physical barrier against other microorganisms, but also to facilitate access to oxygen (present in higher concentration at the surface of the culture medium) and nutrients (higher availability inside the membrane, due to its adsorptive properties) [1,13,14].

Contrarily to wood and plant cellulose, BC is produced free of hemicellulose, lignin and other polymers, saving steps and chemical reagents in the purification operation. However, wood and plant biomass is abundant and cheap. The large scale production of BC at low cost, allowing market competition, has been approached in several ways: using agro-industrial wastes as a carbon source, strain selection and genetic manipulation to improve productivity and BC yield, and development of new bioreactors to allow continuous production – with limited success so far [13,19,20].

Typically, at laboratory scale, BC-producing bacteria of the genus *Komagataeibacter* are cultivated in synthetic Hestrin-Schramm (HS) medium (containing glucose, peptone, yeast extract, disodium phosphate and citric acid) [21]. However, for large-scale production, pure chemicals are a costly solution and many authors have found nutrient-rich alternatives amongst agro-industrial by-products and wastes. Substrates such as glycerol and sunflower seed residues from biodiesel production, flour hydrolysates from confectionary industries [22], rotten or leftover fruits, milk whey [23–25], sugarcane molasses, corn steep liquor [26], and even recycled paper sludge [27], have been employed successfully and show the variety of otherwise waste products that can be used in a cost-contained production of BC. Some of these alternative substrates contain a variety of sugars, proteins, salts and vitamins that is hard and expensive to replicate in synthetic media and have, in many cases, been found to generate much higher yields and productivities than standard HS medium. The use of different carbon sources, or different substrate media in general, can also translate in different physicochemical and textural BC properties [17,28].

The search for new cellulose-producing bacterial strains is still in progress, with recent examples such as the isolation of *Komagataeibacter* sp. strain W1 from fermented vinegar and its gene analysis [29], isolation of *K. rhaeticus* K3 [30] and *K. xylinus* K2G30 [31] from Kombucha tea, and of *K. saccharivorans* strains BC1 and MD1 from rotten grapes and fermented beverages, respectively [24,32]. Sequencing and analysis of the naturally occurring strains' genomes allows to understand the factors influencing BC metabolism and productivity, generating new tools for genetic improvements. Enhancement of production through genetic engineering/modification of bacterial strains has been attempted by several authors, as

well as the production of BC from alternative substrates or with tailored properties [13,33]. Some examples include the enhancement of cellulose production in genetically modified *K. xylinus* BPR2001 [34], the development of genetic tools to manipulate BC production in a strain of *K. rhaeticus* that can grow in low-cost, low-nitrogen media [35], BC production from sweet potato pulp using an engineered *K. xylinus* BPR2001 mutant with improved glucose conversion [36], and production of BC in agitated culture using a stable mutant *Escherichia coli* genetically modified with high-yield *K. hansenii* ATCC 53582 genes [37].

BC biosynthesis is typically carried out in static culture, where the formed membrane (Figure 2.4), given enough time to develop, adopts the shape of the vessel. The use of templates allows to obtain different 3D shaped hydrogels for specific uses, such as blood vessel substitutes, prosthetics and heart valves for biomedicine. Another strategy, employed to improve the productivity and/or lower the costs of an up-scaled BC production, relies on the use of continuous or semi-continuous bioreactors, decreasing the requirements for space, time and labour of batch fermentations, as well as allowing for a tighter control of production and characteristics of the final product [6,13,38].

BC production in agitated conditions or stirred tanks is faster, generally taking 2 to 4 days (whereas static cultures take 2 to 4 weeks); however, small flocs or spherical particles are produced instead of a continuous membrane, and the volumetric yields are usually lower. Besides, agitation promotes the growth of mutant non-cellulose producing strains [6,13,20,39]. Taking this into account, new bioreactors try to incorporate an automated and continuous production with the benefits of static cultivation. Examples of this are: rotating disk reactors, where the motion allows for contact of the bacteria with both air and nutrient media, alternately; aerosol bioreactors, where medium and oxygen can be sprayed on top of the growing culture; membrane bioreactors with large interfacial areas that allow diffusion of nutrients and oxygen to static BC pellicles [13,19]; the Horizontal Lift reactor (HoLiR technology), where the BC is produced in a long horizontal tank being lifted from the growth medium and extracted at one end, as it reaches the desired thickness, creating a continuous mantle [40]; and the Mobile Matrix Reservoir Technology (MMR Tech), where a template is dipped in culture medium and lifted up in an alternate way, allowing a new BC layer to be synthesized around the template in every cycle in contact with air (not depending on the diffusion of oxygen through the liquid medium) [38].

The large-scale production of BC in an economically competitive manner has raised great interest, and has been the subject of a thorough software-assisted process simulation and techno-economic evaluation, where the authors from the Minho University concluded that it is possible to devise an economically feasible process, although the final product's cost would restrict its market to high-value niches [41].

Later, the same group reported a study on the treatment of the BC production wastewaters - which contain high organic loads from the culture media and bacteria – by anaerobic digestion in an Upflow Anaerobic Sludge Blanket reactor and their valorisation to produce biogas. The authors reported that low-cost media have the drawback of resulting in wastewaters with higher solid contents and organic loads, thus requiring more demanding and costly processing before being discharged [42].

Large-scale production of BC as a foodstuff is common in some Asian countries, where BC is consumed as *nata de coco*, a traditional desert fermented from coconut water. Nowadays, production of more advanced BC products that meet quality requirements for specific applications (for instance, medical and cosmetic applications) is also taking place in a few companies, in pilot or semi-industrial facilities. Some multinational companies are also commercializing BC-based hydrocolloids for use in liquid detergents and personal care products [6,20,43,44].

2.3 - BC'S PROPERTIES AND CHARACTERIZATION

BC shares many characteristics with other celluloses but has also particular features that make it a unique and exceptional material. One of the major differences resides in its morphology: BC is organized in elementary fibrils with a lateral size of 6 nm to 10 nm, which assemble into ribbon-shaped microfibrils with less than 100 nm wide and several micrometres in length [1,6]. Accurately measuring untreated and isolated BC fibres is not an easy task, since they are produced as a mesh of interconnected fibres and can easily interact with each other, aggregating in bundles after a wet-grinding or homogenization process. However, single BC fibres have been prepared by aqueous counter collision, displaying around 30 nm in width and 3 μm in length. The high length to width relation results in a high aspect ratio, in the range of 100, and a high specific surface area, as is common in nanomaterials [45]. The crystallinity index of BC fibres depends on the bacterial strain and culture medium conditions, but is still among the highest of nanocelluloses: common values are above 70 % [45–47] and can reach over 90 % [24].

When a BC sheet is dried, the fibres collapse in organized and stratified layers. The densely packed nanometre-thick fibres make dry BC sheets optically transparent (because of the absence of inter-fibre small voids that avoid light scattering). A dry BC membrane with a thickness of 40 μm has an average specular transmittance of 60 % in the visible region of the spectrum, and transparent composites of BC and resins with larger thickness have been developed [48–51]. BC fibres also shows excellent mechanical properties when compared to plant cellulose, with high values of Young's modulus, estimated at 114 GPa for single fibres and up to 138 GPa for only crystalline regions (cellulose I), an estimated tensile strength

of 2 GPa and a density of 1.6 g/cm^3 , values comparable to those of aramid fibres (e.g., Kevlar) [1,3,52–55]. Furthermore, a coefficient of thermal expansion (CTE) as low as $1 \times 10^{-7} \text{ }^\circ\text{C}^{-1}$ in the axial direction has been ascribed to BC fibres, which translates in high dimensional stability [1,49,56]. BC films also shows a relatively smooth surface even without surface treatments, after a simple drying process by evaporation (with or without pressing). Together, these are important factors for large-scale manufacturing and deposition processes, and for applications such as optoelectronic devices [48,56].

The thermal properties and stability of cellulosic materials are usually assessed by thermogravimetric analysis (TGA), which measures degradation (weight loss) as a function of temperature for a given heating rate. Typical TGA spectra of dry BC membranes show a first small mass loss around $100 \text{ }^\circ\text{C}$ due to the evaporation of residual moisture, while the actual sample decomposes around $300 \text{ }^\circ\text{C}$. This is the maximum temperature for processing BC, while for traditional paper is approximately $200 \text{ }^\circ\text{C}$, owing to impurities (hemicellulose and lignin) that degrade at lower temperatures [1,48].

Cellulose is insoluble in water, but at the same time is highly hydrophilic. BC membranes in particular can retain large amounts of water: in other words, they have a high water holding capacity, a parameter that is also proportional to the surface area of the fibres and porosity of the mesh. BC membranes have been produced with water holding capacity superior to 99 % (mass of water relatively to the mass of dry BC) [14,17,22,57].

Cellulose insolubility in water can also be explained in part by its amphiphilicity, provided by the crystalline nature of the cellulose molecule. In the crystal structure, which is faceted, there are hydrophobic edge planes (located at the corners of the cellulosic crystals) composed only of $-\text{CH}$, while the other planes (thickness and width of the crystal) are hydrophilic due to the high density of $-\text{OH}$ groups. Despite being overall a hydrophilic material, the less significant hydrophobic domains exposing non-polar groups at the surface result in an amphiphilic character, and greatly contribute for the Pickering stabilization properties (discussed in detail in subchapter 2.4) [5,57–59]. Figure 2.5 shows the hydrophilic and hydrophobic parts of a cellulose molecule (structural anisotropy), and the arrangement into a crystalline structure exposing hydrophilic and hydrophobic planes.

Cellulose is also an uncharged molecule, and consequently its particles have a high tendency to aggregate. Its neutrality and water-insolubility may pose some obstacles when trying to obtain stable particle suspensions, particularly after drying. The properties of BC's membranes and fibres, namely their high water retention and swelling, are mostly lost upon drying. As water evaporates from the voids, the fine BC fibres come closer, interact via inter-molecule hydrogen bonding and aggregate irreversibly due to cocrystallization mechanism of adjacent fibres. These interactions are not broken upon resuspension

in water unless there is a significant energy input. This results in a so called hornified cellulose, a very aggregated material with no swelling ability [2,60].

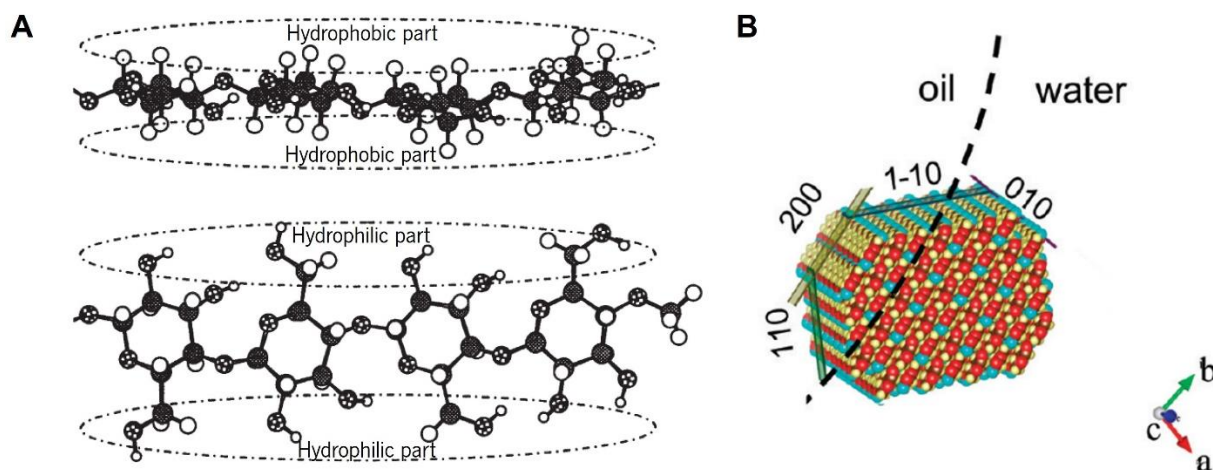


Figure 2.5 – Amphiphilic character of cellulose: (A) side and front view of a cellulose chain, with dashed lines marking the hydrophobic and hydrophilic parts of the molecule (adapted from [58]); (B) schematic representation of the transverse section of a cellulose nanocrystal (Iβ allomorph) at the oil/water interface, exposing the hydrophobic edge plane (200) to the oil phase (retrieved from [59]).

The most usual approach to prevent aggregation and hornification relies on creating a steric and/or electrostatic barrier between the cellulose particles. This can be achieved either by acid hydrolysis, which imparts negative surface charge to the cellulose itself, or by mixing with an additive, such as charged polysaccharides. As an example, the addition of carboxymethyl cellulose (CMC) to MCC before drying is a common practice in industry, in the production of hydrocolloidal cellulose products. The production method of CNCs (i.e., acid hydrolysis) also prevents their aggregation. These strategies contribute to a better dispersion and colloidal stability of the cellulosic particles, as well as improving rehydration and redispersion in liquid media after a drying process [2,61–65]. Drying processes like freeze-drying and spray-drying may also prevent hornification to some extent, but alone cannot prevent aggregation of the dried particles placed back in aqueous media [47,66,67].

Cellulose fibres can be made water-soluble by chemical modification of the surface hydroxyl groups, introducing other functional groups. Some modified (or derivatized) hydrosoluble celluloses include CMC, cellulose acetate (CA), hydroxyethyl cellulose (HEC), hydroxypropyl methyl cellulose (HPMC), among others [68–72]. These cellulose derivatives are used in composites, biomedical and food applications, and BC derivatives in particular have also been produced and reported [73,74].

In fact, the high availability of reactive hydroxyl groups on BC fibres opens the possibility for several types

of chemical modifications. Some examples include surface hydrophobization with organic acids [75], surface acetylation of BC membranes for controlled drug delivery systems [76], surface modification with recombinant proteins to improve cell adhesion [77], and with antibacterial drugs for wound dressings [78].

As an alternative to chemical modifications, the interconnected fibre networks of BC membranes present a highly porous environment suitable for the incorporation of polymers, hydrophilic drugs or drug-loaded particles, for the *in situ* production of metal nanoparticles, and for the easy development of cellulose reinforced composite materials [55,56,79–84]. Incorporation of some compounds of interest can even be done during biosynthesis for modulating the BC membrane's structure and mechanical properties [85,86].

Functional topographies or specific surface patterns may be designed using an appropriate mould during biosynthesis [87–89], or after production by laser perforation [90–92]. It is also possible to produce free-standing three-dimensional BC structures, such as spheres or lens, by tuning the hydrophilicity/hydrophobicity of the culturing surface [93].

A vast number of the reported composites and structures were developed in the scope of medical applications, and this stems from a very important characteristic of BC: its biocompatibility. This highly pure, high-water content and inert material presents no toxic effects on living tissues, and an insignificant foreign body reaction *in vivo* [44,94,95]. Furthermore, the BC fibres can be oxidized or impregnated with cellulases to promote degradation and clearance from inside the body [96–98]. Under environmental conditions, BC is biodegradable in soil and sludge by the action of cellulase producing microorganisms [99,100]. Consequently, BC benefits from the Generally Recognized as Safe (GRAS) status by the United States Food and Drug Administration (FDA) [20,38,101].

All these properties make BC an outstanding and multipurpose biomaterial, presenting a more sustainable and eco-friendly alternative to celluloses of plant origin.

2.4 - STABILIZATION OF HETEROGENEOUS SYSTEMS

Heterogeneous systems are thermodynamically metastable mixtures of two (or more) immiscible phases. Biphasic systems can be categorized as liquid-in-liquid, gas-in-liquid or solid-in-liquid dispersions (or suspensions). Liquid-in-liquid dispersions are commonly known as emulsions; in turn, gas-in-liquid dispersions are denominated foams. Emulsions are obtained from at least two immiscible liquids, when they are mixed together and one of the phases arranges in small droplets (internal phase) dispersed in

the other continuous outer phase. Generally, we speak of oil-in-water (o/w) emulsions, in which the oil is the dispersed/internal phase, and the water is the continuous phase, or water-in-oil (w/o) emulsions, in which the opposite occurs. This sort of mixture is unstable without the addition of an emulsifying agent of some kind. Conventionally, to produce and stabilize an emulsion, surfactant molecules are added in order to lower the surface tension between the immiscible liquid phases – in other words, to reduce the energy of the liquid-liquid interface. Surfactants arrange in the oil-water interface because they are amphiphilic molecules, meaning they have both hydrophilic and hydrophobic moieties (with affinity for water and oil phases, respectively). They stabilize the emulsion by preventing coalescence (merging) of the dispersed phase droplets and consequent aggregation and phase separation [102,103]. Tendency to form oil-in-water or water-in-oil emulsions is traditionally related to the surfactant's Hydrophile-Lipophile Balance (HLB) number [104].

Similarly to emulsions, foams are dispersions of gas bubbles in a liquid continuous phase. The tension at the air-water interface is higher, also because of the large density difference between the two fluids involved, which makes this system even less stable than emulsions [102].

A stable system is one where, in equilibrium, the internal phase is homogeneously (or colloidally) dispersed, and this state is maintained over time and under environmental changes; it is also a system in which the stabilizing agents are able to counteract and prevent thermodynamic phenomena that would ultimately lead to the separation of phases, termed “breaking” of the system. The mechanisms of instability (Figure 2.6) affecting biphasic systems are gravitational separation, coalescence, flocculation and Ostwald ripening. Destabilization by the action of gravity can either be sedimentation of the disperse phase when it has higher density than the continuous phase, or creaming when the opposite occurs. Creaming is associated with oi-in-water emulsions, since oil is less dense and has tendency to ascend, forming a top layer; sedimentation occurs in water-in-oil emulsions, when water deposits in a bottom layer. Ostwald ripening is the mass diffusion of the disperse phase components from smaller to larger droplets, due to the pressure differences (Laplace pressure). This relates, ultimately, to the effect of the curvature on the energy of the molecules present in the curved surface, which is higher the smaller the radius of the droplet [105,106]. Flocculation, sometimes also referred as coagulation or aggregation, happens because of dispersive droplet-droplet interactions, when Van der Waals attractive forces dominate over electrostatic repulsions, according to the DLVO theory. According to this theory, coagulation and flocculation are in fact distinguishable according to the stability of the aggregates: the former relies on a low-distance primary minimum of energy between the particles, hence more stable, requiring a high

amount of energy to overcome; the later relies on a secondary minimum of energy, where particles can be separated with a low energy input (for example, agitation) [107,108].

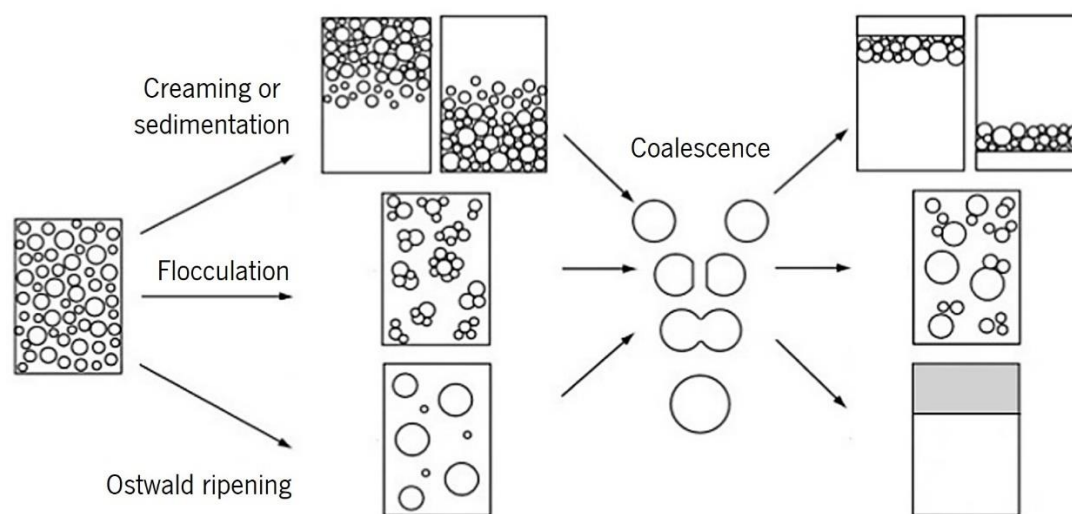


Figure 2.6 – Representation of the destabilization mechanisms of emulsion systems (adapted from [109]).

All of the above-mentioned phenomena can increase the risk of coalescence, which is the merging of adjacent or contacting droplets into larger ones, resulting in a smaller surface area. Coalescence can also occur in the absence of a steric barrier separating the droplets. It is further favoured when the concentration of stabilizing agent is too low to cover/saturate the interface between phases, leading to the necessity of an interfacial rearrangement. Partially covered droplets may also undergo bridging flocculation by sharing the adsorbed stabilizing agent without coalescing. These mechanisms lead to the accumulation of the dispersed phase until it merges and separates from the continuous phase, and it's the role of a stabilizer or emulsifier to prevent them. Smaller droplets with some surface charge and a monodisperse size distribution are less affected by these mechanisms, thus more stable [109–112].

2.4.1 - Particle-stabilized systems: Pickering emulsions and foams

In the past few years, there has been a shift toward studying materials of biological origin for the stabilization of foam and emulsion systems for food, cosmetic and drug delivery applications. Biosurfactants, for example, are less toxic, more biodegradable and can act in a wider range of conditions. The biotechnological production process is more environmentally friendly, as compared to chemically produced surfactants, and industrial by-products can be used in the culture media [103]. On the other hand, particle-stabilized emulsions - known as Pickering emulsions - have also gained increasing interest.

Particles suitable for Pickering stabilization of emulsions and foams strongly and irreversibly adsorb at the interface, depending on their relative affinity for both phases. Organic solid particles, or more precisely biopolymers (polysaccharides, aromatic macromolecules and polypeptides), have been shown to be capable of stabilizing foams and emulsions: they exhibit surface activity at air–liquid and liquid–liquid interfaces [102]. These particles irreversibly adsorb at the interface and form a film (monolayer or multilayer) around the dispersed phase droplets, so they are necessarily smaller than the droplets. The solid particle coating at the droplets surface acts as a mechanical barrier, preventing coagulation and coalescence phenomena [104,112,113].

Size, morphology and affinity for each phase play important roles in the organization of solid particles in the interface between immiscible phases. Pickering stabilization occurs under partial wetting conditions of the solid colloidal particles, meaning at least a small degree of amphiphilicity [112]. The tendency of solid particles to form o/w or w/o emulsions, foams or aerosols (water-in-air dispersions) depends on their wettability, measured by contact angle as depicted in Figure 2.7. Hydrophilic particles are mostly wet by water and have a water contact angle inferior to 90°; on the contrary, hydrophobic ones will reside mostly in the oil or air phase, originating a contact angle greater than 90°. The particle layer around the disperse phase droplets curves in a way that the larger area of the particle surface remains on the external side, facing mostly the phase to which it has higher affinity, originating an air-in-water or oil-in-water system when particles are hydrophilic (<90°) and water-in-air or water-in-oil systems when are hydrophobic (>90°). However, it must be noted that very hydrophilic or very hydrophobic particles might give rise to very large drops, more prone to coalescence and loss of stability, or might be completely dispersed in one of the phases instead of adsorbed at the interface, not leading to emulsification at all [102,104,112]. Since foams are a more challenging system, particles capable of stabilizing emulsions may not have the capacity to stabilize foams.

Theoretically, the free energy of spontaneous desorption - the energy required to remove the particle from the interface - for a spherical particle, is given by equation 1:

$$\Delta G_d = \pi r^2 \gamma_{1,2} (1 - |\cos \theta|)^2 \quad (\text{eq. 1})$$

where r is the particle radius, $\gamma_{1,2}$ is the interfacial tension between the two phases and θ is the contact angle of the particle (relatively to the aqueous phase) [102,104,111]. This energy - that has a maximum for an angle of 90° - is always much larger than the thermal energy, and that is the reason why solid particles adsorption at an interface between two immiscible liquids becomes irreversible in practice. According to the equation, larger particles will be more strongly adsorbed since the energy needed for

desorption is higher, but even nanoparticles have free energy of desorption higher than the thermal energy. This equation only applies to particles small enough to neglect the effect of gravity (under 1 μm in diameter). Cellulose materials are normally found as fibres or crystals, so the relationship needs to be adapted for the morphology [112,114].

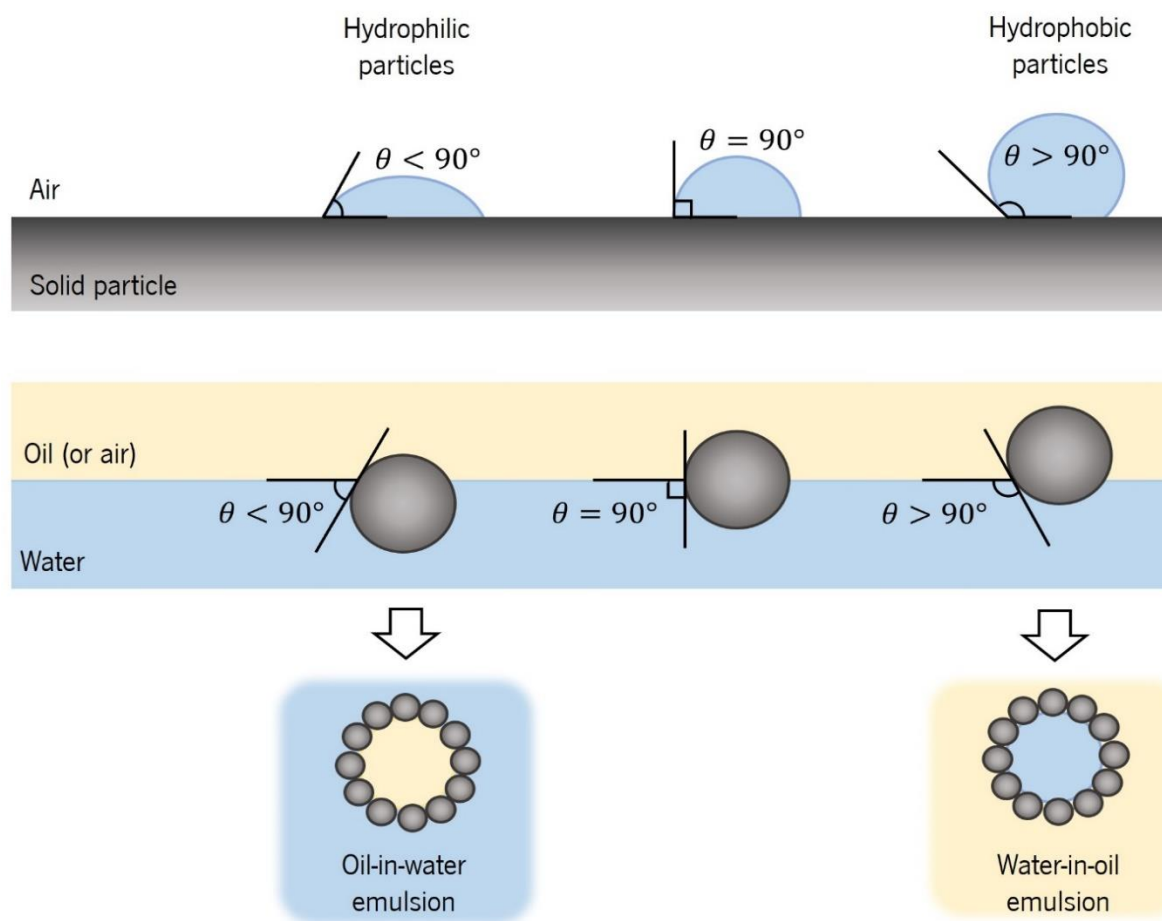


Figure 2.7 – Wettability of a solid surface, as measured by contact angle with a water drop (top); position of a spherical solid particle at a planar oil/water (or air/water) interface, according to its contact angle, and corresponding position at a curved interface resulting in oil-in-water or water-in-oil emulsions (bottom).

Given the irreversible nature of adsorption to the interface, solid particles stabilized systems show a high resistance to coalescence, even with a very small concentration of particles – only enough to cover the interfacial area, even if partially. The amount of solid particles will also influence the interfacial area of the system: increasing the concentration also increases the droplets surface area that can be covered, originating smaller and more stable droplets. A further increase in concentration, over the limit of the interfacial area, will result in the dispersion and accumulation of the solid particles in the continuous phase, which may further add to the stabilization through steric effects, as discussed ahead [104,112].

For o/w emulsions, Cherhal et al. [115] also observed that droplet size is dependent on the amount of oil and concentration of solid particles needed to cover the resultant interfacial area; after the irreversible adsorption takes place, a further increase in the water content does not compromise stability. Besides concentration, particle size is also directly correlated to Pickering emulsion droplet size. Smaller particles originate smaller emulsion droplet sizes, which ultimately translates in higher stability with regards to the action of gravity. Niu et al. [116] prepared Pickering o/w emulsions with CNCs produced from increasing hydrolysis durations. They observed that the morphology of the emulsion droplets became much more uniform and less flocculation occurred for the particles obtained using longer hydrolysis time, attributing this to the higher number of smaller particles, which could then cover a larger surface area.

Besides the stabilization attained by adsorption to the interface of two fluids, solid particles have yet another mechanism of stabilization: structuring the continuous phase. When the interfacial area of a biphasic system is completely covered, and an excess amount of particles remains in the continuous phase, they interact with each other and can form a three-dimensional structure. The viscosity of the continuous phase increases, providing higher support to the disperse phase droplets, reducing coalescence and creaming. Thickening of the emulsions and foams slows down the processes that lead to phase separation, improving long-time storage, an interesting outcome for some applications [102,104,112]. Consistency and texture are advantages proceeding from the increase in viscosity, namely regarding uses in food and cosmetic industries.

2.4.2 - Cellulose particles as Pickering stabilizers

Solid cellulosic particles, in the form of nano- or micro- fibres or crystals, show capability to form Pickering emulsions and foams. Hydrocolloidal microcrystalline cellulose, from plant sources, is already widely used in food and cosmetic industry to regulate the stability, rheology and organoleptic properties of the formulations [117–119]. More recently, research has been focusing on the use of cellulose nanoparticles as stabilizers of biphasic systems, mainly emulsions. Nanocelluloses possess particular characteristics that suit appropriately for oil/water interface stabilization; at the same time, some other features must be controlled to ensure the best outcome.

The first important property of cellulose particles is their structural anisotropy leading to an amphiphilic character. As referred before, strictly hydrophilic materials would not be able to adsorb at the oil/water or air/water interface. Cellulose crystals are amphiphilic, since the smaller edge planes of the crystallites are richer in less polar domains (-CH), derived from the molecular alignment, resulting in a hydrophobic region; meanwhile, the larger planes are rich in polar groups (-OH) and bear hydrophilic character. This

means that a small area of the particles has affinity to oil (or air), while the largest area of the molecule is preferentially wetted by water ($CA < 90^\circ$), being suitable for systems with an aqueous continuous phase and a hydrophobic disperse phase such as oil or air [9,109,120].

Cellulose amphiphilicity has been used to explain its behaviour at interfaces and its stabilizing effects. The understanding of this property has also opened possibilities towards tuning the hydrophobicity of cellulose nanoparticles and better controlling their wettability [58,59]. Hydrophobization of cellulose nanoparticles can also be attained by surface modification, useful to produce water-in-oil emulsions [9,120,121].

The source of cellulose alone does not have a direct impact on the emulsification and stabilization properties, since native celluloses have a common crystal allomorph, cellulose I, with varying proportions of $I\alpha$ and $I\beta$ structures - BC is richer in $I\alpha$ (60 % and above), while wood and plant celluloses are richer in $I\beta$ [1,7,20,45,120]. On the other hand, the size, aspect ratio and surface charge of the particles, which depend on the source, crystallinity and extraction/purification processes, can influence their organization in the interface, their interaction in the continuous phase and therefore the stabilizing efficacy.

Being anisotropic particles with high aspect ratio, cellulose nanofibers and nanocrystals tend to one-dimensionality since the width and height can be negligible in comparison with the length [9]. This type of particles can organize in different orientations and interact with each other at the interface, creating a steric barrier even at low concentrations; plus, when the interface is mostly covered, the excess particles interact in the continuous phase forming self-assembled networks or gels. The interfacial area is also, in part, defined by the amount of particles available to cover it: a low concentration of particles can only effectively cover (even if partially) a small interfacial area, resulting in large droplets of oil; increasing particle concentration, it is possible to cover a larger area - higher number of smaller droplets. In general, this happens until a plateau where the increase in particle concentration no longer affects the droplet size, but instead the particles remain and accumulate in the continuous phase. In this case, a higher energy processing might further decrease the droplet size [122].

A decrease in the emulsion droplet size with increasing particle concentration has been observed for milled cellulose particles [123], CNCs obtained from wood [124] and cotton [115], and bacterial cellulose nanocrystals (BCNC) [63]. Cherhal et al. [115] emphasize not only the particle concentration in the emulsion, but also the oil/aqueous phase ratio and the amount of particles per volume of oil, since a higher oil/water volume ratio will also result in larger droplet sizes and need a higher concentration of particles for full stabilization of the interfacial area. These authors state that the parameters influencing the droplet sizes in oil-in-water emulsions are the amount of CNCs and the volume of oil to be dispersed,

while the volume of water has no effect. Li et al. [125], using bacterial cellulose nanofibrils (BCNF) also demonstrated that the emulsion droplet size has a direct correlation with the oil ratio, and is inversely proportional to the particle concentration. An increase in the hydrolysis time of CNCs' production, and consequent decrease in size, has also been correlated to smaller and more stable emulsion droplets [116,126].

When using particles of known dimensions, it is possible to calculate the percentage of surface coverage of the droplets. Kalashnikova et al. [127] showed that the aspect ratio of CNCs directly influences the coverage ratio and structure of oil-in-water emulsions. High coverage of the droplets surface, over 80 %, was obtained with low aspect ratio CNCs at low concentration, and the droplets remained individualized in emulsions with increasing particle concentrations. On the other hand, high aspect ratio CNCs resulted in lower surface coverage, around 40 %, and increasing concentrations promoted a particle networking system in the continuous phase. The droplet coverage obtained by the different aspect ratio particles in this work can be seen in Figure 2.8. The short CNCs stabilize the interface by packing at the surface of oil droplets, whereas the long CNCs form several interconnecting points with each other and with multiple droplets, creating an overall structure that stabilizes the emulsion with lower concentration of particles and only partially covered droplets. The same authors had previously reported stable emulsions at 60 % coverage with BCNCs [63]. Souza et al. [128] obtained stable Cardamom oil-in water emulsions at only 25 % coverage using wood pulp CNFs.

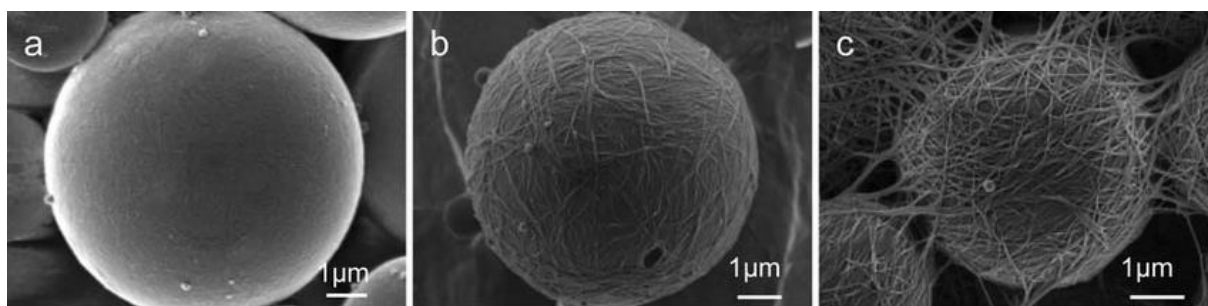


Figure 2.8 – Scanning electron microscope images of polymerised styrene-in-water emulsions stabilised by CNCs of different aspect ratios: (a) cotton nanocrystals with aspect ratio of 13; (b) bacterial cellulose nanocrystals with aspect ratio of 47; (c) *Cladophora* nanocrystals with aspect ratio of 160 (retrieved from [127]).

Using mangosteen rind MFC, Winuprasith & Suphantharika [129] also observed an increase in the fibre structure formation in the continuous phase, with increasing particle concentration, playing a major role in oil-in-water emulsion stability. However, in this case, the increase in viscosity of the continuous phase

at higher MFC concentrations (0.7 %) led to a decrease in the homogenization efficiency, resulting in larger oil droplets.

As a general rule, the size of particles suitable for Pickering stabilization must be smaller than that of the disperse phase droplets. First, because large or denser particles are more susceptible to the effect of gravity, which leads to poor suspension stability and sedimentation; second, because the particles must adsorb to a curved surface, and large particles would protrude or stick out of the droplet surface (or the droplets would have to be much larger to accommodate the entirety of a stiff particle on its surface). Smaller particles can arrange more easily side by side at the interface, covering it more efficiently without deforming it. Nanocelluloses have an advantage on this point, because of their small sizes. Although they can have several μm in length, some studies have noted that these materials are flexible enough to adjust to the curved interface, slightly bending on top of the oil droplets [9]. This behaviour has been observed both in bacterial cellulose nanofibrils (BCNF) [125] and bacterial cellulose nanocrystals (BCNC) [63,127], among others. Thus, flexibility arises as a relevant feature for Pickering stabilization.

Besides flexibility, the location and organization of cellulose particles at the interface, although irreversibly adsorbed, can be dynamic. The ability of particles to reorganize in the interface of a Pickering system can be exploited, for example, to include more internal (dispersed) phase in an emulsion without compromising its stability, since the particles shift to a smaller area arrangement. Capron & Cathala [130] have produced oil-in-water high internal phase emulsions (HIPE) stabilized with CNCs, using a two-step process: a primary Pickering emulsion was prepared with 10:90 oil/water ratio, and then more oil was added. This way, they obtained HIPEs with over 90 % internal phase stabilized with less than 0.1 % CNC concentration. This is possible because the oil added in the second stage of the process accumulates in the previously formed oil droplets, already stabilized with the CNCs in the first step. Close packing and deformation of the interface were observed, and a final gel-like behaviour, as can be seen in Figure 2.9.

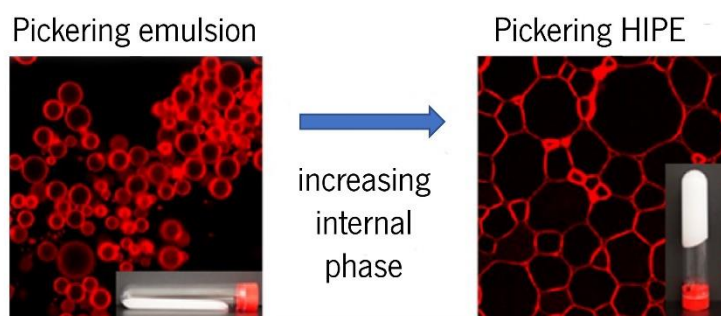


Figure 2.9 - Confocal laser scanning micrographs of a pickering emulsion stabilized with cotton CNCs containing 10 % of internal phase, and the resulting HIPE with 85.6% of internal phase (retrieved from [130]).

The formation of direct HIPEs in a single-step homogenization was not viable, but after adsorption of the CNCs to the interface it was possible to increase the oil/water ratio beyond the limit of surface coverage due to a new arrangement of the microstructure in large oil globules.

In addition to the steric stabilization obtained by the physical barrier of particles adsorbed at the interface and the three-dimensional networks preventing droplets coalescence, Pickering stabilizers might also provide an electrostatic barrier resulting from the particles' surface chemistry. A study on the interfacial layer morphology of oil-in-water Pickering emulsions, using cotton cellulose nanocrystals, suggested that these solid particles arrange in a monolayer varying in surface density depending on the particle charge [115]. Particles surface charge can play an important role on their ability to stabilize biphasic systems, since it might lead to repulsions between particles at the interface and, therefore, to a less stable particle layer. CNCs prepared by hydrochloric acid hydrolysis are weakly negatively charged; on the other hand, those produced by sulphuric acid hydrolysis have a highly negative charge density due to sulphate groups, leading to strong interparticle repulsions and consequently a good colloidal stability in aqueous media [2]. However, this is not advantageous for Pickering systems since the repulsions between particles lead to a low surface coverage, weak mechanical barrier and easier destabilization of the interface. Neutral or low charged particles with poor colloidal stability tend to aggregate in aqueous media, which is beneficial in the scope of Pickering systems because it allows the creation of a denser layer due to overlapping and multiple interconnections of the particles [9,109]. This way, emulsions with neutral particles are less susceptible to environmental changes (pH, ionic strength, temperature), and resist to centrifugation due to their structural stability [120,131]. Kalashnikova et al. also suggested that the electrostatic interactions play an important role in the exposure of the hydrophobic planes of CNCs to the oil phase. In the same report, the authors compare sulphated and desulphated cotton CNCs and BCNCs and concluded that, regardless of the source, a surface charge density above 0.03 e/nm^2 was incompatible with efficient interface stabilization [59]. For attaining stable Pickering emulsions, electrostatic repulsions between neighbouring adsorbed sulphated CNCs can be prevented by charge screening with NaCl; another possibility is to neutralize the particles with a desulphation post-treatment [9,59,109].

Nevertheless, when well characterized and controlled, surface charges can still be compatible and even beneficial for Pickering emulsification. Aaen et al. [131] prepared oil-in-water emulsions with low-charged CNFs obtained by enzymatic treatment and highly charged carboxylated CNFs from TEMPO (2,2,6,6-tetramethylpiperidine-1-oxyl) oxidation. The emulsions produced with TEMPO-oxidized CNFs showed higher viscosity and resistance to creaming during centrifugation, but were susceptible to the presence of salt and acetic acid, breaking during centrifugation. On the other hand, the low charge CNFs generated

less viscous emulsions that underwent creaming during centrifugation, but no coalescence or phase separation were observed for any of the tested conditions.

Saelices & Capron [122] produced oil-in-water emulsions with sulphated CNCs, TEMPO-oxidized CNFs and unmodified (neutral and less fibrillated) CNFs, resorting to charge screening with 50 mM NaCl. The TEMPO-oxidized CNFs, which had the higher surface charge, originated emulsions with better stability than the sulphated CNCs and neutral CNFs. Moreover, the TEMPO-oxidized CNFs and the sulphated CNCs were able to produce nanoemulsions. Jia et al. [132] prepared BCNFs with different degrees of TEMPO-oxidation and obtained the best emulsion stability results with the lowest oxidation degree, but not with the native BC. The low-oxidation degree BCNFs showed, apart from native BC, the larger particle size but lower carboxyl content, charge density and hydrophilicity. Overall, these reports indicate that particle surface charge can improve stability against coalescence and creaming due to the creation of an electrostatic barrier between emulsion droplets but, on the other side, excessive surface charge might compromise the mechanical barrier if not properly screened with salts to prevent interparticle repulsions. Although stable emulsions containing nanocelluloses have been reported in many studies, the case of foams requires further investigation and tailoring of the cellulose surface properties to achieve good results, since the interfacial tension (IFT) at the air-water interface is significantly higher than that of oil-water systems [113,133]. CNCs have been reported not to decrease the air-water tension significantly, having low surface activity in this interface. CNFs, although possessing low surface activity as well, are capable of stabilizing foams through other mechanisms. The higher aspect ratio, namely, seems to favour the gel formation at the interface and improve stability [9]. Most of the literature reporting cellulose foams is in fact referring to solid or dry aerogels (sponge-like), not air-in-water dispersions. Notwithstanding, in the few reports of cellulose stabilized aqueous foams, the particles are usually modified or combined with surfactants.

Hu et al. [134] reported aqueous foams generated from sulphated CNCs and methylcellulose (MC), a stabilizer used in food industry. They proposed that the MC adsorbs onto the CNCs and positions at the air-water interface, since CNCs alone did not lower the surface tension nor could produce stable foams. Increasing CNC concentration in the MC stabilized foams promoted air incorporation, producing higher foam volumes with lower density and smaller air bubbles. Plus, the authors verified that the CNCs did not drain from the foam over time, and this stability allowed for air-drying and resistance to high temperatures. Cervin et al. [135] modified the surface of charged CNFs with octylamine by simple electrostatic adsorption, mixing the two components. This modification increased the contact angle of the CNFs from 20° to 40°, rendering less hydrophilic particles. The produced foams were stable and resistant to

temperature and water drainage, allowing for drying and attainment of strong, porous dry materials. Later, the mechanisms behind the foam stabilizing ability of these surface-modified CNFs was studied. The authors compared TEMPO-oxidized CNFs of varying charge densities, modified with octylamine or decylamine, with CNCs prepared from the same fibres and with the same modifications. Overall they concluded that the ability of CNFs to stabilize aqueous foams even at low concentrations (from 5 g/L) was due to two main factors: i) their high aspect ratio that potentiates the creation of intertwined networks and gel formation at the interface, immobilizing water, strengthening the interface and preventing drainage; ii) the charge density that creates repulsive electrostatic pressure between the bubbles (disjoining pressure), contributing to their stability over time [136]. Surface activity and foaming ability have also been reported for CNCs from rice straw holocellulose (less pure, containing hemicellulose and residues of silica and lignosulphonate), with the particularity of being more hydrophobic than their pure cellulose counterparts [137].

Numerous works have mentioned the networking ability of cellulose particles in aqueous media, regardless of the morphology but depending on the aspect ratio and concentration [61,123,127–129,138]. The ability of celluloses to structure the continuous phase by creating networks of interconnected particles also allows the stabilization of solid particle suspensions in liquid media. For instance, Yaginuma & Kijima [117] studied the suspension stability of cocoa beverages containing commercial Avicel RC-591, a hydrocolloidal MCC product with 11 % CMC. The authors found that a concentration of 0.5 % (w/w) of this cellulose prevents the sedimentation of the solid cocoa particles after heat sterilization. In a similar system (a chocolate drink) Okiyama et al. [139] achieved complete suspension stability with only 0.25 % BC.

In summary, solid cellulosic nanoparticles possess several features that make them suitable as Pickering stabilizers of emulsions and foams, as well as suspending agents. BC exhibits all these features and can be easily modified for further improvement. It is a pure and sustainable source of nanocellulose, not requiring extensive purification or extraction processes. Its morphology is particularly suited for surface action, given its high aspect ratio and flexibility. These advantages can be exploited in some specific applications, as will be shown in the next section.

2.5 - APPLICATIONS OF BC IN FOOD AND COSMETICS

Given the well-recognized potential of cellulose particles as Pickering stabilizer of foams, emulsions and other multiphasic systems, they are actually found in many industries and in everyday products. BC

possesses the properties and ability to compete with, or even outperform, other cellulose particles; however, less studies have been conducted with this biomaterial and its transition to the market is delayed in comparison to plant-derived cellulose products. BC's suitability has yet to be attested in some markets where plant-derived cellulose products are already well integrated, and new applications can be developed, taking advantage of its particular features. Two of the most promising, yet less explored areas, are food and cosmetics. The work reported so far in these areas, as well as the identified investigation and development gaps, are discussed ahead.

2.5.1 - Food Applications

Dietary fibre - non-digestible carbohydrates - provides a beneficial effect to consumer's health, primarily by promoting a feeling of "fullness" without additional energy intake (since the fibres cannot be digested) and improving laxation and bowel function; indirectly, it can help reduce the risk of diabetes, obesity, cardiovascular disease and other chronic diseases. Cellulose is among the fibres that are naturally present in food products, representing a significant part of the available dietary fibre, more specifically insoluble fibre. BC possesses the same health benefits as other insoluble dietary fibres and celluloses from different sources. It is consumed and commercialized in Asian countries as *Nata de coco*, a traditional dessert originated in the Philippines. It is produced by static fermentation of coconut wastewaters; the membrane is then cut in cubes and soaked in sugar syrup to be sweetened and chewable [17,101,118,119].

Despite being highly hydrophilic and having high water holding capacity, wet BC membranes exhibit some syneresis over time (excess water drains from the membrane). However, when impregnated with a viscous solution (polyols and polysaccharides have been used for this purpose), water is better immobilized in the fibrous network and the overall structure becomes more 'self-supporting', softer, more penetrable and fracturable; the use of such additives helps retaining water and avoiding syneresis. Processed with e.g., sugar alcohol syrup the membrane goes from tough, difficult to chew, and with low fracturability, to significantly softer and bearing a texture similar to fruit, such as grapes. Also, it changes from opaque to translucent, indicating a swelling and loosen of the network caused by the solutes. On the other hand, processed with alginate and calcium chloride the total texture profile is different, and more resembling of molluscs, such as squids [18]. This shows that texture can be modulated through impregnation with polymers or gelling agents, making the processed membrane an edible non-fat/high-fibre foodstuff that can be impregnated with sweeteners, natural flavours and colours to mimic fruits and be incorporated in low-calorie desserts, yoghurts or drinks.

The potential of BC as a food additive has been acknowledged many years ago and is still an investigation topic. In a former report, Okiyama et al. [139] proposed the use of a wet BC paste as an additive for chocolate drinks, ice cream, hamburgers, sausages, tofu, and more. BC showed higher viscosity, better suspending ability and resistance to heat treatment of the chocolate drink than xanthan gum (XG); BC improved the body of ice cream and prevented melting for 60 min; it increased the gel strength of tofu, at low concentrations, although altering its texture in a perceptible way to consumers; used as bulking agent, it allowed the production of low-fat meat products without affecting their texture.

In more recent works, Paximada et al. [140] prepared olive oil-in-water (10:90) emulsions stabilized with wet BC paste, and compared it with soluble celluloses used in food industry, namely CMC and HPMC. BC emulsions showed to be more viscous, less susceptible to changes in pH, temperature and salinity, with larger droplets but, nonetheless, more stable, as measured by serum index (percentage of the serum layer, the aqueous sub-phase that appears at the bottom when the o/w emulsion starts to cream). The effect of BC as a thickener for the continuous phase of the same emulsions was also studied, using whey protein isolate as emulsifier. Higher amounts of BC led to an increase in the stability of the emulsions and decrease of creaming effect. Comparing the rheology with emulsions prepared with xanthan gum and locust bean gum (LBG), the authors concluded that BC is a good alternative to these commonly used thickeners, even in smaller amounts [141].

Other recently studied examples of BC-based stabilizers for food-grade emulsions include BC nanoparticles produced by hydrochloric acid hydrolysis, with ability to lower the IFT of peanut oil/water interface [142], BCNCs modified with surface carboxyl groups for improved emulsifying performance compared to native BC [46], and BCNFs prepared by HPH [125].

As far as this review could ascertain, no systematic reports concerning BC-stabilized aqueous foams for food applications have been published in scientific literature. However, the interest in this topic seems to be rising, since edible BC solid foams [143] and foam templated biofilms [144] have been recently reported.

In short, pure and modified BC fibres can be used as an edible additive in many heterogeneous food systems. The ultrathin and long BC fibres present an improved alternative to commonly used stabilizers such as surfactants, gums and other hydrocolloidal particles, or even other cellulosic materials. BC shows potential to be applicable as a low-calorie thickener, stabilizer and texture modifier of processed foods and beverages, to improve their overall quality. It is however important to notice that all of the cited works have been performed with never-dried BC particles, whereas a product available in dry form would be

advantageous from an economic and practical standpoint when envisioning real, large-scale, industrial applications.

2.5.2 - Cosmetic applications

Cosmetic formulations, in general, are multiphase systems composed of many substances with specific properties or functions: water, oils and other moisturizing substances, active agents (antiwrinkle, antioxidant, vitamins, makeup, sunlight protecting, cleansing), preservatives, perfumes, texturing agents, and finally emulsifiers to keep all the components mixed in a stable formulation. Conventional surfactants may cause irritancy or other adverse reactions to the skin, and that is why surfactant-free dermal formulations are desirable. Also, the increasing environmental awareness is leading to the search of alternatives such as biosurfactants or biopolymers, which are produced biotechnologically and easier to degrade in the environment. Besides the beautifying or health benefits, other important parameters for consumers in the evaluation of cosmetic formulations are the organoleptic properties: visual aspect, smell, texture, consistency and spreadability, among others. Oil-in-water emulsions are more frequent in the cosmetic field because water, as external phase, provides a cooler, less greasy and lighter feel when applied to the skin [145–150].

Two desired properties of cosmetic or cleansing formulations include shear-thinning behaviour and particle suspension capabilities. This can be achieved by structuring the liquid composition, providing a distinctive rheological behaviour and the ability for suspending liquid or solid particles over long periods of time. The suspended materials to be incorporated in cosmetic formulations can be functional (abrasives, oils, encapsulates, active agents), non-functional (aesthetic, optical particles) or both. Ideally, the structuring agent (thickener or viscosity modifier) must be capable of providing both shear-thinning behaviour and suspension ability with the smallest concentration possible, to avoid overly viscous (non-pourable), opaque or cloudy formulations, which can be undesirable in some products [151–153].

Some natural polymers can change the organoleptic properties and the flow behaviour of emulsions, in addition to improving their stability, even at low concentrations [154–156]. Formulations of plant cellulose with other compounds, to render easier dispersibility, have long been known and their application to cosmetics has been patented [157,158]. Besides cosmetics, these products can also find applications in the pharmaceutical industry, in the formulation of ointments and other pharmaceutical formulations [61]. In this scope, BC may offer a great alternative as a natural, biocompatible, non-toxic and non-irritating stabilizing and thickening agent for application in cosmetics, given its proven structuring and suspending capabilities. Despite this clear potential and an apparent growing interest, BC has not yet been largely

explored for cosmetic applications and there are only few reports among the scientific literature [159]. Up to now, the majority of the reported cosmetic uses of BC refer to skin dressings, such as face masks. BC membranes show interesting properties for this specific use, namely the biocompatibility and non-toxicity, the high water content and water holding capacity, that promote skin hydration, and the high porosity that enables the incorporation and release of drugs, active ingredients or natural extracts. In fact, BC face masks are manufactured in some countries and commercialized globally [44,150,160–162]. They have shown to increase the skin moisture uptake and have positive user acceptance and satisfaction [163]. Some common skincare ingredients, such as hyaluronic acid (hydrophilic) and retinol (hydrophobic) have been incorporated in BC membranes using different approaches [86,164].

The great technological potential of BC as stabilizer and suspending agent for cosmetic creams and cleansing compositions has been mostly exploited by multinational companies, and this knowledge is presently found in the form of intellectual property. Examples include patent US 2007/019777 A1 from CP Kelco, regarding BC containing formulations for use as rheology modifier in products such as hair conditioners and hair styling products [165]; patent WO 2011/019876 A2 from The Procter and Gamble Company, referring to personal cleansing formulations containing BC in combination with a cationic polymer as an external structuring system [166]; patent US 6534071 B1 from L'Oréal, concerning oil-in-water emulsions for cosmetic uses containing commercial BC formulations [145]; and others, such as Colgate Palmolive [153] and Unilever [152]. All of these documents suggest a strong industrial interest in BC formulations for cosmetic and personal care products, that must be further investigated and reported in a systematic way among scientific literature.

2.6 - BIBLIOGRAPHIC REFERENCES

- [1] R.J. Moon, A. Martini, J. Nairn, J. Simonsen, J. Youngblood, Cellulose nanomaterials review: Structure, properties and nanocomposites, 2011. <https://doi.org/10.1039/c0cs00108b>.
- [2] D. Klemm, F. Kramer, S. Moritz, T. Lindström, M. Ankerfors, D. Gray, A. Dorris, Nanocelluloses: A new family of nature-based materials, *Angew. Chemie - Int. Ed.* 50 (2011) 5438–5466. <https://doi.org/10.1002/anie.201001273>.
- [3] S.J. Eichhorn, A. Dufresne, M. Aranguren, N.E. Marcovich, J.R. Capadona, S.J. Rowan, C. Weder, W. Thielemans, M. Roman, S. Renneckar, W. Gindl, S. Veigel, J. Keckes, H. Yano, K. Abe, M. Nogi, A.N. Nakagaito, A. Mangalam, J. Simonsen, A.S. Benight, A. Bismarck, L.A. Berglund, T. Peijs, Review: Current international research into cellulose nanofibres and nanocomposites, 2010. <https://doi.org/10.1007/s10853-009-3874-0>.
- [4] Y. Habibi, L.A. Lucia, O.J. Rojas, Cellulose nanocrystals: Chemistry, self-assembly, and applications, *Chem. Rev.* 110 (2010) 3479–3500. <https://doi.org/10.1021/cr900339w>.
- [5] B. Medronho, B. Lindman, Competing forces during cellulose dissolution: From solvents to mechanisms,

- Curr. Opin. Colloid Interface Sci. 19 (2014) 32–40. <https://doi.org/10.1016/j.cocis.2013.12.001>.
- [6] D. Klemm, E.D. Cranston, D. Fischer, M. Gama, S.A. Kedzior, D. Kralisch, F. Kramer, T. Kondo, T. Lindström, S. Nietzsche, K. Petzold-Welcke, F. Rauchfuß, Nanocellulose as a natural source for groundbreaking applications in materials science: Today's state, *Mater. Today*. 21 (2018) 720–748. <https://doi.org/10.1016/j.mattod.2018.02.001>.
- [7] I.M. Saxena, R.M. Brown, Cellulose biosynthesis: Current views and evolving concepts, *Ann. Bot.* 96 (2005) 9–21. <https://doi.org/10.1093/aob/mci155>.
- [8] D.A.B. Martins, H.F.A. do Prado, R.S. Ribeiro Leite, H. Ferreira, M.M. de Souza Moretti, R. da Silva, E. Gomes, Agroindustrial Wastes as Substrates for Microbial Enzymes Production and Source of Sugar for Bioethanol Production, in: S. Kumar (Ed.), *Integr. Waste Manag.* - Vol. II, InTech, Rijeka, Croatia, 2011. <https://doi.org/10.5772/23377>.
- [9] I. Capron, O.J. Rojas, R. Bordes, Behavior of nanocelluloses at interfaces, *Curr. Opin. Colloid Interface Sci.* 29 (2017) 83–95. <https://doi.org/10.1016/j.cocis.2017.04.001>.
- [10] G. Alborno-Palma, F. Betancourt, R.T. Mendonça, G. Chinga-Carrasco, M. Pereira, Relationship between rheological and morphological characteristics of cellulose nanofibrils in dilute dispersions, *Carbohydr. Polym.* 230 (2020) 115588. <https://doi.org/10.1016/j.carbpol.2019.115588>.
- [11] N. Stevulova, V. Hospodarova, Cellulose Fibres Used in Building Materials, *Proc. REHVA Annu. Conf. 2015 "Advanced HVAC Nat. Gas Technol.* (2015). <https://doi.org/10.7250/rehvaconf.2015.031>.
- [12] Y. Habibi, A.L. Goffin, N. Schiltz, E. Duquesne, P. Dubois, A. Dufresne, Bionanocomposites based on poly(ϵ -caprolactone)-grafted cellulose nanocrystals by ring-opening polymerization, *J. Mater. Chem.* 18 (2008) 5002–5010. <https://doi.org/10.1039/b809212e>.
- [13] K.Y. Lee, G. Buldum, A. Mantalaris, A. Bismarck, More than meets the eye in bacterial cellulose: Biosynthesis, bioprocessing, and applications in advanced fiber composites, *Macromol. Biosci.* 14 (2014) 10–32. <https://doi.org/10.1002/mabi.201300298>.
- [14] D. Mamlouk, M. Gullo, Acetic Acid Bacteria: Physiology and Carbon Sources Oxidation, *Indian J. Microbiol.* 53 (2013) 377–384. <https://doi.org/10.1007/s12088-013-0414-z>.
- [15] L. Stasiak, S. Błaejak, Acetic acid bacteria-perspectives of application in biotechnology-a review, *Polish J. Food Nutr. Sci.* 59 (2009) 17–23.
- [16] S.M. Keshk, Bacterial Cellulose Production and its Industrial Applications, *J. Bioprocess. Biotech.* 04 (2014). <https://doi.org/10.4172/2155-9821.1000150>.
- [17] A. Jagannath, S.S. Manjunatha, N. Ravi, P.S. Raju, The effect of different substrates and processing conditions on the textural characteristics of bacterial cellulose (nata) produced by *Acetobacter xylinum*, *J. Food Process Eng.* 34 (2011) 593–608. <https://doi.org/10.1111/j.1745-4530.2009.00403.x>.
- [18] A. Okiyama, M. Motoki, S. Yamanaka, Bacterial cellulose II. Processing of the gelatinous cellulose for food materials, *Top. Catal.* 6 (1992) 479–487. [https://doi.org/10.1016/S0268-005X\(09\)80033-7](https://doi.org/10.1016/S0268-005X(09)80033-7).
- [19] M.U. Islam, M.W. Ullah, S. Khan, N. Shah, J.K. Park, Strategies for cost-effective and enhanced production of bacterial cellulose, *Int. J. Biol. Macromol.* 102 (2017) 1166–1173. <https://doi.org/10.1016/j.ijbiomac.2017.04.110>.
- [20] C. Zhong, Industrial-Scale Production and Applications of Bacterial Cellulose, *Front. Bioeng. Biotechnol.* 8 (2020) 1–19. <https://doi.org/10.3389/fbioe.2020.605374>.
- [21] S. HESTRIN, M. SCHRÄMM, Synthesis of cellulose by *Acetobacter xylinum*. II. Preparation of freeze-dried cells capable of polymerizing glucose to cellulose., *Biochem. J.* 58 (1954) 345–352. <https://doi.org/10.1042/bj0580345>.
- [22] E. Tsouko, C. Kourmentza, D. Ladakis, N. Kopsahelis, I. Mandala, S. Papanikolaou, F. Paloukis, V. Alves,

- A. Koutinas, Bacterial cellulose production from industrial waste and by-product streams, *Int. J. Mol. Sci.* 16 (2015) 14832–14849. <https://doi.org/10.3390/ijms160714832>.
- [23] A.F. Jozala, R.A.N. Pértile, C.A. dos Santos, V. de Carvalho Santos-Ebinuma, M.M. Seckler, F.M. Gama, A. Pessoa, Bacterial cellulose production by *Gluconacetobacter xylinus* by employing alternative culture media, *Appl. Microbiol. Biotechnol.* 99 (2015) 1181–1190. <https://doi.org/10.1007/s00253-014-6232-3>.
- [24] D. Abol-Fotouh, M.A. Hassan, H. Shokry, A. Roig, M.S. Azab, A.E.H.B. Kashyout, Bacterial nanocellulose from agro-industrial wastes: low-cost and enhanced production by *Komagataeibacter saccharivorans* MD1, *Sci. Rep.* 10 (2020) 1–14. <https://doi.org/10.1038/s41598-020-60315-9>.
- [25] J.V. Kumbhar, J.M. Rajwade, K.M. Paknikar, Fruit peels support higher yield and superior quality bacterial cellulose production, *Appl. Microbiol. Biotechnol.* 99 (2015) 6677–6691. <https://doi.org/10.1007/s00253-015-6644-8>.
- [26] A.C. Rodrigues, A.I. Fontão, A. Coelho, M. Leal, F.A.G. Soares da Silva, Y. Wan, F. Dourado, M. Gama, Response surface statistical optimization of bacterial nanocellulose fermentation in static culture using a low-cost medium, *N. Biotechnol.* 49 (2019) 19–27. <https://doi.org/10.1016/j.nbt.2018.12.002>.
- [27] F.A.G. Soares da Silva, M. Fernandes, A.P. Souto, E.C. Ferreira, F. Dourado, M. Gama, Optimization of bacterial nanocellulose fermentation using recycled paper sludge and development of novel composites, *Appl. Microbiol. Biotechnol.* 103 (2019) 9143–9154. <https://doi.org/10.1007/s00253-019-10124-6>.
- [28] F. Mohammadkazemi, M. Azin, A. Ashori, Production of bacterial cellulose using different carbon sources and culture media, *Carbohydr. Polym.* 117 (2015) 518–523. <https://doi.org/10.1016/j.carbpol.2014.10.008>.
- [29] S.S. Wang, Y.H. Han, Y.X. Ye, X.X. Shi, P. Xiang, D.L. Chen, M. Li, Physicochemical characterization of high-quality bacterial cellulose produced by *Komagataeibacter* sp. strain W1 and identification of the associated genes in bacterial cellulose production, *RSC Adv.* 7 (2017) 45145–45155. <https://doi.org/10.1039/c7ra08391b>.
- [30] P. Jacek, F.A.G. Soares, F. Dourado, M. Gama, Optimization and characterization of bacterial nanocellulose produced by *Komagataeibacter rhaeticus* K3, 2 (2021). <https://doi.org/10.1016/j.carpta.2020.100022>.
- [31] M. Gullo, S. La China, G. Petroni, S. Di Gregorio, P. Giudici, Exploring K2G30 genome: A high bacterial cellulose producing strain in glucose and mannitol based media, *Front. Microbiol.* 10 (2019) 1–12. <https://doi.org/10.3389/fmicb.2019.00058>.
- [32] G. Gopu, S. Govindan, Production of bacterial cellulose from *Komagataeibacter saccharivorans* strain BC1 isolated from rotten green grapes, *Prep. Biochem. Biotechnol.* 48 (2018) 842–852. <https://doi.org/10.1080/10826068.2018.1513032>.
- [33] M. Jedrzejczak-Krzepkowska, K. Kubiak, K. Ludwicka, S. Bielecki, Bacterial NanoCellulose Synthesis, Recent Findings, in: M. Gama, F. Dourado, S. Bielecki (Eds.), *Bact. Nanocellulose - From Biotechnol. to Bio- Econ.*, Elsevier B.V., 2016. <https://doi.org/10.1016/B978-0-444-63458-0.00002-0>.
- [34] T. Nakai, N. Tonouchi, T. Konishi, Y. Kojima, T. Tsuchida, F. Yoshinaga, F. Sakai, T. Hayashi, Enhancement of cellulose production by expression of sucrose synthase in *Acetobacter xylinum*, *Proc. Natl. Acad. Sci. U. S. A.* 96 (1999) 14–18. <https://doi.org/10.1073/pnas.96.1.14>.
- [35] M. Florea, H. Hagemann, G. Santosa, J. Abbott, C.N. Micklem, X. Spencer-Milnes, L. De Arroyo Garcia, D. Paschou, C. Lazenbatt, D. Kong, H. Chughtai, K. Jensen, P.S. Freemont, R. Kitney, B. Reeve, T. Ellis, Engineering control of bacterial cellulose production using a genetic toolkit and a new celluloseproducing strain, *Proc. Natl. Acad. Sci. U. S. A.* 113 (2016) E3431–E3440. <https://doi.org/10.1073/pnas.1522985113>.
- [36] T. Shigematsu, K. Takamine, M. Kitazato, T. Morita, T. Naritomi, S. Morimura, K. Kida, Cellulose production

- from glucose using a glucose dehydrogenase gene (*gdh*)-deficient mutant of *gluconacetobacter xylinus* and its use for bioconversion of sweet potato pulp, *J. Biosci. Bioeng.* 99 (2005) 415–422. <https://doi.org/10.1263/jbb.99.415>.
- [37] G. Buldum, A. Bismarck, A. Mantalaris, Recombinant biosynthesis of bacterial cellulose in genetically modified *Escherichia coli*, *Bioprocess Biosyst. Eng.* 41 (2018) 265–279. <https://doi.org/10.1007/s00449-017-1864-1>.
- [38] D. Klemm, K. Petzold-Welcke, F. Kramer, T. Richter, V. Raddatz, W. Fried, S. Nietzsche, T. Bellmann, D. Fischer, Biotech nanocellulose: A review on progress in product design and today's state of technical and medical applications, *Carbohydr. Polym.* 254 (2021) 117313. <https://doi.org/10.1016/j.carbpol.2020.117313>.
- [39] A. Krystynowicz, W. Czaja, A. Wiktorowska-Jezierska, M. Gonçalves-Miśkiewicz, M. Turkiewicz, S. Bielecki, Factors affecting the yield and properties of bacterial cellulose, *J. Ind. Microbiol. Biotechnol.* 29 (2002) 189–195. <https://doi.org/10.1038/sj.jim.7000303>.
- [40] D. Kralisch, N. Hessler, D. Klemm, R. Erdmann, W. Schmidt, White biotechnology for cellulose manufacturing - The HoLiR concept, *Biotechnol. Bioeng.* 105 (2010) 740–747. <https://doi.org/10.1002/bit.22579>.
- [41] F. Dourado, A.I. Fontão, M. Leal, A.C. Rodrigues, M. Gama, Process Modeling and Techno-Economic Evaluation of an Industrial Bacterial NanoCellulose Fermentation Process, in: M. Gama, F. Dourado, S. Bielecki (Eds.), *Bact. Nanocellulose - From Biotechnol. to Bio- Econ.*, Elsevier B.V., 2016. <https://doi.org/https://doi.org/10.1016/B978-0-444-63458-0.00012-3>.
- [42] F.A.G.S. da Silva, J. V. Oliveira, C. Felgueiras, F. Dourado, M. Gama, M.M. Alves, Study and valorisation of wastewaters generated in the production of bacterial nanocellulose, *Biodegradation.* 31 (2020) 47–56. <https://doi.org/10.1007/s10532-020-09893-z>.
- [43] M. Moniri, A.B. Moghaddam, S. Azizi, R.A. Rahim, A. Bin Ariff, W.Z. Saad, M. Navaderi, R. Mohamad, Production and status of bacterial cellulose in biomedical engineering, *Nanomaterials.* 7 (2017) 1–26. <https://doi.org/10.3390/nano7090257>.
- [44] K. Ludwicka, M. Jedrzejczak-Krzepkowska, K. Kubiak, M. Kolodziejczyk, T. Pankiewicz, S. Bielecki, Medical and Cosmetic Applications of Bacterial NanoCellulose, in: M. Gama, F. Dourado, S. Bielecki (Eds.), *Bact. Nanocellulose - From Biotechnol. to Bio-Economy*, Elsevier B.V., 2016: pp. 145–165.
- [45] T. Kondo, P. Rytczak, S. Bielecki, Bacterial NanoCellulose Characterization, in: M. Gama, F. Dourado, S. Bielecki (Eds.), *Bact. Nanocellulose - From Biotechnol. to Bio- Econ.*, Elsevier B.V., 2016: pp. 59–71.
- [46] H. Yan, X. Chen, H. Song, J. Li, Y. Feng, Z. Shi, X. Wang, Q. Lin, Synthesis of bacterial cellulose and bacterial cellulose nanocrystals for their applications in the stabilization of olive oil pickering emulsion, *Food Hydrocoll.* 72 (2017) 127–135. <https://doi.org/10.1016/j.foodhyd.2017.05.044>.
- [47] N. Pa'E, N.I.A. Hamid, N. Khairuddin, K.A. Zahan, K.F. Seng, B.M. Siddique, I.I. Muhamad, Effect of different drying methods on the morphology, crystallinity, swelling ability and tensile properties of nata de coco, *Sains Malaysiana.* 43 (2014) 767–773.
- [48] E. Fortunato, D. Gaspar, P. Duarte, L. Pereira, H. Águas, A. Vicente, F. Dourado, M. Gama, R. Martins, Optoelectronic devices from bacterial nanocellulose, in: M. Gama, F. Dourado, S. Bielecki (Eds.), *Bact. Nanocellulose - From Biotechnol. to Bio- Econ.*, Elsevier B.V., 2016: pp. 179–199.
- [49] H. Yano, J. Sugiyama, A.N. Nakagaito, M. Nogi, T. Matsuura, M. Hikita, K. Handa, Optically transparent composites reinforced with networks of bacterial nanofibers, *Adv. Mater.* 17 (2005) 153–155. <https://doi.org/10.1002/adma.200400597>.
- [50] C. Legnani, H.S. Barud, J.M.A. Caiut, V.L. Calil, I.O. Maciel, W.G. Quirino, S.J.L. Ribeiro, M. Cremona, Transparent bacterial cellulose nanocomposites used as substrate for organic light-emitting diodes, *J.*

- Mater. Sci. Mater. Electron. 30 (2019) 16718–16723. <https://doi.org/10.1007/s10854-019-00979-w>.
- [51] S. Ummartyotin, J. Juntaro, M. Sain, H. Manuspiya, Development of transparent bacterial cellulose nanocomposite film as substrate for flexible organic light emitting diode (OLED) display, Ind. Crops Prod. 35 (2012) 92–97. <https://doi.org/10.1016/j.indcrop.2011.06.025>.
- [52] G. Guhados, W. Wan, J.L. Hutter, Measurement of the elastic modulus of single bacterial cellulose fibers using atomic force microscopy, Langmuir. 21 (2005) 6642–6646. <https://doi.org/10.1021/la0504311>.
- [53] Y.C. Hsieh, H. Yano, M. Nogi, S.J. Eichhorn, An estimation of the Young's modulus of bacterial cellulose filaments, Cellulose. 15 (2008) 507–513. <https://doi.org/10.1007/s10570-008-9206-8>.
- [54] D. Zhu, B. Mobasher, S.D. Rajan, Characterization of Mechanical Behavior of Kevlar 49 Fabrics, Exp. Appl. Mech. 6 (2011) 377–384. <https://doi.org/10.1007/978-1-4614-0222-0>.
- [55] N. Pogorelova, E. Rogachev, I. Digel, S. Chernigova, D. Nardin, Bacterial Cellulose Nanocomposites: Morphology and Mechanical Properties, Materials (Basel). (2019) 87–105. https://doi.org/10.1007/978-3-030-05825-8_5.
- [56] M. Nogi, H. Yano, Transparent nanocomposites based on cellulose produced by bacteria offer potential innovation in the electronics device industry, Adv. Mater. 20 (2008) 1849–1852. <https://doi.org/10.1002/adma.200702559>.
- [57] B. Medronho, A. Romano, M.G. Miguel, L. Stigsson, B. Lindman, Rationalizing cellulose (in)solubility: Reviewing basic physicochemical aspects and role of hydrophobic interactions, Cellulose. 19 (2012) 581–587. <https://doi.org/10.1007/s10570-011-9644-6>.
- [58] C. Yamane, T. Aoyagi, M. Ago, K. Sato, K. Okajima, T. Takahashi, Two different surface properties of regenerated cellulose due to structural anisotropy, Polym. J. 38 (2006) 819–826. <https://doi.org/10.1295/polymj.PJ2005187>.
- [59] I. Kalashnikova, H. Bizot, B. Cathala, I. Capron, Modulation of cellulose nanocrystals amphiphilic properties to stabilize oil/water interface, Biomacromolecules. 13 (2012) 267–275. <https://doi.org/10.1021/bm201599j>.
- [60] R.H. Newman, Carbon-13 NMR evidence for cocrystallization of cellulose as a mechanism for hornification of bleached kraft pulp, Cellulose. 11 (2004) 45–52. <https://doi.org/10.1023/B:CELL.0000014768.28924.0c>.
- [61] G.H. Zhao, N. Kapur, B. Carlin, E. Selinger, J.T. Guthrie, Characterisation of the interactive properties of microcrystalline cellulose-carboxymethyl cellulose hydrogels, Int. J. Pharm. 415 (2011) 95–101. <https://doi.org/10.1016/j.ijpharm.2011.05.054>.
- [62] H.T. Winter, C. Cerclier, N. Delorme, H. Bizot, B. Quemener, B. Cathala, Improved colloidal stability of bacterial cellulose nanocrystal suspensions for the elaboration of spin-coated cellulose-based model surfaces, Biomacromolecules. 11 (2010) 3144–3151. <https://doi.org/10.1021/bm100953f>.
- [63] I. Kalashnikova, H. Bizot, B. Cathala, I. Capron, New pickering emulsions stabilized by bacterial cellulose nanocrystals, Langmuir. 27 (2011) 7471–7479. <https://doi.org/10.1021/la200971f>.
- [64] P. Nechita, D.M. Panaitescu, Improving the dispersibility of cellulose microfibrillated structures in polymer matrix by controlling drying conditions and chemical surface modifications, Cellul. Chem. Technol. 47 (2013) 711–719.
- [65] J. Laine, T. Lindstrom, G.G. Nordmark, G. Risinger, Studies on topochemical modification of cellulosic fibres Part 1. Chemical conditions for the attachment of carboxymethyl cellulose onto fibres, Nord. Pulp Pap. Res. J. 15 (2000). <https://doi.org/10.3183/npprj-2003-18-03-p325-332>.
- [66] C. Clasen, B. Sultanova, T. Wilhelms, P. Heisig, W.M. Kulicke, Effects of different drying processes on the material properties of bacterial cellulose membranes, Macromol. Symp. 244 (2006) 48–58. <https://doi.org/10.1002/masy.200651204>.

- [67] M.C.I.M. Amin, A.G. Abadi, H. Katas, Purification, characterization and comparative studies of spray-dried bacterial cellulose microparticles, *Carbohydr. Polym.* 99 (2014) 180–189. <https://doi.org/10.1016/j.carbpol.2013.08.041>.
- [68] E.S. Abdel-Halim, Chemical modification of cellulose extracted from sugarcane bagasse: Preparation of hydroxyethyl cellulose, *Arab. J. Chem.* 7 (2014) 362–371. <https://doi.org/10.1016/j.arabjc.2013.05.006>.
- [69] M. Wrona, M.J. Cran, C. Nerin, S.W. Bigger, Development and characterisation of HPMC films containing PLA nanoparticles loaded with green tea extract for food packaging applications, *Carbohydr. Polym.* 156 (2017) 108–117. <https://doi.org/10.1016/j.carbpol.2016.08.094>.
- [70] S. Gorgieva, V. Kokol, Synthesis and application of new temperature-responsive hydrogels based on carboxymethyl and hydroxyethyl cellulose derivatives for the functional finishing of cotton knitwear, *Carbohydr. Polym.* 85 (2011) 664–673. <https://doi.org/10.1016/j.carbpol.2011.03.037>.
- [71] R.G. Candido, A.R. Gonçalves, Synthesis of cellulose acetate and carboxymethylcellulose from sugarcane straw, *Carbohydr. Polym.* 152 (2016) 679–686. <https://doi.org/10.1016/j.carbpol.2016.07.071>.
- [72] C.A. Kumar Varma, R.K. Koley, S. Singh, A.K. Sen, K.J. Kumar, Homogeneous carboxymethylated orange pulp cellulose: Characterization and evaluation in terms of drug delivery, *Int. J. Biol. Macromol.* 93 (2016) 1141–1146. <https://doi.org/10.1016/j.ijbiomac.2016.09.084>.
- [73] K. Schluffer, T. Heinze, Carboxymethylation of bacterial cellulose, *Macromol. Symp.* 294 (2010) 117–124. <https://doi.org/10.1002/masy.200900054>.
- [74] A. Casaburi, Ú. Montoya Rojo, P. Cerrutti, A. Vázquez, M.L. Foresti, Carboxymethyl cellulose with tailored degree of substitution obtained from bacterial cellulose, *Food Hydrocoll.* 75 (2018) 147–156. <https://doi.org/10.1016/j.foodhyd.2017.09.002>.
- [75] K.Y. Lee, F. Quero, J.J. Blaker, C.A.S. Hill, S.J. Eichhorn, A. Bismarck, Surface only modification of bacterial cellulose nanofibres with organic acids, *Cellulose*. 18 (2011) 595–605. <https://doi.org/10.1007/s10570-011-9525-z>.
- [76] M. Badshah, H. Ullah, A.R. Khan, S. Khan, J.K. Park, T. Khan, Surface modification and evaluation of bacterial cellulose for drug delivery, *Int. J. Biol. Macromol.* 113 (2018) 526–533. <https://doi.org/10.1016/j.ijbiomac.2018.02.135>.
- [77] R. Pértile, S. Moreira, F. Andrade, L. Domingues, M. Gama, Bacterial cellulose modified using recombinant proteins to improve neuronal and mesenchymal cell adhesion, *Biotechnol. Prog.* 28 (2012) 526–532. <https://doi.org/10.1002/btpr.1501>.
- [78] I. Orlando, P. Basnett, R. Nigmatullin, W. Wang, J.C. Knowles, I. Roy, Chemical Modification of Bacterial Cellulose for the Development of an Antibacterial Wound Dressing, *Front. Bioeng. Biotechnol.* 8 (2020) 1–19. <https://doi.org/10.3389/fbioe.2020.557885>.
- [79] M. Zeng, A. Laromaine, W. Feng, P.A. Levkin, A. Roig, Origami magnetic cellulose: Controlled magnetic fraction and patterning of flexible bacterial cellulose, *J. Mater. Chem. C*. 2 (2014) 6312–6318. <https://doi.org/10.1039/c4tc00787e>.
- [80] A. Khalid, R. Khan, M. Ul-Islam, T. Khan, F. Wahid, Bacterial cellulose-zinc oxide nanocomposites as a novel dressing system for burn wounds, *Carbohydr. Polym.* 164 (2017) 214–221. <https://doi.org/10.1016/j.carbpol.2017.01.061>.
- [81] R.J.B. Pinto, P.A.A.P. Marques, M.A. Martins, C.P. Neto, T. Trindade, Electrostatic assembly and growth of gold nanoparticles in cellulosic fibres, *J. Colloid Interface Sci.* 312 (2007) 506–512. <https://doi.org/10.1016/j.jcis.2007.03.043>.
- [82] N. Ferreira, A. Marques, H. Águas, H. Bandarenka, R. Martins, C. Bodo, B. Costa-Silva, E. Fortunato, Label-Free Nanosensing Platform for Breast Cancer Exosome Profiling, *ACS Sensors*. 4 (2019) 2073–2083.

- <https://doi.org/10.1021/acssensors.9b00760>.
- [83] N. Shah, M. Ul-Islam, W.A. Khattak, J.K. Park, Overview of bacterial cellulose composites: A multipurpose advanced material, *Carbohydr. Polym.* 98 (2013) 1585–1598. <https://doi.org/10.1016/j.carbpol.2013.08.018>.
 - [84] R.D. Pavaloïu, A. Stoica-Guzun, M. Stroescu, S.I. Jinga, T. Dobre, Composite films of poly(vinyl alcohol)-chitosan-bacterial cellulose for drug controlled release, *Int. J. Biol. Macromol.* 68 (2014) 117–124. <https://doi.org/10.1016/j.ijbiomac.2014.04.040>.
 - [85] M. de Lima Fontes, A.B. Meneguim, A. Tercjak, J. Gutierrez, B.S.F. Cury, A.M. dos Santos, S.J.L. Ribeiro, H.S. Barud, Effect of in situ modification of bacterial cellulose with carboxymethylcellulose on its nano/microstructure and methotrexate release properties, *Carbohydr. Polym.* 179 (2018) 126–134. <https://doi.org/10.1016/j.carbpol.2017.09.061>.
 - [86] X. Wang, J. Tang, J. Huang, M. Hui, Production and characterization of bacterial cellulose membranes with hyaluronic acid and silk sericin, *Colloids Surfaces B Biointerfaces.* 195 (2020) 111273. <https://doi.org/10.1016/j.colsurfb.2020.111273>.
 - [87] F. Robotti, S. Botton, F. Frascchetti, A. Mallone, G. Pellegrini, N. Lindenblatt, C. Starck, V. Falk, D. Poulikakos, A. Ferrari, A micron-scale surface topography design reducing cell adhesion to implanted materials, *Sci. Rep.* 8 (2018) 1–13. <https://doi.org/10.1038/s41598-018-29167-2>.
 - [88] F. Robotti, I. Sterner, S. Botton, J.M. Monné Rodríguez, G. Pellegrini, T. Schmidt, V. Falk, D. Poulikakos, A. Ferrari, C. Starck, Microengineered biosynthesized cellulose as anti-fibrotic in vivo protection for cardiac implantable electronic devices, *Biomaterials.* 229 (2020) 119583. <https://doi.org/10.1016/j.biomaterials.2019.119583>.
 - [89] M. Jin, W. Chen, Z. Li, Y. Zhang, M. Zhang, S. Chen, Patterned bacterial cellulose wound dressing for hypertrophic scar inhibition behavior, *Cellulose.* 25 (2018) 6705–6717. <https://doi.org/10.1007/s10570-018-2041-7>.
 - [90] P.M. Favi, S.P. Ospina, M. Kachole, M. Gao, L. Atehortua, T.J. Webster, Preparation and characterization of biodegradable nano hydroxyapatite–bacterial cellulose composites with well-defined honeycomb pore arrays for bone tissue engineering applications, *Cellulose.* 23 (2016) 1263–1282. <https://doi.org/10.1007/s10570-016-0867-4>.
 - [91] W. Jing, Y. Chunxi, W. Yizao, L. Honglin, H. Fang, D. Kerong, H. Yuan, Laser patterning of bacterial cellulose hydrogel and its modification with gelatin and hydroxyapatite for bone tissue engineering, *Soft Mater.* 11 (2013) 173–180. <https://doi.org/10.1080/1539445X.2011.611204>.
 - [92] H. Ahrem, D. Pretzel, M. Endres, D. Conrad, J. Courseau, H. Müller, R. Jaeger, C. Kaps, D.O. Klemm, R.W. Kinne, Laser-structured bacterial nanocellulose hydrogels support ingrowth and differentiation of chondrocytes and show potential as cartilage implants, *Acta Biomater.* 10 (2014) 1341–1353. <https://doi.org/10.1016/j.actbio.2013.12.004>.
 - [93] A. Laromaine, T. Tronser, I. Pini, S. Parets, P.A. Levkin, A. Roig, Free-standing three-dimensional hollow bacterial cellulose structures with controlled geometry: Via patterned superhydrophobic-hydrophilic surfaces, *Soft Matter.* 14 (2018) 3955–3962. <https://doi.org/10.1039/c8sm00112j>.
 - [94] N. Petersen, P. Gatenholm, Bacterial cellulose-based materials and medical devices: Current state and perspectives, *Appl. Microbiol. Biotechnol.* 91 (2011) 1277–1286. <https://doi.org/10.1007/s00253-011-3432-y>.
 - [95] H.G. de Oliveira Barud, R.R. da Silva, H. da Silva Barud, A. Tercjak, J. Gutierrez, W.R. Lustri, O.B. de Oliveira, S.J.L. Ribeiro, A multipurpose natural and renewable polymer in medical applications: Bacterial cellulose, *Carbohydr. Polym.* 153 (2016) 406–420. <https://doi.org/10.1016/j.carbpol.2016.07.059>.
 - [96] E.C. Queirós, S.P. Pinheiro, J.E. Pereira, J. Prada, I. Pires, F. Dourado, P. Parpot, M. Gama, Hemostatic

- Dressings Made of Oxidized Bacterial Nanocellulose Membranes, Polysaccharides. 2 (2021) 80–99. <https://doi.org/10.3390/polysaccharides2010006>.
- [97] S. Peng, Y. Zheng, J. Wu, Y. Wu, Y. Ma, W. Song, T. Xi, Preparation and characterization of degradable oxidized bacterial cellulose reacted with nitrogen dioxide, *Polym. Bull.* 68 (2012) 415–423. <https://doi.org/10.1007/s00289-011-0550-8>.
- [98] Y. Hou, X. Wang, J. Yang, R. Zhu, Z. Zhang, Y. Li, Development and biocompatibility evaluation of biodegradable bacterial cellulose as a novel peripheral nerve scaffold, *J. Biomed. Mater. Res. - Part A.* 106 (2018) 1288–1298. <https://doi.org/10.1002/jbm.a.36330>.
- [99] M.S.A. Camargo, A.P. Cercal, V.F. Silveira, K.C.B. Mancinelli, R.M.M. Gern, M.C.F. Garcia, G.P. Apati, A.L. dos Santos Schneider, A.P.T. Pezzin, Evaluation of Wet Bacterial Cellulose Degradation in Different Environmental Conditions, *Macromol. Symp.* 394 (2020) 1–8. <https://doi.org/10.1002/masy.202000149>.
- [100] S.B. Schröpfer, M.K. Bottene, L. Bianchin, L.C. Robinson, V. De Lima, V.D. Jahno, H. Da Silva Barud, S.J.L. Ribeiro, Biodegradation evaluation of bacterial cellulose, vegetable cellulose and poly (3-hydroxybutyrate) in soil, *Polimeros.* 25 (2015) 154–160. <https://doi.org/10.1590/0104-1428.1712>.
- [101] Z. Shi, Y. Zhang, G.O. Phillips, G. Yang, Utilization of bacterial cellulose in food, *Food Hydrocoll.* 35 (2014) 539–545. <https://doi.org/10.1016/j.foodhyd.2013.07.012>.
- [102] S. Lam, K.P. Velikov, O.D. Velev, Pickering stabilization of foams and emulsions with particles of biological origin, *Curr. Opin. Colloid Interface Sci.* 19 (2014) 490–500. <https://doi.org/10.1016/j.cocis.2014.07.003>.
- [103] D.K.F. Santos, R.D. Rufino, J.M. Luna, V.A. Santos, L.A. Sarubbo, Biosurfactants: Multifunctional biomolecules of the 21st century, *Int. J. Mol. Sci.* 17 (2016) 1–31. <https://doi.org/10.3390/ijms17030401>.
- [104] B.P. Binks, Particles as surfactants - similarities and differences, *Curr. Opin. Colloid Interface Sci.* 7 (2002) 21–41.
- [105] S. Ariyaprakai, S.R. Dungan, Influence of surfactant structure on the contribution of micelles to Ostwald ripening in oil-in-water emulsions, *J. Colloid Interface Sci.* 343 (2010) 102–108. <https://doi.org/10.1016/j.jcis.2009.11.034>.
- [106] M.Y. Koroleva, E. V. Yurtov, Effect of ionic strength of dispersed phase on Ostwald ripening in water-in-oil emulsions, *Colloid J.* 65 (2003) 40–43. <https://doi.org/10.1023/A:1022362807131>.
- [107] M. Salou, B. Siffert, A. Jada, Study of the stability of bitumen emulsions by application of DLVO theory, *Colloids Surfaces A Physicochem. Eng. Asp.* 142 (1998) 9–16. [https://doi.org/10.1016/S0927-7757\(98\)00406-3](https://doi.org/10.1016/S0927-7757(98)00406-3).
- [108] W.R. Schowalter, A.B. Eidsath, Brownian flocculation of polymer colloids in the presence of a secondary minimum, *Proc. Natl. Acad. Sci.* 98 (2001) 3644–3651. <https://doi.org/10.1073/pnas.061028498>.
- [109] C. Costa, B. Medronho, A. Filipe, I. Mira, B. Lindman, H. Edlund, M. Norgren, Emulsion formation and stabilization by biomolecules: The leading role of cellulose, *Polymers (Basel).* 11 (2019) 1–18. <https://doi.org/10.3390/polym11101570>.
- [110] E. Dickinson, Hydrocolloids and emulsion stability, in: G.O. Philips, P.A. Williams (Eds.), *Handb. Hydrocoll.*, 2 Ed, Woodhead Publishing, 2009: pp. 23–49. <https://doi.org/10.1533/9781845695873.23>.
- [111] E. Dickinson, Use of nanoparticles and microparticles in the formation and stabilization of food emulsions, *Trends Food Sci. Technol.* 24 (2012) 4–12. <https://doi.org/10.1016/j.tifs.2011.09.006>.
- [112] Y. Chevalier, M.A. Bolzinger, Emulsions stabilized with solid nanoparticles: Pickering emulsions, *Colloids Surfaces A Physicochem. Eng. Asp.* 439 (2013) 23–34. <https://doi.org/10.1016/j.colsurfa.2013.02.054>.

- [113] Z. Hu, S. Ballinger, R. Pelton, E.D. Cranston, Surfactant-enhanced cellulose nanocrystal Pickering emulsions, *J. Colloid Interface Sci.* 439 (2015) 139–148. <https://doi.org/10.1016/j.jcis.2014.10.034>.
- [114] R. Aveyard, B.P. Binks, J.H. Clint, Emulsions stabilised solely by colloidal particles, *Adv. Colloid Interface Sci.* 100–102 (2003).
- [115] F. Cherhal, F. Cousin, I. Capron, Structural Description of the Interface of Pickering Emulsions Stabilized by Cellulose Nanocrystals, *Biomacromolecules.* 17 (2016) 496–502. <https://doi.org/10.1021/acs.biomac.5b01413>.
- [116] F. Niu, B. Han, J. Fan, M. Kou, B. Zhang, Z.J. Feng, W. Pan, W. Zhou, Characterization of structure and stability of emulsions stabilized with cellulose macro/nano particles, *Carbohydr. Polym.* 199 (2018) 314–319. <https://doi.org/10.1016/j.carbpol.2018.07.025>.
- [117] Y. Yaginuma, T. Kijima, Effects of microcrystalline cellulose on suspension stability of cocoa beverage, *J. Dispers. Sci. Technol.* 27 (2006) 941–948. <https://doi.org/10.1080/01932690600766306>.
- [118] J. Nsor-Atindana, M. Chen, H.D. Goff, F. Zhong, H.R. Sharif, Y. Li, Functionality and nutritional aspects of microcrystalline cellulose in food, *Carbohydr. Polym.* 172 (2017) 159–174. <https://doi.org/10.1016/j.carbpol.2017.04.021>.
- [119] F. Dourado, M. Leal, D. Martins, A. Fontão, A. Cristina Rodrigues, M. Gama, Celluloses as Food Ingredients/Additives: Is There a Room for BNC?, in: M. Gama, F. Dourado, S. Bielecki (Eds.), *Bact. Nanocellulose From Biotechnol. to Bio-Economy*, Elsevier B.V, 2016: pp. 123–133. <https://doi.org/10.1016/B978-0-444-63458-0.00007-X>.
- [120] S. Fujisawa, E. Togawa, K. Kuroda, Nanocellulose-stabilized Pickering emulsions and their applications, *Sci. Technol. Adv. Mater.* 18 (2017) 959–971. <https://doi.org/10.1080/14686996.2017.1401423>.
- [121] M. Andresen, P. Stenius, Water - in - oil Emulsions Stabilized by Hydrophobized Microfibrillated Cellulose Water-in-oil Emulsions Stabilized by Hydrophobized Microfibrillated Cellulose, 2691 (2007). <https://doi.org/10.1080/01932690701341827>.
- [122] C. Jiménez Saelices, I. Capron, Design of Pickering Micro- and Nanoemulsions Based on the Structural Characteristics of Nanocelluloses, *Biomacromolecules.* 19 (2018) 460–469. <https://doi.org/10.1021/acs.biomac.7b01564>.
- [123] X. Lu, H. Zhang, Y. Li, Q. Huang, Fabrication of milled cellulose particles-stabilized Pickering emulsions, *Food Hydrocoll.* 77 (2018) 427–435. <https://doi.org/10.1016/j.foodhyd.2017.10.019>.
- [124] L. Bai, S. Lv, W. Xiang, S. Huan, D.J. McClements, O.J. Rojas, Oil-in-water Pickering emulsions via microfluidization with cellulose nanocrystals: 1. Formation and stability, *Food Hydrocoll.* 96 (2019) 699–708. <https://doi.org/10.1016/j.foodhyd.2019.04.038>.
- [125] Q. Li, Y. Wang, Y. Wu, K. He, Y. Li, X. Luo, B. Li, C. Wang, S. Liu, Flexible cellulose nanofibrils as novel pickering stabilizers: The emulsifying property and packing behavior, *Food Hydrocoll.* 88 (2019) 180–189. <https://doi.org/10.1016/j.foodhyd.2018.09.039>.
- [126] B. Medronho, A. Filipe, C. Costa, A. Romano, B. Lindman, H. Edlund, M. Norgren, Microrheology of novel cellulose stabilized oil-in-water emulsions, *J. Colloid Interface Sci.* 531 (2018) 225–232. <https://doi.org/10.1016/j.jcis.2018.07.043>.
- [127] I. Kalashnikova, H. Bizot, P. Bertoncini, B. Cathala, I. Capron, Cellulosic nanorods of various aspect ratios for oil in water Pickering emulsions, *Soft Matter.* 9 (2013) 952–959. <https://doi.org/10.1039/c2sm26472b>.
- [128] A.G. Souza, R.R. Ferreira, L.C. Paula, L.F.G. Setz, D.S. Rosa, The effect of essential oil chemical structures on Pickering emulsion stabilized with cellulose nanofibrils, *J. Mol. Liq.* 320 (2020) 114458. <https://doi.org/10.1016/j.molliq.2020.114458>.
- [129] T. Winuprasith, M. Suphantharika, Properties and stability of oil-in-water emulsions stabilized by

- microfibrillated cellulose from mangosteen rind, *Food Hydrocoll.* 43 (2015) 690–699. <https://doi.org/10.1016/j.foodhyd.2014.07.027>.
- [130] I. Capron, B. Cathala, Surfactant-free high internal phase emulsions stabilized by cellulose nanocrystals, *Biomacromolecules.* 14 (2013) 291–296. <https://doi.org/10.1021/bm301871k>.
- [131] R. Aaen, F.W. Brodin, S. Simon, E.B. Heggset, K. Syverud, Oil-in-water emulsions stabilized by cellulose nanofibrils—The effects of ionic strength and pH, *Nanomaterials.* 9 (2019) 1–14. <https://doi.org/10.3390/nano9020259>.
- [132] Y. Jia, X. Zhai, W. Fu, Y. Liu, F. Li, C. Zhong, Surfactant-free emulsions stabilized by tempo-oxidized bacterial cellulose, *Carbohydr. Polym.* 151 (2016) 907–915. <https://doi.org/10.1016/j.carbpol.2016.05.099>.
- [133] C.J. van Oss, R.F. Giese, A. Docoslis, Hyperhydrophobicity of the water-air interface, *J. Dispers. Sci. Technol.* 26 (2005) 585–590. <https://doi.org/10.1081/DIS-200057645>.
- [134] Z. Hu, R. Xu, E.D. Cranston, R.H. Pelton, Stable Aqueous Foams from Cellulose Nanocrystals and Methyl Cellulose, *Biomacromolecules.* 17 (2016) 4095–4099. <https://doi.org/10.1021/acs.biomac.6b01641>.
- [135] N.T. Cervin, L. Andersson, J.B.S. Ng, P. Olin, L. Bergström, L. Waišberg, Lightweight and strong cellulose materials made from aqueous foams stabilized by nanofibrillated cellulose, *Biomacromolecules.* 14 (2013) 503–511. <https://doi.org/10.1021/bm301755u>.
- [136] N.T. Cervin, E. Johansson, J.W. Benjamins, L. Wågberg, Mechanisms behind the Stabilizing Action of Cellulose Nanofibrils in Wet-Stable Cellulose Foams, *Biomacromolecules.* 16 (2015) 822–831. <https://doi.org/10.1021/bm5017173>.
- [137] F. Jiang, Y. Lo Hsieh, Holocellulose Nanocrystals: Amphiphilicity, Oil/Water Emulsion, and Self-Assembly, *Biomacromolecules.* 16 (2015) 1433–1441. <https://doi.org/10.1021/acs.biomac.5b00240>.
- [138] D. Tatsumi, S. Ishioka, T. Matsumoto, Effect of particle and salt concentrations on the rheological properties of cellulose fibrous suspensions, *Nihon Reorogi Gakkaishi.* 27 (1999) 243–248. <https://doi.org/10.1678/rheology.27.243>.
- [139] A. Okiyama, M. Motoki, S. Yamanaka, Bacterial cellulose IV. Application to processed foods, *Food Hydrocoll.* 6 (1993) 503–511. [https://doi.org/10.1016/S0268-005X\(09\)80074-X](https://doi.org/10.1016/S0268-005X(09)80074-X).
- [140] P. Paximada, E. Tsouko, N. Kopsahelis, A.A. Koutinas, I. Mandala, Bacterial cellulose as stabilizer of o/w emulsions, *Food Hydrocoll.* 53 (2016) 225–232. <https://doi.org/10.1016/j.foodhyd.2014.12.003>.
- [141] P. Paximada, A.A. Koutinas, E. Scholten, I.G. Mandala, Effect of bacterial cellulose addition on physical properties of WPI emulsions. Comparison with common thickeners, *Food Hydrocoll.* 54 (2016) 245–254. <https://doi.org/10.1016/j.foodhyd.2015.10.014>.
- [142] X. Zhai, D. Lin, D. Liu, X. Yang, Emulsions stabilized by nanofibers from bacterial cellulose: New potential food-grade Pickering emulsions, *Food Res. Int.* 103 (2018) 12–20. <https://doi.org/10.1016/j.foodres.2017.10.030>.
- [143] X. Zhang, J. Zhou, J. Chen, B. Li, Y. Li, S. Liu, Edible foam based on pickering effect of bacterial cellulose nanofibrils and soy protein isolates featuring interfacial network stabilization, *Food Hydrocoll.* 100 (2020) 105440. <https://doi.org/10.1016/j.foodhyd.2019.105440>.
- [144] P.A. Rühs, F. Storz, Y.A. López Gómez, M. Haug, P. Fischer, 3D bacterial cellulose biofilms formed by foam templating, *Npj Biofilms Microbiomes.* 4 (2018) 1–6. <https://doi.org/10.1038/s41522-018-0064-3>.
- [145] F. Tournilhac, R. Lorant, US 6534071 B1 - COMPOSITION IN THE FORM OF AN OIL IN-WATER EMULSION CONTAINING CELLULOSE FIBRILS, AND ITS USES, ESPECIALLY COSMETIC USES, 2003.
- [146] D.J. McClements, C.E. Gumus, Natural emulsifiers — Biosurfactants, phospholipids, biopolymers, and colloidal particles: Molecular and physicochemical basis of functional performance, *Adv. Colloid Interface Sci.* 234 (2016) 3–26. <https://doi.org/10.1016/j.cis.2016.03.002>.

- [147] L. Gilbert, G. Savary, M. Grisel, C. Picard, Predicting sensory texture properties of cosmetic emulsions by physical measurements, *Chemom. Intell. Lab. Syst.* 124 (2013) 21–31. <https://doi.org/10.1016/j.chemolab.2013.03.002>.
- [148] S. Bom, J. Jorge, H.M. Ribeiro, J. Marto, A step forward on sustainability in the cosmetics industry: A review, *J. Clean. Prod.* 225 (2019) 270–290. <https://doi.org/10.1016/j.jclepro.2019.03.255>.
- [149] P. Dubuisson, C. Picard, M. Grisel, G. Savary, How does composition influence the texture of cosmetic emulsions?, *Colloids Surfaces A Physicochem. Eng. Asp.* 536 (2018) 38–46. <https://doi.org/10.1016/j.colsurfa.2017.08.001>.
- [150] F. Freitas, V.D. Alves, M.A.A. Reis, Bacterial Polysaccharides: Production and Applications in Cosmetic Industry, *Polysaccharides*. (2014) 1–2241. https://doi.org/10.1007/978-3-319-03751-6_63-1.
- [151] M. Caggioni, R. Ortiz, F.A. Barnabas, R.V. Nunes, J.A. Flood, F. Corominas, US 8716213 B2 - Liquid Detergent Composition comprising an external structuring system comprising a bacterial cellulose network, 2014.
- [152] Y.T. Hu, C.S. Palla-Venkata, M.S. Vethamuthu, WO2012065925 A1 - Liquid surfactant compositions structured with fibrous polymer and further comprising citrus fibers having no flow instability or shear banding, n.d.
- [153] R. D'Ambrogio, D.A. Peru, J.E. Gambogi, K.M. Kinscherf, D. Patel, R. Tavares, WO 2011/056951 A1 - Microfibrous cellulose having a particle size distribution for structured surfactant compositions, 2011.
- [154] R.P. Vianna-Filho, C.L.O. Petkowicz, J.L.M. Silveira, Rheological characterization of O/W emulsions incorporated with neutral and charged polysaccharides, *Carbohydr. Polym.* 93 (2013) 266–272. <https://doi.org/10.1016/j.carbpol.2012.05.014>.
- [155] L. Gilbert, V. Loisel, G. Savary, M. Grisel, C. Picard, Stretching properties of xanthan, carob, modified guar and celluloses in cosmetic emulsions, *Carbohydr. Polym.* 93 (2013) 644–650. <https://doi.org/10.1016/j.carbpol.2012.12.028>.
- [156] L. Gilbert, C. Picard, G. Savary, M. Grisel, Rheological and textural characterization of cosmetic emulsions containing natural and synthetic polymers: relationships between both data, *Colloids Surfaces A Physicochem. Eng. Asp.* 421 (2013) 150–163.
- [157] P.J. Tiemstra, Microcrystalline cellulose compositions co-dried with hydrocolloids, 1971.
- [158] W. Claudie, FR2769836A1.pdf, (n.d.).
- [159] R.T. Bianchet, A.L. Vieira Cubas, M.M. Machado, E.H. Siegel Moecke, Applicability of bacterial cellulose in cosmetics – bibliometric review, *Biotechnol. Reports.* 27 (2020) e00502. <https://doi.org/10.1016/j.btre.2020.e00502>.
- [160] H. Ullah, H.A. Santos, T. Khan, Applications of bacterial cellulose in food, cosmetics and drug delivery, *Cellulose*. 23 (2016) 2291–2314. <https://doi.org/10.1007/s10570-016-0986-y>.
- [161] I.F. Almeida, T. Pereira, N.H.C.S. Silva, F.P. Gomes, A.J.D. Silvestre, C.S.R. Freire, J.M. Sousa Lobo, P.C. Costa, Bacterial cellulose membranes as drug delivery systems: An in vivo skin compatibility study, *Eur. J. Pharm. Biopharm.* 86 (2014) 332–336. <https://doi.org/10.1016/j.ejpb.2013.08.008>.
- [162] P. Perugini, M. Bleve, F. Cortinovis, A. Colpani, Biocellulose masks as delivery systems: A novel methodological approach to assure quality and safety, *Cosmetics*. 5 (2018). <https://doi.org/10.3390/cosmetics5040066>.
- [163] T. Amnuakitt, T. Chusuit, P. Raknam, P. Boonme, Effects of a cellulose mask synthesized by a bacterium on facial skin characteristics and user satisfaction, *Med. Devices Evid. Res.* 4 (2011) 77–81. <https://doi.org/10.2147/MDER.S20935>.
- [164] Y. Numata, L. Mazzarino, R. Borsali, A slow-release system of bacterial cellulose gel and nanoparticles for

- hydrophobic active ingredients, Int. J. Pharm. 486 (2015) 217–225.
<https://doi.org/10.1016/j.ijpharm.2015.03.068>.
- [165] Z.-F. Yang, N.A. Morrison, T.A. Talashek, D.F. Brinkmann, D. DiMasi, Y.L. Chen, US 2007/019777 A1 - Bacterial Cellulose-containing formulations, 2007.
- [166] B.P. Heath, T.W. Coffindaffer, K.E. Kyte, E.D. Smith, S.D. McConaughy, WO 2011/019876 A2 - PERSONAL CLEANSING COMPOSITIONS COMPRISING A BACTERIAL CELLULOSE NETWORK AND CATIONIC POLYMER, 2011.
- [167] A. Naderi, T. Lindström, J. Sundström, G. Flodberg, Can redispersible low-charged nanofibrillated cellulose be produced by the addition of carboxymethyl cellulose prior to its drying?, Nord. Pulp Pap. Res. J. 30 (2015).

Chapter 3

Dry BC:CMC formulations with interfacial-active performance: processing conditions and redispersion

Dry or powdered formulations of food additives facilitate transportation, storage, preservation and handling. In this work, dry formulations of bacterial cellulose and carboxymethyl cellulose (BC:CMC), easily redispersible and preserving the functionality of the never-dried dispersions are reported. Different processing parameters and their effect on the materials properties were evaluated, namely: i) wet-grinding of BC (Hand-blender, Microcut Head Impeller, High-pressure Homogenizer), ii) drying of BC:CMC mixtures (fast drying at ≈ 130 °C and slow drying at 80 °C) and subsequent iii) comminution to different particle sizes. The dispersibility of the obtained BC:CMC powders was evaluated, and their functionality after redispersion was assessed by measuring the dynamic viscosity, the effect in oil/water interfacial tension (liquid-liquid system) and the stabilization of cocoa in milk (solid-liquid system).

The size of BC fibre bundles was of paramount relevance to its stabilizing ability in multiphasic systems. A more extensive wet grinding of the BC fibres was accompanied by a loss in the BC:CMC functionality, related to the increasingly smaller size of the BC bundles. Indeed, as the $Dv(50)$ of the wet BC bundles was reduced from 1228 to 55 μm , the BC:CMC viscosity profile dropped and the effect on interfacial tension decreased. This effect was observed both on the never-dried and dry BC:CMC formulations. On the other hand, the drying method did not play a major effect in the materials' properties. In a benchmarking study, the BC:CMC formulations, at a low concentration (0.15 %), had better stabilizing ability of the cocoa particles than several commercial cellulose products.

3.1 - INTRODUCTION

Bacterial cellulose (BC) is an exopolysaccharide synthesized by certain acetic acid bacteria, the *Komagataeibacter* genus being the most important due to the high cellulose yield. As *Komagataeibacter* microorganisms are mandatory aerobes, under static conditions BC is synthesized at the air/liquid interface of the culture medium in the form of a fibrous membrane comprising 99 % water and 1 % cellulose. Morphologically, this biopolymer is organized in elementary nanofibrils with a lateral size of 6 nm to 7 nm, which assemble into ribbon-shaped fibrils less than 100 nm wide and several micrometres in length [1–4]. This high aspect ratio, nanoscale thickness, good mechanical properties and the ability to arrange into structured three-dimensional networks even at low concentrations [5] account for the good performance of BC fibres as a texture/rheology modifier and stabilizer of heterogeneous systems, including food products [6–8].

For bulk commercial applications, dry formulations offer several advantages over aqueous suspensions, such as a decrease in the size and mass, thus lower storage space and transportation costs, improved storage stability and lower risk of contamination. As with plant cellulose, the properties of BC are mostly lost upon drying due to irreversible structural changes - a phenomenon called hornification. One of the most accepted mechanisms for hornification is cocrystallization of the cellulose fibres. As water evaporates, the thin fibres come closer and aggregate, establishing hydrogen bonds between adjacent crystalline domains. These bonds are not broken upon resuspension in water without a significant energy input, resulting in a so called hornified material [2,9].

One of the most usual approaches to prevent hornification is to mix cellulose with an additive to create a steric barrier prior to drying, such as carbohydrates or biopolymers. These polymers might bare a charge, as in the case of the water-soluble polyanionic Carboxymethyl Cellulose (CMC), one of the most commonly used additives in hydrocolloidal cellulose formulations [2,10]. CMC is generally recognized as safe (GRAS) for food consumption by the American Food and Drug Administration and approved by the European Food Safety Authority, often found in food products as Cellulose Gum or E466. It is used as thickener, stabilizer, gelling agent and texture modifier, alone or in combination with non-modified plant-derived celluloses. Being a modified cellulose, CMC shows a selective adsorption towards non-modified cellulose fibres, since it has chemically similar backbone segments, facilitating cooperative hydrogen bonding [11,12]. Bearing negatively charged carboxylic groups, CMC imparts a surface charge to cellulose structures upon adsorption. The electrostatic repulsion forces increase the swelling and dispersion of cellulose in aqueous media, improving its colloidal stability and contributing to the three-dimensional network formation [5].

On the other hand, the presence of a charged drying-aid prevents cooperative hydrogen bonding between adjacent cellulose polymer chains during water evaporation, avoiding hornification. In this type of formulations CMC plays a dual role as co-drying agent and stability enhancer. This methodology has been used for plant cellulose fibres and crystals, in order to obtain dry materials with improved dispersion [13,14]. When redispersed in water, the CMC layer coating the cellulose particles rehydrates, freeing the particles. The material then recovers its initial gel-like form with a microscopic network of interconnected fibres or crystals, preserving, in theory, the functional properties as those of the never-dried material [10,15].

Only a few works have yet focused on obtaining rehydratable or redispersible cellulose from bacterial sources [16,17]; in fact, most of the reports on dry BC formulations are published as patents, which suggests the industrial interest in the use of such materials for areas ranging from food and cosmetics to reinforcement materials and composites [18–21]. Some of these works claim the restoration of the BC fibres properties, as compared to those of the never-dried versions. However, the redispersion methods involve the use of high energy mixing, high temperature, long dispersion times or combinations of these, as well as the use of additives in excess amounts. These energy and time-intensive processes represent high capital and operating costs when considering industrial applications. Furthermore, most of the reports are mainly focused on demonstrating the BC's redispersibility, not clearly demonstrating the recovery of the BC technological properties upon redispersion, as compared to the never-dried material. On the path of devising methods for drying cellulose particles, the effect of processing conditions and their impact in the redispersibility, rehydration and final properties has also been studied by some authors [22–24]. In particular, some work has also been done with BC alone [17,25].

In this work, dry powdered and easily rehydratable BC formulations with CMC (BC:CMC) are reported, which can achieve full redispersion in water under low-energy mixing and within a few minutes, contrarily to other dry (plant based) cellulose products available in the market. To produce the dry powder formulations, different grinding, drying and dispersing methods were evaluated for their impact on the final product's properties. This study presents, for the first time, a systematic approach towards the understanding of the relevant processing conditions for the development of dry BC:CMC formulations bearing suitable redispersion ability, while not compromising the functional features. In particular, in this work we analyse the impact of the extension of grinding (both in wet or dry state) on the size of the obtained fibre bundles and on its functional properties. To our knowledge, the relevance of the size of the bacterial cellulose fibre bundles on its performance as a hydrocolloid has never been reported.

3.2 - MATERIALS AND METHODS

3.2.1 - Preparation of the BC:CMC powders

The different process conditions used to prepare the dry BC:CMC samples are outlined in Figure 3.1.

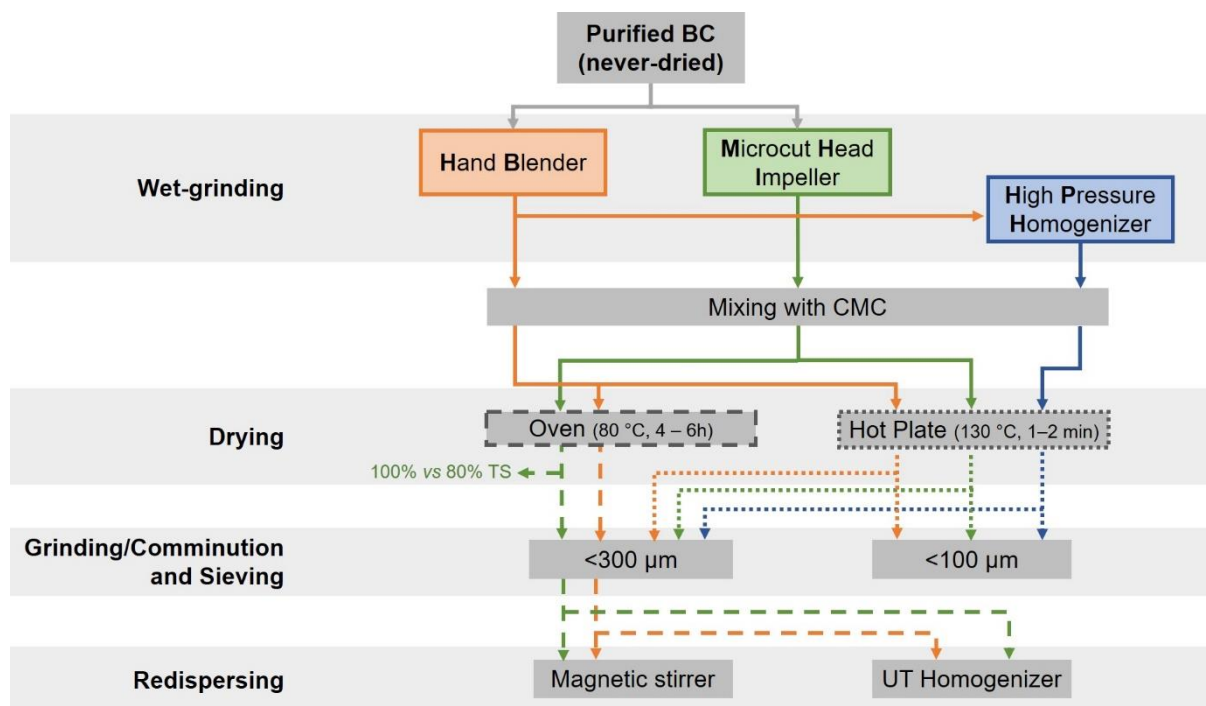


Figure 3.1 - Scheme of the several steps and processing conditions used in this work to obtain the different dry BC:CMC powders.

3.2.1.1 - BC production and purification

BC membranes were produced by static culture using *Komagataeibacter xylinus* BPR 2001 (ATCC 700178), according to the optimized parameters described by Rodrigues et al. (2019). Briefly, the strain was grown in Hestrin-Schramm culture medium (in m/v): 2.0 % glucose (Fisher Chemical), 0.5 % peptone (OXOID), 0.5 % yeast extract (OXOID), 0.27 % disodium phosphate (Panreac) and 0.115 % citric acid (Panreac), initial pH 5.5 set by using 18% (v/v) HCL (Fisher-Chemical). This culture (inoculum) was incubated for 2 d at 30 °C under static conditions. Afterwards, it was transferred to large square containers with a different culture medium, making up 10 % of the final volume. This cultured medium consisted of 0.27 % (m/v) disodium phosphate, 0.115 % (m/v) citric acid, 5.38 % (m/v, sugar basis) molasses (a gift from RAR Refinarias de Açúcar Reunidas, S.A.; Portugal), 1.91 % (m/v, protein basis) CSL (a gift from COPAM Companhia Portuguesa de Amidos, S.A.; Portugal), 0.63 % (m/v) ammonium

sulphate (Panreac) and 1.38 % (v/v) ethanol (Fisher-Chemical), pH 5.5 (set with 18 % HCl). The culture was incubated in static conditions for 30 days at 30 °C.

After cultivation, the BC membranes were washed with distilled water, then thoroughly with 0.1 M NaOH (Fisher-Chemical) at room temperature, with changes twice a day, until the membranes turned completely white. Then, they were washed again with distilled water until reaching the same pH as that of distilled water.

3.2.1.2 - Wet grinding of BC

Purified bacterial cellulose membranes were wet-ground by three different methods (Figure 3.1):

- Using a Sammic fixed speed hand blender (HB), 9000 rpm (model TR250, Samic, S.L.), for about 1 min until a visually homogeneous pulp was obtained;
- Submitting the BC membranes (previously cut in cubes) to 2 passages through a Microcut Head Impeller (MHI), Comitrol® Processor Model 1700 (Urschel Laboratories Inc.). In each passage, grinding of BC was done at 900 Rpm, using a labyrinth Vericut impeller and a cutting head 160 at 5° inclination;
- The pulp obtained with the hand blender was further processed in a High-Pressure Homogenizer (HPH) using a GEA Niro Soavi, model Panther NS3006L, at 600 Bar. BC was collected after 1 cycle (HPH-1), 2 cycles (HPH-2) and 6 cycles (HPH-6), through the High-Pressure Homogenizer.

3.2.1.3 - Mixing Bacterial Cellulose with sodium Carboxymethyl Cellulose

The wet-ground BC pulp obtained by the three different methods described in the previous section, was mixed with a solution of sodium Carboxymethyl Cellulose (CMC, 90 KDa, D.S.= 0.7, Sigma) at a mass ratio of 1:1 (BC:CMC), to a final solids content of 2 %. This mixture was left under magnetic stirring overnight at room temperature.

3.2.1.4 - Drying of the BC:CMC mixtures

To study the effect of the drying method, wet BC:CMC mixtures obtained from section 2.1.3 (HB, MHI and HPH ground BC:CMC) were dried by two different methods:

- Fast drying in a hot plate (HP), an Ariette Crepes Maker, model 183. A thin layer of BC:CMC sample was spread over the hot plate at 130 °C, for only a few minutes (1-2 min). With this process, a completely dry BC:CMC product was obtained (100 % total solids (TS)).
- Slow drying in an oven (OV), in aluminium pans for 4 h to 6 h, at 80 °C. MHI ground samples were retrieved at 80 % TS and 100 % TS, to evaluate the effect of residual moisture on the dispersibility of BC:CMC formulations.

3.2.1.5 - Grinding and sieving

The HP and OV dried materials were ground with a High Power Herb Grain Grinder Cereal Mill Powder Grinding Machine Flour 600G. To assess the effect of particle size on the properties of the BC:CMC formulations, the ground powders were then sieved to different particle size ranges: <100 µm (Endecotts, Ltd, aperture 106 µm), <300 µm (Endecotts, Ltd, aperture 300 µm).

3.2.2 - Evaluation of the dispersibility

To evaluate the dispersibility of the dry and ground BC:CMC mixtures, samples were prepared at 0.5 % (m/v on dry basis, by correcting the amount of residual moisture of BC:CMC) in water, at room temperature, by two methods:

- Low mechanical shearing, using a magnetic stirrer (MS) plate (Stuart SD162), at 900 Rpm for 5 min;
- High shear mixing, using an Ultra-turrax Homogenizer (UT) Unidrive X1000D (CAT Scientific) with a T20-F generator dispersing tool, at 15000 Rpm for 5 min.

The dispersed materials were spread over a petri dish and observed at naked eye.

3.2.3 - Microscopic observations

For fluorescence optical microscopy, never-dried BC samples (0.01 % m/v, dry basis) wet-ground by the above-mentioned methods, were placed on glass slides, stained with 10 µg/mL Calcofluor White stain (Sigma) for 1 min (protected from light), coverslipped and visualized on an Olympus BX51 fluorescence microscope with a DAPI filter (Excitation wavelength: 365 – 370 nm; Emission wavelength: 421 nm).

BC:CMC powders observation was performed using a desktop Scanning Electron Microscope (SEM) coupled with energy-dispersive X-ray spectroscopy analysis (Phenom ProX, Phenom-World BV). Samples were added to aluminium pin stubs with electrically conductive adhesive carbon tape and coated with 2 nm Au prior to analysis.

3.2.4 - Size measurements

The measurement of the BC bundle size was carried out in a Malvern Mastersizer 3000 laser diffraction instrument equipped with a Hydro EV sample dispersion unit (Malvern Panalytical, Malvern, UK). Aqueous suspensions of wet-ground BC samples were added to the sample dispersion unit prefilled with tap water, until an obscuration level between 10 and 20 % (as recommended by the equipment manufacturer) was reached. The stirring rate in the dispersion unit was set at 1500 rpm with initial ultrasonication (35 W)

for 10 s. The detector array measured the scattering pattern during 30 s. Five measurements were performed per sample. The refractive index of cellulose and water were assumed as 1.468 and 1.330 respectively (as provided by the software's database) and Mie scattering model was used for non-spherical particles. The particles size was then expressed as the volume distribution percentiles, Dv(50) (Mass Median Diameter, the size at which 50 % of the sample is smaller and 50 % is larger), Dv(10) and Dv(90) (the size of particle below which 10 % and 90 % of the sample lies, respectively); also the Volume Moment Mean, D[4,3], and the Surface Area Mean, D[3,2].

3.2.5 - Viscosity measurements

The viscosity profiles of the redispersed BC:CMC samples were measured in a controlled stress rheometer (DHR-1, TA instruments) with TRIOS Software (TA Instruments) at 25 °C using a cone and plate geometry (60 mm, 2.006° cone angle, 64 µm gap). Prior to analysis, dried and ground samples were redispersed either by magnetic stirring or Ultra-turrax homogenizer. Flow tests were performed in duplicate at increasing shear rates (0.01 to 100 s⁻¹). Shear rate versus viscosity graphs were drawn in semi-log scale to better visualise the different rheological profiles at low shear rates.

3.2.6 - Interfacial tension

Interfacial tension between isohexadecane and aqueous suspensions of the non-dried and dry BC:CMC materials (prepared by magnetic stirring) was measured with the pendant drop method using Optical Contact Angle (OCA 20, DataPhysics), and SCA 20 Software module 22 (DataPhysics). A volume of 2 mL of isohexadecane was placed on a disposable optical polystyrene macro standard fluorescence cuvette (1 cm x 1 cm x 4.5 cm) (Labbox). A disposable 1 mL syringe with a needle of 0.71 mm outer diameter, containing the aqueous sample suspensions (heavier phase) was introduced in the cuvette, with the needle always at the same depth. First, maximum drop volume was determined for each sample. For each drop, profile extraction and IFT calculation were made automatically, 10 times per minute until 25 readings, in triplicate for each sample and at 20 ± 1 °C.

Statistical analysis of these results was performed using GraphPad Prism 5 (GraphPad Software). Results were expressed as mean of three separate measurements and respective Standard Deviation. A one-way analysis of variance (ANOVA) was performed, followed by Tukey's Multiple Comparison Test to establish the significance of differences with the H₂O control and between all datasets.

3.2.7 - Effect of BC:CMC formulations on the suspension stability of cocoa beverage

3.2.7.1 - Effect of drying and grinding

The effect of particle size of BC:CMC formulations on the suspension stability of cocoa particles in a chocolate milk beverage, was evaluated. For this, BC:CMC samples (i) never-dried; ii) dried in Hot Plate, ground and sieved to different particle size ranges), were used at a final concentration of 0.15 % (m/v dry basis). Pure cocoa (1.2 % m/v) and BC:CMC were added to 15 mL of medium-skimmed milk. The mixtures were stirred in a vortex (2,800 rpm) for 3 min at room temperature and then pasteurized at 75 °C for 15 seconds. A control, where no BC:CMC was added, was also prepared in the same manner. Samples were stored at room temperature and the cocoa particles sedimentation was evaluated over time. The stabilization of the chocolate drinks was quantified by calculating the percentage of cocoa sedimentation, according to equation 2:

$$Stability (\%) = \frac{Volume\ of\ Milk\ with\ suspended\ Cocoa}{Total\ Milk\ Volume} \times 100 \quad (eq. 2)$$

where 100 % stability corresponds to a fully stabilized cocoa suspension.

3.2.7.2. Benchmark assay

Several plant-derived commercial celluloses were used in a benchmarking study: hydrocolloidal microcrystalline Avicel RT1133 and CM2159 with CMC, and non-colloidal Avicel LM310 (FMC Biopolymer); microcrystalline Novagel RCN-15 and RCN-10 (FMC Biopolymer), with Guar gum; sulphated Celluforce NCC nanocrystals (from Celluforce Inc.). These materials - differing in size, morphology, presence of additives and chemical modification - are all marketed as stabilizers and rheology/texture modifiers for food products and have been previously characterized [5]. Furthermore, Bioplus-L Fibrils (lignin-coated cellulose nanofibrils from wood, American Process, Inc.), although not being commercialized for food applications, were also used for their fibrillar nature and nanoscale thickness, similar to BC. According to the manufacturer, these fibres are 5 - 200 nm wide and 500 nm to several micron in length.

An assay was done using the same conditions as in section 3.2.7.1, with above referred celluloses and CMC. All Avicel and Novagel celluloses were previously activated, for 30 min, at 23 800 Rpm, according to the specification's sheets.

3.3 - RESULTS

BC membranes obtained by static culture were processed by wet grinding, mixed with CMC, dried, ground (or dry comminuted) and sieved to different size ranges. The effect of these different and sequential processing methods on the size of BC, dispersibility, rheological behaviour (viscosity) of BC:CMC and its stabilizing effect on a solid/liquid suspension were studied.

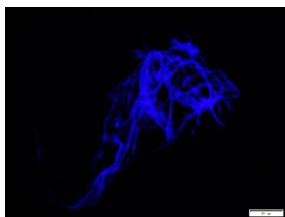
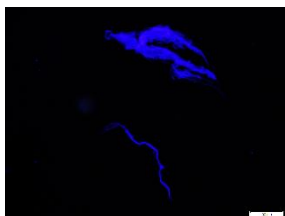
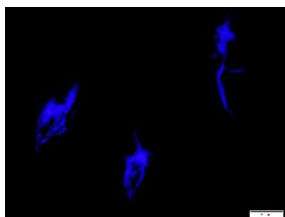
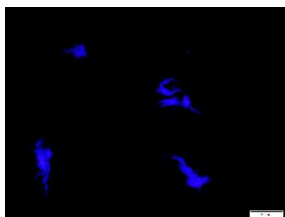
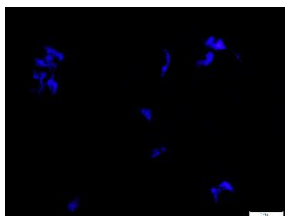
3.3.1 - Effect of wet-grinding method on BC bundle size

Three BC homogenization methods were used, providing different levels of shear force, leading to different degrees of fibre comminution or disaggregation of the fibre bundles. Table 3.1 shows the results of the size of the fibre aggregates or flocs, as measured by laser diffraction, as well as illustrative micrographs obtained by staining with Calcofluor White.

When produced under static conditions, BC fibres are organized as a 3D nanofibrillar network of entangled fibres. When submitted to mechanical shear, the fibre network is broken down into fleeces of flocs, composed mainly by fibre bundles of variable size and shape. These bundles have a star-resembling structure, with loose fibre branches emerging from a deeply entangled core. With increasing grinding shear (HB<MHI<HPH), the size of the bundles decreases, the branches become less evident and the core becomes denser. This is especially the case with the use of HPH, where the BC bundles are submitted to cycles of compression and decompression, contrarily to HB and MHI, where the BC bundles are obtained through the mechanical action of the high shear spinning blades.

Regarding the particle size characterization, the D[4,3] reflects the size of those particles which constitute the bulk of the sample volume, while D[3,2] is most sensitive to the presence of fine particulates in the size distribution. The differences between these two mean values for the same sample, plus the large variation of the percentiles, indicate its wide size distribution (more evident in the case of HB). HB ground BC showed the highest mean size of fibre bundles. With the increase in the shearing stress (to MHI and HPH) and compression/decompression cycles (HPH 1 to 6 cycles), an increase in the BC defibrillation/fragmentation occurred, as observed in all the values of the percentiles and mean diameters. In all HPH samples only micrometric fragments were observed, most of them being below 100 μm , the micrographs also suggesting that these bundles bear higher density, as mentioned, likely due to the compression forces associated with the homogenization process.

Table 3.1 - Percentiles and Mean Diameters of the particle size distribution (by volume) of BC samples wet-ground by different methods, and respective micrographs (scale bars correspond to 100 μm). All measurements satisfy the quality criteria since the Residuals (%) and Weighted Residuals (%) are $\leq 1\%$

	Percentiles (μm)			Span	Mean Diameters (μm)		
	Dv(10)	Dv(50)	Dv(90)		D[4,3]	D[3,2]	
HB	254	1228	2299	2	1205	514	
MHI	108	575	1700	3	757	254	
HPH-1	24	79	229	3	107	52	
HPH-2	24	71	187	2	91	50	
HPH-6	22	55	139	2	70	43	

3.3.2 - Properties of the never-dried BC formulations after CMC addition

Well-dispersed suspensions are a prerequisite in many industrial applications. Suspensions of cellulosic materials, such as BC, exhibit pronounced aggregation in aqueous media due to strong interfibrillar hydrogen bonds and Van der Waals attractions [15]. To overcome this issue, CMC was added to BC, at

mass ratio of 1:1 as described in 3.2.1.3. The water-soluble anionic polyelectrolyte plays a determinant role in ensuring the dispersibility of the BC fibres and allowing their stabilization in aqueous media. The negative charge of CMC contributes to the improved dispersion of the BC fibres due to steric hindrance. Non-adsorbed CMC may also prevent the agglomeration of BC fibres due to the creation of a hydration shell around BC, thus also contributing to the improved dispersibility and stability in aqueous media. The presence of CMC improves the final performance of the formulation, even though BC fibres are the responsible for the product's viscosity and stabilizing ability. The properties of a BC:CMC mixture have been shown to be superior to BC or CMC alone [5].

The never-dried BC:CMC samples were magnetically stirred (low energy mixing), or homogenized with Ultra-turrax (high shear mixing). Samples dispersed using only magnetic stirring still showed small fibre bundles and agglomerates, but after treatment with UT a homogeneous suspension was obtained (minimum of fibre bundles were visually observed). These results also show that, in the conditions used, the wet-grinding of BC is insufficient to yield a fully dispersed fibre suspension after adding CMC, an additional high energy mixing with the UT being necessary to achieve that goal. The viscosity profiles of the BC:CMC samples dispersed with UT are shown in Figure 3.2. Although not shown, the analysis of the never-dried BC:CMC samples without UT treatment was performed and the general trend is similar to the one obtained with those processed with the UT, suggesting that UT does not compromise the fibres viscosity - it mainly further disaggregates the larger bundles producing a more homogeneous mixture.

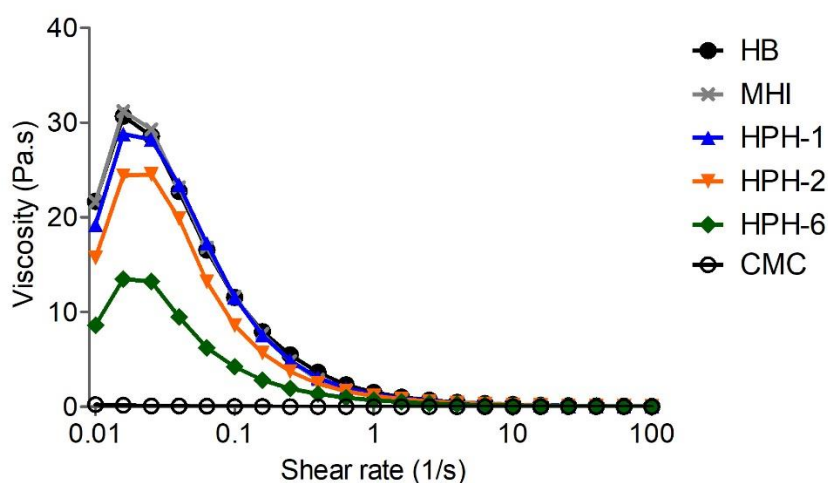


Figure 3.2 - Viscosity profiles of 0.5% (m/v) of CMC and never-dried BC:CMC mixtures with BC from the different grinding methods, diluted and dispersed using Ultra-turrax.

From Figure 3.2 it can be seen that after a first shearing, where the molecules in the sample rearrange and orient, all BC:CMC samples show a shear-thinning behaviour. It is also clear that the wet grinding method affected the viscosity profile of the BC:CMC mixtures: in general, the smaller the initial BC fibre bundle size, the lower the viscosity of the BC:CMC dispersions. CMC alone has much lower viscosity than the BC:CMC formulations at the same concentration, so the increase in viscosity can be imparted on the BC fibres.

It was not possible to analyse samples of wet-ground BC without CMC. BC suspensions exhibit pronounced aggregation in aqueous media, making it impossible for the sample to be continuously sheared in the rheometer without entanglements (for the viscosity measurements), or to flow through a syringe (for the IFT determination, further below).

Figure 3.3 shows the results of the interfacial tension between water dispersions of never-dried BC:CMC and isohexadecane, using the Pendant Drop method.

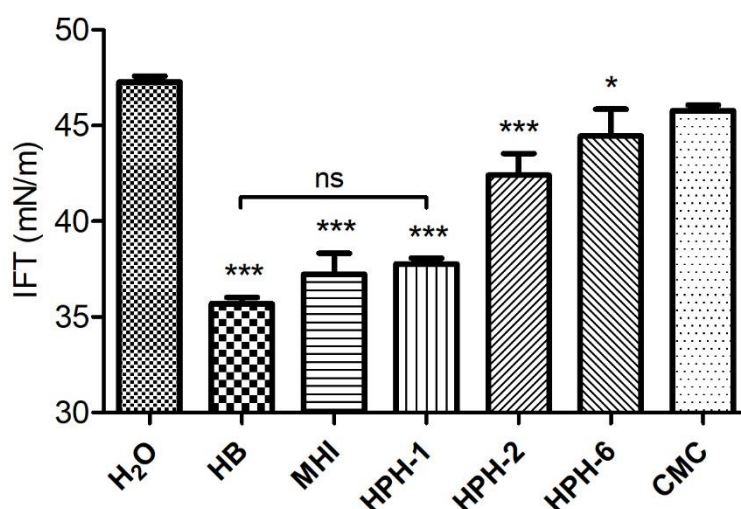


Figure 3.3 - Effect of wet grinding of BC on the Interfacial Tension of Isohexadecane/Water containing 0.5 % (m/v) never-dried BC:CMC. Results are expressed as average of triplicate measurements and bars are representative of the Standard Deviation. All datasets were compared with each other using one-way ANOVA followed by Tukey's Multiple Comparison Test (significant at * $p < 0.05$, *** $p < 0.001$, when compared with the H₂O control; ns – not significant comparing HB with HPH-1).

Isohexadecane is a lightweight hydrocarbon (0.79 g/mL at 20 °C) used in cosmetic applications and the energy of its interface with distilled water was 47.3 ± 0.3 mN/m. The IFT value significantly decreased in the presence of 0.5 % BC:CMC, in BC samples wet ground by HB, MHI and HPH-1, indicating that, despite differences in the mean particle size (Table 3.1), the fibres possess similar interface activity and can promote the stabilization of this heterogeneous liquid-liquid system. However, the IFT reduction was less

and less evident as the BC was more fragmented, becoming very close to that of pure water for the HPH-6 sample. As the effect of non-dried BC:CMC on the isohexadecane/water interface becomes smaller, we can say there's a decrease in the formulation's functionality with the reduction in fibres' size. A similar effect and functionality loss was observed for the viscosity with increasing fragmentation of the fibres (Figure 3.2).

3.3.3 - Effect of drying and redispersion methods

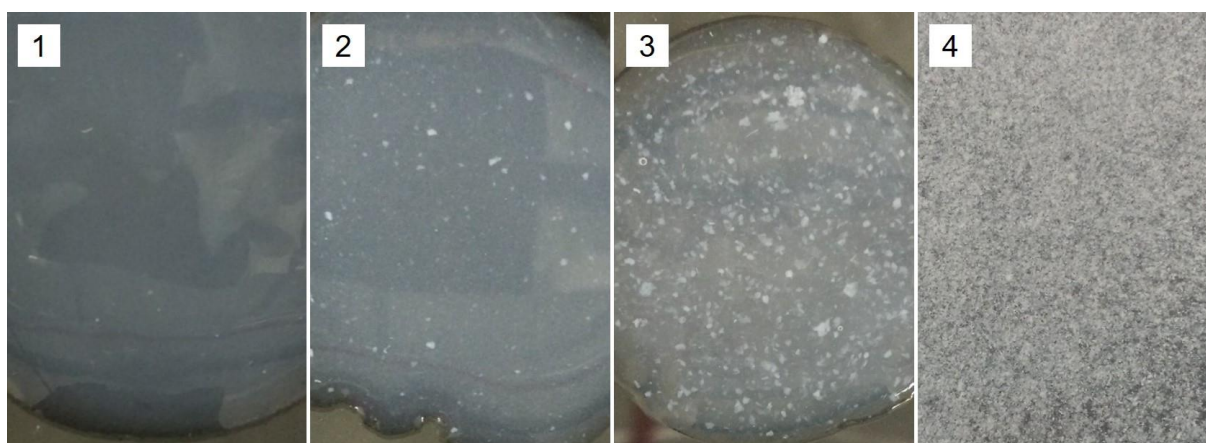
Different drying methods have been tested with nanocelluloses [24], including BC [16,17,25]. Freeze-drying yields best results in preventing hornification in whole BC membranes, since the water is sublimated and the 3D structure is maintained, avoiding collapsing and aggregation of the fibres [17,25,26]. However, freeze-drying is an expensive technology for a scaled-up production process. On the other hand, Amin et al. [16] also prepared dry powders with purified BC by spray-drying. They employed particle size analysis to determine the ease of redispersion of the powders, only concluding that no further agglomeration occurred between the particles after drying. Besides, the reported swelling index and water retention capacity values show that the powders were only limitedly redispersible, as compared to the water retention capacity of the never-dried BC (over 100 fold the dry weight) [26]. In addition, no further tests were performed to assess the preservation of the fibres functionality. In this work we produced a fully redispersible powdered BC:CMC formulation, using simple and more scalable methods: hot plate and oven drying.

Table 3.2 summarizes the aqueous dispersibility scores for the dried and ground BC:CMC mixtures (size <300 µm). Dispersibility of the formulations was classified as follows: 1 - sample is homogeneous and no visible particles or aggregates are observable; 2 - sample contains some very small particles or aggregates; 3 - the sample contains some larger particles or aggregates; 4 - non-dispersible, the water remains transparent and the well separated particles or aggregates are observed. Corresponding images of samples bearing the different dispersibility scores can be found in Figure 3.4.

For dried BC:CMC samples redispersed in water under low shear (magnetic stirring) some fibre bundles or particle fragments were still visible at naked eye, whereas with a high shear treatment (UT), the BC fibres were completely dispersed. This behaviour was consistent in all samples regardless of the wet grinding method; moreover, the material dispersibility was also independent of the presence of residual moisture in the sample, for both 80 % and 100 % TS materials showed good dispersion in water (also further improved with UT homogenization).

Table 3.2 - Dispersibility of BC:CMC mixtures after drying, grinding and sieving to a particle size of <300 µm

Wet grinding	Drying	Dispersion	Dispersibility
HB	Hot Plate	Magnetic stirrer	2
	Oven		
MHI	Hot Plate	UT Homogenizer	1
	80% TS		
	Oven 100% TS		
HPH-1			
HPH-2	Hot plate	Magnetic stirrer	2
		UT Homogenizer	1
HPH-6			

**Figure 3.4** - Classification of the dispersibility of dry BC:CMC formulations in water, at 0.5 % (m/v): 1 - sample is homogeneous and no visible particles or aggregates are observable; 2 - sample contains some very small particles or aggregates; 3 – the sample contains some larger particles or aggregates; 4 – non-dispersible, the water remains transparent and the well separated particles or aggregates are observed.

It is worth to mention that UT homogenization is efficient in redispersing all BC:CMC formulations in aqueous media, independently of the previous processing used; furthermore, with UT homogenization it was also possible to disperse larger size fractions than <300 µm, and even the whole BC:CMC dry powders before sieving. The need for a formulation with smaller sized particles is only applicable when pursuing a material that can be redispersed using low energy mixing.

In addition to Table 3.2, redispersion of dry BC (HB treatment, hot plate and oven dried, sieved to <300 µm) without CMC was unsuccessful – classified as 4, non-dispersible, even after UT homogenization.

BC:CMC samples dried by either of the tested methods and then ground and sieved to different granulometries were redispersed using low shear (magnetic stirring) and high shear (UT homogenizer). The obtained samples were analysed by rheological tests (Figure 3.5).

As observed previously for the never-dried samples, the harsher the wet-grinding treatments (yielding smaller wet BC fibre bundles), the lower the viscosity of the corresponding samples obtained after undergoing drying and redispersion. This tendency can be observed in all graphics from Figure 3.5, for both drying methods and for the different dry particle sizes. Thus, the influence of wet-grinding of the BC membranes on viscosity still remains following drying and redispersion.

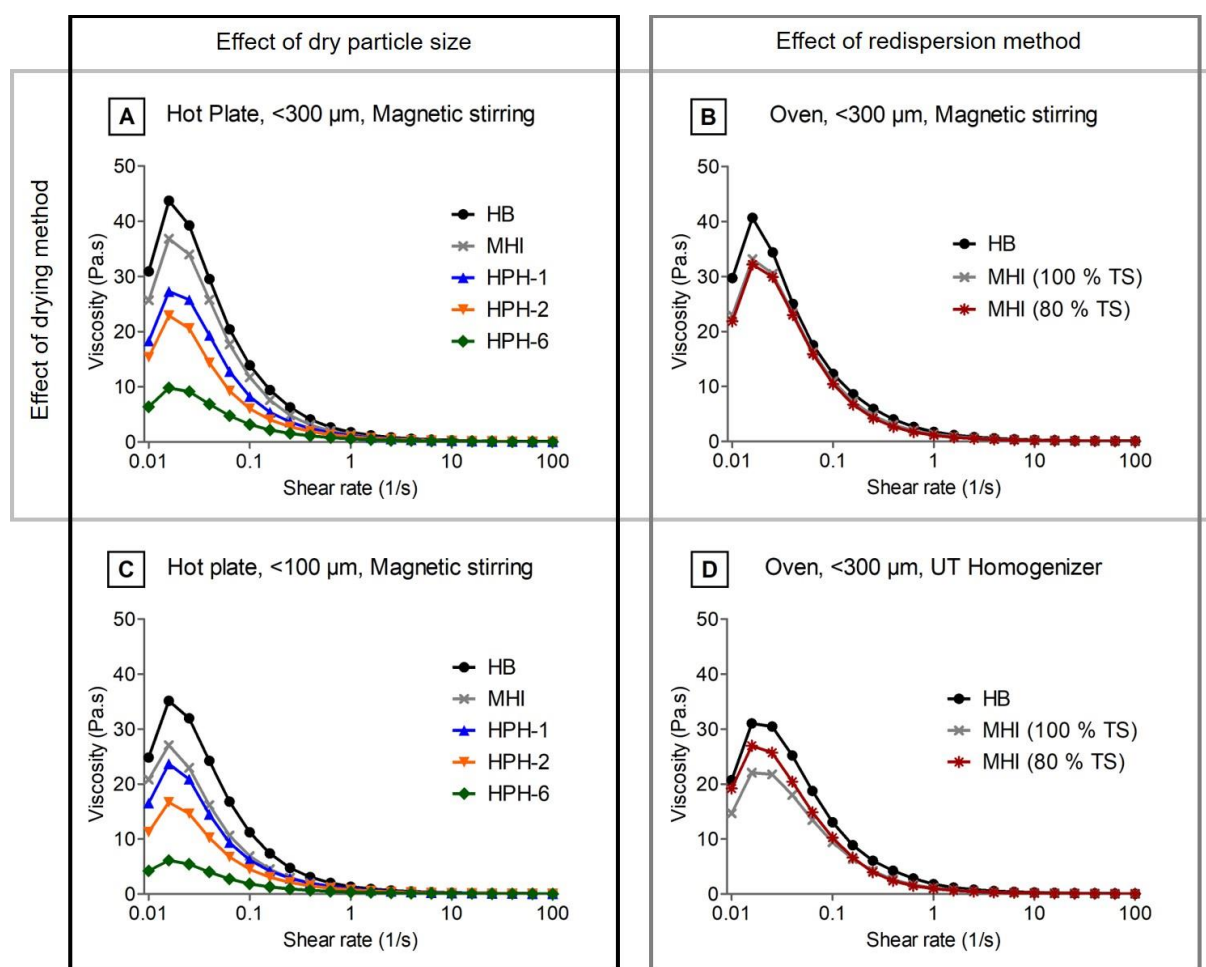


Figure 3.5 - Dynamic viscosity profiles of 0.5 % (m/v) BC:CMC powders redispersed in water, following different drying (hot plate or oven) and comminution (to sizes <300 µm or <100 µm), and redispersed using UT homogenizer or Magnetic stirring.

Furthermore, a comparison of Figure 3.5-A and 3.5-C shows that samples processed similarly (wet grinding, drying, redispersion), but dry ground to different granulometry present significantly different

viscosity profiles. Samples with particle size $<100\ \mu\text{m}$ present much lower viscosity than the $<300\ \mu\text{m}$ counterpart, confirming the relevance of the grinding process (both on the wet and dry state) on the viscosity of the BC:CMC fibrous suspensions.

Comparing Figure 3.5-A and 3.5-B, the drying method (slow oven drying or the fast hot plate drying) did not affect significantly the viscosity profile of redispersed BC:CMC, with the HB and MHI samples having close viscosity profiles for the two drying methods. Also, regarding residual moisture, the MHI sample dried to 80 % TS had equal profile to the one dried to 100 % TS (Figure 3.5-B), such that the extent of drying also does not significantly affect the viscosity.

All the redispersed samples in Figure 3.5-A showed a similar or higher viscosity than the never-dried ones (Figure 3.2). Thus, redispersion using low shear stress mixing, at room temperature and under 5 minutes, was enough to allow for the recovery (even slight improvement) of the rheological profile of the non-dried BC:CMC formulations. However, the occurrence of small aggregates of BC in the redispersed BC:CMC suspension (Table 3.2) may contribute to the increase in the apparent viscosity profile. Indeed, dispersion of the dry materials with UT slightly reduced the rheological profile (as compared to the samples dispersed in the magnetic stirrer), as can be seen from the HB and MHI samples viscosity in Figure 3.5-A and 3.5-D, possibly due a better hydration of the powders and the reduction of some fibre agglomerates.

Overall, these results demonstrate that it is the BC wet-grinding, not the drying process, that has a relevant impact on the properties of its powdered formulations. In the presence of CMC, BC fibres are somewhat protected and less exposed to the negative effects that some drying methods might have on the fibres. This way, higher temperatures and less time and energy consuming processes can be employed, without jeopardizing the functionality of the material after redispersion and rehydration. In sum, the drying method (either slower or faster) and temperature do not affect the redispersion and the rheological profile of BC:CMC formulations and, contrarily to what has been proposed in other works [19], drying can be done to the full extent.

3.3.4 - Effect of dry comminution

As an example, Figure 3.6 shows SEM micrographs of BC:CMC powders produced from HB processed BC and comminuted to different particle sizes.

The separation of the BC:CMC particles after grinding was done by mechanical means (sieves with different mesh apertures). The BC:CMC powders resemble thin flakes of varying shape, such that some particles with larger length than the mesh aperture may have passed perpendicularly through the sieve.

Thus, although the size assigned to the samples (<100 or <300 μm) is in fact indicative, two populations of particles (larger and smaller) were obtained through sieving.

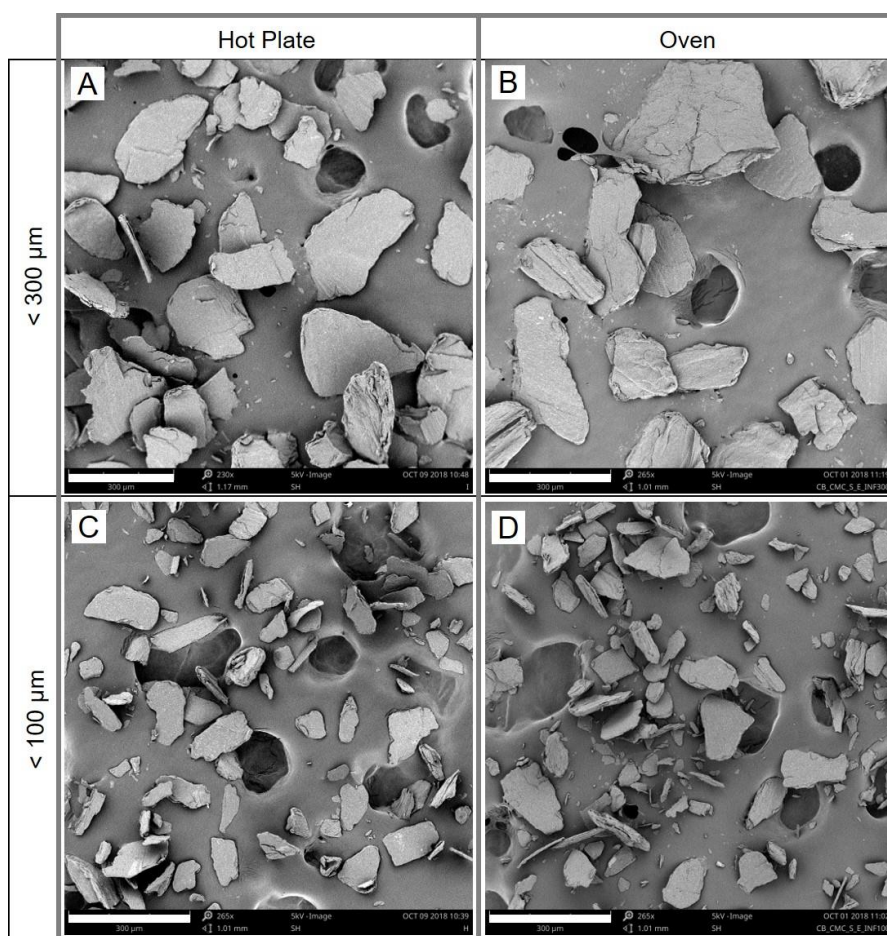


Figure 3.6 - SEM images of BC:CMC powders obtained from HB processed BC, (A) dried in a Hot plate, ground and sieved to <300 μm ; (B) dried in an Oven, ground and sieved to <300 μm ; (C) dried in a Hot plate, ground and sieved to <100 μm ; (D) dried in an Oven, ground and sieved to <100 μm . All white scale bars correspond to 300 μm .

Table 3.3 summarizes the main observations pertaining to the dispersibility of BC:CMC dry formulations ground and sieved to a size < 100 μm . To simplify the demonstration of the results, only hot plate dried samples' results are shown. The same profile was observed for samples dried in an oven.

Decreasing the dry particle size of the BC:CMC samples to <100 μm allows for a faster dispersion (complete under 1 min) of the powders at low shear magnetic stirring (Table 3.3), as compared to particles <300 μm , where a complete dispersion was only achieved after UT homogenization of all samples (Table 3.2).

Table 3.3 - Dispersibility of BC:CMC mixtures after drying, grinding and sieving to a particle size <100 μm

Wet Grinding	Drying	Dispersion	Dispersibility
HB			
MHI			
HPH-1	Hot Plate	Magnetic stirrer	1
HPH-2		UT Homogenizer	
HPH-6			

However, with the decrease in particle size there is also a decrease in the viscosity profile, as noted previously (Figure 3.5-A and 3.5-C). Increasing the particle size (from <100 μm to <300 μm), decreases the ease of dispersion under low shear mixing, but maintains more of the fibre's functionality, as perceived by the higher viscosity profiles.

The redispersed samples were also analysed for their ability to stabilize isohexadecane/water interfaces (Figure 3.7).

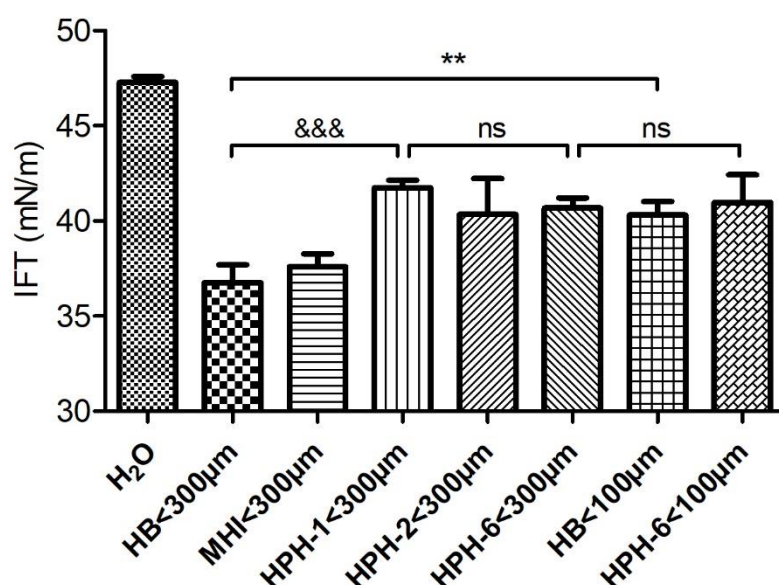


Figure 3.7 - Interfacial tension of Isohexadecane/Water containing dried BC:CMC at 0.5%, ground and sieved to different size ranges. Results are expressed as average of triplicate measurements and bars are representative of the Standard Deviation. All datasets were compared with each other using one-way ANOVA followed by Tukey's Multiple Comparison Test (all samples were significantly different at $p < 0.001$ when comparing with the H₂O control; &&& $p < 0.001$ comparing HB<300 μm with HPH-1<300 μm ; ** $p < 0.01$, comparing HB<300 μm and HB<100 μm ; ns – not significant, comparing HPH-1<300 μm with HPH-6<300 μm , and HPH-6<300 μm with HPH-6<100 μm).

Overall, the effect of the technology used for BC wet-grinding on the ability of BC:CMC to reduce the interfacial tension, observed in the non-dried samples (Figure 3.3), is still patent in the corresponding samples obtained after drying and redispersion. Actually, the results obtained with samples HB and MHI after drying and redispersion are similar to those of the never dried counterpart (Figure 3.7 vs Figure 3.3), while a deterioration of the activity of the sample HPH-1 was observed as a consequence of further processing. Further decreasing the size of wet BC (from HPH-1 Pass to HPH-6), has no further influence on the IFT values. Importantly, these results also show that too extensive dry comminution (e. g. HB, ground from <300 to <100 μm) affects the functionality of the BC:CMC mixture, as shown also concerning the viscosity of the samples (Fig. 3.5-A and 3.5-C).

3.3.5 - Functionality assessment: Suspension Stability of a Cocoa Beverage

The dried and non-dried BC:CMC were used in a stability test using a solid-in-liquid suspension, a cocoa and milk system. The stabilizing effect of the different samples was determined using equation 2 and the results are summarized in Table 3.4. An example of the aspect of samples with different levels of stabilization percentage can be found in Figure 3.8. Percentages of stability under 10 % were considered as complete sedimentation (c.s.) of the cocoa particles. Only one of each Avicel and Novagel celluloses are shown because all the results were similar.

Hydrocolloids are used in heterogeneous systems such as chocolate milk and other beverages (solid-in-liquid suspensions) to increase their viscosity, having a double function of improving the mouthfeel and preventing the sedimentation of suspended particles - improved rheology [27]. Microcrystalline cellulose (MCC) and cellulose derivatives, namely CMC, are employed for this purpose. Concentrations over 0.75 % of CMC are needed for the change in rheological behaviour of milk to be noticeable [28]. For MCCs such as Avicel products, concentrations of 0.5 % are necessary to completely avoid cocoa particles sedimentation. MCC acts beyond the simple thickening of the media: it forms aggregate structures with the cocoa particles, also further interacting with the milk components, creating network structures responsible for the stable suspensions [29]. BC:CMC formulations (1:1) are also able of creating structured networks and having a positive effect on rheological properties of heterogeneous systems, at concentrations as low as 0.1 % [5].

Results in Table 3.4 were obtained with only 0.15 % of the different powders or non-dried formulations, and simple vortex agitation was employed, followed by a short heat treatment. HB and MHI samples preserved their stabilizing capabilities after drying and comminution, even with the smaller sizes (<100 μm), maintaining fully stable suspensions for up to 4 days. A more extensive homogenization with HPH-

1 only showed stability for the never-dried BC:CMC and the dry formulation with a size of <300 µm; for 2 and 6 cycles of HPH, not even the never dried material was capable of complete stabilization for 4 days, and the difference in the dry particle size becomes more evident, as the materials <100 µm are much less efficient than the ones <300 µm. As seen before, extensive grinding of the wet fibres, and then of the dried material to a particle size <100 µm, reduces the stabilizing effect of BC:CMC.

Table 3.4 - Stabilization of cocoa particles in chocolate milk, with BC:CMC, added at 0.15% (m/v), at room temperature (c.s. – complete sedimentation)

Wet grinding	Drying	Particle size (µm)	Stability (%)		
			1 h	24 h	4 days
HB	Hot plate	<100	100	100	83
		<300	100	100	100
	Never-dried		100	100	100
MHI	Hot plate	<100	100	100	100
		<300	100	100	100
	Never-dried		100	100	100
HPH-1	Hot plate	<100	100	67	50
		<300	100	100	100
	Never-dried		100	100	100
HPH-2	Hot plate	<100	100	67	50
		<300	100	100	83
	Never-dried		100	100	83
HPH-6	Hot plate	<100	100	27	33
		<300	100	100	50
	Never-dried		87	83	67
Avicel CM 2159	UT, 30 min		95	c.s.	c.s.
Novagel RCN-15			96	c.s.	c.s.
Bioplus-L Fibrils			70	40	35
CelluForce NCC			100	100	100
CMC			40	c.s.	c.s.
Control			c.s.	c.s.	c.s.

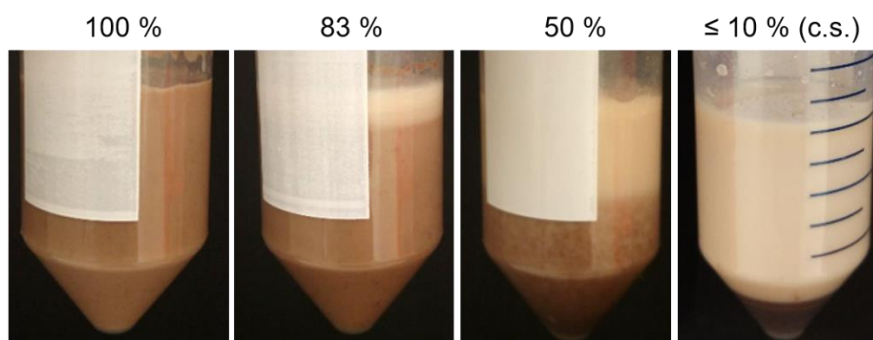


Figure 3.8 - Examples of the aspect of samples with different levels of stability percentage of cocoa particles in chocolate milk. Percentages of stability under 10 % were considered as complete sedimentation (c.s.) of the cocoa particles (control without stabilizing agent).

To the exception of Celluforce, all colloidal plant celluloses and nanocelluloses used as benchmark showed a very low stabilizing effect on cocoa particles. It is also worth to notice that CMC alone was unable to fully stabilize the system, so the stabilizing effect can be imparted to the BC fibres in the BC:CMC formulations.

3.4 - CONCLUSIONS

Dry formulations of BC:CMC, able to redisperse in a few minutes under magnetic stirring, were developed. The redispersed material preserves the properties of the non-dried samples, namely concerning viscosity, the reduction of the interfacial activity of oil/water interface and the stabilization of multiphasic systems (liquid-liquid and solid-liquid).

It is demonstrated for the first time that the size of the BC fibre bundles is of paramount relevance concerning BC:CMC functionality and potential applications in the food and cosmetic fields. Thus, the control of the grinding process, both on the wet and dry materials, is of utmost importance, while the drying process (time and temperature) seems not to be very relevant in this regard after adding CMC as co-drying agent.

3.5 - BIBLIOGRAPHIC REFERENCES

- [1] S.M. Keshk, Bacterial Cellulose Production and its Industrial Applications, J. Bioprocess. Biotech. 04 (2014). <https://doi.org/10.4172/2155-9821.1000150>.
- [2] D. Klemm, F. Kramer, S. Moritz, T. Lindström, M. Ankerfors, D. Gray, A. Dorris, Nanocelluloses: A new family of nature-based materials, Angew. Chemie - Int. Ed. 50 (2011) 5438–5466. <https://doi.org/10.1002/anie.201001273>.

- [3] T. Kondo, P. Rytczak, S. Bielecki, Bacterial NanoCellulose Characterization, in: M. Gama, F. Dourado, S. Bielecki (Eds.), *Bact. Nanocellulose - From Biotechnol. to Bio- Econ. .*, Elsevier B.V., 2016: pp. 59–71.
- [4] K.Y. Lee, G. Buldum, A. Mantalaris, A. Bismarck, More than meets the eye in bacterial cellulose: Biosynthesis, bioprocessing, and applications in advanced fiber composites, *Macromol. Biosci.* 14 (2014) 10–32. <https://doi.org/10.1002/mabi.201300298>.
- [5] D. Martins, B. Estevinho, F. Rocha, F. Dourado, M. Gama, A Dry and Fully Dispersible Bacterial Cellulose Formulation as a Stabilizer for Oil-in-Water Emulsions, *Carbohydr. Polym.* 230 (2020) 115657. <https://doi.org/10.1016/j.carbpol.2019.115657>.
- [6] H. Ougiya, K. Watanabe, Y. Morinaga, F. Yoshinaga, Emulsion-stabilizing Effect of Bacterial Cellulose, *Biosci. Biotechnol. Biochem.* 61 (1997) 1541–1545. <https://doi.org/10.1271/bbb.61.1541>.
- [7] P. Paximada, E. Tsouko, N. Kopsahelis, A.A. Koutinas, I. Mandala, Bacterial cellulose as stabilizer of o/w emulsions, *Food Hydrocoll.* 53 (2016) 225–232. <https://doi.org/10.1016/j.foodhyd.2014.12.003>.
- [8] X. Zhai, D. Lin, D. Liu, X. Yang, Emulsions stabilized by nanofibers from bacterial cellulose: New potential food-grade Pickering emulsions, *Food Res. Int.* 103 (2018) 12–20. <https://doi.org/10.1016/j.foodres.2017.10.030>.
- [9] R.H. Newman, Carbon-13 NMR evidence for cocrystallization of cellulose as a mechanism for hornification of bleached kraft pulp, *Cellulose.* 11 (2004) 45–52. <https://doi.org/10.1023/B:CELL.0000014768.28924.0c>.
- [10] G.H. Zhao, N. Kapur, B. Carlin, E. Selinger, J.T. Guthrie, Characterisation of the interactive properties of microcrystalline cellulose-carboxymethyl cellulose hydrogels, *Int. J. Pharm.* 415 (2011) 95–101. <https://doi.org/10.1016/j.ijpharm.2011.05.054>.
- [11] R. Kargl, T. Mohan, M. Bračč, M. Kulterer, A. Doliška, K. Stana-Kleinschek, V. Ribitsch, Adsorption of carboxymethyl cellulose on polymer surfaces: Evidence of a specific interaction with cellulose, *Langmuir.* 28 (2012) 11440–11447. <https://doi.org/10.1021/la302110a>.
- [12] F.L. Zemljic, P. Stenius, J. Laine, K. Stana-Kleinschek, V. Ribitsch, Characterization of Cotton Fibres Modified By Carboxymethyl Cellulose, *Lenzinger Berichte.* 85 (2006) 68–76.
- [13] N. Butchosa, Q. Zhou, Water redispersible cellulose nanofibrils adsorbed with carboxymethyl cellulose, *Cellulose.* 21 (2014) 4349–4358. <https://doi.org/10.1007/s10570-014-0452-7>.
- [14] A. Naderi, T. Lindström, J. Sundström, G. Flodberg, Can redispersible low-charged nanofibrillated cellulose be produced by the addition of carboxymethyl cellulose prior to its drying?, *TAPPI Int. Conf. Nanotechnol. Renew. Mater.* 2016. 30 (2015) 939–953.
- [15] D. Agarwal, W. MacNaughtan, T.J. Foster, Interactions between microfibrillar cellulose and carboxymethyl cellulose in an aqueous suspension, *Carbohydr. Polym.* 185 (2018) 112–119. <https://doi.org/10.1016/j.carbpol.2017.12.086>.
- [16] M.C.I.M. Amin, A.G. Abadi, H. Katas, Purification, characterization and comparative studies of spray-dried bacterial cellulose microparticles, *Carbohydr. Polym.* 99 (2014) 180–189. <https://doi.org/10.1016/j.carbpol.2013.08.041>.
- [17] N. Pa'E, N.I.A. Hamid, N. Khairuddin, K.A. Zahan, K.F. Seng, B.M. Siddique, I.I. Muhamad, Effect of different drying methods on the morphology, crystallinity, swelling ability and tensile properties of nata de coco, *Sains Malaysiana.* 43 (2014) 767–773.
- [18] P. Tammarate, US Patent 5,962,676 - Process for the modification and utilization of bacterial cellulose, 1999.
- [19] K. Watanabe, A. Shibata, H. Ougiya, N. Hioki, Y. Morinaga, US Patent 6,153,413 - Method for processing bacterial cellulose, 2000.

- [20] Z.-F. Yang, S. Sharma, C. Mohan, J. Kobzeff, Patent WO 01/05838 A1 - Process for drying reticulated bacterial cellulose without co-agents, 2001.
- [21] Z.-F. Yang, N.A. Morrison, T.A. Talashek, D.F. Brinkmann, D. DiMasi, Y.L. Chen, US Patent 8,053,216 B2 - Bacterial cellulose-containing formulations, 2011.
- [22] V. Khoshkava, M.R. Kamal, Effect of drying conditions on cellulose nanocrystal (CNC) agglomerate porosity and dispersibility in polymer nanocomposites, *Powder Technol.* 261 (2014) 288–298. <https://doi.org/10.1016/j.powtec.2014.04.016>.
- [23] P. Nechita, D.M. Panaitescu, Improving the dispersibility of cellulose microfibrillated structures in polymer matrix by controlling drying conditions and chemical surface modifications, *Cellul. Chem. Technol.* 47 (2013) 711–719.
- [24] Y. Peng, D.J. Gardner, Y. Han, A. Kiziltas, Z. Cai, M.A. Tshabalala, Influence of drying method on the material properties of nanocellulose I: Thermostability and crystallinity, *Cellulose.* 20 (2013) 2379–2392. <https://doi.org/10.1007/s10570-013-0019-z>.
- [25] C. Clasen, B. Sultanova, T. Wilhelms, P. Heisig, W.M. Kulicke, Effects of different drying processes on the material properties of bacterial cellulose membranes, *Macromol. Symp.* 244 (2006) 48–58. <https://doi.org/10.1002/masy.200651204>.
- [26] D. Klemm, D. Schumann, U. Udhardt, S. Marsch, Bacterial synthesized cellulose - Artificial blood vessels for microsurgery, *Prog. Polym. Sci.* 26 (2001) 1561–1603. [https://doi.org/10.1016/S0079-6700\(01\)00021-1](https://doi.org/10.1016/S0079-6700(01)00021-1).
- [27] D. Saha, S. Bhattacharya, Hydrocolloids as thickening and gelling agents in food: A critical review, *J. Food Sci. Technol.* 47 (2010) 587–597. <https://doi.org/10.1007/s13197-010-0162-6>.
- [28] S. Bayarri, L. González-Tomás, E. Costell, Viscoelastic properties of aqueous and milk systems with carboxymethyl cellulose, *Food Hydrocoll.* 23 (2009) 441–450. <https://doi.org/10.1016/j.foodhyd.2008.02.002>.
- [29] Y. Yaginuma, T. Kijima, Effects of microcrystalline cellulose on suspension stability of cocoa beverage, *J. Dispers. Sci. Technol.* 27 (2006) 941–948. <https://doi.org/10.1080/01932690600766306>.

Chapter 4

A Dry and Fully Dispersible BC Formulation as a Stabilizer for Oil-in-Water Emulsions

Bacterial cellulose is an emerging alternative to plant cellulose in different applications. Several works demonstrated the potential of never-dried BC; however, envisioning real industrial applications, a dry product retaining its functional properties upon rehydration is preferable.

A dry and completely redispersible formulation of BC with carboxymethyl cellulose (CMC) was prepared by Spray-drying. The obtained material showed a Zeta Potential of (-67.0 ± 3.9) mV, a $Dv(50)$ of (601 ± 19.7) μm and was able to decrease the oil/water interface energy.

The dry BC:CMC formulation was employed as stabilizer in oil-in-water emulsions, in parallel with commercial plant celluloses and Xanthan gum. The emulsions were monitored over time by optical microscopy and characterized by rheological measurements. BC:CMC effectively stabilized emulsions against coalescence and creaming, at a concentration of 0.50 % - contrarily to other commercial dry celluloses – due to the Pickering effect and to the structuring of the continuous phase, as seen with Cryo-SEM.

4.1 - INTRODUCTION

Emulsions may be stabilized by particles (Pickering effect) instead of surfactant amphiphilic molecules. Organic solid particles have shown to stabilize liquid–liquid interfaces when bearing a contact angle around 90° at the interface. These particles irreversibly adsorb at the interface, forming a layer around the surface of the disperse phase droplets that acts as a mechanical barrier, preventing coagulation and coalescence phenomena [1,2]. A very small concentration of particles – enough to cover only a fraction of the interfacial area – may suffice to stabilize the emulsion. When an excess of particles remains in the continuous phase, they interact with each other and can form a three-dimensional structure, further enhancing the stabilization effect by steric hindrance. Also, the viscosity of the continuous phase increases, providing higher support to the disperse phase droplets, reducing coalescence and creaming (thus improving long-time storage) [1–3].

Hydrocolloidal microcrystalline cellulose (MCC) from plant sources is widely used in the food industry to regulate the stability, texture, rheology and organoleptic properties [4]. Many works refer to the use of cellulosic particles for oil-in-water Pickering emulsions stabilization [5–11]. Cellulose particles are suitable for stabilizing Pickering emulsions because they have both hydrophilic and hydrophobic regions within the cellulose crystal structure [12,13]. Some work has also been done with never-dried BC [14–18].

However, for the sake of storage, economy and practicality, it is important that additives for food and cosmetic industry can be provided in their dried form. Drying cellulose originates a so called “hornified” product, due to the establishment of inter-chain hydrogen bonds that are hardly broken when the material is placed in contact with water again. The rehydration of these products and generation of colloidal particles requires a substantial input of energy [19,20]. Acid hydrolysis mitigates this effect by imparting negative charges on the crystallites’ surface which improve their stability in aqueous media [18]. Alternatively, co-drying with charged polysaccharides may be used. Being a negatively charged polymer, CMC imparts a surface charge to cellulose fibres where it adsorbs, improving their dispersion due to electrostatic repulsions. Also, upon drying, the presence of a charged drying-aid prevents the formation of hydrogen bonds between cellulose polymer chains during water removal, avoiding hornification. This results in improved redispersion of the cellulose fibres when rehydrated, thus preserving and re-establishing the functional properties as those of the never-dried material [19,21,22].

Dry commercial products of MCC and nano crystalline cellulose (NCC) from plant sources are available, and fibrillary dry products have also been reported [19,21,22]. However, dry cellulose from bacterial source has only seldom been reported [23,24], even more rarely in powder form [25]. Most of the reports

consist in patents [26–29], which do not clearly show the rehydrating ability of the prepared materials nor analyse the post-processing retrieval of the functional properties (i.e., maintaining the ability to stabilize heterogeneous systems). Achieving a dry, rehydratable and functional product could be a step ahead in placing BC as a competitor in the hydrocolloid market, along with the existing plant celluloses and other widely used polysaccharides as Xanthan gum. In this work, a dry formulation of BC and CMC was prepared, which is fully rehydratable within few minutes using low energy stirring. These features are of utmost importance for the industry, as they impact on the operating costs, for hydrocolloidal microcrystalline cellulose requires high energy mixing for optimal functionalization. A benchmarking study with several commercially available cellulose dry products and Xanthan gum as emulsion stabilizers was performed, revealing the retrieval of the BC functionality after drying and rehydration, and its suitability as a stabilizer.

4.2 - MATERIALS AND METHODS

4.2.1 - Materials and Reagents

Carboxymethyl cellulose (90 kDa, degree of substitution of 0.7) was supplied by Acros Organics (New Jersey, USA), Xanthan gum was bought from Sigma (St. Louis, Missouri, USA), and isohexadecane was gently provided by Lanxess (Leverkusen, Germany). Colloidal MCC Avicel RT1133 (containing 11.9 % CMC), non-colloidal MCC Avicel LM310 and non-colloidal MCC Novagel RCN15 (with 15 % Guar gum) were provided by FMC Corporation (Philadelphia, Pennsylvania, USA). Hydrophilic sulphated cellulose nanocrystals, Celluforce NCC, was provided by Celluforce (Montreal, Quebec, Canada).

4.2.2 - BC:CMC preparation

BC membranes (HTK Food CO. Ltd, Vietnam) were washed in a 0.1 M NaOH solution, rinsed thoroughly with distilled water until the pH reached that of the distilled water and then wet ground using a Sammic fixed speed blender, model TR250 at 9000 Rpm (Sammic, S.L.). The solid fraction of the obtained pulp was determined and adjusted to 1 % (m/v). The effect of different BC:CMC ratios on the dry materials redispersion was preliminarily studied and the optimal ratio was found to be 1:1. This proportion was selected to proceed with the experiments for giving the best redispersion results. Thus, to the 1% BC pulp, the same volume of 1 % (m/v) CMC (90 kDa) was added, making up a 1:1 mixture (BC:CMC) of 1 % total solids. This mixture was left under magnetic stirring overnight at room temperature and then autoclaved at 121 °C for 20 min. The formulation was then dried in a pilot Spray-Dryer (GEA Niro A/S Production

Minor) with a 2 mm Nozzle (3.5 bar), using an inlet flow rate of approximately 10 kg/h of 1 % BC:CMC mixture in water, inlet temperature of 210 °C and outlet temperature of 115 °C. High temperatures were used to ensure a completely dry product in the outlet (since CMC and BC are very hydrophilic, and BC has high water holding capacity), to minimize losses by adhesion to the equipment walls and to minimize the processing time. This was possible due to cellulose's high thermal stability.

4.2.3 - Contact angles of BC and BC:CMC

BC and BC:CMC dispersions (0.50 % m/v) were layered onto glass slides and dried at 37 °C to assure flat and smooth films. Contact angles were determined by the sessile drop method using Optical Contact Angle (OCA 20, DataPhysics) and SCA 20 Software module 22 (DataPhysics). Drops of 2 µL of ultrapure (MilliQ) water were deposited on top of the films with a Hamilton 500 mL syringe and left in contact for 120 s, at 20 ± 1 °C, while recording with the equipment's video camera. Movie records were analysed frame by frame to determine the contact angles over time. Glass slides without any film were used as control.

4.2.4 - Particles Zeta Potential and size measurements

The Zeta Potential of the used celluloses was measured using a Zetasizer Nano ZS (Malvern Instruments Ltd.). Avicel and Novagel products (1.5 % m/v in distilled water) were first activated, according to the manufacturer's recommendation, for 20 min at 20 000 rpm in a Unidrive X1000D homogenizer (CAT Scientific) with a T20 F Shaft and Generator assembly. The other celluloses were dispersed in distilled water at a concentration of 0.50 % (m/v) and stirred with magnetic agitation (20 min at 500 rpm). All samples were further diluted to 0.1 % in distilled water and analysed three times in a disposable folded capillary cell (Malvern Instruments).

The particles' size by volume of the different celluloses was determined using a Mastersizer 3000 particle size analyser equipped with a Hydro EV wet dispersion unit (Mastersizer 3000, Malvern Instruments Ltd.). Aqueous dispersions of BC, BC:CMC, activated and non-activated Avicel and Novagel products were analysed six times at an obscuration level between 10 and 20 %. Taking into account that these were non-spherical particles, Mie scattering model was used for the analysis and the refractive index of cellulose and water were assumed as 1.468 and 1.330 respectively (as provided by the software's database). For irregular shaped particles, the Mastersizer takes the volume of the particle and calculates the diameter of an imaginary sphere that is equivalent in volume. The particles size was then expressed as the Mass Median Diameter, Dv(50) (the size at which 50 % of the sample is smaller and 50 % is larger, considering

the volume distribution), Dv(10) and Dv(90) (the size of particle below which 10 % and 90 % of the sample lies, respectively).

4.2.5 - Interfacial tension measurements

4.2.5.1 - Pendant Drop method

Interfacial tension was measured with the pendant drop method using Optical Contact Angle (OCA 20, DataPhysics), and SCA 20 Software module 22 (DataPhysics). 2 mL of isohexadecane was placed on a disposable optical polystyrene macro standard fluorescence cuvette (1 cm x 1 cm x 4.5 cm) (Labbox). A Hamilton 500 mL syringe (0.71 mm outer needle diameter) containing the aqueous sample suspensions (heavier phase) was introduced in the cuvette, with the needle always at the same depth. First, maximum drop volume was determined for each sample. For each drop, profile extraction and IFT calculation were made automatically, 10 times per minute until 25 readings, in triplicate for each sample and at 20 ± 1 °C.

4.2.5.2 - Du Noüy ring method

A K20 Force Tensiometer (Kruss) with a RI21 platinum-iridium alloy wire ring was used for the Du Noüy ring method. BC:CMC dispersions density was assumed the same as that of the distilled water at 20 °C, 1.00 g/mL, and isohexadecane's density was 0.79 g/mL at 20 °C. Ten mL of each phase were placed in a glass sample vessel (70 mm outer diameter), and analyses were performed according to the equipment's manual. Readings were performed in triplicate for each sample, at 21 ± 1 °C.

4.2.5.3 - Statistical analysis

Statistical analysis was performed using GraphPad Prism 5 (GraphPad Software). Results were expressed as mean \pm standard deviation. A one-way analysis of variance (ANOVA) was performed, followed by Tukey's Multiple Comparison Test, to establish the significance of differences.

4.2.6 - Emulsions' preparation

MCC (Avicel and Novagel products) were activated as described in section 2.4 before dilution. Celluforce, BC:CMC, CMC and Xanthan were dispersed in distilled water with magnetic stirring (20 min at 500 rpm), in the required amounts.

Isohexadecane-in-water emulsions (10:90) were each prepared in the presence of 0.50 % of the different polymers, in a total volume of 100 mL. Samples were homogenized in a Unidrive X1000D for 4 minutes at a speed of 20 000 rpm and stored at room temperature. Additionally, emulsions with lower BC:CMC

concentrations - 0.25 % and 0.1 % - were prepared in the same conditions. Photos were taken at different timepoints after preparation, for at least one month.

BC alone was not used in these assays because it aggregates and creates fibre bundles under high-shear stirring/mixing.

4.2.7 - Microscopy

For optical microscopy observations, a drop of each sample was placed on a slide, coverslipped and visualized on an Olympus BX51 fluorescence microscope using bright field.

For optical microscopy of stained cellulose 20 μL of each suspension were placed and spread on a glass slide and oven-dried at 40 °C. A drop of 10 $\mu\text{g/mL}$ Calcofluor White stain (Sigma) was placed on top of the dry samples (protected from light), coverslipped and visualized on an Olympus BX51 fluorescence microscope with a DAPI filter (Excitation wavelength: 365 – 370 nm; Emission wavelength: 421 nm).

Spray-dried BC:CMC observation was performed using a desktop Scanning Electron Microscope (SEM) coupled with energy-dispersive X-ray spectroscopy analysis (Phenom ProX, Phenom-World BV). Samples were added to aluminium pin stubs with electrically conductive carbon adhesive tape and coated with 2 nm Au prior to analysis.

Cryo-SEM observations were performed in the Laboratory for Scanning Electron Microscopy and X-Ray Microanalysis, at Materials Centre of the University of Porto (CEMUP), using a High-resolution Scanning Electron Microscope (JEOL JSM 6301F) with X-Ray Microanalysis (Oxford INCA Energy 350) and CryoSEM experimental facilities (Gatan Alto 2500). Each sample was rapidly cooled in sub-cooled nitrogen and transferred under vacuum to the cold stage of the preparation chamber. The specimen was fractured, sublimated for 120 s at -90 °C, and coated with Au/Pd by sputtering for 50 s and with 12 mA current. The sample was then transferred into the SEM chamber and observed at a temperature of -150 °C.

4.2.8 - Rheological analysis of the emulsions

Rheological analysis of the emulsions was performed in a controlled stress rheometer (DHR-1, TA instruments) with TRIOS Software (TA Instruments) at 25 °C using a cone and plate geometry (60 mm, 2.006° cone angle, 64 μm gap). Samples shear stress and viscosity were measured in triplicate by flow sweep tests at increasing shear rates (0.01 to 1000 s^{-1}). Oscillatory strain sweep tests were carried out to determine the sample's linear viscoelastic region (LVR) at a frequency of 1 rad/s and strain amplitude from 0.1 to 100 %. Oscillatory frequency sweep tests were performed in triplicate at a strain within the LVR (0.25 % strain), with angular frequency ranging from 0.1 to 100 rad/s.

4.3 - RESULTS AND DISCUSSION

CMC adsorbs onto and coats BC fibres in a water suspension, due to structural similarities that allow cooperative hydrogen bonding between the free cellulose segments on the CMC backbone and the cellulose fibre surfaces [30–32]. CMC is also responsible for preventing further fibre aggregation during the drying process – acting as co-drying and dispersant agent, due to its negative charge that is imparted onto the BC fibres, resulting in better redispersion owing to electrostatic repulsion forces [19,22]. Thus, when rehydrated, the BC fibres remain well separated and the gel recovers its original well dispersed structure and rheological properties. We observed that the spray-dried BC:CMC formulation reported herein could actually be completely redispersible in water at a concentration of 0.50 % (m/v), through simple magnetic stirring at 500 rpm for 5 min. To the best of our knowledge, this is the first report on co-drying BC and CMC into a dry formulation with such excellent water redispersion (Figure 4.1-A and B). Pa'E et al. [24] tested different drying methods of BC membranes, but these samples were not ground or powdered, and only the swelling ability was assessed. Amin et al. [25] prepared dry powders with blended BC and acid treated BC by freeze-drying or spray-drying, reporting limited swelling index and water retention capacity values after redispersion, as compared to the water retention capacity of the never-dried BC.

In a similar approach to ours, Butchosa & Zhou [19] used a 250 kDa CMC (DS = 0.90) to prepare water-redispersible plant cellulose nanofibrils (CNFs). After high-shear mixing with Ultra-turrax, heat treatment and oven drying, a fully water-redispersible and stable suspension was obtained, preserving the original properties of never dried CNFs (namely the viscosity). However, the reported resuspension process requires magnetic stirring overnight followed by mixing with an Ultra-turrax for 15 min, thus requiring much more energy and time than the here reported BC:CMC formulation. Later, Naderi et al. [167] using also nanofibrillated cellulose from wood pulp (low-charged), were able to prepare a redispersible dry product retaining “close-to-maintenance” rheological properties, adding low amounts of CMC (1 %) and a low-shear mixing protocol.

Figure 4.1 shows Cryo-SEM micrographs of the BC:CMC mixture before drying (A), after redispersion in water (B) (through magnetic stirring) and also a SEM micrograph of the spray-dried powder (C). The redispersed BC:CMC presents a good dispersion at the fibre level as observed at the Cryo-SEM (Figure 4.1-B), although not as homogeneous as the one obtained before drying, some small aggregates being detectable. Nevertheless, considering the ease and swiftness of the redispersion (5 min under 500 rpm),

the result is rather promising. Figure 4.2 shows the microscopical appearance (rather homogeneous) of the dry and redispersed material in contrast with the never-dried BC fibres without CMC.

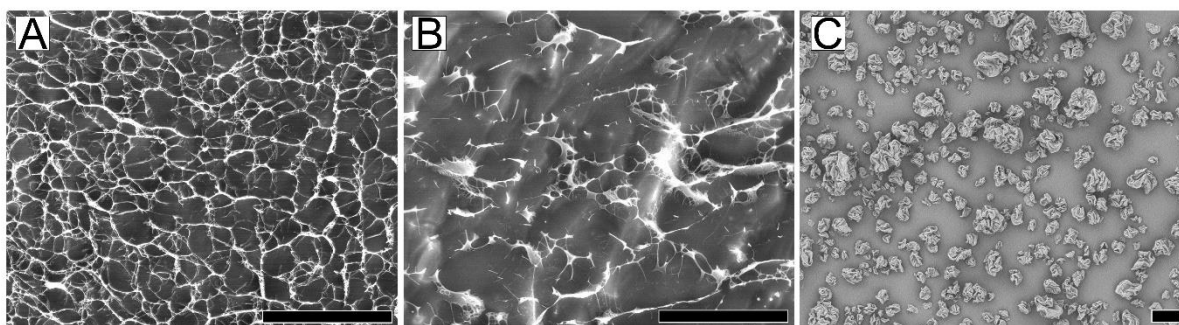


Figure 4.1 - Cryo-SEM images (2000X magnification) of (A) 0.50 % non-dried BC:CMC; (B) 0.50 % dried and redispersed BC:CMC; (C) SEM image (890X magnification) of spray-dried BC:CMC. All black scale bars correspond to 20 µm.

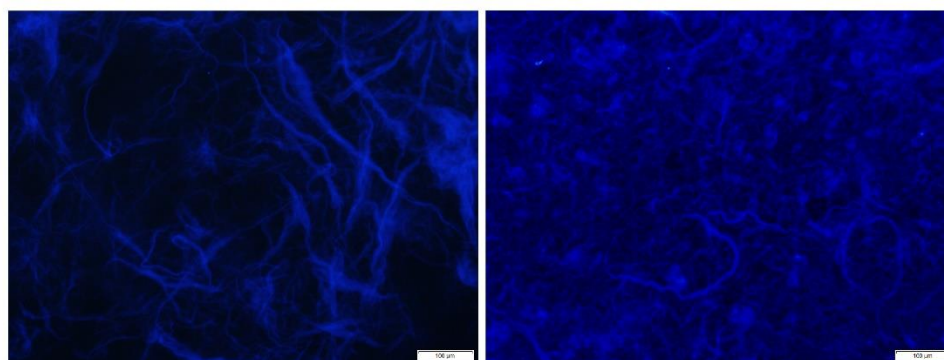


Figure 4.2 - Optical micrographs (10X magnification) of ground BC (left) and redispersed BC:CMC formulation after spray-drying (right), stained with Calcofluor White. Scale bars correspond to 100 µm.

Several plant-derived celluloses were used in parallel as a benchmarking study, varying in size, morphology and chemical modification: colloidal Avicel RT1133 and non-colloidal Avicel LM310 are used as stabilizers of emulsions and suspended particles, and also texture modifiers for cosmetics or food products and beverages; Novagel RCN15 is recommended as fat replacer and as a rheology modifier in food products; finally, Celluforce NCC has a vast recommended application spectra - for reinforcing Agent in Textiles and additive in thermoplastic composites, adhesives and paints, personal care products and food and beverages to improve texture and suspension qualities. All these products are commercially available, and this information is provided by the suppliers in the materials' datasheets and catalogues. Microscopic images of these products can be found in Figure 4.3. Celluforce NCC images were not

possible to obtain with this technique. Celluforce morphology images can be found at: <https://www.celluforce.com/en/products/cellulose-nanocrystals/>.

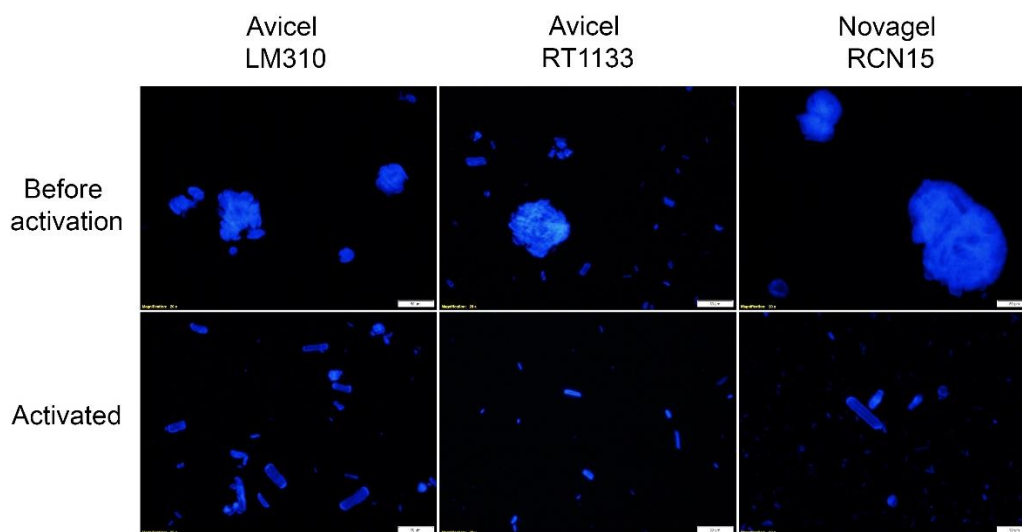


Figure 4.3 - Optical micrographs (20X magnification) of Avicel LM310, Avicel RT1133 and Novagel RCN15, dispersed in water and stained with Calcofluor White, before and after activation. Scale bars correspond to 50 μm .

4.3.1 - Assessment of the surface hydrophilicity by contact angles measurement

The contact angle of a water drop deposited on a surface depends on the material's hydrophobicity.

Figure 4.4 shows the contact angles of water with BC and BC:CMC.

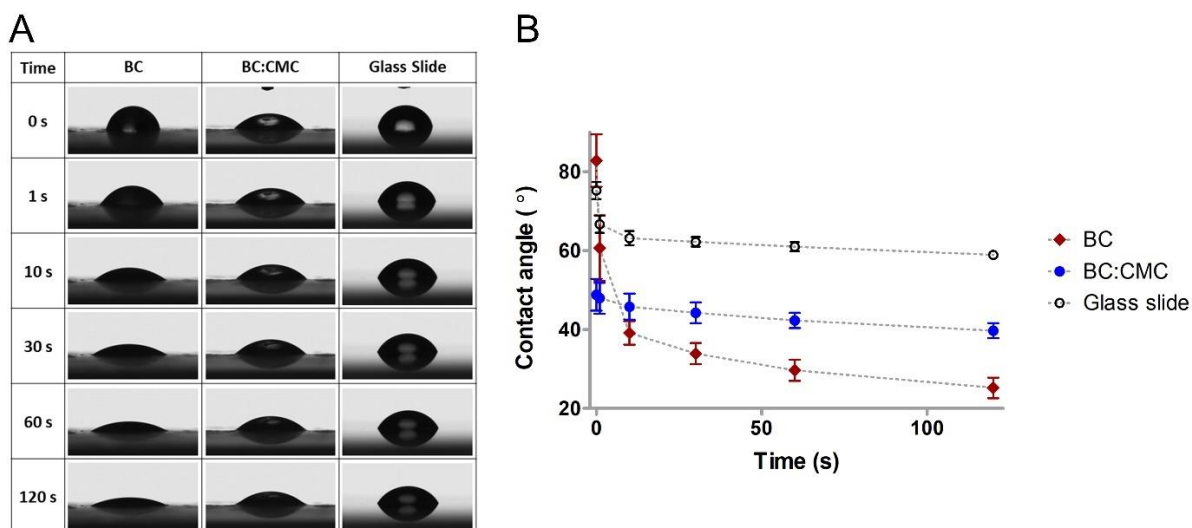


Figure 4.4 - (A) Micrographs of the evolution of a 2 μL water drop on top of BC and BC:CMC dry films over time (glass was used as a control); (B) Contact angles of water with BC and BC:CMC films over time, as determined by the sessile drop method.

An equilibrium contact angle was not observed (not even in glass), probably due to water evaporation (as the relative humidity of the room was not controlled) and in the case of polysaccharides, also due to water absorption and/or spreading. As observed in Figure 4.4, for BC films the contact angle changes from over 80° to less than 40° in just 10 s, further dropping to around 20°, clearly demonstrating the material's hydrophilicity. In the case of BC:CMC films the contact angle remained above 40°. This is a bit surprising, since CMC is a water-soluble polymer and could be expected to improve the materials hydrophilicity; however, the results suggest that water spreading and/or absorption on BC was more favourable than on BC:CMC. In both cases, the materials are highly hydrophilic.

4.3.2 - Surface charge assessment through Zeta Potential measurements

The Zeta Potential is a stability indicator for colloidal suspensions: samples showing highly positive or negative Zeta Potential ($> |30|$ mV) will have a lower tendency to aggregate and flocculate, owing to inter-particle repulsion forces. Table 4.1 shows the Zeta Potential values for the used materials.

Table 4.1 - Zeta Potential (Z) and particle size of different cellulose aqueous suspensions, represented as the average and standard deviation (a- Before activation; b- After activation; c – Information provided by the supplier)

	BC	BC:CMC	Avicel LM310	Avicel RT1133	Novagel RCN15	Celluforce NCC
Z (mV)	-23.3±0.9	-67.0±3.9	-22.6±0.7	-64.9±0.5	-1.4±0.2	-51.3±2.3
Size (µm)	Dv(10)	184±5.26	98.2±1.57	16.7±0.04 ^a / 3.42±0.004 ^b	3.02±0.01 ^a / 2.76±0.03 ^b	35.9±0.13 ^a / 16.3±0.08 ^b
	Dv(50)	1080±26.1	601±19.7	38.6±0.09 ^a / 10.3±0.02 ^b	10.4±0.10 ^a / 7.9±0.04 ^b	116±1.08 ^a / 59.8±0.45 ^b
	Dv(90)	2360±16.5	1850±51.4	76.2±0.20 ^a / 26.4±0.14 ^b	55.9±2.37 ^a / 222.5±0.55 ^b	304±4.60 ^a / 189±4.38 ^b
						Diameter: 2.3-4.5 nm; Length: 44-108 nm ^c

Although not included in Table 4.1, CMC and Xanthan gum are known to be negatively charged given the presence of carboxylic groups. Novagel is a mixture of cellulose with Guar gum, a cationic polysaccharide, which is likely to neutralize the anions that adsorb onto solid surfaces in aqueous suspensions, hence the almost neutral Zeta Potential. Celluforce's significant negative charge is due to the sulphate groups at the surface of the fibres. Interestingly, products containing only cellulose – BC and Avicel LM310 - showed similar values of Zeta Potential (around -20 mV). On the other hand, the formulations containing CMC

present lower Zeta Potential (around -60 to 70 mV), indicating a good colloidal stability. As mentioned before, CMC imparts a negative charge on BC fibres, resulting in a more negative Zeta Potential of BC:CMC, comparing with BC alone. These results, however, should be regarded as merely indicative, due to the differences in size and shape among the different cellulose samples (the Zetasizer Nano ZS is mostly suited for particles from 5 nm to 10 μ m). Nevertheless, overall, the values compare well with those reported in the literature, e.g. in the case of BC fibres and the BC:CMC formulation [33].

Table 4.1 also shows the results of median size distribution measurements of the materials, by volume, or the size indicated by the supplier. BC was characterized in the never-dried form, and BC:CMC after drying and redispersion in water. The presence of CMC (in the BC:CMC formulation) decreased the value observed for the BC fibres' median size, which is most probably due to the improved dispersion of BC in the presence of CMC. Nevertheless, the Dv(50) value for this material is over 10-fold higher than the MCCs after the activation process (advised by the manufacturer as a means to destroy aggregates). Indeed, as shown in Table 4.1, the high energy mixing resulted in a decrease of the MCCs particle size, more noticeably in the case of Avicel LM310 and Novagel RCN15 (Figure 4.3).

4.3.3 - Interfacial tension

The chosen biphasic o/w system is a challenging one, given the difference in density between the oily and aqueous phases, a main driving force for creaming and phase separation [34]. The lightweight of isohexadecane (0.79 g/mL at 20 °C) favours its use in cosmetic formulations. Other oils, mainly vegetable oils used in food, have density values closer to that of water (e.g. sunflower oil, 0.922 g/mL [35]). Nonetheless, this more demanding system allows to better assess the performance of the new presented material, BC:CMC.

The interfacial tension (determined by the pendant drop method) between isohexadecane and water was (47.3 ± 0.3) mN/m, while for commercial sunflower oil and water is much lower (27.7 ± 0.6) mN/m. Figure 4.5 shows the results obtained using two different methods to determine the interfacial tension between water dispersions of the different materials and isohexadecane. The large size and non-colloidal nature of Novagel made it difficult to analyse by the Pendant Drop method. Furthermore, a control with wet-ground BC alone was impossible to perform given the tendency of the fibres to aggregate in bundles that could not pass through the syringe and would cling to the tensiometer ring, not providing reliable measurements.

The high viscosity of the 0.50 % Xanthan gum dispersion made it impossible to analyse with the ring method. Using the pendant drop method, this problem was overcome by allowing the drop to equilibrate

for a few minutes before starting the tension measurements. BC:CMC, CMC, Xanthan and Celluforce drops were clear and transparent, while Novagel and Avicel ones had an opaque appearance. BC:CMC and xanthan drops were less round-shaped, more elongated and smaller.

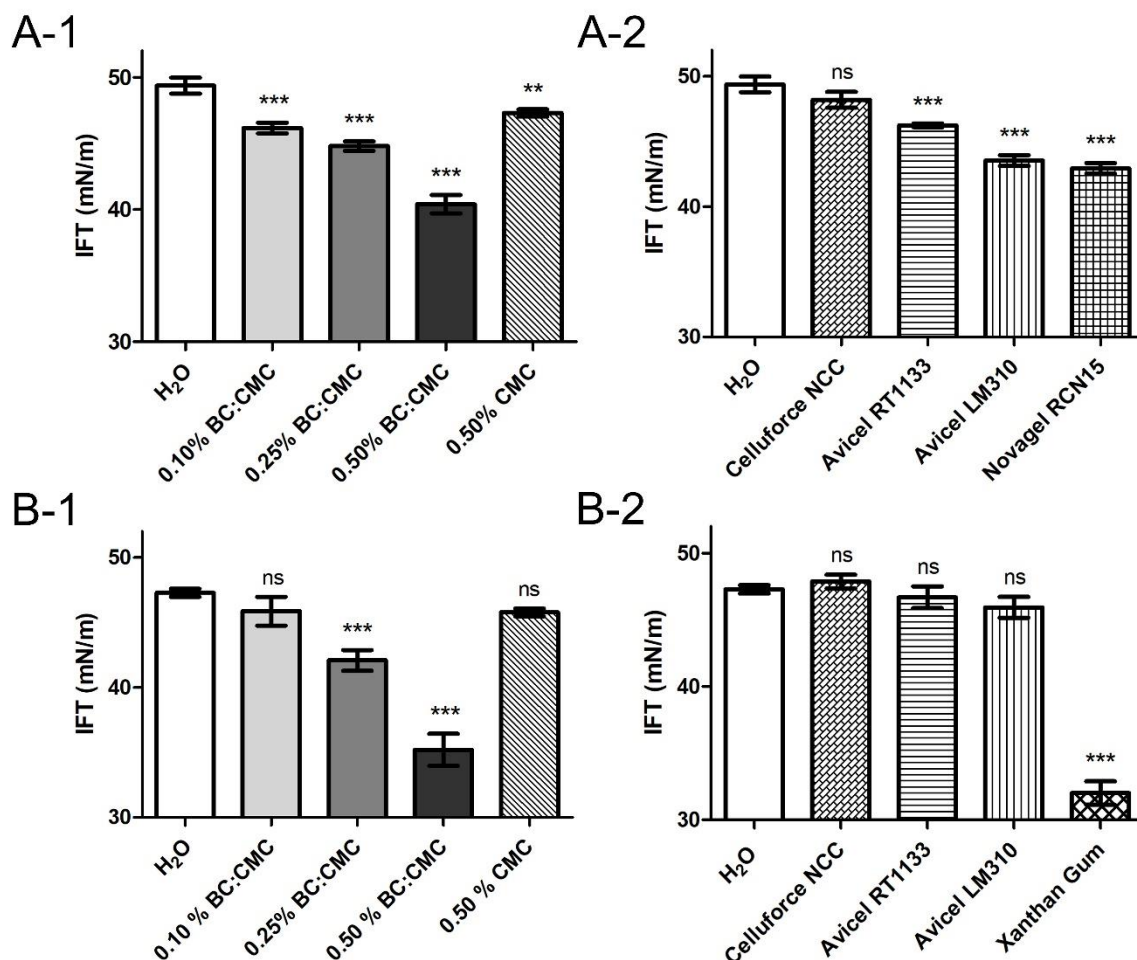


Figure 4.5 - Isohexadecane/water interfacial tension measurements performed by (A) Du Noüy Ring method and (B) Pendant Drop method, in the presence of (1) different concentrations of the BC:CMC dry formulation (0.10 %, 0.25 % and 0.50 %) and 0.50 % CMC, and (2) 0.50 % of plant celluloses (Avicel RT1133, Avicel LM310, Novagel RCN15, Celluforce NCC) and Xanthan gum. Results are the average of triplicate measurements and bars represent standard deviation. All the results were compared with the control (H₂O) using one-way ANOVA and Tukey's Multiple Comparison Test (ns – not significant, * p < 0.05, ** p < 0.01, *** p < 0.001).

Although the interfacial tension values obtained by each method were not the same, the tendency is quite similar for the BC:CMC dispersions: the IFT significantly decreased with increasing BC:CMC concentration. A 0.50 % CMC solution showed IFT values closer to water and very different from the BC:CMC dispersion at the same concentration. We can then impart the IFT decrease to the BC fibres in

the formulation, since CMC alone is unable to induce such marked reduction of the interfacial forces between oil and aqueous phase.

The similarities between both methods are not so evident for the commercial products. For the pendant drop method (Figure 4.5-B), Celluforce and both Avicel products showed no significant differences from the water control; in the ring method (Figure 4.5-A) however, the Avicel celluloses seem to be able of lowering the IFT. While the ring method could be a more sensitive method for the plant celluloses, this was not the case for the BC:CMC and CMC samples.

Although the emulsion stabilizing ability of MCCs, NCCs and even BC have been reported, we could not find a systematic study on how and why these materials affect the IFT [9,15,18]. Overall, under the pendant drop method, xanthan yielded a slightly higher reduction in IFT than BC:CMC. On the other hand, it is clear that the BC:CMC formulation induced a greater decrease in the IFT than all of the commercial plant celluloses.

4.3.4 - Emulsion stability over time

The visual aspect of the emulsions was recorded for several weeks (Figures 4.6 and 4.7), allowing the observation of the creaming effect (whitish emulsified layer on the top of the vessel, separating from the continuous phase). In some cases, the separation of the oil phase is also detectable (broken emulsion). The oil droplets size was also assessed by optical microscopy observations. The emulsion with only CMC was unstable just 1 day after preparation, had substantial creaming and very large droplets of oil, these becoming quite evident after 30 days (Figure 4.6). Different concentrations of BC:CMC were tested, showing that even small amounts of this formulation (0.10 % and 0.25 %) are capable of preventing droplets aggregation and coalescence of the oil phase for up to 90 days, despite the visible creaming effect. Indeed, the size of the droplets remains constant throughout the assay. On the other hand, when using 0.50 % of BC:CMC, no changes were detected and the emulsion remained fully stable (no creaming, no phase separation) (Figure 4.6). When using 0.50 % BC:CMC, some larger oil microdroplets were observed from the beginning, most probably due to a decreased distribution of the shear forces during homogenization in a more viscous system. Similar results were attained by Winuprasith & Supphantharika [11], using microfibrillated cellulose from mangosteen rind.

The formation of creaming just after 1 storage day was evident in all the commercial plant derived celluloses (Figure 4.7). There is a direct correlation between particle size and Pickering emulsion droplet size. Smaller particles originate smaller emulsion droplet sizes, which ultimately translates into higher stability, because gravity has less effect on them [10]. That is one of the reasons why Novagel, having

large particles and lack of colloidal stability, is not recommended for Pickering stabilization, showing large coagulated oil droplets and phase separation (Figure 4.7). Sulphated Celluforce, although being much smaller, has higher hydrophilicity and thus lower affinity for the oil phase, as pointed out by Kalashnikova et al. [12], stabilizing the oil droplets only to some extent (under the conditions tested). Large size droplets appeared over time, and a thin layer of separated oil was also detected.

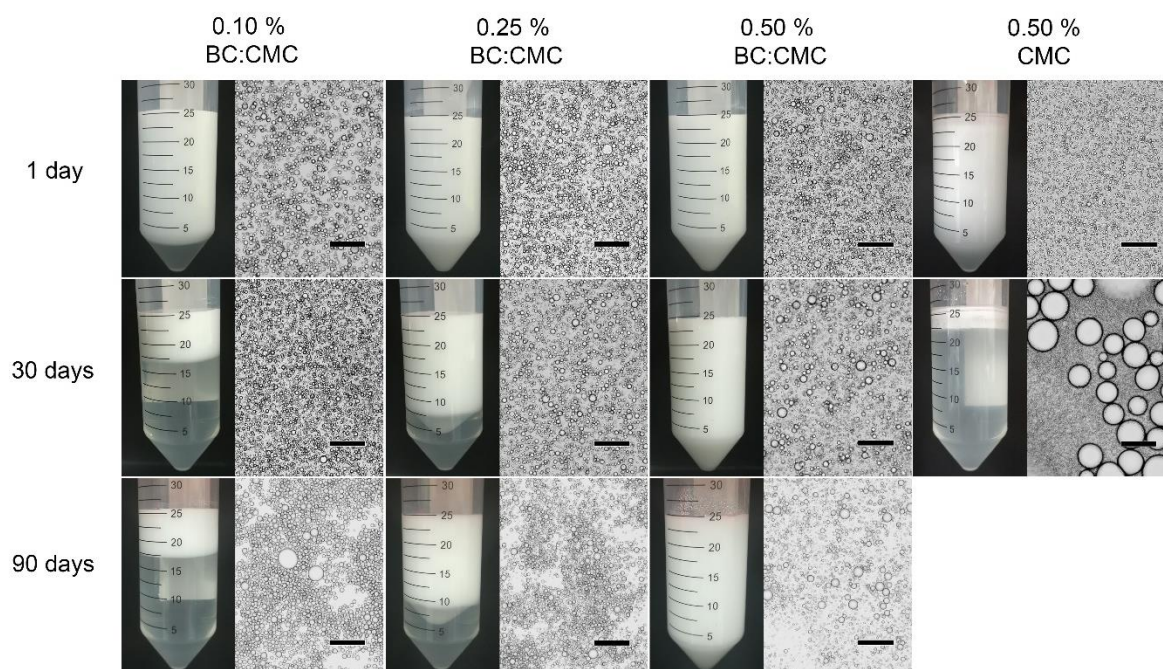


Figure 4.6 - Photographs and optical micrographs (10X magnification) of 10 % isohexadecane-in-water emulsions prepared with different concentrations of BC:CMC dry formulation (0.10 %, 0.25 % and 0.50 %) and with 0.50 % CMC, taken 1 day after preparation and after a storage time of 30 and 90 days, at room temperature. Black scale bars correspond to 100 µm.

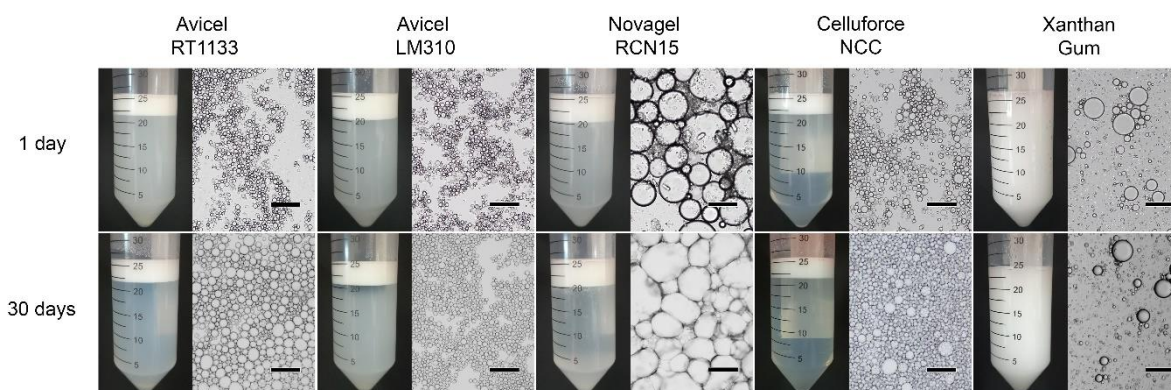


Figure 4.7 - Photographs and optical micrographs (10X magnification) of 10 % isohexadecane-in-water emulsions prepared with 0.50 % of different materials (Avicel RT1133, Avicel LM310, Novagel RCN15, Celluforce NCC and Xanthan gum), taken 1 day after preparation and after a storage time of 30 days at room temperature. Black scale bars correspond to 100 µm.

For the two Avicel samples, LM301 preserved the small size of the o/w droplets, whilst they slightly appeared to increase in the case of RT1133. Overall, among the plant derived celluloses, the smaller, non-modified particles - Avicel celluloses - performed better, as they were able to prevent the oil droplets coagulation and oil separation, showing why they are meant to be used for emulsion stabilization purposes.

Fibrillar materials with high aspect ratios generate entangled and disordered networks [11]. Although several celluloses with different sizes and surface charge were tested, they all were ineffective comparatively to BC:CMC formulations. The fibrous three-dimensional network generated by the swollen BC fibres (Figure 4.8) even at lower concentrations (<0.50 %), allowed for a better control of the creaming effect. Thus, in addition to the Pickering effect, structuring of the water phase also contributed to the oil droplets' stabilization. Although cellulose microcrystals are also known for creating a network capable of structuring the continuous phase, relatively high concentrations are needed, since their aspect ratio (length/width) is far lower than that of BC nanofibres – in the range of 100 (as reported for single BC fibres prepared with aqueous counter collision) [36]. For colloidal MCC to form a stable gel network, concentrations of 1.5 % are commonly used and a rest time is needed, following activation with high shear mixing, to achieve full structural equilibrium [20,37]. The same applies to nanocrystals - even BC nanocrystals - which have lower aspect ratios than BC whole fibres [14]. Thus, BC nanofibres, at much lower concentrations, being longer, flexible and thinner, have a structural advantage for covering the oil droplets and creating a mechanical network capable of sustaining and stabilizing the oil phase.

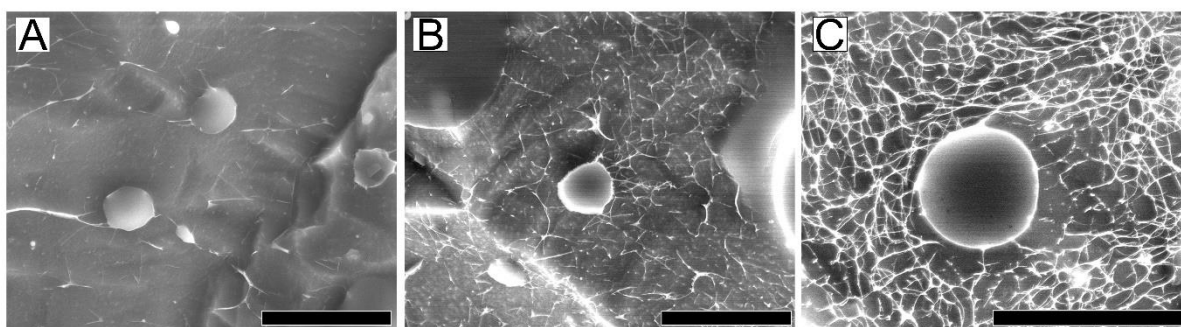


Figure 4.8 - Cryo-SEM images (different magnifications) of 10 % isohexadecane-in-water emulsions prepared with (A) 0.10 %, (B) 0.25 % and (C) 0.50 % of the BC:CMC dry formulation in the day after preparation. All black scale bars correspond to 20 μm .

Xanthan gum is a standard polysaccharide ingredient in the food and cosmetic industries, used as thickener and stabilizing aid in many products. Xanthan gum emulsions were also stable and did not

significantly change over time. Although showing large oil droplets from time zero (possibility also due to the higher viscosity of the continuous phase), they did not show aggregation or coalescence over time. Cryo-SEM images of Figure 4.8 clearly show the formation of an entangled network that develops in the continuous phase and around the disperse, ranging from a looser mesh at lower BC:CMC concentration (Figure 4.8-A), to a very dense, tight and structured network at higher concentration (Figure 4.8-C). BC's long but thin fibres, thus more flexible, can easily bend and shape to the interface. Several works have also shown the arrangement of cellulose fibres at the interface, covering the dispersed oil droplets [8,11,12,15]. However, only Winuprasith & Suphantharika [11] mentioned the three-dimensional networks formed by fibres in the continuous aqueous phase and how they play a structural supporting role for the emulsion droplets. This effect strongly helps to improve the stability of the emulsion. In addition to allowing the redispersion of the BC fibres, CMC may also contribute to the functional properties of the redispersed formulation, by improving the swelling and water dispersion of the BC fibres, which may be relevant to the emulsion stabilizing effect of the BC:CMC formulation by structuring the continuous water phase.

4.3.5 - Rheological analysis

The viscosity of BC:CMC emulsions (Figure 4.9) increased with the concentration, as would be expected, and decreased with the increase in the shear rates, showing a characteristic shear-thinning behaviour. At 0.50 % concentration, BC:CMC emulsions showed a rheologic behaviour closer to that of Xanthan gum emulsions, the later reaching a higher maximum viscosity value (126.2 Pa·s *versus* 73.5 Pa·s). The lower viscosity is not necessarily a disadvantage, as long as other rheologic parameters satisfy the demands for a stable emulsion. High viscosity might actually be an obstacle for proper sample homogenization, requiring higher shear stress, hence higher energy input, an economic disadvantage for industrial applications. As noted above, the size of the oil droplets was larger when using Xanthan gum.

It is also worth to mention that the emulsion with 90 kDa CMC alone has a very different profile and significantly lower viscosity. Thus, the viscosity of the BC:CMC dispersions is to be assigned mainly to the well dispersed BC fibres, as also noted by other authors [20]. Neither BC:CMC or Xanthan emulsions showed a yield stress value. The viscosity curves in Figure 4.9 do not increase indefinitely towards the lower shear rates, and the emulsions flow at rest conditions (near-zero shear stress).

Dynamic mechanical rheological testing was applied to the more stable systems amongst the tested ones: Xanthan gum and BC:CMC (Figure 4.10).

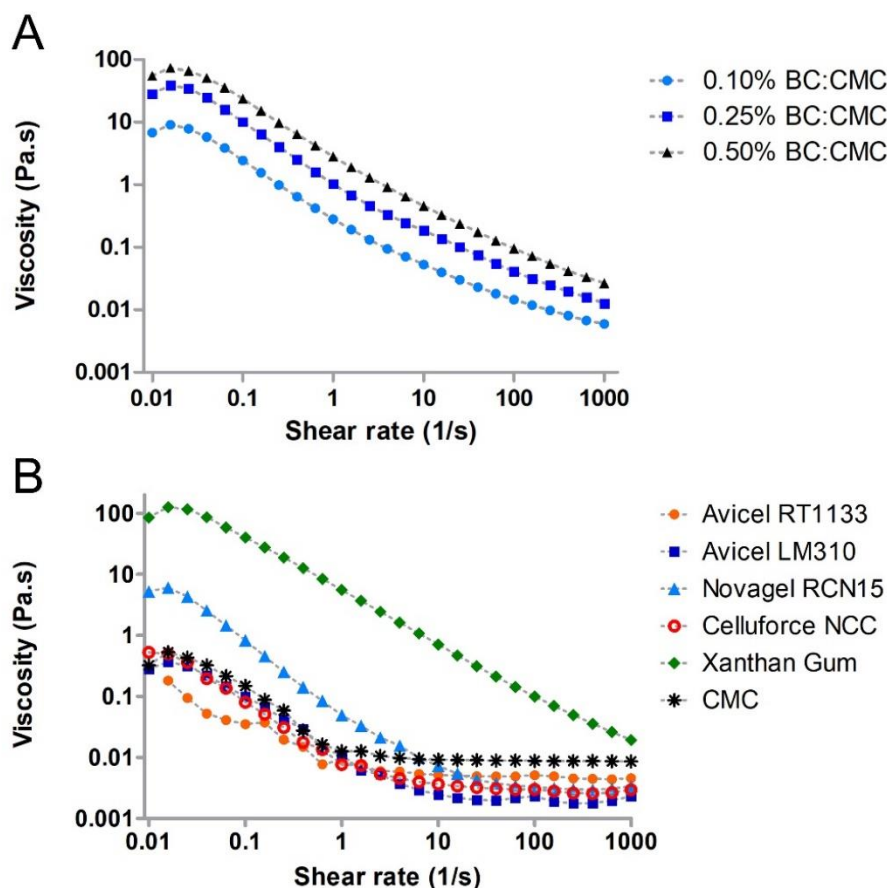


Figure 4.9 - Flow sweep curves of 10 % isohexadecane-in-water emulsions prepared with (A) different concentrations of the BC:CMC dry formulation (0.10 %, 0.25 % and 0.50 %); (B) 0.50 % of different materials (Avicel RT1133, Avicel LM310, Novagel RCN15, Celluforce NCC, Xanthan gum and CMC), obtained from the average of triplicate samples.

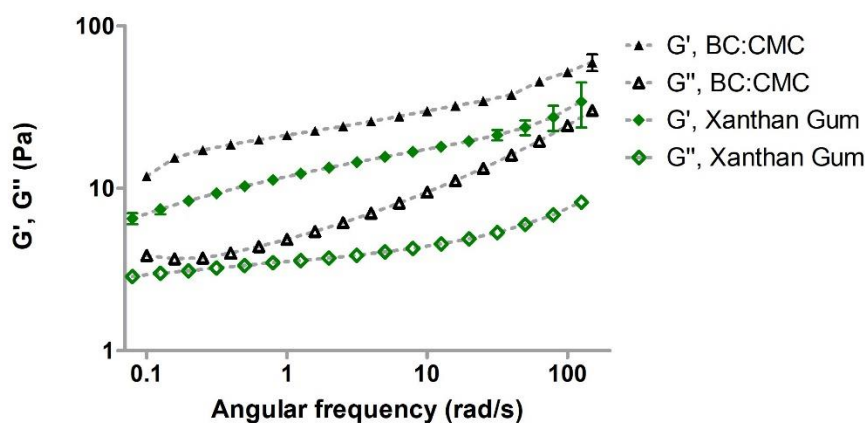


Figure 4.10 - Oscillatory frequency sweep curves of 10 % isohexadecane-in-water emulsions prepared with 0.50 % BC:CMC and Xanthan gum, obtained from the average of triplicate samples. Bars represent standard deviation.

First, a strain sweep was performed (data not shown) to establish the extent of the emulsions' linearity range - the LVR - where the storage modulus (G') and loss modulus (G'') are approximately constant. The LVR was maintained up to 1 % strain amplitude for the 0.50 % BC:CMC emulsions, and extended up to 10 % for the Xanthan gum emulsions. A strain of 0.25 % was chosen to proceed for the frequency sweep test.

There must be a sufficient degree of structure in an emulsion to avoid creaming and separation. The storage modulus G' is a good indicator of the emulsion's elastic (solid-like) behaviour coming from the inherent network structure, when it exists. When phases separate in an emulsion, it loses the solid-like character and becomes more fluid.

From Figure 4.10, emulsions prepared with BC:CMC and Xanthan exhibit a predominant elastic behaviour within the LVR, since G' was higher than G'' . Interestingly, despite the higher viscosity on the Xanthan gum emulsions, the results point to a stronger network in the samples stabilized with BC:CMC, as G' is higher for BC:CMC emulsions than Xanthan. This could be due to a stiffer network created in the BC:CMC emulsions by the insoluble BC fibres.

As shown in Figure 4.6, well separated oil droplets were still observed in the creaming layer of the emulsions processed with the plant celluloses, although the stability of these formulations was rather poor. It seems thus likely that these commercial celluloses are achieving some IFT reduction and acting as Pickering agents. However, the lack of aqueous phase structuring results in quick creaming and eventually phase separation. In turn, BC:CMC reduces more effectively the IFT, likely owing to the thinner and more flexible fibres, an effect that is reinforced by the relevant water structuring effect, as demonstrated by the Cryo-SEM and rheology studies. We speculate that the slightly lower hydrophilicity of the BC:CMC as compared BC alone, may be relevant to achieve a more favourable contact angle at the oil-water interface. In addition, we also hypothesize that CMC, by improving the fibres swelling by repelling each other due to the negative charges, may significantly contribute to the emulsions stabilization by promoting the three-dimensional structuring effect.

4.4 - CONCLUSIONS

In short, the BC:CMC formulation used in o/w emulsions showed to possess crucial characteristics for emulsion stability: surface charge, formation of a three-dimensional network, reduction of the interfacial energy and high viscosity (thickener). The ultrathin and very long BC fibres represent a radically different material as compared to some commonly available dry celluloses recommended as stabilizers, as the ones used as benchmark in this study, which are either soluble or lower aspect ratio hydrocolloidal

cellulose particles. In general, these commercial dry products are obtained from plant/wood biomass, thus needing more processing steps to achieve a high purity and low size range, need much higher energy mixing to reach their full capabilities, which translate in lower efficiencies in the interfacial surface coverage and in the formation of a three-dimensional network for structuring the aqueous phase, in the case of emulsions. In this study, the prepared dry BC formulation was technically superior to the dry commercial celluloses used in parallel as benchmark: it showed better stabilizing performance and was easily and rapidly redispersible, with no need of activation or high energy processing prior to use. Due to its intrinsic structural and rheological properties, BC could be applicable as a thickener, stabilizer and texture modifier for food and cosmetic applications. At a concentration of 0.50 %, the dry BC:CMC formulation was able to effectively stabilize low density oil-in-water emulsions against coalescence or creaming for up to 90 days without the need to add any other emulsifying agents, thus confirming the potential of BC as a Pickering emulsions stabilizer.

4.5 - BIBLIOGRAPHIC REFERENCES

- [1] B.P. Binks, Particles as surfactants - similarities and differences, *Curr. Opin. Colloid Interface Sci.* 7 (2002) 21–41.
- [2] S. Lam, K.P. Velikov, O.D. Velez, Pickering stabilization of foams and emulsions with particles of biological origin, *Curr. Opin. Colloid Interface Sci.* 19 (2014) 490–500. <https://doi.org/10.1016/j.cocis.2014.07.003>.
- [3] Y. Chevalier, M.A. Bolzinger, Emulsions stabilized with solid nanoparticles: Pickering emulsions, *Colloids Surfaces A Physicochem. Eng. Asp.* 439 (2013) 23–34. <https://doi.org/10.1016/j.colsurfa.2013.02.054>.
- [4] F. Dourado, M. Leal, D. Martins, A. Fontão, A. Cristina Rodrigues, M. Gama, Celluloses as Food Ingredients/Additives: Is There a Room for BNC?, in: M. Gama, F. Dourado, S. Bielecki (Eds.), *Bact. Nanocellulose From Biotechnol. to Bio-Economy*, Elsevier B.V., 2016: pp. 123–133. <https://doi.org/10.1016/B978-0-444-63458-0.00007-X>.
- [5] L. Bai, S. Lv, W. Xiang, S. Huan, D.J. McClements, O.J. Rojas, Oil-in-water Pickering emulsions via microfluidization with cellulose nanocrystals: 1. Formation and stability, *Food Hydrocoll.* 96 (2019) 699–708. <https://doi.org/10.1016/j.foodhyd.2019.04.038>.
- [6] L. Bai, S. Huan, W. Xiang, O.J. Rojas, Pickering emulsions by combining cellulose nanofibrils and nanocrystals: Phase behavior and depletion stabilization, *Green Chem.* 20 (2018) 1571–1582. <https://doi.org/10.1039/c8gc00134k>.
- [7] I. Capron, B. Cathala, Surfactant-free high internal phase emulsions stabilized by cellulose nanocrystals, *Biomacromolecules.* 14 (2013) 291–296. <https://doi.org/10.1021/bm301871k>.
- [8] F. Cherhal, F. Cousin, I. Capron, Structural Description of the Interface of Pickering Emulsions Stabilized by Cellulose Nanocrystals, *Biomacromolecules.* 17 (2016) 496–502. <https://doi.org/10.1021/acs.biomac.5b01413>.
- [9] Z. Hu, S. Ballinger, R. Pelton, E.D. Cranston, Surfactant-enhanced cellulose nanocrystal Pickering emulsions, *J. Colloid Interface Sci.* 439 (2015) 139–148. <https://doi.org/10.1016/j.jcis.2014.10.034>.

- [10] F. Niu, B. Han, J. Fan, M. Kou, B. Zhang, Z.J. Feng, W. Pan, W. Zhou, Characterization of structure and stability of emulsions stabilized with cellulose macro/nano particles, *Carbohydr. Polym.* 199 (2018) 314–319. <https://doi.org/10.1016/j.carbpol.2018.07.025>.
- [11] T. Winuprasith, M. Supphantharika, Properties and stability of oil-in-water emulsions stabilized by microfibrillated cellulose from mangosteen rind, *Food Hydrocoll.* 43 (2015) 690–699. <https://doi.org/10.1016/j.foodhyd.2014.07.027>.
- [12] I. Kalashnikova, H. Bizot, B. Cathala, I. Capron, Modulation of cellulose nanocrystals amphiphilic properties to stabilize oil/water interface, *Biomacromolecules.* 13 (2012) 267–275. <https://doi.org/10.1021/bm201599j>.
- [13] C. Yamane, T. Aoyagi, M. Ago, K. Sato, K. Okajima, T. Takahashi, Two different surface properties of regenerated cellulose due to structural anisotropy, *Polym. J.* 38 (2006) 819–826. <https://doi.org/10.1295/polymj.PJ2005187>.
- [14] I. Kalashnikova, H. Bizot, B. Cathala, I. Capron, New pickering emulsions stabilized by bacterial cellulose nanocrystals, *Langmuir.* 27 (2011) 7471–7479. <https://doi.org/10.1021/la200971f>.
- [15] H. Ougiya, K. Watanabe, Y. Morinaga, F. Yoshinaga, Emulsion-stabilizing Effect of Bacterial Cellulose, *Biosci. Biotechnol. Biochem.* 61 (1997) 1541–1545. <https://doi.org/10.1271/bbb.61.1541>.
- [16] P. Paximada, E. Tsouko, N. Kopsahelis, A.A. Koutinas, I. Mandala, Bacterial cellulose as stabilizer of o/w emulsions, *Food Hydrocoll.* 53 (2016) 225–232. <https://doi.org/10.1016/j.foodhyd.2014.12.003>.
- [17] P. Paximada, A.A. Koutinas, E. Scholten, I.G. Mandala, Effect of bacterial cellulose addition on physical properties of WPI emulsions. Comparison with common thickeners, *Food Hydrocoll.* 54 (2016) 245–254. <https://doi.org/10.1016/j.foodhyd.2015.10.014>.
- [18] X. Zhai, D. Lin, D. Liu, X. Yang, Emulsions stabilized by nanofibers from bacterial cellulose: New potential food-grade Pickering emulsions, *Food Res. Int.* 103 (2018) 12–20. <https://doi.org/10.1016/j.foodres.2017.10.030>.
- [19] N. Butchosa, Q. Zhou, Water redispersible cellulose nanofibrils adsorbed with carboxymethyl cellulose, *Cellulose.* 21 (2014) 4349–4358. <https://doi.org/10.1007/s10570-014-0452-7>.
- [20] G.H. Zhao, N. Kapur, B. Carlin, E. Selinger, J.T. Guthrie, Characterisation of the interactive properties of microcrystalline cellulose-carboxymethyl cellulose hydrogels, *Int. J. Pharm.* 415 (2011) 95–101. <https://doi.org/10.1016/j.ijpharm.2011.05.054>.
- [21] D. Agarwal, W. MacNaughtan, T.J. Foster, Interactions between microfibrillar cellulose and carboxymethyl cellulose in an aqueous suspension, *Carbohydr. Polym.* 185 (2018) 112–119. <https://doi.org/10.1016/j.carbpol.2017.12.086>.
- [22] A. Naderi, T. Lindström, J. Sundström, G. Flodberg, Can redispersible low-charged nanofibrillated cellulose be produced by the addition of carboxymethyl cellulose prior to its drying?, *Nord. Pulp Pap. Res. J.* 30 (2015).
- [23] C. Clasen, B. Sultanova, T. Wilhelms, P. Heisig, W.M. Kulicke, Effects of different drying processes on the material properties of bacterial cellulose membranes, *Macromol. Symp.* 244 (2006) 48–58. <https://doi.org/10.1002/masy.200651204>.
- [24] N. Pa'E, N.I.A. Hamid, N. Khairuddin, K.A. Zahan, K.F. Seng, B.M. Siddique, I.I. Muhamad, Effect of different drying methods on the morphology, crystallinity, swelling ability and tensile properties of nata de coco, *Sains Malaysiana.* 43 (2014) 767–773.
- [25] M.C.I.M. Amin, A.G. Abadi, H. Katas, Purification, characterization and comparative studies of spray-dried bacterial cellulose microparticles, *Carbohydr. Polym.* 99 (2014) 180–189. <https://doi.org/10.1016/j.carbpol.2013.08.041>.
- [26] P. Tammarate, US Patent 5,962,676 - Process for the modification and utilization of bacterial cellulose, 1999.

- [27] K. Watanabe, A. Shibata, H. Ougiya, N. Hioki, Y. Morinaga, US Patent 6,153,413 - Method for processing bacterial cellulose, 2000.
- [28] Z.-F. Yang, N.A. Morrison, T.A. Talashek, D.F. Brinkmann, D. DiMasi, Y.L. Chen, US Patent 8,053,216 B2 - Bacterial cellulose-containing formulations, 2011.
- [29] Z.-F. Yang, S. Sharma, C. Mohan, J. Kobzeff, Patent WO 01/05838 A1 - Process for drying reticulated bacterial cellulose without co-agents, 2001.
- [30] S. Ahola, P. Myllytie, M. Österberg, T. Teerinen, J. Laine, Effect of Polymer Adsorption on Cellulose, *BioResources*. 3 (2008) 1315–1328. http://ojs.cnr.ncsu.edu/index.php/BioRes/article/viewFile/BioRes_03_4_1315_Ahola_MOTL_Poly_Adsorp_Cellulose_Nanofiber_Water_Binding/285.
- [31] R. Kargl, T. Mohan, M. Bračč, M. Kulterer, A. Doliška, K. Stana-Kleinschek, V. Ribitsch, Adsorption of carboxymethyl cellulose on polymer surfaces: Evidence of a specific interaction with cellulose, *Langmuir*. 28 (2012) 11440–11447. <https://doi.org/10.1021/la302110a>.
- [32] J. Laine, T. Lindstrom, G.G. Nordmark, G. Risinger, Studies on topochemical modification of cellulosic fibres Part 1. Chemical conditions for the attachment of carboxymethyl cellulose onto fibres, *Nord. Pulp Pap. Res. J.* 15 (2000). <https://doi.org/10.3183/npprj-2003-18-03-p325-332>.
- [33] R. Silva-Carvalho, J.P. Silva, P. Ferreira, A.F. Leitão, F.K. Andrade, R.M. Gil da Costa, C. Cristelo, M.F. Rosa, M. Vilanova, F.M. Gama, Inhalation of Bacterial Cellulose Nanofibrils triggers an inflammatory response and changes lung tissue morphology of mice, *Toxicol. Res.* 35 (2019) 45–63. <https://doi.org/10.5487/TR.2019.35.1.045>.
- [34] T. Tadros, Application of rheology for assessment and prediction of the long-term physical stability of emulsions, 2004. <https://doi.org/10.1016/j.cis.2003.10.025>.
- [35] D.L. Lamas, D.T. Constenla, D. Raab, Effect of degumming process on physicochemical properties of sunflower oil, *Biocatal. Agric. Biotechnol.* 6 (2016) 138–143. <https://doi.org/10.1016/j.bcab.2016.03.007>.
- [36] T. Kondo, P. Rytczak, S. Bielecki, Bacterial NanoCellulose Characterization, in: M. Gama, F. Dourado, S. Bielecki (Eds.), *Bact. Nanocellulose - From Biotechnol. to Bio- Econ.*, Elsevier B.V., 2016: pp. 59–71.
- [37] V.S. Rudraraju, C.M. Wyandt, Rheological characterization of Microcrystalline Cellulose/Sodiumcarboxymethyl cellulose hydrogels using a controlled stress rheometer: Part I, *Int. J. Pharm.* 292 (2005) 53–61. <https://doi.org/10.1016/j.ijpharm.2004.10.011>.

Chapter 5

BC:CMC dry formulation as stabilizer and texturizing agent for surfactant-free cosmetic formulations

Generic cosmetic creams (oil-in-water emulsions) were prepared using dry Bacterial Cellulose and Carboxymethyl Cellulose (BC:CMC) to study the possibility of partially or completely replacing surfactants, while ensuring a long-term stability and the required organoleptic characteristics. BC:CMC was benchmarked against two hydrocolloidal Avicel products (PC-591 and PC-611), commonly used as thickeners and stabilizing aids in cosmetics production. The emulsions were then characterized regarding storage stability, rheology, texture and microscopic features.

The full replacement of 5.5% surfactants with only 0.75% BC:CMC consistently showed similar results to those obtained with surfactants, namely concerning viscosity and texture. Although producing emulsions with larger oil droplets, BC:CMC provided for a very effective stabilization through a Pickering effect and by structuring the continuous phase. The more effective Avicel tested (PC-591) required a higher concentration (1.5 %) to achieve similar rheological profile but was ineffective in stabilizing the oil phase in a surfactant-free formulation with the adopted protocol. By replacing surfactants, dry BC:CMC matches a strong market need since both end users and manufacturers increasingly seek natural ingredients for cosmetic formulations.

5.1 - INTRODUCTION

Cosmetic formulations are very complex mixtures, comprising water, oils, alcohols, active agents, preservatives, fragrances and others. Surfactants allow to balance all these components into a stable mixture. Besides their main role as emulsion stabilizers, surfactants also improve the rheological behaviour and texture of the formulations. In products such as cleansers, shampoos, washes and other personal hygiene products, they are the main ingredient, responsible for the cleaning function. Often surfactants can be irritating or sensitizing, depending on their chemical nature and concentration, originating or aggravating existent skin issues. Due to an increasing awareness and concern about these effects, more products are being formulated with milder or more natural surfactant systems, or partially replacing surfactants with polymeric thickeners such as xanthan gum, cellulose derivatives (e.g., hydroxypropyl methyl cellulose) and microcrystalline cellulose (MCC), among others. Thickeners help improving stability and rheology, and even bringing more pleasant sensory attributes to low-surfactant formulations [1–5].

MCC is already widely used in cosmetic products, often in combination with carboxymethyl cellulose (CMC). MCC particles can interact with each other in aqueous dispersions to form a network structure, after being subjected to high-energy mixing. MCC particles can help emulsification by Pickering stabilization; the three-dimensional polymer networks increase viscosity and create a solid-like rheological behaviour. Altogether, these properties help stabilizing emulsions and dispersions [6–9].

Cellulose from bacterial sources (e.g., *Komagataeibacter* genus) is chemically identical to wood or plant cellulose, but is obtained through fermentation in a pure state, consisting of long fibres with nanoscale thickness (high aspect ratio) [10,11]. Bacterial cellulose (BC) has already been studied notably in biomedical applications and also in the production of composites for the most diverse areas, the production and stabilization of emulsions and other food systems, optoelectronics and others [12–16].

In cosmetics, BC has been commercialized as face masks. The high water content and water retention capacity of the BC membrane can increase water uptake by the skin and improve hydration. Due to its high porosity, several drugs and active ingredients can be incorporated and released to skin under a controlled manner [17–21]. Other applications for BC as an ingredient for personal care and cosmetics have been studied and developed in recent decades, mostly found in patents. Examples include patent US 2007/019777 A1 [22] referring to mixtures of BC and CMC dried after alcohol precipitation (and spray-drying) for use as rheology modifier in a plethora of applications, including hair conditioners and hair styling products; patent WO 2011/019876 A2 [23] referring to personal cleansing formulations

containing BC in combination with a cationic polymer as an external structuring system, to compensate for a smaller amount of internal structurants (surfactants); patent US 6534071 B1 [24] related to oil-in-water emulsions for cosmetic uses, free of surfactants, and containing cellulose fibrils, namely some commercial powdered BC formulations with CMC; and others (WO 2011/056951 A1 [25], US 8716213 B2 [26]). These documents strongly demonstrate the growing commercial interest in BC for cosmetics and personal care market segments, but also a strong market need for BC products in their dry form. Indeed, dry products have advantages in transportation and storage since they occupy a smaller volume, plus are less prone to contaminations and can have longer shelf-life than hydrated forms.

Dry BC:CMC formulations have been recently reported by our group, which require low-energy mixing and short mixing time (under 5 min) at room temperature, to achieve complete redispersion. These BC:CMC formulations display high viscosity and thickening power, ability to decrease oil/water interfacial tension and the capability to form three-dimensional networks in aqueous media, acting as an external structurant. Even in low concentrations they are able to stabilize different heterogeneous systems for long periods of time, such as liquid-in-liquid emulsions (stability for over 90 days against coalescence and creaming, at 0.5 %) and solid-in-liquid dispersions (stability for over 4 days against sedimentation, at 0.15 %). Moreover, BC:CMC was able to outperform some commercially available MCCs in these systems [27,28].

Having proved the emulsifying, thickening and stabilizing capabilities of BC:CMC in a simple emulsion system, it is important to ascertain its performance in a complex matrix such as that of cosmetic products; it is also still necessary to validate its performance in the presence of - or in combination with - surfactants, once they serve a specific purpose in many products and are therefore indispensable. Furthermore, a surfactant substitute such as BC:CMC must not only stabilize cosmetic creams, it must also replicate relevant rheological and textural characteristics of traditional creams. This would allow to secure consumer acceptance, unlike what happens with other ingredients from natural sources.

In this work, generic cosmetic cream analogues (oil-in-water emulsions) have been prepared with dry BC:CMC in order to study the possibility of replacing, partially or completely, the surfactants in the cosmetic formulation, while maintaining a long-term stability and the characteristic rheological and organoleptic properties of the creams. A short-time mixing protocol was employed. Furthermore, a benchmark was made with MCC products that are optimized for cosmetic applications, to demonstrate that BC:CMC can have a competitive advantage against some of the already marketed plant-based celluloses.

5.2 - MATERIALS AND METHODS

5.2.1 - Materials and Reagents

BC wet membranes were supplied by HTK Food CO., Ltd (Ho Chi Minh, Vietnam). Carboxymethyl cellulose (90 kDa, Degree of Substitution of 0.7) was supplied by Acros Organics (Geel, Belgium). Isohexadecane (Purolan IHD) was gently provided by Lanxess (Leverkusen, Germany). Steareth 21 (Brij S721) was purchased from Croda (Goole, United Kingdom). Liquid paraffin was provided by Labchem (Loures, Portugal). Butylene glycol, Dimethicone, Stearic acid, Steareth 2 (Brij S2), Nile Red, Calcofluor White and Sodium azide were purchased from Sigma (St. Louis, Missouri, USA).

Avicel® colloidal MCCs are widely known and used in several industry fields. For this work, two were chosen for being specifically indicated for cosmetic applications, and used as received: Avicel PC-611 (low viscosity, containing 11.3 to 18.8 % CMC) and Avicel PC-591 (medium viscosity, containing 9.0 to 15.0 % CMC), kindly provided by DuPont (Wilmington, Delaware, USA).

5.2.2 - BC:CMC preparation

Dried BC:CMC was prepared using a methodology adapted from Martins et al. [27]. BC membranes were left in 0.1 M NaOH solution for 4 days (with daily solution exchange), at room temperature, then washed thoroughly with distilled water until the pH was that of the distilled water. The washed membranes were then wet ground using first a fixed speed hand blender (Sammic blender TR250, Sammic S. L.) at 9000 rpm until a homogeneous pulp was obtained, and then using a high-speed blender (Moulinex Ultrablend 1500W) at 24 000 rpm for 1 min. The solid fraction of the obtained pulp was determined by dry weight and adjusted to 0.5 % (m/v). To this pulp, the same volume of 0.5 % (m/v) CMC (90 kDa) was added, making up a 1:1 mixture (BC:CMC) of 0.5 % total solids. This mixture was left under magnetic stirring overnight and autoclaved at 121 °C for 20 min. The formulation was freeze-dried for 5 days at -100 °C and approximately 0.05 mbar and stored in a desiccator until use. A similar BC:CMC material (spray-dried) has been previously characterized [27], showing Zeta potential of (-67.0 ± 3.9) mV and a mean diameter, $D_v(50)$, of (601 ± 19.7) μm in aqueous suspension.

5.2.3 - Emulsions preparation

Generic cosmetic cream emulsions were prepared (Table 1) in triplicate, using a methodology adapted from Gilbert et al. [29–31], where Steareth 2, Steareth 21 (non-ionic) and stearic acid were used as surfactants. The full formulation (FF), as described in the cited literature is displayed in Table 5.1,

containing a total surfactants concentration of 5.5 % (in mass). Samples with added polymers (BC:CMC or MCC) were prepared with only 10 % of that amount (0.55 % of total surfactants) and designated “Low Surfactant Formulations” (LSF). This concentration was chosen after several exploratory tests, for lying below the stability threshold of the emulsion (which was determined to be around 1.38 % of total surfactants, where creaming started to occur). A low surfactant control (“LS Control”) cream was also prepared without any polymer (the amount of polymer was substituted by distilled water).

Furthermore, to investigate the stabilizing properties of the polymers alone, emulsions were also prepared without surfactants (designated “No Surfactant Formulations”, NSF). No control was made in this case since emulsions could not be obtained.

Table 5.1 - Composition, in mass fraction (% w/w), of the generic cosmetic cream emulsions (* - Full formulation of the generic cream, prepared according to Gilbert et al. [29–31])

		Low surfactants formulations (LSF)							No surfactants formulations (NSF)			
	FF*	LS Control	LS BC:CMC		LS PC-591		LS PC-611		NS BC:CMC		NS PC-591	
Polymer	-	-	0.5	0.75	0.75	1.5	0.75	1.5	0.5	0.75	0.75	1.5
Distilled water	81	85.95	85.45	85.2	85.2	84.45	85.2	84.45	86	85.75	85.75	85
Butylene glycol	4											
Steareth2	3	0.3							-			
Steareth 21	2	0.2							-			
Stearic acid	0.5	0.05							-			
Iso-hexadecane	7											
Dimethicone	1											
Paraffin	1.5											

It has been previously reported that a dry formulation of BC:CMC at a concentration of 0.5 % was capable of fully stabilizing a 10 % isohexadecane emulsion up to 90 days [27]. Therefore, for this work with a similar material, a concentration of 0.5 % BC:CMC was chosen; additionally, a concentration of 0.75 % BC:CMC was also tested in order to increase the viscosity and possibly improve the textural profile of the cosmetic cream formulation. On the other hand, MCCs usually require higher amounts to create a

structuring network within the sample, up to 1.5 % [9]; besides, a lower concentration of 0.75 % was also tested for Avicels to have a comparison point with BC:CMC.

BC:CMC, Avicel PC-591 and Avicel PC-611 were pre-dispersed in half of the volume of water used in each formulation, with magnetic stirring for 10 min at 700 rpm, at room temperature.

For the FF and LSF samples, the oil phase components and the surfactants were firstly mixed together in a magnetic stirrer at 200 rpm and approximately 75 °C, to melt the surfactants into the oils. Warm distilled water and butylene glycol were then added to the oil phase under vigorous stirring (700 rpm) for 2 min, promoting a primary coarse emulsion, also at approximately 75 °C. Afterwards, for the LSF samples, the pre-dispersed polymer was added under continuous agitation, and mixed for 1 min more. Each sample (FF and LSF) was then immediately emulsified for 2 min at 15 000 rpm in a T 25 digital Ultra-turrax (IKA, Germany) with a S25 N-18 G dispersing tool. Finally, the emulsions were left to cool to room temperature, under magnetic stirring.

For the NSF samples, oil phase components were mixed under magnetic stirring at 200 rpm and room temperature. The polymers were pre-dispersed in the total amount of distilled water and butylene glycol was added. This aqueous phase was stirred vigorously with the oil phase and emulsified in the rotor-stator homogenizer as previously described.

Emulsions of 100 g were prepared in triplicate for each condition. Sodium azide (0.02 %) was then added to all emulsions to prevent microbial contamination, and the samples were stored at room temperature in well-sealed containers to prevent water evaporation until analysis.

5.2.4 - Evaluation of stability

The samples' stability over time, at room temperature, was assessed by visual inspection and optical microscopy. An aliquot of 10 mL of each sample was transferred into a tube just after emulsion preparation and kept sealed. Photographs were taken after 1 and 30 days of preparation. For microscopic analyses, a drop of each emulsion was placed on a glass slide, coverslipped and visualized on bright field in an Olympus BX51 fluorescence microscope with Cellsense software and 10X magnification objective lens (Olympus Europa SE & Co. KG, Hamburg, Germany).

5.2.5 - Rheological analysis of the emulsions

Rheological tests were performed in a DHR-1 controlled stress rheometer with Trios version 4 software for Windows (TA Instruments, New Castle, Delaware, USA) at 25 °C using a cone and plate geometry (60 mm, 2.006° cone angle, 64 µm gap). In a flow sweep test, samples shear stress and viscosity were

measured at varying shear rate. Shear rate was increased from 0.01 s^{-1} to 1000 s^{-1} , then decreased to 0.01 s^{-1} , and finally increased once again to 1000 s^{-1} (logarithmic mode, 5 points per decade), and the values from the first and third sweeps were considered for analysis. Results were plotted as the average and standard deviation of the triplicate samples.

A Three Interval Thixotropy Test (3ITT) was performed in controlled shear rate mode to investigate the time-dependent behaviour of the formulations, through monitoring the samples' viscosity. Samples were deformed with a shear rate of 0.1 s^{-1} for 150 s in the first interval, 300 s^{-1} for 60 s in the second interval, and finally back to 0.1 s^{-1} for 600 s to allow for structure recovery.

An oscillatory strain sweep test was carried out to determine the Linear Viscoelastic Region (LVR) of the different samples. Frequency was set at 1 rad/s and strain amplitude was increased from 0.02 % to 500 %. An oscillatory frequency sweep test was performed (after a pre-shear from 1 s^{-1} to 100 s^{-1} , and 100 s^{-1} to 1 s^{-1}), with angular frequency ranging from 0.05 to 200 rad/s at a strain of 0.3 %, within the LVR as determined from the previous strain sweep test. Results were plotted as the average and standard deviation of the triplicate samples.

Cream emulsions were lastly monitored for changes in the rheological behaviour while subjected to oscillatory temperature cycles. Silicon oil was used to prevent solvent evaporation. The storage modulus was recorded as samples were cooled and heated between $10 \text{ }^{\circ}\text{C}$ and $50 \text{ }^{\circ}\text{C}$, at a constant angular frequency of 10 rad/s and 0.3 % strain, according to the following steps: (1) initial hold at $10 \text{ }^{\circ}\text{C}$, 240 s; (2) temperature ramp from $10 \text{ }^{\circ}\text{C}$ to $50 \text{ }^{\circ}\text{C}$ at a heating rate of $5 \text{ }^{\circ}\text{C}/\text{min}$, followed by a soak time of 600 s at $50 \text{ }^{\circ}\text{C}$; (3) temperature ramp from $50 \text{ }^{\circ}\text{C}$ to $10 \text{ }^{\circ}\text{C}$ at a cooling rate of $5 \text{ }^{\circ}\text{C}/\text{min}$, followed by a soak time of 600 s at $10 \text{ }^{\circ}\text{C}$; (4) repeat step 2; (5) repeat step 3.

5.2.6 - Textural analysis

Texture analysis was performed in a TA.HD Plus Texture analyser (Stable Micro Systems, Godalming, United Kingdom) with a 5 kg load cell. Samples were analysed in cylindrical cups (50 mm diameter, 75 mm height), and sample height was 35 mm.

A Penetration test was made with a P/10 probe, pre-test speed of 0.5 mm/s , test speed of 2 mm/s and post-test speed of 2 mm/s . The trigger force was set at 0.5 g, and the probe penetrated 20 mm into the sample. Firmness (the maximum penetration force) and consistency (the work of penetration, area below the curve up to the point of the maximum force) were automatically calculated by the Exponent software. Results were calculated as the mean and standard deviation of the triplicate samples for each condition.

For the Back-extrusion test, a 45 mm diameter disc was used; pre-test speed was 1mm/s, test speed was 1 mm/s and post-test speed was 2 mm/s. The trigger force was set at 0.5 g and the disc penetrated 35 mm into the sample. Firmness, consistency, cohesiveness (maximum negative force) and index of viscosity (or 'work of cohesion', the area of the negative region of the curve that represents resistance to withdrawal) were automatically calculated by the Exponent software version 6 for Windows (Stable Micro Systems). Results were calculated as the mean and standard deviation of the triplicate samples for each condition.

Statistical analysis was performed using GraphPad Prism version 5 for Windows (GraphPad Software Inc., San Diego, California, USA). Results were expressed as mean \pm standard deviation. A one-way analysis of variance (ANOVA) was performed, followed by Dunnett's Multiple Comparison Test, to establish the significance of differences.

5.2.7 - Confocal Laser Scanning Microscopy (CLSM)

Before observation, aliquots of emulsions were stained with 1 % of Nile Red solution (0.5 mg/mL in acetone) and 4 % of Calcofluor White stain solution (0.02 mg/mL in distilled water). A sample of 10 μ L was placed on a glass slide and coverslipped. Observation was made in a Confocal Laser Scanning Microscope Olympus BX61, model FluoView FV1000 (version 4), with an objective lens of 10X magnification (Olympus Europa SE & Co. KG).

The excitation and emission wavelengths used for Nile red detection were 559 nm and 592 nm, respectively, and for Calcofluor white stain were 405 nm and 461 nm, respectively.

5.3 - RESULTS AND DISCUSSION

5.3.1 - Evaluation of stability over time

The visual aspect of the cosmetic emulsions was recorded photographically at 1 and 30 days after preparation (Figure 5.1), at room temperature. Phase separation and creaming effects were observed in some cases, pointed out in Figure 5.1 with red arrows. In the case of the LSF, the addition of Avicel PC-611 did not effectively stabilize the emulsions. These samples started to show instability 1 day after preparation. The more concentrated samples (LS 1.5 PC-611) showed a small but visible creaming, remaining unaltered until the 30th day of storage, while the ones with lower concentration (LS 0.75 PC-611) exhibited very pronounced creaming and even sedimentation. Creaming is the rise of the disperse phase droplets to the top of the emulsion, a phenomenon that depends on droplet size, viscosity of the

continuous phase and density differences between continuous and dispersed phases [32]. In this case, the observation of creaming suggests low viscosity and/or insufficient continuous phase structuring in these samples, a polymer network that would immobilize the oil droplets and prevent their buoyancy driven by gravity. This will be further evaluated in the section regarding rheology experiments.

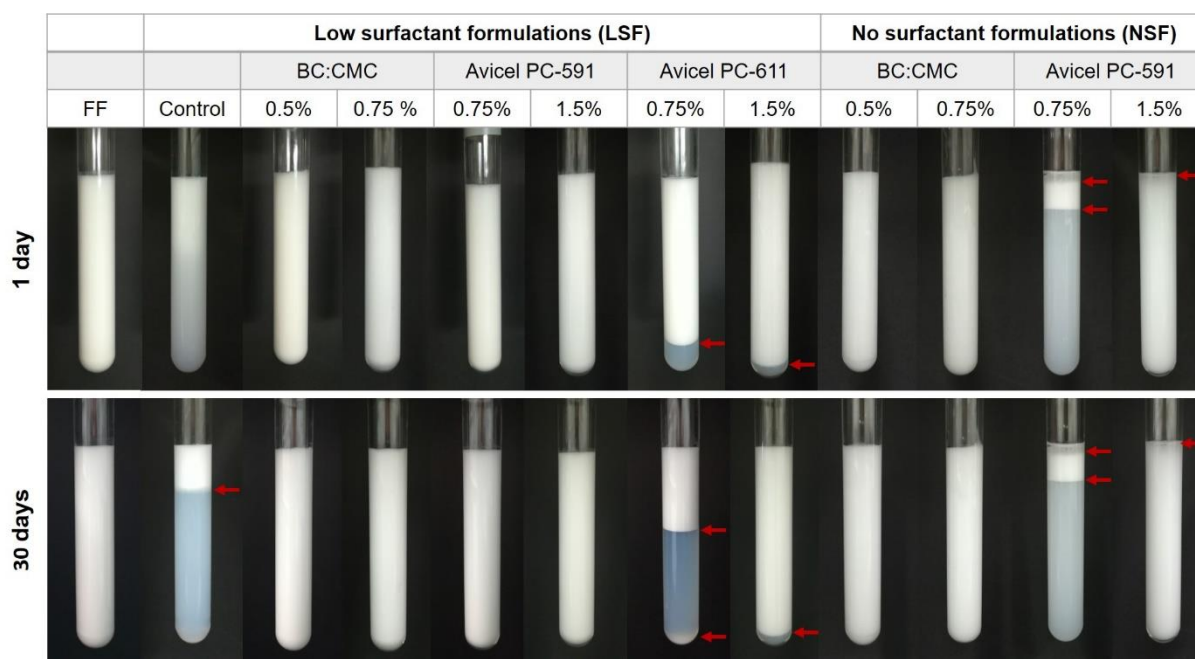


Figure 5.1 - Photographs of the cosmetic emulsions stabilized with different concentrations of BC:CMC, Avicel PC-591 and Avicel PC-611, taken 1 day after preparation and after 30 days of storage, at room temperature. Red arrows indicate visible lines of phase separation, creaming effect or sedimentation.

No oil separation was visible because the small amount of surfactants in the emulsions was sufficient to stabilize the oil phase, as can be understood from the LS Control assay. For BC:CMC and Avicel PC-591, at both concentrations, emulsions remained fully stable as no creaming nor phase separation were observed. It has been previously shown that dry BC:CMC has the ability to reduce the oil/water interfacial tension [27,28], a property associated to emulsifying agents. Therefore, emulsions were also prepared without surfactants (NSF), to evaluate the effect of the cellulose products alone in the stabilization of the oil phase. With NS Avicel PC-611, even at 1.5 %, phase separation occurred immediately after preparation, so this assay was discontinued. Avicel PC-591 was also incapable of stabilizing the emulsions, in the conditions of the adopted protocol (at a concentration of 1.5 % there was a visible line of oil at the surface of the emulsion). Contrarily, the emulsions with BC:CMC, at both tested concentrations, showed stability throughout the 30-day storage period, without visually detectable changes. Due to the pronounced

instability of the emulsions prepared with Avicel PC-611, only the LS 1.5 PC-611 was included in the following analyses; the condition NS 0.75 PC-591 was also disregarded.

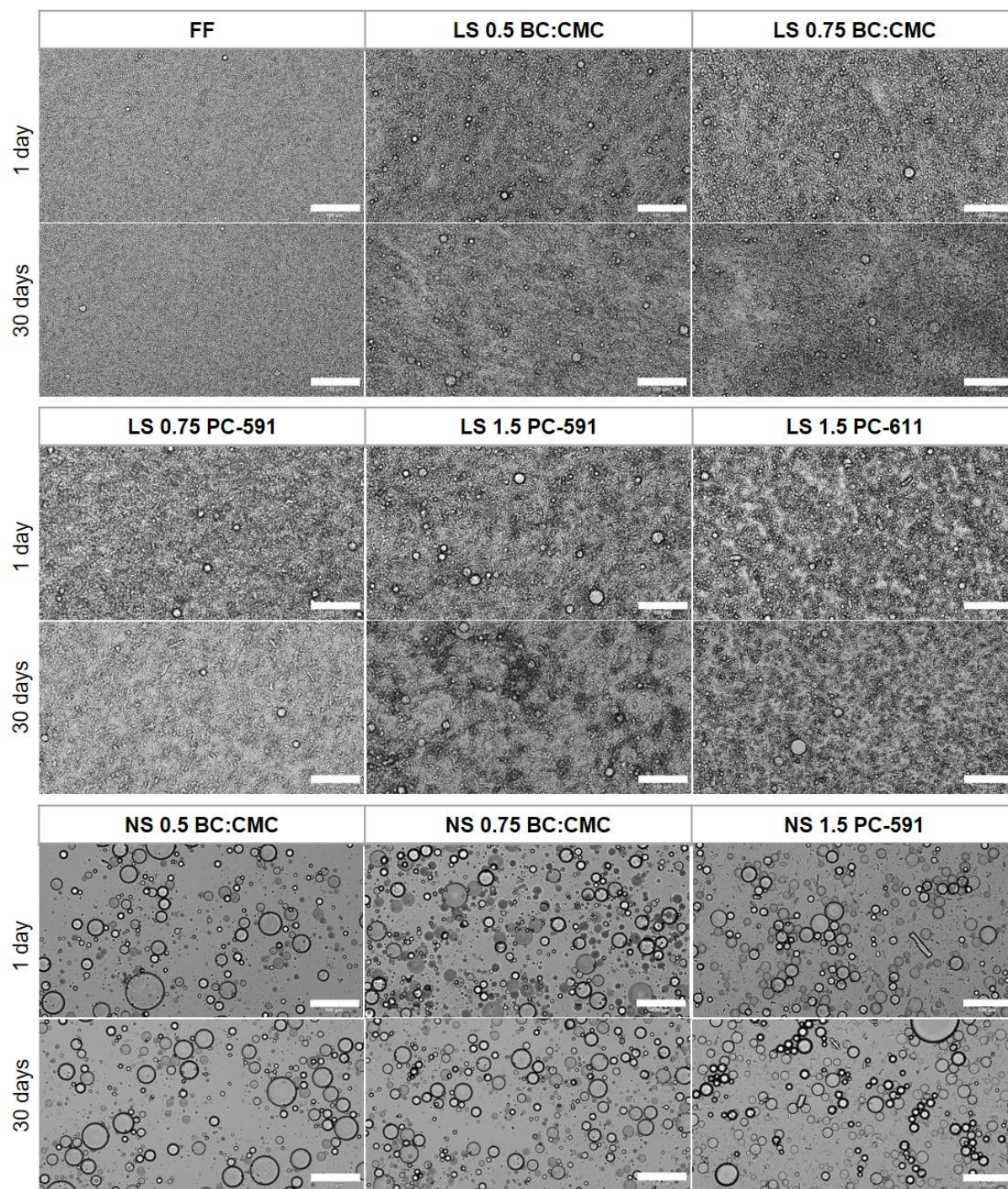


Figure 5.2 - Optical micrographs (10X magnification) of the cosmetic emulsions stabilized with different concentrations of BC:CMC, Avicel PC-591 and Avicel PC-611, taken after a storage time of 1 day and 30 days, at room temperature. Scale bars correspond to 100 μm .

In many cosmetic emulsions, surfactants are the main emulsifier/stabilizer and additional thickeners only serve rheological and textural purposes. In Figure 5.2 it is visible that the emulsion droplet sizes increase with the decrease in added surfactants and their replacement with polymers: FF emulsion has an almost homogeneous microscopic appearance; LSF show some larger droplets than FF; and then NSF show even larger droplets, more heterogeneous in size (broad distribution). In FF, higher surfactant concentration allows for a larger oil-water interfacial area and reduced interfacial tension, resulting in decreased oil droplet size.

In LSF, surfactants are still the main emulsifying agent, as the oil is much better dispersed than in the corresponding NSF (where oil globules reach several tens of micrometres). However, as a proof of concept, this experiment allowed us to further demonstrate that BC:CMC alone is capable of stabilizing the oil phase of a generic cosmetic emulsion. Figure 5.2 also shows the microscopic evolution of the emulsions over time, comparing images obtained 1 and 30 days after preparation. No significant changes in the microstructure are apparent during the storage period as there is no significant variation in the emulsion size distribution, confirming the emulsions' stability over time. This is most relevant in the case of the NS BC:CMC formulations, which display larger, yet well dispersed droplets even after 30 days, no noticeable evolution in size being detected. The significant size of the oil droplets did not translate in a loss of stability - a particular characteristic of Pickering emulsions. Particle-stabilized emulsions often have larger droplet sizes (at times reaching few millimetres) that, contrarily to surfactant-stabilized emulsions, are very stable against coalescence due to the steric (mechanical) barrier created by the solid particles adsorbed around the oil droplets [33–35].

By CLSM (Figure 5.3), the spatial distribution of the fibres in a NSF, namely NS 0.5 BC:CMC, was investigated. The BC fibres (stained in blue) can be seen all around the oil droplets (stained in red). This is more clearly visible in the bottom section of the scan, where arrows point out a more intense blue fibre network covering oil droplets. As the scan moves upwards on the sample, in the middle section a blue halo is also evident around the oil droplets, in the oil/water interface (pointed by arrows). These observations support the Pickering emulsion mechanism in the NS BC:CMC. Additionally, BC fibres can be seen in all images in the bulk of the aqueous phase, creating a dense 3D network probably responsible for stabilizing the droplets in suspension and preventing their coalescence.

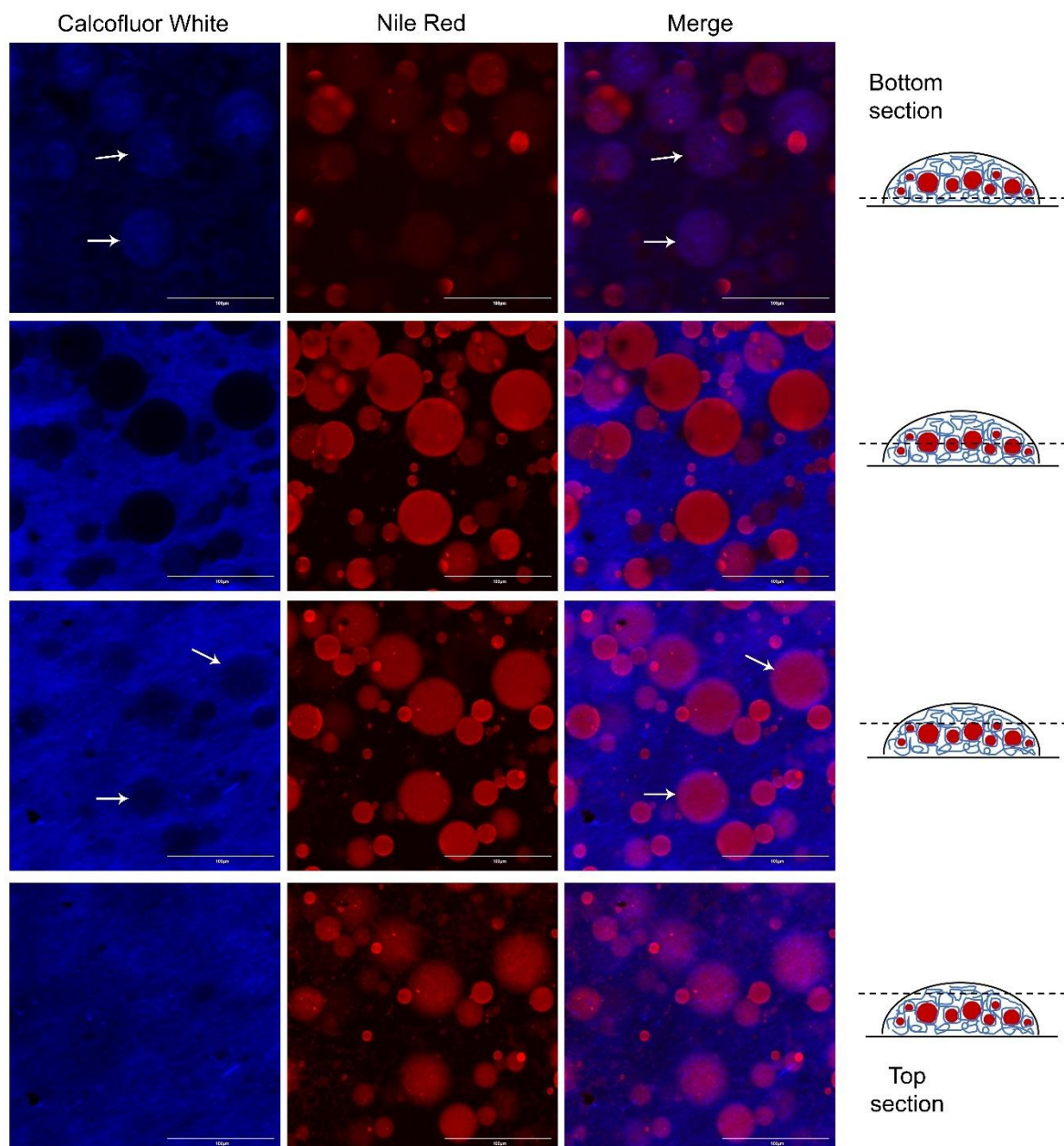


Figure 5.3 - CLSM micrographs (10x magnification) of NS 0.5 BC:CMC. Oil phase is stained in red by Nile Red dye, and BC fibers are stained blue by Calcofluor White stain. Scale bars correspond to 100 μm .

5.3.2 - Rheological assessment

Figure 5.4 shows that the different tested celluloses in aqueous suspensions present quite distinct viscosity profiles (from higher to lower): BC:CMC, Avicel PC-591 and Avicel PC-611 (the two Avicel samples have medium and low viscosity, respectively, as reported by the supplier). All dispersions showed a shear thinning behaviour, widely common in complex fluids, resulting from the progressive entanglement breakdown. This effect is sharper for BC:CMC mixtures and much smoother for PC-611, and can be associated with different degrees of hydrogen bonding. Since BC fibres are much longer and

thinner (in the order of nanometres) than microcrystalline cellulose, they have a higher aspect ratio and specific surface area [11]. For this reason they are more flexible, which favours interaction points between them via hydrogen bonds. MCC particles are crystals of larger diameter, having smaller specific surface area and lower flexibility, so there are fewer possibilities for interaction. A concentration effect is also observed in the results of Figure 5.4, usually ascribed to the presence of more entanglement points [36].

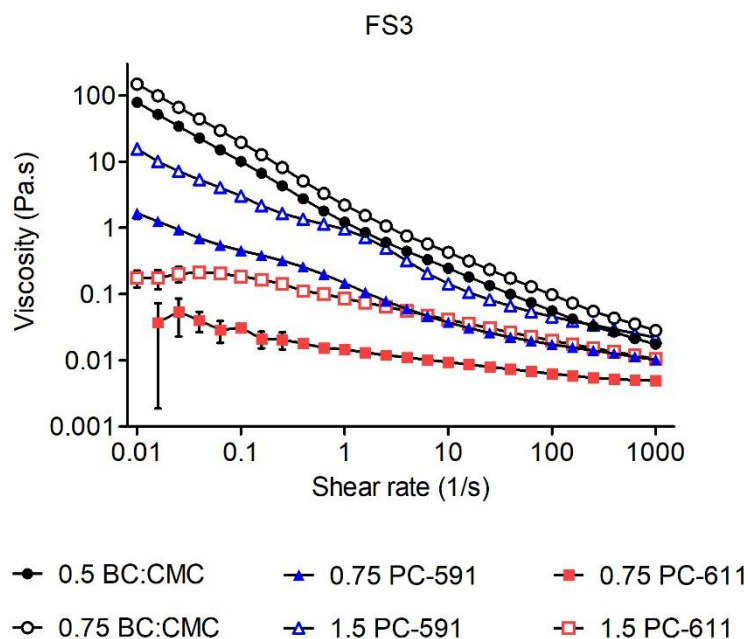


Figure 5.4 - Flow curves of aqueous dispersions of the polymers used in this study, at different concentrations. Results are the average of triplicate samples, obtained from the third consecutive flow sweep (FS3). Bars represent standard deviation.

5.3.2.1 - Low surfactant formulations

Results of the first (FS1) and third (FS3) consecutive flow-sweeps of the emulsions are shown in Figures 5.5-A and 5.5-B, respectively. The first flow sweep emulates flow behaviour of the samples after storage in commercial recipients. The purpose of the third flow-sweep is to investigate the stability of the formulations after undergoing multiple shearing steps, removing forces that might have built up during storage and revealing more of the intrinsic structure of the emulsion.

From Figure 5.5 (A and B), all LSF and FF samples viscosities decreased with the increase in the shear rate, characteristic of a shear-thinning (pseudoplastic) behaviour. This is an important property for cosmetic creams, as when applying the cream on the skin (under shearing force applied by hand) the viscosity decreases and spreading is facilitated. Shear rates involved in rubbing creams or lotions on the skin can vary from 10^2 to 10^4 s⁻¹; on the other hand, draining under gravity corresponds to shear rates

between 10^{-1} and 10^1 s^{-1} , and sedimentation of particles in a suspending liquid happens below 10^{-3} s^{-1} [37]. In the LSF samples the viscosity also increases with the respective polymer's concentration.

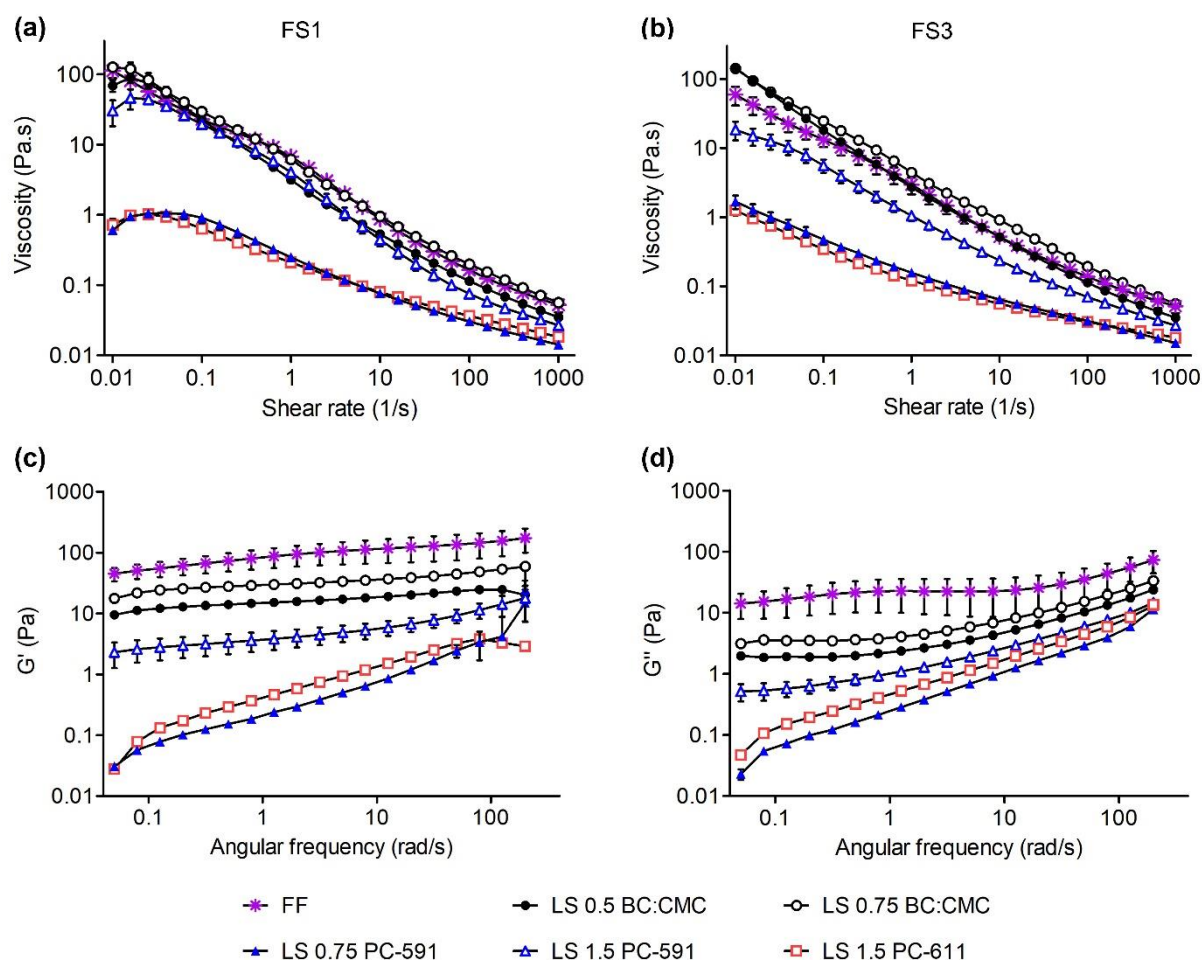


Figure 5.5 - Rheological evaluation of the FF and LSF after 1 day of storage at room temperature: flow curves taken from (a) the first flow sweep, FS1, and (b) the third consecutive flow sweep, FS3; (c) storage modulus, G' , and (d) loss modulus, G'' , taken from oscillatory frequency sweep tests. Results are the average of triplicate samples. Bars represent standard deviation.

The emulsions prepared with BC:CMC present similar shear viscosity values to those of its aqueous suspensions (Figure 5.4). Thus, for these samples it can be said that the surfactants (present in low concentration – 10 % relatively to the control) were not playing the major viscosifying role and that the overall viscosity pattern is controlled by the continuous phase: an aqueous network of cellulosic particles which may interact cohesively by hydrogen bonds while repulsive electrostatic forces arising from the presence of the polyelectrolyte (CMC) counterbalances these forces, promoting the full spreading or swelling of the fibres, strongly contributing to the structuring effect. In this case the different oil droplet

patterns do not seem to lead to differences in the interaction between droplets that could interfere with the viscosity (e.g., through the formation of droplet clusters), or these differences are overlapped by the continuous phase governance. On the other hand, FF does not contain any polymer, so its viscosity is related to the microstructure of the emulsion: influence of the surfactant, size distribution of the oil droplets and their interaction, which offer resistance to movement under shearing.

The flow curves of LSF PC-591 and PC-611 show higher viscosity in comparison to the respective polymers' suspensions. The overall flow profile in this case depends on both the viscosity of the suspended solid particles (which is relatively low), but also on the microstructure of the emulsion – a combination of continuous and dispersed phase contributions.

As seen in Figure 5.5-A, the FF shows a tendency of ever-increasing viscosity towards lower shear rates, while the cellulose-stabilized LSF creams demonstrate a plateau or slight increase of viscosity in the first points of the graphic, until a critical shear rate (below 0.1 s^{-1}). This may indicate that in the range of very low shear rates, the disordered entangled network is only slightly disturbed and is able to recover. Despite this narrow initial plateau, most samples' behaviour approximate the FF for the rest of the shear rate interval tested, with a disordered entangled network disruption rate higher than the recovery rate resulting in the decrease of the viscosity with the increase of shear rate. Both concentrations of BC:CMC were able to thicken the samples to a viscosity close to FF (LS 0.5 BC:CMC) or identical (LS 0.75 BC:CMC). The LS 1.5 PC-591 sample also has a viscosity profile that approximates to FF around 0.1 s^{-1} , with a lower viscosity profile onwards. Further, the third flow sweep (Figure 5.5-B) reveals that this sample loses viscosity after shearing, so the higher apparent initial viscosity could be due to weak interactions between the components, built up during rest time, that were eliminated by the application of a shear force. A small decrease in viscosity was also observed in the FF; samples with BC:CMC showed high structural integrity even after the multiple shearing cycles, maintaining a high viscosity. The viscosity plateau disappeared in the third flow sweep for all the polymer-stabilized emulsions.

At low shear rates, below 0.1 s^{-1} , the average viscosity of the samples with 0.5 % BC:CMC is not much different from the 0.75 % ones. This behaviour changed after 30 days of storage, as seen in Figure 5.6, the differences at low shear rates becoming more defined between the two concentrations, as in the polymers' viscosity graphic of Figure 5.4.

Creams prepared with Avicel PC-611 and PC-591 could not match the rheological profile of the control even at 1.5 %, always showing lower viscosities. These MCCs, at the concentrations tested, could not provide the necessary viscosity in a formulation with reduced surfactants. Comparing both Avicel at the

same concentration (0.75 %) with BC:CMC, the later had much higher thickening power, as could be already induced from the behaviour of the dispersions of the polymer mixtures alone.

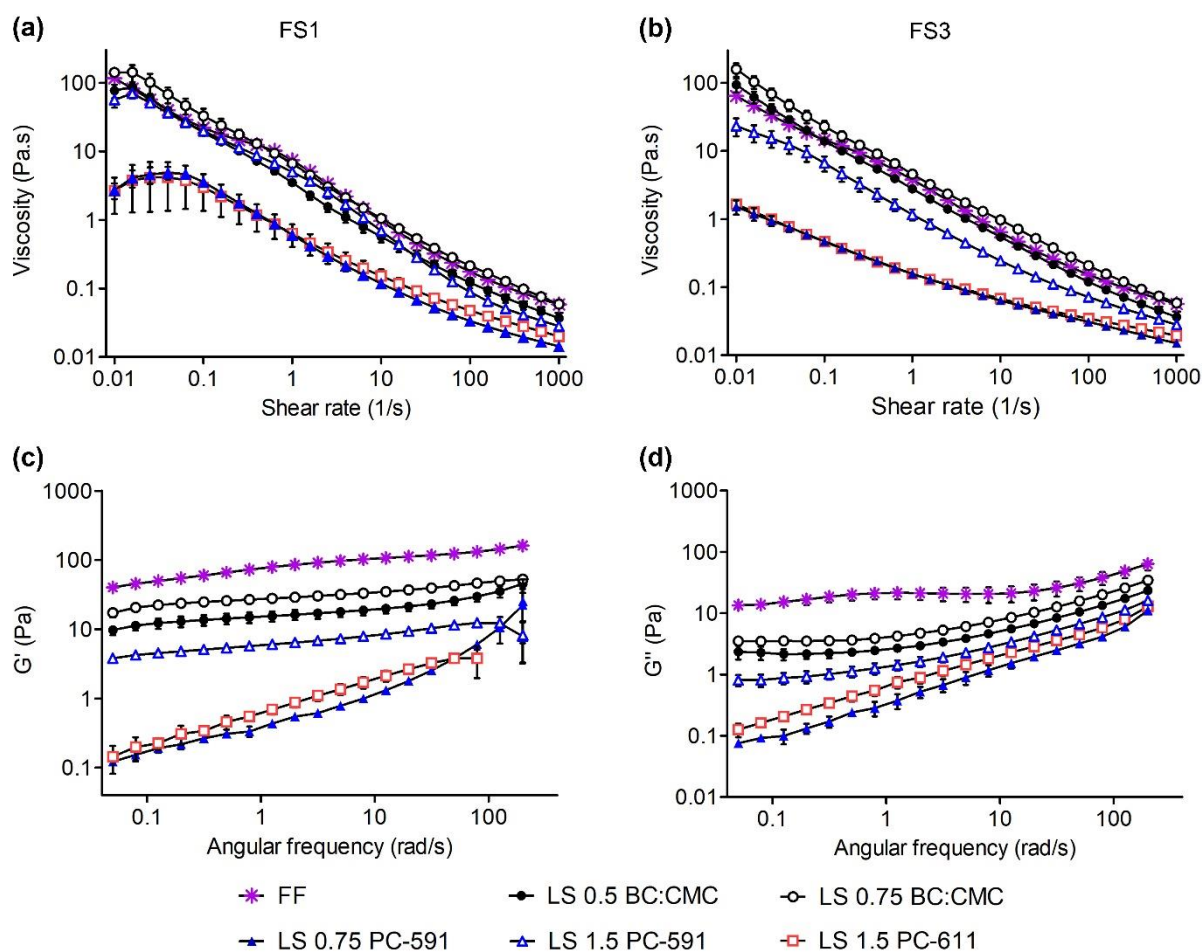


Figure 5.6 - Rheological evaluation of the FF and LSF after 30 days of storage at room temperature: flow curves taken from (a) the first flow sweep, FS1, and (b) the third consecutive flow sweep, FS3; (c) storage modulus, G' , and (d) loss modulus, G'' , taken from oscillatory frequency sweep tests. Results are the average of triplicate samples. Bars represent standard deviation.

Regarding the dynamic tests, the storage/elastic modulus (G') and loss/viscous modulus (G'') of the samples were analysed. Solid materials are characterized by an elastic behaviour, whereas fluid materials have viscous behaviour. Viscoelastic/pseudoplastic materials such as polymeric dispersions or emulsions are neither true fluids nor solids by definition, but share behavioural characteristics of both - an elastic component represented by G' , and a viscous component represented by G'' [36,37]. Materials with a more pronounced solid behaviour component are more capable of keeping particles in suspension, which in this case are oil droplets. The materials with the largest solid component are, in theory, more stable. Results from the oscillatory strain sweep tests are reported in Figure 5.7.

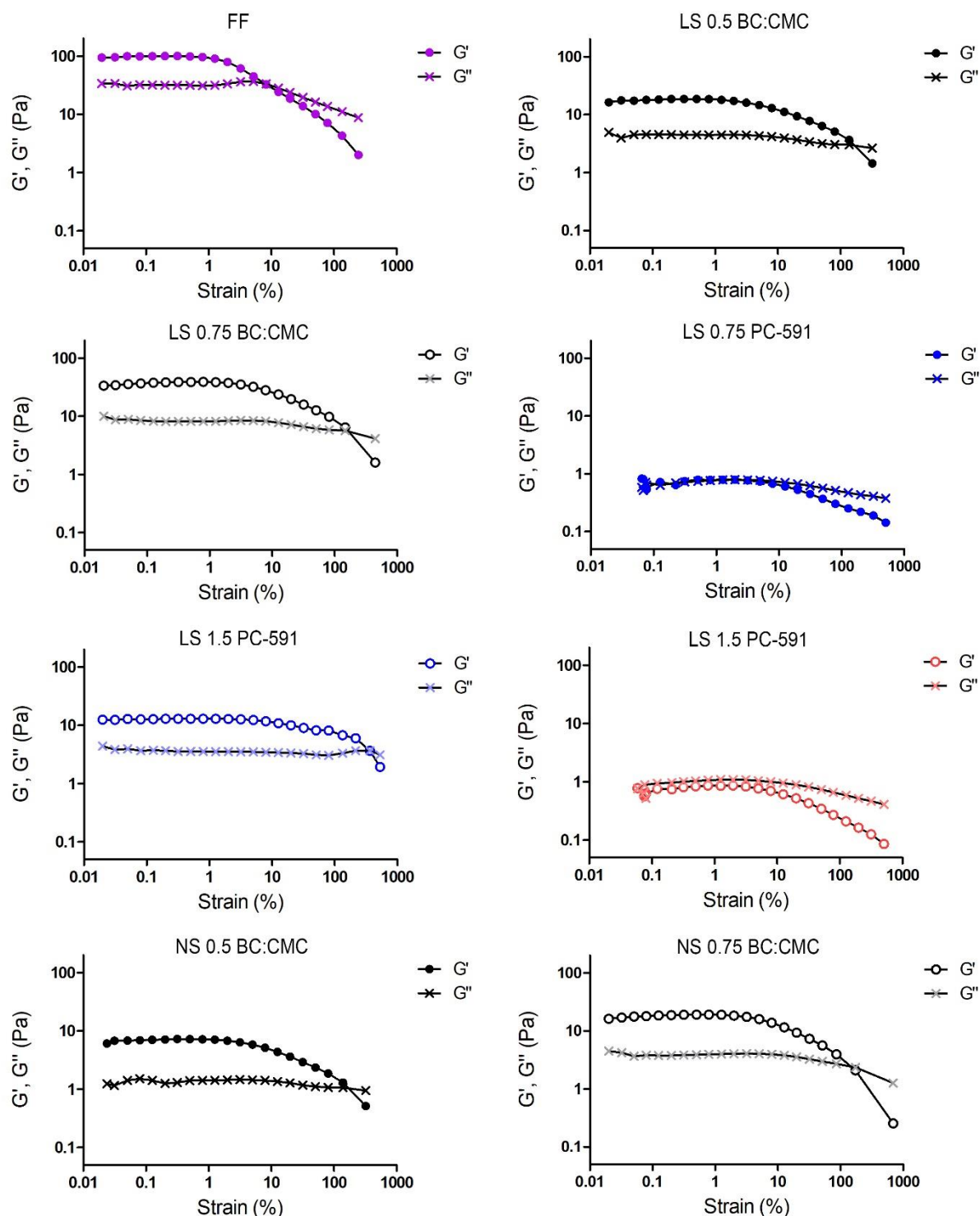


Figure 5.7 - Oscillatory strain sweeps of the FF and LSF after 1 day of storage at room temperature.

The emulsion LS 1.5 PC-611 shows a predominant viscous behaviour throughout the entire strain interval, which is in accordance with the creaming effect verified in Figure 5.1 due to insufficient structuring of the continuous phase. LS 0.75 PC-591 also displays a weak phase structuring, with nearly $G' = G''$ until 10 % strain, from where G' further decreases. All the other samples show a main elastic behaviour at the

LVR, but varying on the critical strain and the G'/G'' crossing point. The critical point is when the viscoelastic material's rheological properties are no longer independent on the strain: where the LVR ends, and structure disruption starts. With further increasing strain, G' will decrease. At some point, it will become lower than G'' and the behaviour of the material changes to fluid-like. In the FF cream this happens below 10 % strain, while for the LS and NS BC:CMC and the LS 1.5 PC-591 emulsions the critical strain is higher than 10 % and the crossover point only occurs around 100 % strain.

Regarding now the oscillatory frequency sweep tests, conducted at a strain of 0.3 % within the LVR of all samples, G' and G'' are presented in Figure 5.5-C and 5.5-D, respectively. In emulsions LS 0.75 PC-591 and LS 1.5 % PC-611, G' and G'' are comparable; all the other samples have $G' > G''$, indicating a prevalence of the elastic component, with a gel-like behaviour. The FF emulsions present the highest values of G' despite not having the highest viscosity in the flow curves (Figure 5.5-A and B), showing the importance of surfactants and microstructure in the rheology of the system, resulting in a more structured network. Indeed, this formulation was observed to have the smallest oil droplets, more tightly packed, and very good storage stability. On the other hand, LSF and NSF have a less organized microstructure due to the reduction of surfactants, which is compensated with the continuous phase structure given by the network of solid cellulosic particles. A stronger structuring effect is achieved with BC:CMC, amongst the cellulosic materials. As observed with the rheological profiles, compared to Avicels, BC:CMC has a superior stabilization effect, and PC-591 performs better than PC-611. The recorded mechanical spectra (G' and G'') show a behaviour nearly independent from the frequency (with almost flat slope), which is typical of gel samples, except for samples with Avicel PC-611. The slight dependence observed can be ascribed to the predominance of non-covalent bonds in the network, independently from the strength of the network (for purely chemically bonded polymers, the slope would be zero) [36].

Similar observations were recorded after 30 days of storage (Figure 5.6), with small deviations in all samples, probably due to stabilization of the formulation components (surfactants) to an equilibrium state. In particular, BC:CMC samples showed a constant behaviour from the beginning and good reproducibility from the followed protocol. Despite the larger oil droplets in the BC:CMC samples, these emulsions were spatially stabilized by the BC fibre 3D network and the effect of a higher viscosity, which effectively prevented the lipid globules from coalescing through all the storage period tested.

5.3.2.2 - No surfactant formulations

The NSF produced with BC:CMC exhibited again the same viscosity pattern as the correspondent low surfactant formulations (Figure 5.8-A and B), also indicating that the continuous phase properties are ruling the overall emulsion rheological behaviour. Similarly, G' and G'' profile showed a solid-like behaviour

predominance (Figure 5.8-C), with a very slight increase in the moduli values over the tested angular frequency range, indicative of the predominance of physical bonds in the entangled network, as in the correspondent LSF. Also in this case there were no changes in the average rheological parameters of the samples after a 30-day storage period (Figure 5.9). Therefore, in terms of rheological properties, there is a good indication towards the feasibility of totally replacing the use of surfactants by BC:CMC particles in this type of cosmetic formulations.

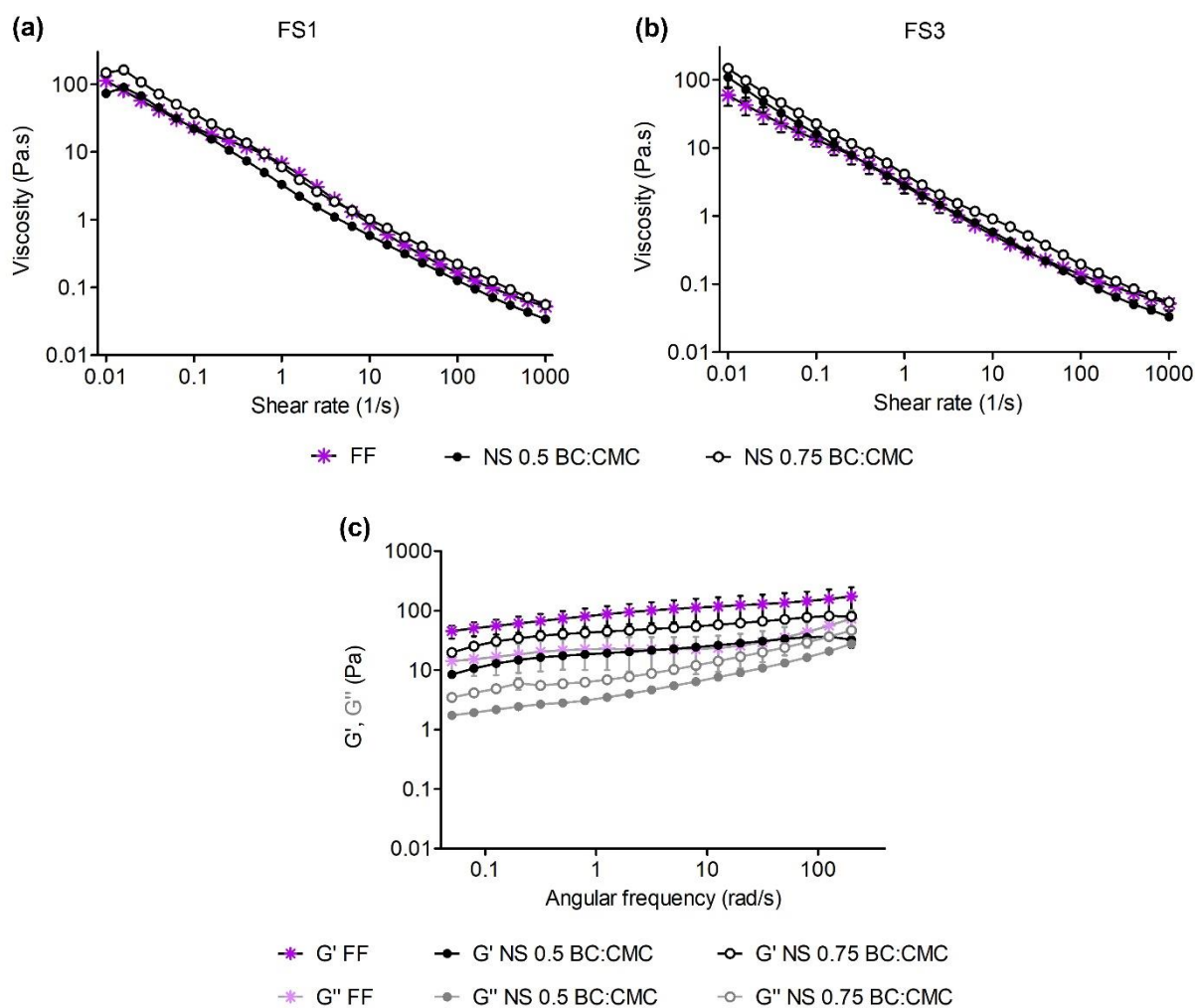


Figure 5.8 - Rheological evaluation of NSF after 1 day of storage at room temperature: flow curves taken from (a) the first flow sweep, FS1, and (b) the third consecutive flow sweep, FS3; (c) storage modulus, G' , and loss modulus, G'' , taken from oscillatory frequency sweep tests. Results are the average of triplicate samples. Bars represent standard deviation.

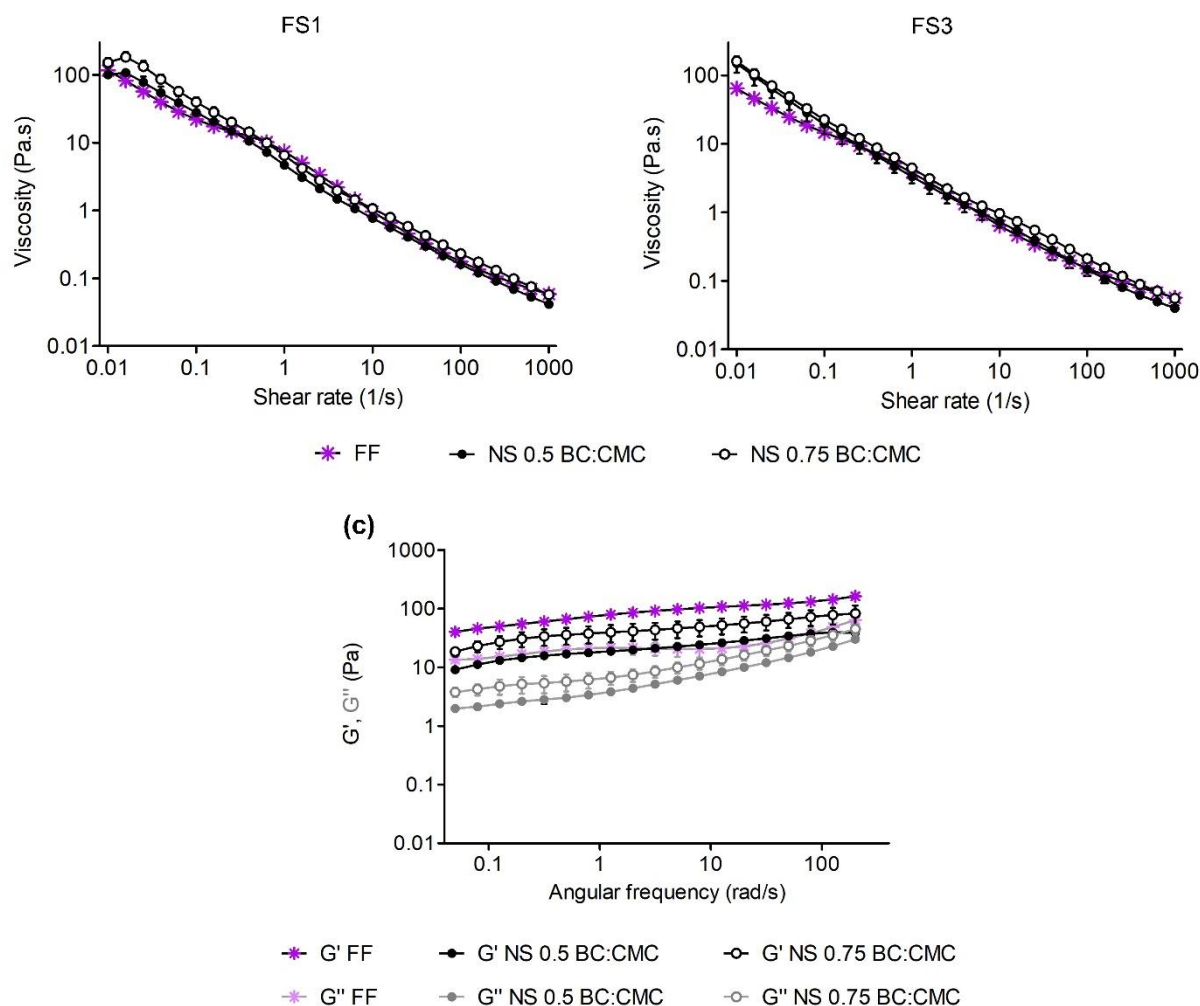


Figure 5.9 - Rheological evaluation of NSF after 30 days of storage at room temperature: flow curves taken from (a) the first flow sweep, FS1, and (b) the third consecutive flow sweep, FS3; (c) storage modulus, G' , and loss modulus, G'' , taken from oscillatory frequency sweep tests. Results are the average of triplicate samples. Bars represent standard deviation.

5.3.2.3 - Three Interval Thixotropy Test

3ITT methodology was applied to investigate the emulsion's time-dependent behaviour. The test begins at a low shear rate, in ideally near-rest conditions; in the second stage, a high shear rate is applied in order to break the internal structure; finally, in the third stage, the material is allowed to recover/rebuild its initial structure under low-shear (near-rest) conditions. In this way, this methodology can show how much of the material's structure can be recovered, and how quickly [38,39]. Thixotropic materials undergo structure breakdown under shear and take time to rebuild at rest. This feature allows cosmetics to flow smoothly as they are rubbed in, and recover their structure to stop flowing once they sit on the skin. Regarding the results from Figure 5.10, the FF cream shows some degree of thixotropy as it takes

some time but manages to rebuild the structure and regain its initial viscosity. Recovery of the steady-state viscosity achieved at the end of interval 1, approximately 40 Pa·s, is reached back within 255 s of interval 3 (at $t = 465$ s).

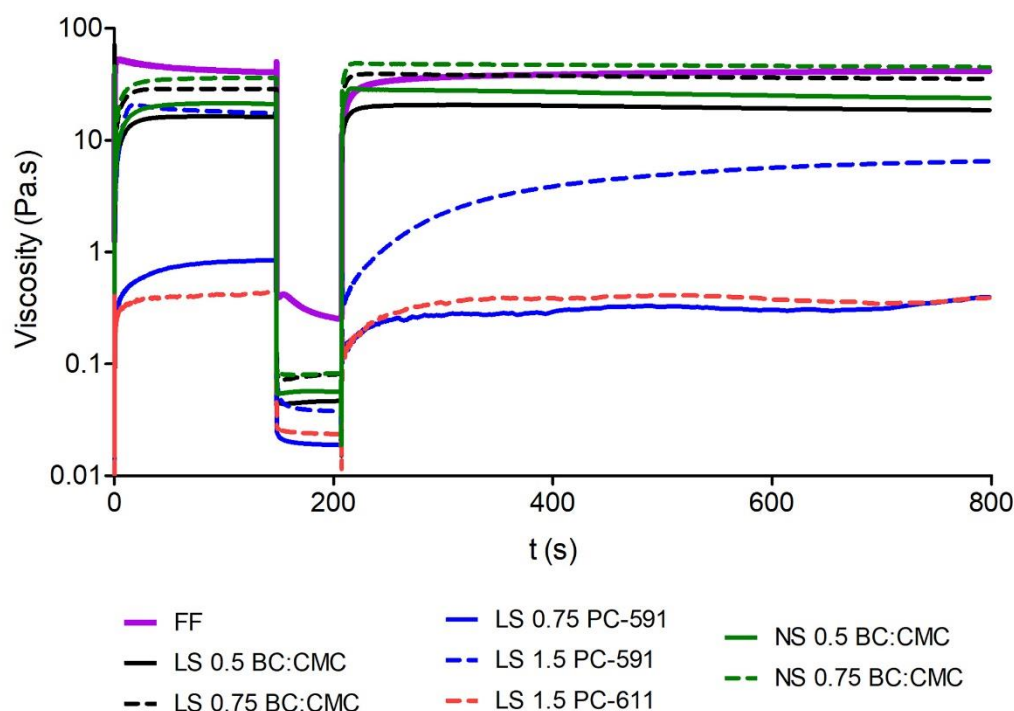


Figure 5.10 – Three interval thixotropy flow curves of the cosmetic cream analogues after 1 day of storage, at room temperature

BC: CMC emulsions (LS and NS) show a lower thixotropy degree than FF. The internal structured network of dispersed BC:CMC quickly reaches the equilibrium state between breakdown and rebuild when the shear conditions are changed. The recovery was almost immediate (within approximately 1 s) and resulted in a slightly higher viscosity than that observed in the first stage, possibly due to an improved dispersion of the fibres after the high shear period [38]. Avicel creams, on the other hand, showed greater lag in the structure recovery phase and did not return to the initial viscosity within the analysed time interval.

5.3.2.4 - Viscoelastic behaviour under oscillatory temperature cycles

Figure 5.11 displays the behaviour of the cosmetic cream analogues when submitted to temperature cycles. The most evident result in this dynamic temperature test concerns the surfactant-stabilized FF cream, which undergoes drastic variation in the elastic behaviour, G' , when subjected to temperature changes. The sample shows high G' values at low temperatures and low G' at higher temperatures (from

a practical point of view, this facilitates application of the product to the warm skin, since the solid-like behaviour becomes less pronounced). At the final 10 °C plateau, after 2 complete cycles, G' remained high and close to the initial value. There is a slight rise tendency towards the end of the graphic that is common to all samples, therefore most probably due to some degree of structure rearrangements under oscillation, or to the method itself (for example, a more appropriate solvent trap could eliminate this effect). On the other hand, on the second 50 °C plateau, the G' dropped relatively to the first cycle, laying below the unit. Lower temperatures do not seem to impact much on the viscoelasticity, but cycles of high temperatures may cause loss of stability in the FF cream. From this result, it is also expected that organoleptic characteristics will vary with temperature, potentially changing the way the product feels on the hand or is applied to the skin. Contrarily to this, the samples that were totally or partially stabilized with cellulose solid particles maintain a much more constant behaviour despite the temperature, indicating a good storage stability even in uncontrolled environments and the maintenance of organoleptic properties regardless of the temperature.

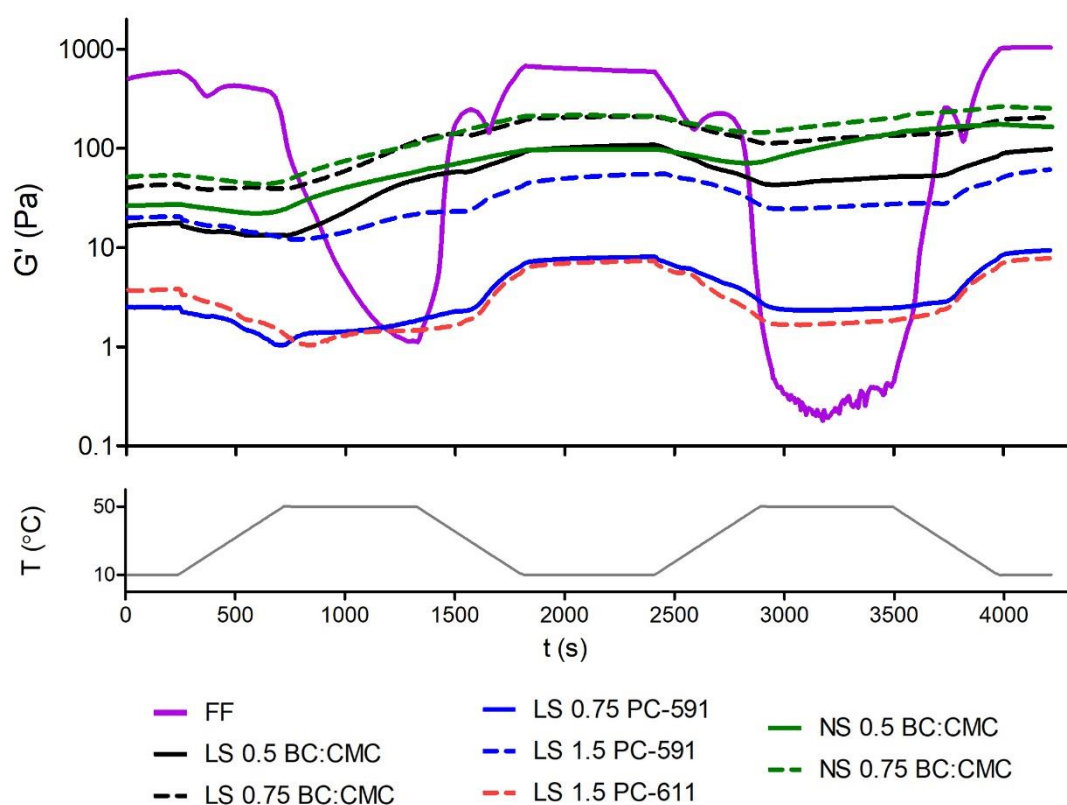


Figure 5.11 - Temperature dependence of G' in oscillatory temperature cycles, between 10 °C and 50 °C, of the cosmetic cream analogues after 1 day of storage at room temperature.

5.3.3 - Texture assessment

Texture analysis is a tool based on the conversion of quantitative force measurements into qualitative organoleptic parameters, thus making an approximation to the sensory description of the materials. Two different tests were made: a penetration test, using a cylindrical probe with a small contact area, and a back-extrusion test using a large contact area probe. The penetration test is less sensitive to differences in force; the back-extrusion test, having greater contact area with the sample, besides being more sensitive can also provide information on more textural parameters.

The penetration test would be the equivalent to dipping a finger inside a cream. The main parameters measured in this test are the firmness (maximum force that the sample exerts on the probe during penetration), and consistency (total work performed by the probe to penetrate the sample to a defined depth). In the back-extrusion test, these same parameters are measured in the downward movement; in the upward movement, the sample's cohesiveness (the maximum absolute force measured during probe withdrawal), and the respective work - the index of viscosity - are determined. This last test is applied to the almost entirety of the sample in the container. With these tests it is possible to replicate different kinds of cosmetic cream handling, more gentle or more intense (corresponding to gentle finger dipping or extrusion of a large amount of sample), and to validate whether the differences between each sample and the control can be felt regardless of the kind or intensity of handling.

Looking at the texture analysis results from Figure 5.12 it is noticeable that, overall, the FF cream has higher mean values for all the parameters, which can be attributed to the microstructure. A narrower size distribution, tighter packing of emulsion droplets and the structuring effect of the surfactant in a more consistent network offer a resistance to movement that translates in higher forces necessary for the probes' motion. However, the standard deviations are also much larger. The properties of the surfactant-stabilized FF, besides being dependent on the production parameters like temperature and agitation, are also time dependent and could reach an equilibrium stage (in terms of chemical and steric interactions) later in time, meaning the deviations could be smaller on a later analysis. This cannot be shown directly since texture analysis was not performed after the 30-day storage period, but is inferred from the rheology results (Figure 5.5 and 5.6), where a drop in the standard deviation values is observed from 1 to 30 days after preparation. On the other hand, the stability, rheological and textural properties of the polymer-stabilized creams (LSF and NSF) were not dependent on the microstructure alone, but more on the cellulose type and concentration, resulting in smaller deviations and more consistent results. This is further demonstrated by comparing the emulsions of LS 0.5 BC:CMC and LS 0.75 BC:CMC with their NS counterparts, where the physical properties between matching concentrations are similar in every test

performed, although different production processes were employed (the samples without surfactants were simply homogenized at room temperature). This can actually be a major advantage in terms of manufacture, since it does not require high energy expenses to heat large volumes, and in terms of formulation it allows for the incorporation of heat-sensitive active ingredients.

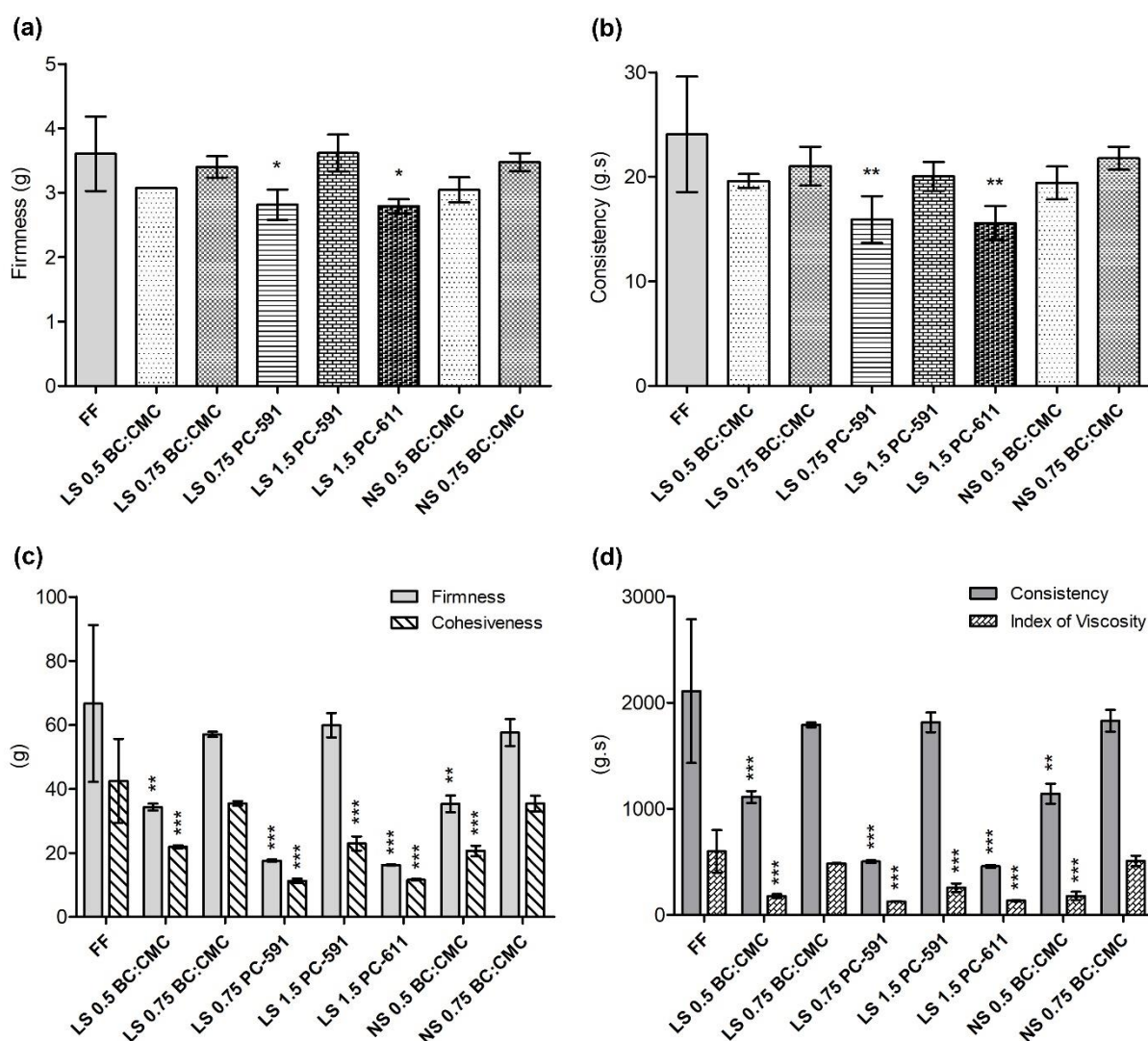


Figure 5.12 - Textural parameters of the cosmetic emulsions after 1 day of storage at room temperature: Firmness (a) and Consistency (b) were taken from a puncture test; Firmness and Cohesiveness (c), Consistency and Index of Viscosity (d) were taken from a back-extrusion test. Results are the average of triplicate samples and bars represent standard deviation. All the results were compared with the FF cream using one-way ANOVA and Tukey's Multiple Comparison Test (* p < 0.05, ** p < 0.01, *** p < 0.001).

Regarding the sensory properties in more detail, in terms of firmness in the back-extrusion tests (Figure 5.12-C), 3 samples showed no significant differences from the control, consistent with the viscosity profiles of these samples, in particular from the first flow rate sweep: the LS and NS 0.75 BC:CMC

emulsions, and LS 1.5 PC-591. The same is observed in the consistency results from back-extrusion (Figure 5.12-D). Although the absolute values are not directly comparable, the penetration test showed similar firmness and consistency tendencies (Figure 5.12-A and B), leading to the same conclusions. However, relative differences (and thus statistical significance) are much higher for the back extrusion tests, both due to the much higher area of contact between the plunger and the sample and to the much larger sample volume moved during the test. Concerning the cohesiveness and index of viscosity parameters (Figure 5.12-C and D), the LS and NS 0.75 BC:CMC also show similar values to the control ($p > 0.05$); on the contrary, the LS 1.5 PC-591 creams display lower values ($p < 0.05$), deviating from the FF in these parameters. In the dynamic viscosity measurements performed in the rheometer, PC-591 samples' viscosity profile was also below the FF and BC:CMC ones, particularly for the third flow sweep step. Further, consistency parameters correlate well with the mechanical spectra (G' and G''), presented in Figures 5.5 and 5.8 and with the “solid-like” character and types of bonds involved in the emulsion network. In fact, both bacterial and plant derived celluloses, namely MCC, are known to create three-dimensional networks [8,9,27] which present an obstacle to the introduction of the probe in the sample, thus increasing the necessary force – resulting in measurable firmness and consistency. However, MCC networks might need higher concentrations and more time to rebuild after shearing [7], explaining why less force is needed in the retrieval of the probe – lower cohesiveness and index of viscosity. This explanation of lower structural integrity or cohesion can also apply to the lower values of G' and G'' , and the decrease in the viscosity profile from the first to the third flow-sweep of LS 1.5 PC-591, as was previously explained.

Overall, the LS and NS emulsions prepared with 0.75 % BC:CMC consistently showed similar results to the FF cream. Formulations with the MCC Avicel PC-591 needed a higher concentration to achieve the same firmness and consistency, still showing lower cohesiveness. The low viscosity MCC Avicel PC-611 fell short to the FF in all assessed parameters.

5.4 - CONCLUSIONS

A BC:CMC formulation was used for the first time to produce a cosmetic cream, allowing a significant or even total elimination of the need for a chemical surfactant. The utilized BC:CMC is a dry powder which can be quickly incorporated in the formulation, not requiring high energy or long mixing periods to achieve good stabilizing and thickening results. From the results of this work, BC:CMC's technological potential

seems to be high and might fulfil a market need for more natural cosmetic ingredients, without compromising the performance or sensorial attributes of the formulations.

Samples prepared with 0.75 % BC:CMC consistently showed similar results to the FF control cream, in all the performed tests (visual observation, storage stability, rheology and texture), suggesting that it was possible to mimic relevant rheological and textural properties in formulations with reduced or no surfactants. BC:CMC also performed better than the MCCs used as benchmark, Avicel PC-591 and PC-611, requiring lower concentrations while stabilizing a formulation without surfactants. Although involving a derivatized cellulose, this formulation is clearly advantageous as compared to chemical surfactants, which are claimed to present some skin-irritation issues.

5.5 - BIBLIOGRAPHIC REFERENCES

- [1] S. Bom, J. Jorge, H.M. Ribeiro, J. Marto, A step forward on sustainability in the cosmetics industry: A review, *J. Clean. Prod.* 225 (2019) 270–290. <https://doi.org/10.1016/j.jclepro.2019.03.255>.
- [2] F. Freitas, V.D. Alves, M.A.A. Reis, Bacterial Polysaccharides: Production and Applications in Cosmetic Industry, *Polysaccharides*. (2014) 1–2241. https://doi.org/10.1007/978-3-319-03751-6_63-1.
- [3] B.A. Khan, N. Akhtar, H.M.S. Khan, K. Waseem, T. Mahmood, A. Rasul, M. Iqbal, H. Khan, Basics of pharmaceutical emulsions: A review, *African J. Pharm. Pharmacol.* 5 (2011) 2715–2725. <https://doi.org/10.5897/AJPP11.698>.
- [4] D.K.F. Santos, R.D. Rufino, J.M. Luna, V.A. Santos, L.A. Sarubbo, Biosurfactants: Multifunctional biomolecules of the 21st century, *Int. J. Mol. Sci.* 17 (2016) 1–31. <https://doi.org/10.3390/ijms17030401>.
- [5] R.P. Vianna-Filho, C.L.O. Petkowicz, J.L.M. Silveira, Rheological characterization of O/W emulsions incorporated with neutral and charged polysaccharides, *Carbohydr. Polym.* 93 (2013) 266–272. <https://doi.org/10.1016/j.carbpol.2012.05.014>.
- [6] M.C. Adeyeye, A.C. Jain, M.K.M. Ghorab, W.J. Reilly, Viscoelastic evaluation of topical creams containing microcrystalline cellulose/sodium carboxymethyl cellulose as stabilizer, *AAPS PharmSciTech.* 3 (2002) 1–10. <https://doi.org/10.1208/pt030208>.
- [7] V.S. Rudraraju, C.M. Wyandt, Rheological characterization of Microcrystalline Cellulose/Sodiumcarboxymethyl cellulose hydrogels using a controlled stress rheometer: Part I, *Int. J. Pharm.* 292 (2005) 53–61. <https://doi.org/10.1016/j.ijpharm.2004.10.011>.
- [8] Y. Yaginuma, T. Kijima, Effect of pH on rheological properties of microcrystalline cellulose dispersions, *J. Dispers. Sci. Technol.* 27 (2006) 365–370. <https://doi.org/10.1080/01932690500359483>.
- [9] G.H. Zhao, N. Kapur, B. Carlin, E. Selinger, J.T. Guthrie, Characterisation of the interactive properties of microcrystalline cellulose-carboxymethyl cellulose hydrogels, *Int. J. Pharm.* 415 (2011) 95–101. <https://doi.org/10.1016/j.ijpharm.2011.05.054>.
- [10] T. Kondo, P. Rytczak, S. Bielecki, Bacterial NanoCellulose Characterization, in: M. Gama, F. Dourado, S. Bielecki (Eds.), *Bact. Nanocellulose - From Biotechnol. to Bio- Econ.*, Elsevier B.V., 2016: pp. 59–71.
- [11] R.J. Moon, A. Martini, J. Nairn, J. Simonsen, J. Youngblood, Cellulose nanomaterials review: Structure, properties and nanocomposites, 2011. <https://doi.org/10.1039/c0cs00108b>.

- [12] M. Gama, F. Dourado, S. Bielecki, *Bacterial Nanocellulose: From Biotechnology to Bio-Economy*, Elsevier B.V., 2016. <https://doi.org/10.1017/CBO9781107415324.004>.
- [13] S.M. Keshk, *Bacterial Cellulose Production and its Industrial Applications*, J. Bioprocess. Biotech. 04 (2014). <https://doi.org/10.4172/2155-9821.1000150>.
- [14] H. Ougiya, K. Watanabe, Y. Morinaga, F. Yoshinaga, *Emulsion-stabilizing Effect of Bacterial Cellulose*, Biosci. Biotechnol. Biochem. 61 (1997) 1541–1545. <https://doi.org/10.1271/bbb.61.1541>.
- [15] P. Paximada, E. Tsouko, N. Kopsahelis, A.A. Koutinas, I. Mandala, *Bacterial cellulose as stabilizer of o/w emulsions*, Food Hydrocoll. 53 (2016) 225–232. <https://doi.org/10.1016/j.foodhyd.2014.12.003>.
- [16] X. Zhai, D. Lin, D. Liu, X. Yang, *Emulsions stabilized by nanofibers from bacterial cellulose: New potential food-grade Pickering emulsions*, Food Res. Int. 103 (2018) 12–20. <https://doi.org/10.1016/j.foodres.2017.10.030>.
- [17] I.F. Almeida, T. Pereira, N.H.C.S. Silva, F.P. Gomes, A.J.D. Silvestre, C.S.R. Freire, J.M. Sousa Lobo, P.C. Costa, *Bacterial cellulose membranes as drug delivery systems: An in vivo skin compatibility study*, Eur. J. Pharm. Biopharm. 86 (2014) 332–336. <https://doi.org/10.1016/j.ejpb.2013.08.008>.
- [18] T. Amnuait, T. Chusit, P. Raknam, P. Boonme, *Effects of a cellulose mask synthesized by a bacterium on facial skin characteristics and user satisfaction*, Med. Devices Evid. Res. 4 (2011) 77–81. <https://doi.org/10.2147/MDER.S20935>.
- [19] N. Chunshom, P. Chuysinuan, S. Techasakul, S. Ummartyotin, *Dried-state bacterial cellulose (Acetobacter xylinum) and polyvinyl-alcohol-based hydrogel: An approach to a personal care material*, J. Sci. Adv. Mater. Devices. 3 (2018) 296–302. <https://doi.org/10.1016/j.jsamd.2018.06.004>.
- [20] K. Ludwicka, M. Jedrzejczak-Krzepkowska, K. Kubiak, M. Kolodziejczyk, T. Pankiewicz, S. Bielecki, *Medical and Cosmetic Applications of Bacterial NanoCellulose*, in: M. Gama, F. Dourado, S. Bielecki (Eds.), *Bact. Nanocellulose - From Biotechnol. to Bio-Economy*, Elsevier B.V., 2016: pp. 145–165.
- [21] Y. Numata, L. Mazzarino, R. Borsali, *A slow-release system of bacterial cellulose gel and nanoparticles for hydrophobic active ingredients*, Int. J. Pharm. 486 (2015) 217–225. <https://doi.org/10.1016/j.ijpharm.2015.03.068>.
- [22] Z.-F. Yang, N.A. Morrison, T.A. Talashek, D.F. Brinkmann, D. DiMasi, Y.L. Chen, US 2007/019777 A1 - *Bacterial Cellulose-containing formulations*, 2007.
- [23] B.P. Heath, T.W. Coffindaffer, K.E. Kyte, E.D. Smith, S.D. McConaughy, WO 2011/019876 A2 - *PERSONAL CLEANSING COMPOSITIONS COMPRISING A BACTERIAL CELLULOSE NETWORK AND CATIONIC POLYMER*, 2011.
- [24] F. Tournilhac, R. Lorient, US 6534071 B1 - *COMPOSITION IN THE FORM OF AN OIL IN-WATER EMULSION CONTAINING CELLULOSE FIBRILS, AND ITS USES, ESPECIALLY COSMETIC USES*, 2003.
- [25] R. D'Ambrogio, D.A. Peru, J.E. Gambogi, K.M. Kinscherf, D. Patel, R. Tavares, WO 2011/056951 A1 - *Microfibrillar cellulose having a particle size distribution for structured surfactant compositions*, 2011.
- [26] M. Caggioni, R. Ortiz, F.A. Barnabas, R.V. Nunes, J.A. Flood, F. Corominas, US 8716213 B2 - *Liquid Detergent Composition comprising an external structuring system comprising a bacterial cellulose network*, 2014.
- [27] D. Martins, B. Estevinho, F. Rocha, F. Dourado, M. Gama, *A Dry and Fully Dispersible Bacterial Cellulose Formulation as a Stabilizer for Oil-in-Water Emulsions*, Carbohydr. Polym. 230 (2019) 115657. <https://doi.org/10.1016/j.carbpol.2019.115657>.
- [28] D. Martins, D. de Carvalho Ferreira, M. Gama, F. Dourado, *Dry Bacterial Cellulose and Carboxymethyl Cellulose formulations with interfacial-active performance: processing conditions and redispersion*, Cellulose. 9 (2020). <https://doi.org/10.1007/s10570-020-03211-9>.

- [29] L. Gilbert, G. Savary, M. Grisel, C. Picard, Predicting sensory texture properties of cosmetic emulsions by physical measurements, *Chemom. Intell. Lab. Syst.* 124 (2013) 21–31. <https://doi.org/10.1016/j.chemolab.2013.03.002>.
- [30] L. Gilbert, C. Picard, G. Savary, M. Grisel, Rheological and textural characterization of cosmetic emulsions containing natural and synthetic polymers: relationships between both data, *Colloids Surfaces A Physicochem. Eng. Asp.* 421 (2013) 150–163.
- [31] L. Gilbert, V. Loisel, G. Savary, M. Grisel, C. Picard, Stretching properties of xanthan, carob, modified guar and celluloses in cosmetic emulsions, *Carbohydr. Polym.* 93 (2013) 644–650. <https://doi.org/10.1016/j.carbpol.2012.12.028>.
- [32] E. Dickinson, Hydrocolloids and emulsion stability, in: G.O. Philips, P.A. Williams (Eds.), *Handb. Hydrocoll.*, 2 Ed, Woodhead Publishing, 2009: pp. 23–49. <https://doi.org/10.1533/9781845695873.23>.
- [33] Y. Chevalier, M.A. Bolzinger, Emulsions stabilized with solid nanoparticles: Pickering emulsions, *Colloids Surfaces A Physicochem. Eng. Asp.* 439 (2013) 23–34. <https://doi.org/10.1016/j.colsurfa.2013.02.054>.
- [34] B.P. Binks, Particles as surfactants - similarities and differences, *Curr. Opin. Colloid Interface Sci.* 7 (2002) 21–41.
- [35] T. Winuprasith, M. Supphantharika, Properties and stability of oil-in-water emulsions stabilized by microfibrillated cellulose from mangosteen rind, *Food Hydrocoll.* 43 (2015) 690–699. <https://doi.org/10.1016/j.foodhyd.2014.07.027>.
- [36] J.W. Goodwin, R.W. Hughes, *Rheology for chemists: an introduction*, Royal Society of Chemistry, 2000. <https://doi.org/10.5860/choice.38-3918>.
- [37] J.F. Steffe, *Rheological Methods in Food Process Engineering*, Second Edi, Freeman Press, 1996.
- [38] B. Basnet, W.Y. Jang, J.G. Park, I.S. Han, T.Y. Lim, H.M. Lim, I.J. Kim, Impact of SiC colloidal suspension properties for the fabrication of highly porous ceramics, *J. Ceram. Process. Res.* 18 (2017) 634–639. <https://doi.org/10.36410/jcpr.2017.18.9.634>.
- [39] O.S. Toker, S. Karasu, M.T. Yilmaz, S. Karaman, Three interval thixotropy test (3ITT) in food applications: A novel technique to determine structural regeneration of mayonnaise under different shear conditions, *Food Res. Int.* 70 (2015) 125–133. <https://doi.org/10.1016/j.foodres.2015.02.002>.

Chapter 6

Effect of ionic strength and pH in the behaviour of re-dispersed BC:CMC - a comparative study with Xanthan Gum

Bacterial cellulose and carboxymethyl cellulose (BC:CMC) dry formulations with mass ratios of 1:1, 1:0.75 and 1:0.5 were produced and studied. Their rheological performance was assessed and compared with that of a commercial xanthan gum. The zero-shear viscosity and the yield stress of these hydrocolloids, at concentrations ranging from 0.001 % to 0.5 % (w/w), were determined by fitting the Cross and Herschel-Bulkley models to the flow curves. Only BC:CMC formulations presented a measurable yield stress, the highest recorded value (1.54 ± 0.17 Pa) being obtained for the 1:0.5 ratio at a concentration of 0.5 %. This formulation also presented the highest values for the dynamic moduli, namely G' , indicating a stronger solid-like character. Contrarily to xanthan gum, BC:CMC formulations' viscosity in aqueous solution was not considerably affected by pH (from 2.8 to 10.4) nor by ionic strength (NaCl from 0 mM to 350 mM). These results support the conclusion that BC:CMC formulations show good colloidal stability, high viscosity and good suspending properties under a wide range of environmental conditions, thus having great potential as hydrocolloid additives for food applications.

6.1 - INTRODUCTION

Cellulose is one of the most used bulk commodities, owing to its exceptional physical and chemical properties, and has found applications in varied areas such as food, cosmetics, paints, composites and construction materials, biomedical devices and pharmaceutical formulations. Cellulose $((C_6H_{10}O_5)_n)$ is composed of glucose monomers linked together through β 1–4 glucosidic bonds, each monomer rotated 180° relatively to the adjacent ones, being cellobiose (a glucose dimer) the repeating unit. The high availability of hydroxyl groups promotes intra- and inter-molecular hydrogen bonding between adjacent cellulose chains, resulting in very stable and stiff fibrils [1–4]. Furthermore, the surface hydroxyl groups allow for several types of chemical modifications of the fibres, namely the production of water-soluble cellulose derivatives such as carboxymethyl cellulose (CMC).

Bacterial cellulose (BC), also referred to as bacterial nanocellulose owing to the diameter of its fibres, is a sophisticated biopolymer produced during fermentation by different microorganisms, but most efficiently by acetic acid bacteria of the genus *Komagataeibacter*. BC's structure is chemically identical to that of cellulose from wood and plants, but differing in purity, crystallinity, size and morphology of the fibres [5–9].

Native cellulose molecules do not bare surface charge and are insoluble in water, so they are prone to aggregation. Upon drying, the fibres aggregate strongly and irreversibly, losing their swelling ability and originating a so-called hornified material that does not rehydrate. To prevent aggregation and hornification, one strategy is to mix cellulose with charged molecules or polymers before drying: the electrostatic repulsions prevent fibre aggregation and cocrystallization during water removal, enable rehydration and dispersion of the material in aqueous media, improving colloidal stability [10–12]. A dry BC and CMC formulation with a ratio of 1:1 has been previously reported, showing fast water redispersion under low-energy mixing [13,14]. This BC:CMC 1:1 dry formulation showed potential for application as a thickener and stabilizer in food emulsions and suspensions, while at the same time it could help increase the dietary fibre content of these products. Non-digestible insoluble fibre, as is the case of cellulose, provides a beneficial effect to consumer's health, primarily by promoting a feeling of “fullness” without additional energy intake and improving laxation and bowel function; indirectly, it can help in reducing the risk of diabetes, obesity, cardiovascular disease and other chronic diseases [15–17]. As a food additive, BC:CMC may improve the product's organoleptic properties and stability, plus increasing its nutritional value.

Nowadays, one of the most versatile hydrocolloids – also widely use in the food industry – is xanthan gum (XG). Xanthan gum is a bacterial exopolysaccharide, being most commonly produced by *Xanthomonas*

campestris. Its structure consists of a main chain of β -1,4 linked glucose monomers (a cellulose-like backbone) with trisaccharide side chains linked at the O-3 position of every other glucose residue. The side chains contain one glucuronic acid between two mannose residues. The mannose linked to the backbone contains an acetyl group, and in average about half of the terminal mannose units contain a pyruvic acid residue. These groups are responsible for the anionic character of the XG molecule. [18–20] XG is used to provide high viscosity and pseudoplasticity, having good suspending and stabilizing properties. It is compatible with high concentrations of salt and stable at a wide range of temperature and pH values. However, it is known that these parameters affect the molecular structure of the polyelectrolyte, leading to a conformational transition that affects its rheological behaviour [21,22].

In this work, new BC:CMC formulations were prepared, by increasing the BC to CMC ratio, in order to increase the fiber content and improve the viscosity and the stabilizing ability of aqueous dispersions. A benchmark was carried out with XG, aiming to highlight the competitive advantages of the new BC:CMC dry formulations for application in food systems.

6.2 - MATERIALS AND METHODS

6.2.1 - Materials and reagents

BC wet membranes were supplied by HTK Food CO., Ltd (Ho Chi Minh, Vietnam). Carboxymethyl cellulose, with average molecular weight of 90 kDa and a degree of substitution of 0.7, was supplied by Acros Organics (Geel, Belgium). Xanthan gum was kindly provided by Jungbunzlauer (Pernhofen, Austria). Xanthan Gum FF is a fine powder, 200 mesh (minimum 92 % < 0.075 mm), with a viscosity between 1400 and 1600 mPa·s at a concentration of 1%, in a solution of 1 % KCl (measured in a Brookfield LVTD viscometer, spindle 3, 60 rpm, 25°C).

Sodium Hydroxide (NaOH) was purchased from Labkem (Barcelona, Spain); sodium chloride from Biochem Chemopharma (Cosne-Cours-sur-Loire, France); citric acid and tri-sodium citrate from Riedel-de Haën (Seelze, Germany); potassium di-hydrogen phosphate and di-sodium hydrogen phosphate from Panreac (Barcelona, Spain); sodium carbonate and sodium bicarbonate were acquired from Sigma (Steinheim, Germany).

6.2.2 - Preparation of BC:CMC dry formulations

BC:CMC dry formulations were prepared according to a previously described protocol [23]. Briefly, BC membranes were soaked in NaOH 0.1 M for 3 days, with daily solution exchange, then washed with

distilled water to remove the alkaline solution, with 3 to 4 daily water exchanges, until the pH of the washing solution was the same of distilled water. The washed BC membranes were disintegrated with a hand blender at 9000 rpm (Sammic blender, model TR250, Sammic S.L.). Samples of the obtained pulp were dried in an oven at 40 °C to determine the solid fraction of the batch, which was then adjusted to 0.5 % (m/v) by adding distilled water. A solution of 0.5 % CMC was added to the BC pulp in the necessary amounts to produce mixtures with BC to CMC ratios of 1:1, 1:0.75 and 1:0.5. These mixtures were left under magnetic stirring overnight at room temperature. Afterwards, the BC:CMC mixtures were wet-ground in a high-speed blender (Moulinex Ultrablend 1500 W) at 24 000 rpm for 1 min, and autoclaved at 121 °C for 20 min. Finally, they were freeze-dried for 5 days at -100 °C, 0.05 mbar, and stored in a desiccator until use.

6.2.3 - Physicochemical characterization of the polysaccharides

Attenuated Total Reflection-Fourier Transform Infrared (ATR-FTIR) spectroscopic analysis was carried out in a Bruker FTIR Spectrometer ALPHA II (Bruker, Massachusetts, USA) in the absorbance mode, within the range of 4000 cm^{-1} and 400 cm^{-1} , operating at a resolution of 4 cm^{-1} . The spectra were taken by averaging 24 scans for each spectrum.

The Differential Scanning Calorimetry (DSC) thermograms were obtained in a Perkin-Elmer DSC 6000 calorimeter (Perkin-Elmer, Massachusetts, USA). A mass of approximately 6 mg of each dry sample was weighted into 20 μL aluminium pans and hermetically sealed. Samples were heated from 20 °C to 400 °C, at a rate of 10 °C/min, under a N_2 atmosphere (20 mL/min). An empty sealed pan was used as reference.

6.2.4 - Preparation of aqueous dispersions

NaCl solutions with concentrations of 5, 50, 150 and 350 mM were prepared in distilled water and filtered through a PES membrane with 0.22 μm pore size. The following buffer solutions were prepared, according to standard laboratory protocols, to a final concentration of 50 mM: citric acid – sodium phosphate buffer, pH 2.8; citric acid – sodium citrate buffer, pH 3.5 and pH 5.3; potassium phosphate – sodium phosphate buffer, pH 7.7; sodium carbonate – sodium bicarbonate buffer, pH 10.4. The buffer solutions were filtered through a PES membrane with 0.22 μm pore size and 0.01% sodium azide was added to prevent microbial growth. The salinity and conductivity of the solutions and buffers were measured with a benchtop multiparameter analyser (model C3010, Consort, Turnhout, Belgium).

Aqueous dispersions of the dry BC:CMC formulations and XG were prepared at room temperature, at a concentration of 0.5 % (m/v) in distilled water, buffer or NaCl solutions, to a final volume of 30 mL, in triplicate. The dry materials were added to the aqueous media and agitated in a vortex mixer, until complete hydration (visually confirmed); the dispersions were then homogenized in a T-25 Ultra-turrax equipped with a S25 N-18 G dispersing tool (IKA, Germany), at 8000 rpm for 1 min.

For the studies at different polymer concentrations, sequential dilutions of the previous 0.5 % dispersions in distilled water were made, in a range from 0.25 % to 0.001 %. Additionally, sequential dilutions of the 0.5 % XG dispersion in 150 mM NaCl were made in the same range.

6.2.5 - Rheological analysis

Rheological measurements of the aqueous dispersions were performed in a Discovery HR-1 hybrid rheometer with TRIOS version 4 software (TA Instruments, Delaware, USA), using a cone and plate geometry (60 mm, 2.006° cone angle, 64 µm gap), at 25 °C. Viscosity and shear stress of the samples were measured in triplicate by flow sweep tests at increasing shear rates, from 0.01 s⁻¹ to 300 s⁻¹. The linear viscoelastic region (LVR) of the samples was observed in oscillatory strain sweep tests carried out at a frequency of 1 Hz and strain amplitude from 0.02 to 100 %. After that, oscillatory frequency sweep tests were performed in triplicate within the LVR (0.25 % strain), with angular frequency ranging from 0.01 to 40 Hz.

Using the analysis tool from TRIOS software, several rheological models were adjusted to the experimental flow curves. The best fit (highest coefficient of determination, $R^2 > 0.990$) to the viscosity (η) vs shear rate ($\dot{\gamma}$) plots was given by the Cross model, shown in equation 3:

$$\eta = \eta_{\infty} + \frac{\eta_0 - \eta_{\infty}}{1 + (k\dot{\gamma})^n} \quad (eq. 3)$$

where η_0 is the zero-rate viscosity, η_{∞} is the infinite-rate viscosity, k is the consistency coefficient and n is the flow behaviour index (or power-law index). Regarding the shear stress (σ) vs shear rate plots, the best fit was given by the Herschel-Bulkley model, shown in equation 4:

$$\sigma = \sigma_0 + k\dot{\gamma}^n \quad (eq. 4)$$

where σ_0 is the yield stress. From the adjustment of these models to the experimental data, the values of η_0 and σ_0 were taken and plotted against the polymer concentration in aqueous dispersion.

Data was processed using GraphPad Prism version 5 software (GraphPad Software Inc., San Diego, California, USA) and the results were expressed as mean \pm standard deviation.

6.3 - RESULTS AND DISCUSSION

6.3.1 - Characterization of the polysaccharides and BC:CMC formulations

Thermal characterization of the polysaccharides and BC:CMC mixtures is shown in the DSC thermograms of Figure 6.1-A.

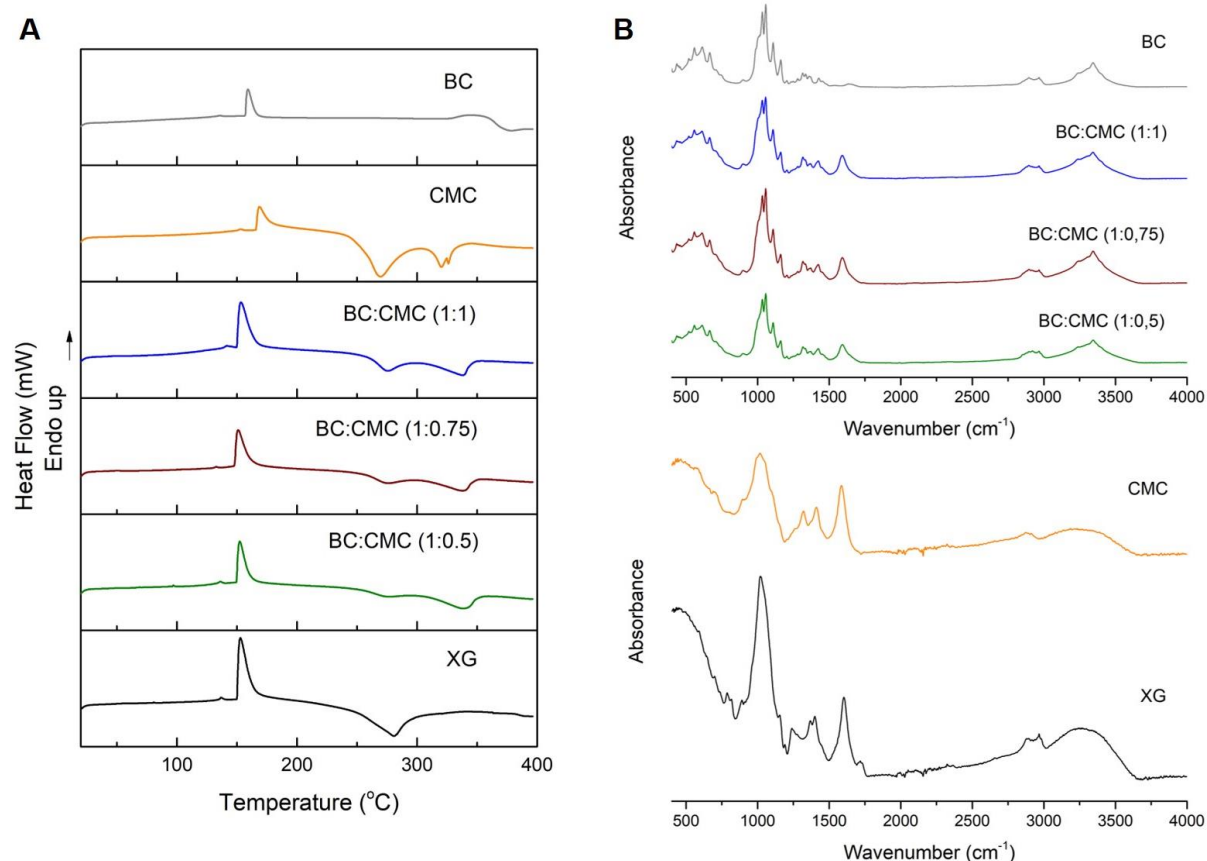


Figure 6.1 - Characterization of BC:CMC formulations, CMC and XG in dry state by: (A) Differential scanning calorimetry, between 20 °C and 400 °C, at a heat rate of 10 °C/min under N₂ atmosphere; (B) Attenuated total reflection-Fourier transform infrared spectroscopy, in absorbance mode in the range of 400 cm⁻¹ to 4000 cm⁻¹.

BC shows an intense endothermic peak at 159 °C, common to all the samples within the temperature range of 150 to 170 °C, that could be ascribed to the desorption of strongly bound water from the polymer chains. BC is then thermally stable until 330 °C, where degradation events start to occur. On

the other hand, CMC shows two exothermic peaks at 270 and 320 °C. The BC:CMC formulations show these same peaks, with a slight shift towards higher temperatures (274 and 338 °C, respectively) that could result from a small protective effect of BC fibres, and the intensity (area) of the peaks decreases with increasing BC to CMC ratio. This is an expected result since the thermograms of the physical mixtures show the events of the individual components, varying in intensity according to the mass fraction of the component in the mixture. Finally, XG shows a single exothermic event with peak at 281 °C, which is in accordance with other reports [24].

Observing Figure 6.1-B, FTIR spectrum of BC shows the characteristic bands well described in literature: a band at 900 cm^{-1} attributed to C-O-C stretching from β -(1,4) glycosidic linkages; peaks corresponding to other C-O bonds between 1030 and 1165 cm^{-1} ; peaks corresponding to C-H bending at 1375 and 1435 cm^{-1} ; a band around 2900 cm^{-1} assigned to C-H stretching; and finally a wide band around 3352 cm^{-1} related to O-H stretching. CMC spectra presents an overall lower intensity with one more band peaking at 1590 cm^{-1} , attributed to the C=O stretching from the carboxylic groups (-COOH) [7,25,26]. BC:CMC formulations have a spectra similar to that of BC, featuring in addition the carboxylic group band from CMC; no other bands are observed in the formulations, an expected result for a physical mixture without chemical interactions between the polymers.

Xanthan gum structure contains many of the same functional groups, so its spectrum shows many similarities: C-O-C stretching of the β -(1,4) glycosidic bonds in the backbone at 900 cm^{-1} ; C-O stretching band around 1030 cm^{-1} ; C-H bending at 1400 cm^{-1} ; C=O stretching of the carboxylic groups from pyruvate and glucuronic acid at 1610 cm^{-1} and an extra peak at 1730 cm^{-1} attributed to the C=O stretching of the acetate group; C-H stretching band around 2900 cm^{-1} and O-H stretching band between 3100 and 3600 cm^{-1} [27–29].

6.3.2 - Rheological characterization of the aqueous dispersions

Figure 6.2 displays the rheological characterization of aqueous dispersions of XG and BC:CMC formulations at a concentration of 0.5 %. Flow profiles of viscosity as a function of shear rate (Figure 6.2-A) show that all samples have a shear-thinning behaviour, characteristic of polysaccharides and other polymeric dispersions. Viscosity is higher at lower shear rates due to the entanglements and physical interactions between polymer chains that hinder the flow, and decreases as the particles align parallel to the direction of flow (hence with less interactions) when higher shear rates are applied [30].

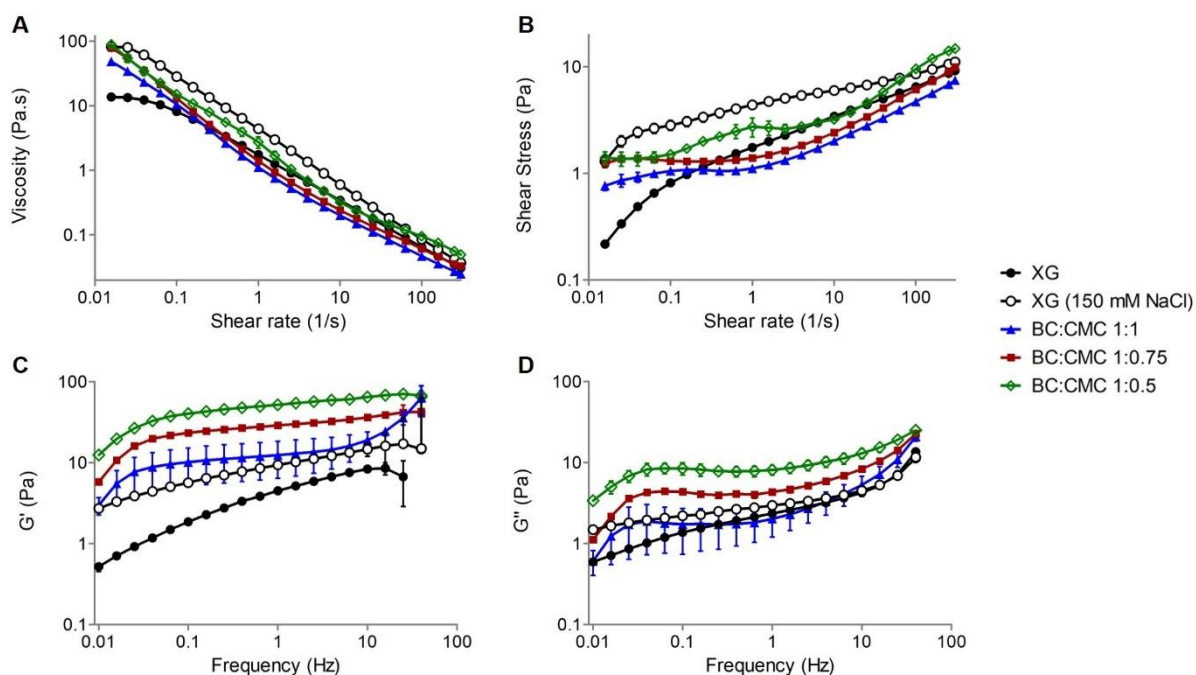


Figure 6.2 - Rheological characterization of BC:CMC and XG dispersions at a concentration of 0.5 % (w/w) in distilled water, plus XG in 150 mM NaCl: (A) viscosity and (B) shear stress, as function of shear rate taken from flow sweep tests in the range of 0.01 to 300 s^{-1} ; (C) storage modulus, G' and (D) loss modulus, G'' , taken from oscillatory frequency sweep tests in the range of 0.01 to 40 Hz. Samples were analysed at 25 °C. Results are the average of triplicate samples and bars represent standard deviations.

Regarding only dispersions in distilled water, XG shows much lower viscosity than BC:CMC formulations, at low shear rates; on the other hand, BC:CMC formulations are more shear-thinning and thus less viscous at high shear rates. Namely BC:CMC formulations with the ratios of 1:1 and 1:0.75 become less viscous than XG between 0.1 and 1 s^{-1} .

Among the BC:CMC formulations, viscosity is directly proportional to the mixture's ratio. In other words, the higher the BC content in the formulation, the higher the viscosity of its aqueous dispersion. The high aspect ratio and insoluble BC fibres are primarily responsible for the viscosity due to the interconnected three-dimensional networks in aqueous media [31]. These networks become denser and more entangled – more structured – as higher amounts of solid BC particles are available for interaction, hindering flow and resulting in higher viscosity. Despite the different viscosity values, all BC:CMC formulations show an ever-increasing viscosity profile towards lower shear rates, whereas XG profiles show tendency to a plateau, corresponding to their viscosity at rest (the zero-shear viscosity).

The curves of shear stress vs shear rate of Figure 6.2-B represent the tension (stress) that has to be applied on the material to promote a certain displacement. This plot confirms the pseudoplasticity of the dispersions, and once again different behaviours towards zero-shear conditions are observed: XG

dispersions show a decrease in stress that ultimately tends to the origin of the graphic, while BC:CMC dispersions show a stress plateau at low shear rates. This constant value is the minimum stress that needs to be applied for a displacement to occur, i.e., to start flow – the yield stress, discussed in more detail in the next subsection. The shear stress is also proportional to the BC:CMC ratio, BC:CMC 1:0.5 showing the higher values despite the more irregular profile (also higher than XG in distilled water).

Despite what was observed so far for the water dispersions, the samples displaying higher viscosity and shear stress were undoubtedly those of XG in NaCl. This result is further analysed and discussed ahead, in the section concerning the effect of salinity.

The viscoelastic behaviour of the dispersions was quantified in terms of elastic (or storage) modulus, G' , and viscous (or loss) modulus, G'' , represented in Figures 6.2-C and 6.2-D, respectively. In all samples, at a concentration of 0.5 %, the contribution of G' is higher than that of G'' , pointing to a more pronounced elastic (solid-like) behaviour of the 0.5 % dispersions, typical of gels, throughout the entire frequency range tested. Differences between the samples are more notorious in the G' plot than in the flow curves, clearly showing that BC:CMC samples have a more pronounced elastic behaviour than XG. Again, the ratio of BC to CMC influences the rheological parameters: the higher the BC content, the denser and more structured the fibrous network becomes. The G' values highlight how an internal structure in an aqueous dispersion can be perceived by its rheological properties, allowing to distinguish materials with similar viscosity profiles. Even though a XG dispersion in salt has higher viscosity than the different BC:CMC formulations, the more pronounced elastic behaviour of the later is an indication of a higher colloidal stability and better particle suspending capabilities.

6.3.3 - Effect of concentration

The flow curves of the dispersions at concentrations ranging from 0.001 % to 0.5 % were adjusted to empirical rheological models. Viscosity *vs* shear rate plots were best fitted by the Cross model, while shear stress *vs* shear rate plots were best fitted by the Herschel-Bulkley model. From the fitted parameters of both models, the zero-shear viscosity (η_0) and the yield stress (σ_0) were selected to investigate the effect of polymer concentration.

The zero-shear viscosity, as the name implies, is the viscosity of the sample determined when the shear rate approaches zero, towards rest conditions. The concentration dependence of the zero-shear viscosity is used to determine the critical aggregation concentration of polymer solutions. This critical concentration marks the transition of the solutions/dispersions from dilute to semi-dilute regime, where higher occurrence of molecule interactions and entanglements lead to an abrupt increase in viscosity and

changes in other rheological parameters [32,33]. From the results of zero-shear viscosity as a function of polymer concentration, Figure 6.3-A, critical aggregation concentration values could not be obtained with precision for all samples. However, it is possible to observe that η_0 increases with concentration for all samples, in different ways. Plots of XG in dH₂O and in 150 mM NaCl cross at a concentration of 0.1 %; BC:CMC profiles are more irregular and show higher deviations; BC:CMC, specifically in the ratio 1:0.5, has higher η_0 values than XG (in water or NaCl) across the whole concentration range. In practice, at low shear, it takes a smaller amount of BC:CMC 1:0.5 to reach the same viscosity of XG solutions.

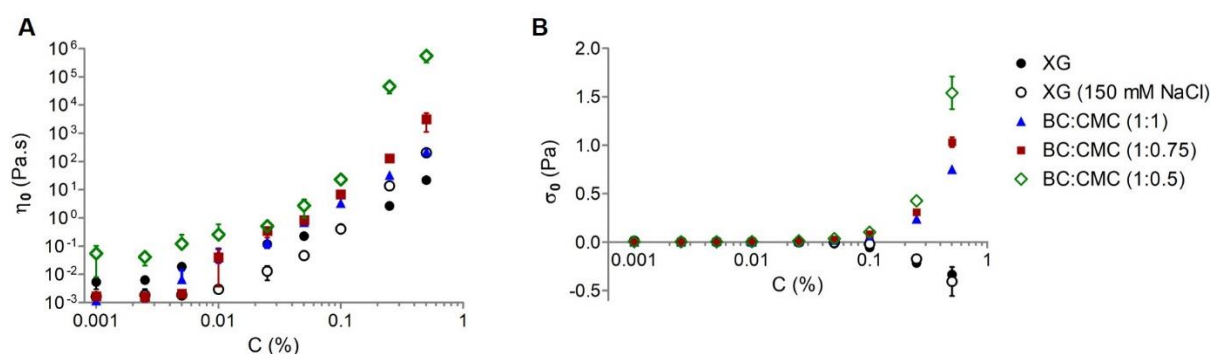


Figure 6.3 - Mass percentage concentration dependence of the (A) zero-shear viscosity, η_0 , and (B) yield stress, σ_0 , for BC:CMC and XG dispersions in distilled water, plus XG in 150 mM NaCl, at 25 °C. Results are the average of triplicate samples and bars represent standard deviations.

Unlike XG, BC:CMC dispersions present a measurable yield stress (Figure 6.3-B), at concentrations higher than 0.1 %, which is directly proportional to the BC:CMC ratio. The yield stress is the minimum stress required to initiate flow, or the threshold value of the transition from solid-like (elastic gel) to fluid-like. It is a good indicator of structural integrity and stability, as no deformation occurs when tensions below the yield stress are applied, e.g., the effect of gravity on suspended particles or droplets might be attenuated or suppressed [34,35]. It is important to note that in a dispersion with a high zero shear viscosity, particles will still slowly sediment, whereas a dispersion with a yield stress will retain its integrity below that value of stress. This is relevant in industry for the formulation of liquid compositions with suspending capabilities and in the assurance of stability over time (storage) [36–38]. The yield stresses at the highest concentration tested, 0.5 %, were (0.75 ± 0.05) Pa for BC:CMC 1:1, (1.03 ± 0.05) Pa for BC:CMC 1:0.75, and (1.54 ± 0.17) Pa for BC:CMC 1:0.5.

6.3.4 - Effect of salinity and pH

To study the effect of salinity and pH on the characteristics of the polysaccharide dispersions, namely their viscosity, solutions with different concentrations of NaCl and buffers with different pH values within a wide range were prepared. The choice of NaCl concentrations was based on values possible to find in food products: sauces and seasonings (such as ketchup and mustard) contain around 1 % salt (≈ 170 mM), broths can have higher salt concentration, and fruit juices and other beverages contain less than 1 mM. For reference, salinity of sea water is 35 (grams of salt per kg, dimensionless). The characterization of the saline solutions was made by measuring their salinity and conductivity, present in Table 6.1, before preparing the dispersions with the polymers. The flow curves of dispersions at a concentration of 0.5 % in aqueous solutions with different salinities are shown in Figure 6.4.

Table 6.1 - Salinity (dimensionless) and conductivity (mS/cm) of the NaCl solutions in distilled water prepared at concentrations ranging from 0 to 350 mM, at room temperature

	dH₂O	NaCl			
Concentration (mM)	0	5	50	150	350
Salinity	0.0	0.2	3.6	11.8	27.3
Conductivity (mS/cm)	1.1×10^{-3}	532×10^{-3}	7.16	20.7	43.95

Plots of BC:CMC formulations (Figure 6.4-B, C and D) are essentially collinear at each ratio, not showing any apparent effect of salinity on the polymeric dispersions' viscosity.

Contrarily, in Figure 6.4-A a pronounced increase in XG viscosity is visible in the presence of salt, as the curve of the dispersion in dH₂O is much lower. After that point, as with BC:CMC, increasing salt concentrations had no significant effect in viscosity [21,32]. Taking this into account, XG dispersions in 150 mM NaCl were also analysed and added to the graphs of Figures 6.2 and 6.3, so that BC:CMC formulations could be compared with XG in its most favourable environment. XG in 150 mM NaCl displays in fact the highest viscosity and stress in Figure 6.2, but is still inferior to BC:CMC formulations when it comes to the dynamic moduli (specially the lower G' values that indicate weaker solid-like behaviour) and yield stress (inexistent for XG in Figure 6.3-B).

Xanthan gum molecules undergo an order-disorder conformational transition in aqueous solution, influenced by temperature, ionic strength and other environmental conditions. They can exhibit either an ordered helical conformation due to hydrogen bonds between the side chains and the backbone, or a disordered coil (broken helix) when the side chains protrude from the main chain owing to electrostatic

repulsions between the negatively charged carboxylic groups [21,22,33,39]. At room temperature the helical conformation is prevalent, but over the transition temperature (around 40 to 50 °C) [21,22,40], hydrogen bonds are weakened and the chain acquires a disordered (more flexible) coil conformation. When salt is added, electrostatic repulsions between carboxylic groups in the side chains disappear due to charge screening; the helical conformation is stabilized, becoming more rigid, and the transition temperature is shifted to higher values. In short, high temperatures promote the transition of xanthan to random coil conformation, while ionic strength promotes a more ordered and stable helix conformation. The two possible configurations, with different flexibility and volume, translate in distinct rheologic behaviours: lower viscosity in solutions of the more rigid and compact helix conformation, and higher for random coils [22,33].

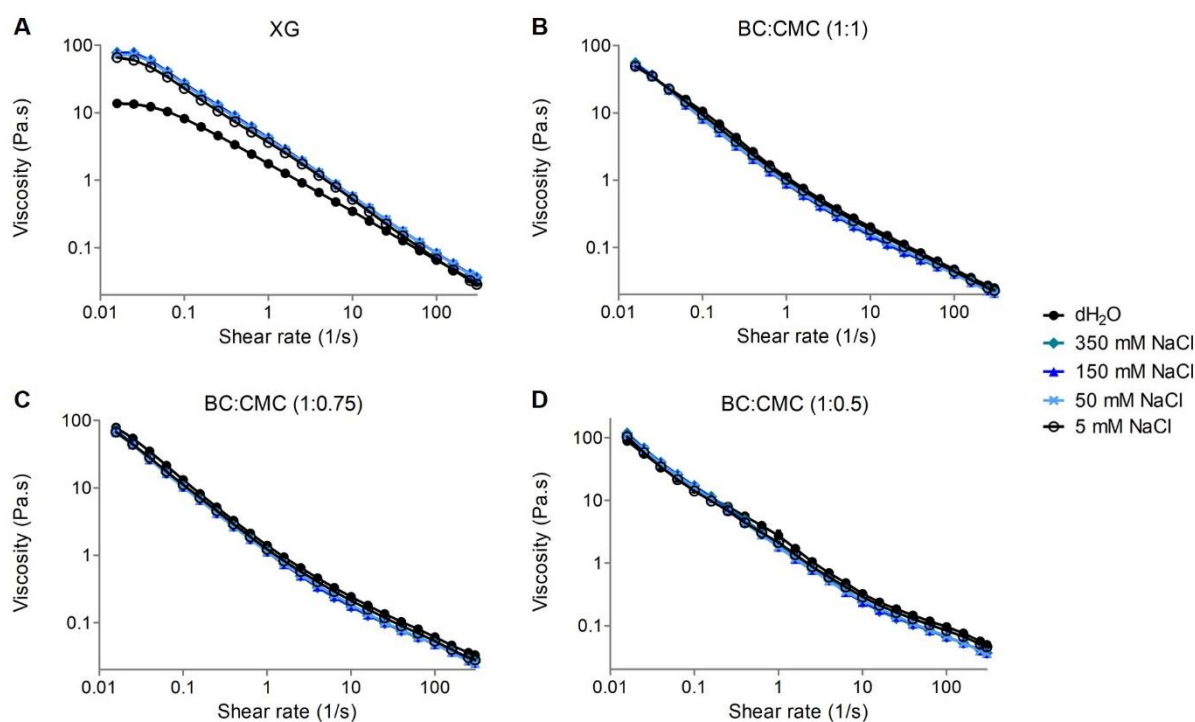


Figure 6.4 - Effect of NaCl concentration in the flow curves (viscosity vs shear rate) of 0.5 % (w/w) dispersions of (A) XG, (B) BC:CMC 1:1, (C) BC:CMC 1:0.75, and (D) BC:CMC 1:0.5. Samples were analysed at 25 °C.

Results are the average of triplicate samples and bars represent standard deviations.

In this work, XG samples were prepared at room temperature and analysed at 25 °C. Thus, the observed difference in XG's viscosity in water or NaCl can be attributed stabilization of the helix conformation in the presence of salts. Although in theory this induces a decrease in viscosity for dilute solutions [22,32,33], the opposite has also been reported for more concentrated (semi-dilute) solutions [21,41,42] and

assigned to the higher lifetime and energy of the transient bonds between XG molecules in helical conformation, in the presence of salt. This is indeed observed in Figure 6.3-A, where XG dispersions in dH₂O show higher zero-shear viscosity up to a concentration of 0.1 %; above this concentration, η_0 is higher for XG in NaCl. Other variables that can affect molecular arrangements and rheology are the acetate to pyruvate ratio and whether the xanthan samples have been renatured (heated above the transition temperature and cooled, becoming less susceptible to environmental changes because the helix conformation cannot be fully recovered) [21,40,41].

The effect of pH was also analysed. The characterization of the buffers used at a concentration of 50 mM is shown in Table 6.2.

Table 6.2 - Salinity (dimensionless) and conductivity (mS/cm) of the buffer solutions in distilled water prepared at a concentration of 50 mM, with pH values ranging from 2.8 to 10.4, at 25 °C

pH	2.8	3.5	5.3	7.7	10.4
Salinity	1.3	1.6	4.8	4.5	4.7
Conductivity (mS/cm)	2.78	3.28	9.37	8.72	9.15

According to the results of Figure 6.5 (B, C and D), pH does not seem to have a significant effect in the viscosity of BC:CMC dispersions, within the tested range. At pH 2.8, some deviation occurs from the global tendency. This is more noticeable in BC:CMC 1:1 ratio, that has relatively higher amount of CMC. This is an anionic polyelectrolyte, becoming protonated and insoluble at low pH values [43,44]. Taking into account the intrinsic dissociation constant of the carboxylic groups in CMC ($pK_a = 3.3$ in salt free solution [45]), an effect of pH is observed only for the more acidic buffer tested. Similarly, XG possesses negatively charged groups ($pK_a = 4.65$ [46]) that can also be screened at low pH values, inducing the conformational transition. Some variation in the viscosity of XG dispersions at different pH values (Figure 6.5-A) was indeed observed at lower shear rates, mainly below 0.1 s^{-1} ; in fact, before this point XG exhibits higher viscosity at pH values closer to neutral (5.3 and 7.7), and lower both in acidic and alkaline media. An increase in XG solution's viscosity with increasing pH values up to $pH = 5$ is in accordance with previous reports [39].

In summary, both CMC and xanthan are polyelectrolytes that are affected by ionic strength, pH and other environmental conditions. In BC:CMC formulations, CMC adsorbed to the BC fibres acts as a co-drying agent to prevent cellulose hornification, and as a dispersing aid due to the negative charges repulsions that prevent fibre aggregation. On the other hand, BC fibres are responsible for the viscosity and other

rheological properties of BC:CMC mixtures, as can be seen from the results obtained with different ratios. After rehydration and activation of BC fibres in water to form a three-dimensional network of solid particles, the effects of pH and salinity on the CMC charge no longer affect the rheological and stabilizing properties of BC. This robust stability of the rheological properties in different environments can represent an advantage for the formulation of foodstuffs or other products.

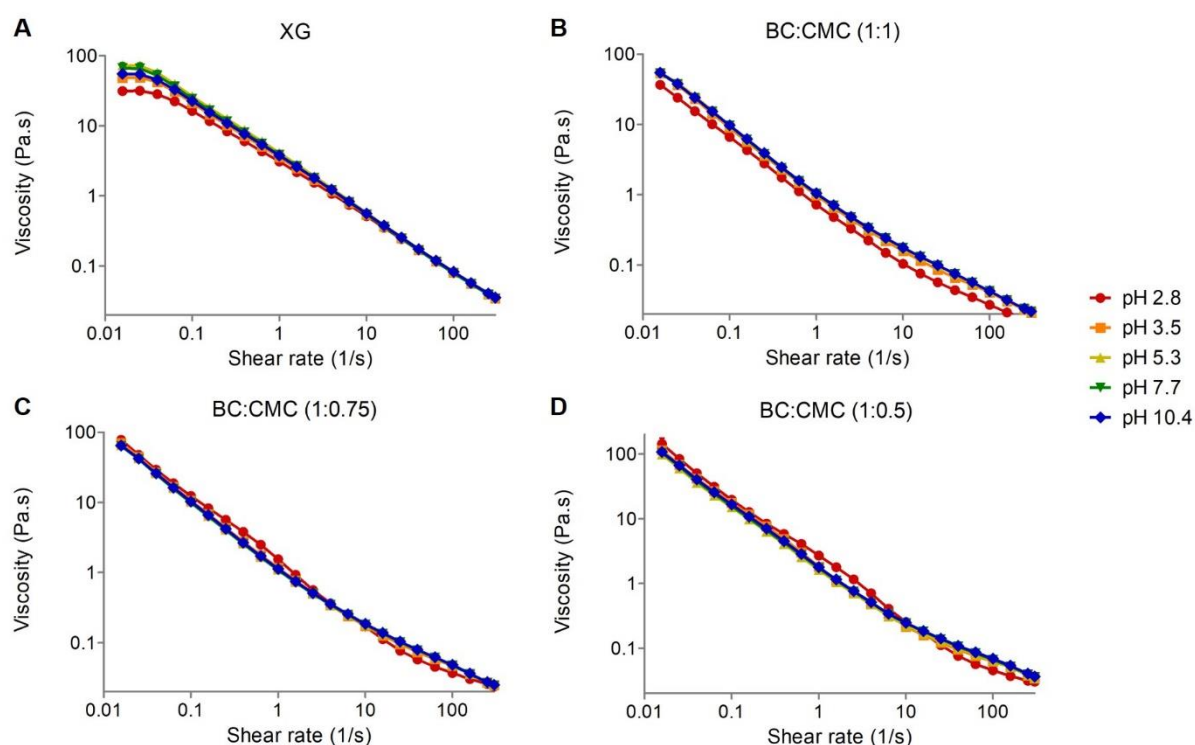


Figure 6.5 - Effect of pH in the flow curves (viscosity vs shear rate) of 0.5 % (w/w) dispersions of (A) XG, (B) BC:CMC 1:1, (C) BC:CMC 1:0.75, and (D) BC:CMC 1:0.5. Samples were analysed at 25 °C. Results are the average of triplicate samples and bars represent standard deviations.

6.4 - CONCLUSIONS

In short, BC:CMC formulations, and particularly BC:CMC 1:0.5, present high values of zero-shear viscosity and a measurable yield stress. These parameters, in addition to the strong elastic gel behaviour, point to a better suspension and emulsion stabilizing ability than xanthan gum in either of its structural conformations. Moreover, BC:CMC formulations showed a constant viscosity behaviour despite the ionic strength or pH of the aqueous media.

Further work should include the study of the effect of temperature (since many food products are submitted to heat treatments in production or consuming steps), as well as the preparation and analysis

of food emulsions to attest the good stabilizing properties hereby suggested by the rheological measurements.

6.5 - BIBLIOGRAPHIC REFERENCES

- [1] B. Medronho, B. Lindman, Competing forces during cellulose dissolution: From solvents to mechanisms, *Curr. Opin. Colloid Interface Sci.* 19 (2014) 32–40. <https://doi.org/10.1016/j.cocis.2013.12.001>.
- [2] R.J. Moon, A. Martini, J. Nairn, J. Simonsen, J. Youngblood, Cellulose nanomaterials review: Structure, properties and nanocomposites, 2011. <https://doi.org/10.1039/c0cs00108b>.
- [3] Y. Habibi, L.A. Lucia, O.J. Rojas, Cellulose nanocrystals: Chemistry, self-assembly, and applications, *Chem. Rev.* 110 (2010) 3479–3500. <https://doi.org/10.1021/cr900339w>.
- [4] D. Klemm, E.D. Cranston, D. Fischer, M. Gama, S.A. Kedzior, D. Kralisch, F. Kramer, T. Kondo, T. Lindström, S. Nietzsche, K. Petzold-Welcke, F. Rauchfuß, Nanocellulose as a natural source for groundbreaking applications in materials science: Today's state, *Mater. Today*. 21 (2018) 720–748. <https://doi.org/10.1016/j.mattod.2018.02.001>.
- [5] D. Mamlouk, M. Gullo, Acetic Acid Bacteria: Physiology and Carbon Sources Oxidation, *Indian J. Microbiol.* 53 (2013) 377–384. <https://doi.org/10.1007/s12088-013-0414-z>.
- [6] S.S. Wang, Y.H. Han, Y.X. Ye, X.X. Shi, P. Xiang, D.L. Chen, M. Li, Physicochemical characterization of high-quality bacterial cellulose produced by *Komagataeibacter* sp. strain W1 and identification of the associated genes in bacterial cellulose production, *RSC Adv.* 7 (2017) 45145–45155. <https://doi.org/10.1039/c7ra08391b>.
- [7] D. Abol-Fotouh, M.A. Hassan, H. Shokry, A. Roig, M.S. Azab, A.E.H.B. Kashyout, Bacterial nanocellulose from agro-industrial wastes: low-cost and enhanced production by *Komagataeibacter saccharivorans* MD1, *Sci. Rep.* 10 (2020) 1–14. <https://doi.org/10.1038/s41598-020-60315-9>.
- [8] P. Jacek, F.A.G. Soares, F. Dourado, M. Gama, Optimization and characterization of bacterial nanocellulose produced by *Komagataeibacter rhaeticus* K3, 2 (2021). <https://doi.org/10.1016/j.carpta.2020.100022>.
- [9] A.C. Rodrigues, A.I. Fontão, A. Coelho, M. Leal, F.A.G. Soares da Silva, Y. Wan, F. Dourado, M. Gama, Response surface statistical optimization of bacterial nanocellulose fermentation in static culture using a low-cost medium, *N. Biotechnol.* 49 (2019) 19–27. <https://doi.org/10.1016/j.nbt.2018.12.002>.
- [10] P. Nechita, D.M. Panaitescu, Improving the dispersibility of cellulose microfibrillated structures in polymer matrix by controlling drying conditions and chemical surface modifications, *Cellul. Chem. Technol.* 47 (2013) 711–719.
- [11] R.H. Newman, Carbon-13 NMR evidence for cocrystallization of cellulose as a mechanism for hornification of bleached kraft pulp, *Cellulose*. 11 (2004) 45–52. <https://doi.org/10.1023/B:CELL.0000014768.28924.0c>.
- [12] D. Klemm, F. Kramer, S. Moritz, T. Lindström, M. Ankerfors, D. Gray, A. Dorris, Nanocelluloses: A new family of nature-based materials, *Angew. Chemie - Int. Ed.* 50 (2011) 5438–5466. <https://doi.org/10.1002/anie.201001273>.
- [13] D. Martins, B. Estevinho, F. Rocha, F. Dourado, M. Gama, A Dry and Fully Dispersible Bacterial Cellulose Formulation as a Stabilizer for Oil-in-Water Emulsions, *Carbohydr. Polym.* 230 (2020) 115657. <https://doi.org/10.1016/j.carbpol.2019.115657>.
- [14] D. Martins, D. de Carvalho Ferreira, M. Gama, F. Dourado, Dry Bacterial Cellulose and Carboxymethyl Cellulose formulations with interfacial-active performance: processing conditions and redispersion, *Cellulose*. 9 (2020). <https://doi.org/10.1007/s10570-020-03211-9>.

- [15] J. Nsor-Atindana, M. Chen, H.D. Goff, F. Zhong, H.R. Sharif, Y. Li, Functionality and nutritional aspects of microcrystalline cellulose in food, *Carbohydr. Polym.* 172 (2017) 159–174. <https://doi.org/10.1016/j.carbpol.2017.04.021>.
- [16] F. Dourado, M. Leal, D. Martins, A. Fontão, A. Cristina Rodrigues, M. Gama, Celluloses as Food Ingredients/Additives: Is There a Room for BNC?, in: M. Gama, F. Dourado, S. Bielecki (Eds.), *Bact. Nanocellulose From Biotechnol. to Bio-Economy*, Elsevier B.V, 2016: pp. 123–133. <https://doi.org/10.1016/B978-0-444-63458-0.00007-X>.
- [17] Z. Shi, Y. Zhang, G.O. Phillips, G. Yang, Utilization of bacterial cellulose in food, *Food Hydrocoll.* 35 (2014) 539–545. <https://doi.org/10.1016/j.foodhyd.2013.07.012>.
- [18] F. García-Ochoa, V.E. Santos, J.A. Casas, E. Gómez, Xanthan gum: Production, recovery, and properties, *Biotechnol. Adv.* 18 (2000) 549–579. [https://doi.org/10.1016/S0734-9750\(00\)00050-1](https://doi.org/10.1016/S0734-9750(00)00050-1).
- [19] D.F.S. Petri, Xanthan gum: A versatile biopolymer for biomedical and technological applications, *J. Appl. Polym. Sci.* 132 (2015). <https://doi.org/10.1002/app.42035>.
- [20] H. Habibi, K. Khosravi-Darani, Effective variables on production and structure of xanthan gum and its food applications: A review, *Biocatal. Agric. Biotechnol.* 10 (2017) 130–140. <https://doi.org/10.1016/j.bcab.2017.02.013>.
- [21] E. Pelletier, C. Viebke, J. Meadows, P.A. Williams, A rheological study of the order–disorder conformational transition of xanthan gum, *Biopolymers.* 59 (2001) 339–346. [https://doi.org/10.1002/1097-0282\(20011015\)59:5<339::aid-bip1031>3.3.co;2-1](https://doi.org/10.1002/1097-0282(20011015)59:5<339::aid-bip1031>3.3.co;2-1).
- [22] C.E. Brunchi, M. Avadanei, M. Bercea, S. Morariu, Chain conformation of xanthan in solution as influenced by temperature and salt addition, *J. Mol. Liq.* 287 (2019) 111008. <https://doi.org/10.1016/j.molliq.2019.111008>.
- [23] D. Martins, C. Rocha, F. Dourado, M. Gama, Bacterial Cellulose-Carboxymethyl Cellulose (BC:CMC) dry formulation as stabilizer and texturizing agent for surfactant-free cosmetic formulations, *Colloids Surfaces A Physicochem. Eng. Asp.* 617 (2021) 126380. <https://doi.org/10.1016/j.colsurfa.2021.126380>.
- [24] K. Venkateswarlu, Evaluation of glibenclamide microspheres for sustained release, 5 (2017).
- [25] A. Casaburi, Ú. Montoya Rojo, P. Cerrutti, A. Vázquez, M.L. Foresti, Carboxymethyl cellulose with tailored degree of substitution obtained from bacterial cellulose, *Food Hydrocoll.* 75 (2018) 147–156. <https://doi.org/10.1016/j.foodhyd.2017.09.002>.
- [26] E.C. Queirós, S.P. Pinheiro, J.E. Pereira, J. Prada, I. Pires, F. Dourado, P. Parpot, M. Gama, Hemostatic Dressings Made of Oxidized Bacterial Nanocellulose Membranes, *Polysaccharides.* 2 (2021) 80–99. <https://doi.org/10.3390/polysaccharides2010006>.
- [27] D. Osiro, R.W.A. Francoa, L.A. Colnago, Spectroscopic characterization of the exopolysaccharide of *Xanthomonas axonopodis* pv. *citri* in Cu²⁺ resistance mechanism, *J. Braz. Chem. Soc.* 22 (2011) 1339–1345. <https://doi.org/10.1590/S0103-50532011000700020>.
- [28] S. Faria, C.L. De Oliveira Petkowicz, S.A.L. De Moraes, M.G.H. Terrones, M.M. De Resende, F.P. De Frana, V.L. Cardoso, Characterization of xanthan gum produced from sugar cane broth, *Carbohydr. Polym.* 86 (2011) 469–476. <https://doi.org/10.1016/j.carbpol.2011.04.063>.
- [29] A. Mohsin, K. Zhang, J. Hu, Salim-ur-Rehman, M. Tariq, W.Q. Zaman, I.M. Khan, Y. Zhuang, M. Guo, Optimized biosynthesis of xanthan via effective valorization of orange peels using response surface methodology: A kinetic model approach, *Carbohydr. Polym.* 181 (2018) 793–800. <https://doi.org/10.1016/j.carbpol.2017.11.076>.
- [30] V. Evageliou, Shear and extensional rheology of selected polysaccharides, *Int. J. Food Sci. Technol.* 55 (2020) 1853–1861. <https://doi.org/10.1111/ijfs.14545>.

- [31] D. Martins, B. Estevinho, F. Rocha, F. Dourado, M. Gama, A dry and fully dispersible bacterial cellulose formulation as a stabilizer for oil-in-water emulsions, *Carbohydr. Polym.* 230 (2020) 115657. <https://doi.org/10.1016/j.carbpol.2019.115657>.
- [32] L. Xu, H. Gong, M. Dong, Y. Li, Rheological properties and thickening mechanism of aqueous diutan gum solution: Effects of temperature and salts, *Carbohydr. Polym.* 132 (2015) 620–629. <https://doi.org/10.1016/j.carbpol.2015.06.083>.
- [33] N.B. Wyatt, M.W. Liberatore, Rheology and Viscosity Scaling of the Polyelectrolyte Xanthan Gum, *J. Appl. Polym. Sci.* 114 (2009). <https://doi.org/10.1002/app>.
- [34] V.S. Rudraraju, C.M. Wyandt, Rheological characterization of Microcrystalline Cellulose/Sodiumcarboxymethyl cellulose hydrogels using a controlled stress rheometer: Part I, *Int. J. Pharm.* 292 (2005) 53–61. <https://doi.org/10.1016/j.ijpharm.2004.10.011>.
- [35] J.F. Steffe, *Rheological Methods in Food Process Engineering*, Second Edi, Freeman Press, 1996.
- [36] M. Caggioni, R. Ortiz, F.A. Barnabas, R.V. Nunes, J.A. Flood, F. Corominas, US 8716213 B2 - Liquid Detergent Composition comprising an external structuring system comprising a bacterial cellulose network, 2014.
- [37] Z.-F. Yang, N.A. Morrison, T.A. Talashek, D.F. Brinkmann, D. DiMasi, Y.L. Chen, US 2007/019777 A1 - Bacterial Cellulose-containing formulations, 2007.
- [38] J.W. Goodwin, R.W. Hughes, *Rheology for chemists: an introduction*, Royal Society of Chemistry, 2000. <https://doi.org/10.5860/choice.38-3918>.
- [39] C.E. Brunchi, M. Bercea, S. Morariu, M. Dascalu, Some properties of xanthan gum in aqueous solutions: effect of temperature and pH, *J. Polym. Res.* 23 (2016). <https://doi.org/10.1007/s10965-016-1015-4>.
- [40] S. Desplanques, F. Renou, M. Grisel, C. Malhiac, Impact of chemical composition of xanthan and acacia gums on the emulsification and stability of oil-in-water emulsions, *Food Hydrocoll.* 27 (2012) 401–410. <https://doi.org/10.1016/j.foodhyd.2011.10.015>.
- [41] E. Choppe, F. Puaud, T. Nicolai, L. Benyahia, Rheology of xanthan solutions as a function of temperature, concentration and ionic strength, *Carbohydr. Polym.* 82 (2010) 1228–1235. <https://doi.org/10.1016/j.carbpol.2010.06.056>.
- [42] E.D. Vega, E. Vásquez, J.R.A. Diaz, M.A. Masuelli, Influence of the Ionic Strength in the Intrinsic Viscosity of Xanthan Gum . An Experimental Review, *J. Polym. Biopolym. Phys. Chem.* 3 (2015) 12–18. <https://doi.org/10.12691/jpbpc-3-1-3>.
- [43] Z. Zare-Akbari, H. Farhadnejad, B. Furughi-Nia, S. Abedin, M. Yadollahi, M. Khorsand-Ghayeni, PH-sensitive bionanocomposite hydrogel beads based on carboxymethyl cellulose/ZnO nanoparticle as drug carrier, *Int. J. Biol. Macromol.* 93 (2016) 1317–1327. <https://doi.org/10.1016/j.ijbiomac.2016.09.110>.
- [44] S. Barkhordari, M. Yadollahi, H. Namazi, PH sensitive nanocomposite hydrogel beads based on carboxymethyl cellulose/layered double hydroxide as drug delivery systems, *J. Polym. Res.* 21 (2014). <https://doi.org/10.1007/s10965-014-0454-z>.
- [45] A.M. Zhivkov, Electric Properties of Carboxymethyl Cellulose, in: T. van de Ven, L. Godbout (Eds.), *Cellul. - Fundam. Asp., InTech, Rijeka, Croatia*, 2013. <https://doi.org/10.5772/56935>.
- [46] V.B. Bueno, D.F.S. Petri, Xanthan hydrogel films: Molecular conformation, charge density and protein carriers, *Carbohydr. Polym.* 101 (2014) 897–904. <https://doi.org/10.1016/j.carbpol.2013.10.039>.

Chapter 7

Conclusions and Future Work

This final chapter consists of an overview of the main breakthroughs of the present thesis, as well as the general conclusions drawn from this work. Some suggestions are outlined for continuing the work on dry BC-based additives; moreover, other areas of application are proposed, where the potential of BC fibres and membranes can still be explored.

CONCLUSIONS

In summary, the work performed for this doctoral thesis led to the development of dry and rehydratable BC:CMC formulations, capable of redispersing in aqueous media in few minutes under low-energy mixing. A dry BC:CMC formulation in a mass ratio of 1:1, when redispersed, preserves the same characteristics as its never-dried counterpart: high viscosity (thickener), colloidal stability, surface activity, creation of entangled structuring networks, among others. These properties, together with the intrinsic characteristics of BC fibres (high purity, high aspect ratio, thermal stability and good mechanical properties) ultimately translate in a great potential as stabilizer, even at low concentrations. It was shown that BC:CMC formulations can be applied in several areas where the stabilization of heterogeneous systems - particularly oil-in-water emulsions and solid particle suspensions - is required. Food and cosmetic systems have been exploited in this work, as examples of future fields of application.

Some other, more specific conclusions can be drawn from this thesis, as follows:

- The addition of CMC to the BC fibres prior to drying prevents hornification and improves redispersion. The anionic polyelectrolyte adsorbs onto BC, imparting a surface charge that leads to electrostatic repulsions between the fibres, hindering aggregation and cocrystallization. This results in a redispersible material with excellent colloidal stability. The addition of CMC as a co-drying and redispersing agent of the BC fibres allows for the use of fast and inexpensive drying methods without compromising the functionality of the formulations.
- After studying various processing parameters, those having the greatest impact on the formulation's functionality were the extent of grinding of the wet BC membranes and the comminution of the dry powders, since these processes cumulatively reduce the size of the fibre bundles. Larger fibres (higher aspect ratio) are more advantageous because they provide higher viscosity and interfacial activity, plus requiring lower concentration to interconnect in entangled networks. Hence, a less extensive processing of the fibres is recommended for preserving the thickening and stabilizing properties.
- The prepared BC:CMC formulations exhibited an optimal combination of properties for stabilizing different heterogeneous systems: colloidal stability due to surface charges imparted by CMC; interfacial active performance, demonstrated by the ability to lower the energy of the water/oil interface; flexibility and adsorption at the interface, defined by BC's amphiphilicity and specific wettability; high viscosity and pronounced solid-like behaviour, plus the presence of a yield stress, at low concentrations; high aspect ratio of the fibres, that facilitates the formation of three-dimensional

networks at low concentration, structuring the aqueous phase and preventing destabilization mechanisms such as sedimentation, creaming and coalescence.

- With the above mentioned combination of features, BC:CMC 1:1 formulations have been capable of effectively stabilizing: a food suspension of solid particles against sedimentation for at least 4 days, at a mass concentration of 0.15 %; an isohexadecane-in-water emulsion against creaming and coalescence for at least 90 days at a concentration of 0.50 %; a complex cosmetic emulsion without surfactants, replicating the rheological and textural properties of a generic cream, for at least 30 days at a concentration of 0.75%.
- Envisioning an additive for application in food products, increasing the fibre content in BC:CMC formulations (from a 1:1 ratio to 1:0.75 and 1:0.5) resulted in improved rheological properties, namely in higher values of zero-shear viscosity, yield stress and storage modulus. The increase in these parameters, in theory, translates in an improvement of the stabilizing effect of the hydrocolloid.
- Despite containing a polyelectrolyte, the BC:CMC formulations at different ratios showed constant behaviour in dispersion, essentially independent of the ionic strength (0 to 350 mM NaCl) and of the pH (2.8 to 10.4) of the environment.
- Within the studied systems, BC:CMC dry formulations consistently demonstrated better results, or the need for lower concentrations, when compared to several different microcrystalline celluloses and xanthan gum.

Finally, it can be concluded that dry BC:CMC formulations may become of commercial interest for application in food and cosmetics, as well as other areas yet to be explored. It is predictable that, in the near future, the large-scale biotechnological production of BC will grow, making BC-based products such as BC:CMC formulations more attractive, as they demonstrate superior properties with lower concentration when compared to other commercial hydrocolloids. Producers may use BC-based dry additives in replacement of surfactants, as a biological, safer and sustainable alternative.

FUTURE WORK

Given the present study and the conclusions drawn from the work, new questions and ideas for investigation arise, paving the way for further research within the scope of this thesis. Thus, some prospects for future work include:

- Study the effect of temperature on BC:CMC dispersions and emulsions more in depth, using higher temperatures and covering the range used in processing and utilization of food products;

- Apply BC:CMC formulations in the ratios of 1:0.75 and 1:0.5 to emulsions and suspensions, to verify and quantify the improvement in stabilizing power in comparison with the 1:1 ratio;
- Subject coarse BC:CMC emulsions to high energy homogenization techniques such as ultrasounds or high pressure homogenization, attempting to produce nanoemulsions;
- Study the behaviour of BC:CMC emulsions through the gastrointestinal tract, to assess the possibility of developing a controlled delivery system for bioactive compounds;
- Understanding the arrangement and dynamics of BC fibres at the oil/water and air/water interfaces, through confocal microscopy techniques using different fibre dyes;
- Developing new edible BC formulations with a more hydrophobic character, showing potential as an additive for stabilization of aqueous foams in food technology.
- Although this work has focused more on the use of ground BC fibres in the form of a dry additive, BC wet membranes' organoleptic properties can be modulated by impregnation with polysaccharides, flavours and other ingredients to resemble fruit pieces that can be incorporated into beverages and desserts.
- Dry BC membranes can also provide an alternative substrate for flexible and recyclable electronics, as well as biodegradable biosensors.

The application of BC in these areas, together with the potential it demonstrated throughout this thesis, outperforming other celluloses, will help turning BC into a multipurpose commodity for the future: one material for multiple products.